JOURNAL OF THE AERONAUTICAL SCIENCES

VOLUME 21 MAY, 1954 NUMBER 5

Wing-Body Interference at Subsonic and Supersonic Speeds—Survey and New Developments

H. R. LAWRENCE* AND A. H. FLAX†

Cornell Aeronautical Laboratory, Inc.

SUMMARY

Recently, wing-body interference effects have assumed greater significance in aerodynamics than heretofore because of the trend toward lower aspect ratios and larger ratios of body diameter to wing span in high-speed aircraft and missiles. It has thus become necessary to effect refinements in the time-honored aerodynamic assumptions concerning wing-body interference for both the subsonic and supersonic speed ranges. In this paper, a critical survey of available theories, simplified analysis methods for use in design, and experimental results is given, including some new developments based on recent work at Cornell Aeronautical Laboratory. Among these are: (1) an approximate subsonic theory for low-aspect-ratio ($AR < 4$) wing-body combinations applicable to the class of wings with straight trailing edges, (2) a simple semiempirical design method for predicting subsonic characteristics of low-aspect-ratio wing-body combinations, (3) a calculation by variational methods of the characteristics of a series of high-aspect-ratio wing-body combinations according to lifting-line theory, (4) supersonic experimental results and analysis for a series of wings with supersonic leading edges of aspect ratios ranging from 0.5 to 5.0, with particular emphasis on body-load distribution, (5) approximate methods for rapid calculation of body loading in supersonic flow for the configurations of (4) above, and (6) general integral relations in the linearized theory of wing-body interference. It is also shown how a unified point of view in constructing approximate theories and design methods, and in interpreting and utilizing experimental data for all speed ranges can be achieved by the application of the general integral relations.

INTRODUCTION

IN RECENT YEARS, the subject of wing-body interference has assumed increased importance in aerodynamics because of the design trend in transonic and supersonic aircraft and missiles toward lower aspect ratios and lower ratios of wing span to body diameter. Many of the time-honored assumptions about wing-body interference which served the aerodynamicist well in analyses of low-speed aircraft have been found to be woefully lacking when applied to some of the high-speed aircraft now under development. For instance, the oft-used assumption that the slope of the lift curve of a wing-body combination can be closely estimated by calculating the slope of the lift curve for the wing alone, including the hypothetical extension of the wing which passes through the body is likely to give within 5 per cent of the correct slope of the lift curve if the ratio of span to body diameter is 10 or greater, but it may lead to errors of the order of 20 per cent if this ratio is 3. The need for increased accuracy in the estimation of wing-body interference effects is not a pleasant idea for the engineer to contemplate, since it suggests the necessity for more complicated, laborious, and time-consuming calculations as part of any design analysis. It appears, however, that the situation may not be as bad as it seems at first sight, since often crude approximations and assumptions based on a sound physical understanding of the problem can lead to results satisfactory for many purposes. For example, in estimating the total lift of a wing-body combination, if interference effects account for 30 per cent of the lift, an error of 20 per cent in estimating the interference effects will lead to an error of 6 per cent in the answer, which is tolerable in many applications. There are few solutions of wing-body problems which are exact, even within the framework of the linearized wing theory. Most theories of wing-body interference are based upon approximations which involve assump-

Presented at the Aerodynamics Session, Annual Summer Meeting, IAS, Los Angeles, July 15–17, 1953.

* Assistant Head, Aerodynamic Research Department.

† Head, Aerodynamic Research Department.

tions in addition to those which are made in the various theories of wings alone. In many practical problems, it is found necessary to use these approximate theories for cases other than those for which they were derived, because of a lack of any theory more applicable to the problem at hand. To do this with any degree of success requires a knowledge of the basic assumptions and limitations of the available approximate theories and their relations to each other, as well as an understanding of the essential physical aspects of wing-body interference. In the present paper, the available theories as well as certain recent extensions and new developments are derived from a common basic formulation insofar as possible, so that the significant assumptions made in developing each theory and the relationships between them can be more clearly seen. A unified point of view is sought in the consideration of the various theories and approximate methods for both the subsonic and supersonic speed ranges. Relationships in the Trefftz plane and the reverse-flow theorems[31] for wing-body combinations are shown to provide useful common bonds between almost all theories in both the subsonic and supersonic speed ranges. Because of limits on the length of this paper, only symmetrical lift problems are considered. While many of the theories and methods discussed apply to antisymmetrical lift problems as well as with minor changes, mention of such applications will usually be omitted.

For subsonic flow, the spanwise lift distribution over a wing-body combination of minimum induced drag was first treated by Lennertz[1] for a body consisting of an infinitely long circular cylinder. His solution was generalized by Pepper[2] to the case of wings in combination with an infinitely long body of any cross-sectional shape or with a multiplicity of such bodies. Lennertz also considered the problem of the longitudinal distribution of lift over the cylindrical body and found a distribution which was symmetrical about an assumed wing lifting-line and which was highly localized in the region of the wings. The case of a high-aspect-ratio wing of given plan form and angle-of-attack distribution mounted on an infinitely long cylinder of any shape was treated by Multhopp,[3] whose solution is based on lifting-line theory. Multhopp also indicated approximate corrections based on slender-body theory to allow for the effects of a noncylindrical body of finite length. Multhopp's treatment of the lift on the body omitted that part of the body lift which would occur on an infinite cylinder of the same cross-sectional shape as the body in the region of the wings. This leads to discontinuities in the body loadings in the vicinity of the wings and requires rather arbitrary assumptions as to the downwash to which the body should be considered subjected. An improved method for calculation of body loading for finite bodies has been developed and is presented herein. This method is based on slender-body theory for the body only and allows the calculation of the loading continuously along the body. For an infinite cylindrical body, Lennertz's results are closely approximated. A solution for the lift of high-aspect-ratio wing-body combinations based on a variational principle in the Prandtl lifting-line theory has been given by Flax and Treanor.[4] Slopes of the lift curve for a large range of wing-body configuration variables have been obtained and some are included herein.

For the case of wings of aspect ratio less than about 6, the Prandtl lifting-line theory predicts slopes of the lift curve for the wing alone which are known to be too high by an appreciable amount, and the same effect may be expected for wing-body combinations of aspect ratio below 6. Also, for swept wing-body combinations, the Prandtl lifting-line approach cannot be used. For wings alone, these cases are handled by the Weissinger[5] theory, but attempts to set up a theory of the Weissinger type for wing-body combinations meet with difficulties in the determination of the downwash produced at the 3/4 chord position of the wing in the presence of the body. Possible methods of attacking this problem are discussed, including one proposed for circular bodies by Zlotnick and Robinson[6] involving the use of a number of horseshoe vortices on the wing, and their images in the body. It appears that while this problem can probably be solved very approximately by any one of a number of methods, the choice of the most suitable method will depend on the results of extensive correlation of theory with experiment.

For slender-winged bodies of revolution having wings with straight trailing edges and cylindrical bodies behind the wings, Spreiter[7] and Ward[8] have given closed solutions of simple form. Ward's results differ from Spreiter's if the body is noncylindrical in the wing region. Miles has pointed out that this discrepancy results from the fact that Spreiter neglected quadratic terms in Bernoulli's equation which effect an interaction between the displacement flow around the body and the lifting flow around the wings. The slender body theory may be expected to be valid for exposed-wing aspect ratios such that the Jones theory[9] is valid for the wing alone. Although the range of these theories is thus limited, the relatively simple form of the results make them very useful in setting up approximations, and in further extensions of the theory. Results of this type for winged bodies of elliptical section have been given by Nonweiler[10] and Kahane,[11] while the case of a body of revolution separated from the wings by a gap has been solved by Mirels. By setting up the Spreiter-Ward formulation of the wing-body problem as a variational problem, it is shown herein that the lift distributions obtained for uniform angle of attack of the wing and body must always be the same as for the classical minimum induced drag case, as has always been observed in all solutions obtained. Further, the total lift of a slender wing-body combination can be readily computed from the results of the minimum induced drag problem with little effort. Another result which speeds up calculations is that the total lift of the

slender wing-body combination is the same as that of the slender wing alone which is obtained from the conformal transformation which maps the body on a vertical slit (Multhopp's transformation). By the use of these two results, the total lift as well as the chordwise distribution of lift can be obtained for a wide variety of cases with little effort, once the transformation appropriate to the body shape is known.

A theory for low-aspect-ratio wings with straight trailing edges centrally mounted on an infinite circular cylinder has been given by Lawrence;[12] this theory is valid for aspect ratios well above those for which slender-configuration theory becomes inaccurate. A generalization of this theory to winged cylindrical bodies of any cross-sectional shape is given in this paper. The results of this theory always lead to an equivalent low-aspect-ratio wing problem, which may then be solved by methods already set up for such problems.[13]

The lift on afterbodies in the presence of wing trailing vortices has been studied by Lagerstrom and Graham,[14] Moskowitz,[15] and Adams and Sears.[16] The work of Lagerstrom and Graham, as well as that of Moskowitz, deals with the forces induced on a long cylindrical afterbody at an angle of attack as the wing vortices pass downstream at an ever-increasing vertical distance from the body. Lagerstrom and Graham found that there was a small additional positive lift on the body, while it can be shown that Moskowitz's method results in a negative lift on the body equal in magnitude to all the positive lift induced on the body by the wing in the first place. It appears that Moskowitz is in error because of his neglect of the pressures induced on the body by the deformed vortex sheet as it passes over the top of the body. Adams and Sears studied the case of an afterbody of decreasing area in the presence of a wing vortex sheet; a small additional positive lift results. The analyses of Adams and Sears, and Lagerstrom and Graham may be applied as a first approximation for slender afterbodies behind nonslender wing-body combinations.

It has been found that rapid estimates of total lift of a winged body which is cylindrical in the region of the wings with constant angle of attack of the wings and body can be made by a relatively simple approximate method, by considering the exposed wings as the basic lifting element. The method was apparently first suggested by Ward,[8] who based it on the results of slender-configuration theory for winged bodies of revolution, but was unable to verify its validity for other cases. In the present work, it is shown on theoretical grounds that the method is approximately valid for both high- and low-aspect-ratio wings in combination with bodies of revolution, and it is shown how the method may be extended to cylindrical bodies of arbitrary shape. There is, however, a need for more experimental data on this subject.

For supersonic flow, the earliest work is apparently that of Kirkby and Robinson,[17] who analyzed the case of a very-high-aspect-ratio wing mounted on a conical body by approximate methods. They did not deal with any action of the wing on the body, and calculated the interference effect as simply the increased lift on wings due to the increase in wing angle of attack produced by the upflow around the body. The next work in this field was that of Ferrari,[18, 19] who considered a rectangular wing of high aspect ratio mounted on a pointed body of revolution. His method involves the use of an iterative process which starts with the calculation of the flow about the wing alone and the flow about the body alone, and proceeds to correct the solutions in such a way that at each stage of the iteration process, the boundary condition on either the wing or the body is satisfied exactly, while the boundary condition on the other component is violated. Since the process can be shown to converge, carrying the procedure through a sufficient number of steps would eventually result in a situation in which the boundary conditions on both the wing and the body are satisfied to any desired numerical accuracy. Actually, the procedure becomes very laborious after the first few steps, and numerical calculations with the theory have never been made beyond the first two steps. While in principle the iterative method will give the correct solution, no matter what initial assumptions are made to start the process, the number of steps required to achieve a given accuracy will obviously depend to a large degree on the strarting point of the iteration. The starting point of the Ferrari method was chosen so as to produce the smallest errors possible in the early steps, subject to the restraining condition that the calculation of the early steps be kept as simple as possible. The results of the first iteration for wing and body show fairly good agreement with experiment.

Morikawa[20] has attacked the problem of a rectangular wing mounted on a cylindrical body when both are at the same angle of attack. The region considered in his analysis is limited to points forward of the wing trailing edge. By using the Laplace transform in the x direction, he has succeeded in finding the Laplace transform of the exact solution to this problem in terms of a series involving the modified Bessel functions. He was, however, unable to invert this transform to obtain the solution. He has given an approximate solution to the problem which should be valid for small distances from the wing leading edge. The accuracy of this solution for practical configurations has not been determined and must depend upon experimental verification. Morikawa[29] also has given the solutions to numerous planar problems intended to simulate the wing-body problem; these solutions may be instructive for qualitative analyses and for setting up approximate methods for use in design. This will be discussed later.

Browne, Friedman, and Hodes,[22] using the powerful methods available for conical-flow problems, have solved the supersonic wing-body problem for the case of a delta wing which starts at the apex of a conical

body. Their solution is exact within the limits of linearized theory. Although the configuration they have considered is not a particularly practical one, the results are useful in checking the validity of those approximate theories which can also be applied to this configuration.

Lagerstrom and Van Dyke[21] have made a very comprehensive study of the supersonic wing-body interference problem. Their arguments and results were, however, entirely qualitative and for the most part based on extension of the results obtained for planar problems. Of special interest in their work is a formulation of the wing-body problem, which was later used by Nielsen[23] in his work. In this formulation, which will be stated here for the case of the wing only at a constant angle of attack, a wing at angle of attack extending through the body is taken as the basic wing. This wing is assumed to have supersonic leading edges. The wing flow then induces normal velocities across the body surface. If a potential can be found satisfying the linearized differential equation for supersonic flow and cancelling these normal velocities at the body surface without producing any velocities normal to the wing surface, the exact solution is the sum of this potential and the basic wing potential. Lagerstrom and Van Dyke have shown that such a solution can be constructed by expanding the potential in a Fourier series in the meridional angle and considering only even terms, each of which contributes zero velocity normal to the wing. This formulation is valid only up to the wing trailing edge.

Nielsen[23] has solved the supersonic problem of a rectangular wing at constant angle of attack centrally mounted on a circular cylindrical body at zero angle to the stream, using the Lagerstrom-Van Dyke formulation of the problem. Nielsen employed the Laplace transform in the stream direction to obtain his solution. He was able to invert the transform of the solution only in terms of a new set of functions, one for each term of the Fourier series. Only the first four of these functions were tabulated, so that only four terms of the Fourier series solution could be used for numerical work. The numerical results showed that the Fourier series solution converged very slowly in the vicinity of the wing leading edge and the solution needed to be faired into a result obtained by another approximation forward of $x = 1.2\sqrt{M^2 - 1}\,R$. More recently, Nielsen and Pitts[24] have given an additional presentation of Nielsen's theory with more emphasis on physical interpretation and application than is to be found in the original paper.

Consideration of the practical side of the wing-body interference problem discloses that, as in the subsonic case, in many instances rather crude approximations will suffice to give satisfactory answers for many purposes. In considering any questions of accuracy in a practical way, due account should be taken of the limitations of the linearized theory itself. Second-order effects on pressures cannot be readily computed for complex configurations, but are known to be of considerable magnitude. Also, the disturbances from wing to body and back do not propagate exactly along the Mach lines as assumed in the theory, and this, too, produces some errors in the theoretical results. Recourse to experiment must be taken to assess the magnitude of such effects in many instances. Cramer[25] has given a comprehensive presentation of experimental pressure distributions at a Mach Number of 2 for a class of wing-body combinations consisting of bodies of revolution with centrally mounted wings having no subsonic edges. The aspect-ratio range covered was from 0.5 to 4.29, based on the exposed span of the models, and the body radius to wing chord ratio was approximately 0.7. Based on these test results, Cramer was able to show that fairly simple "rules of thumb" augmented by the reverse-flow and Trefftz-plane theorems for wings on cylindrical bodies would suffice to give good estimates of the lift on the configurations tested. The results made it clear that the build-up of lift on the body behind the trailing edge contributes the greater part of the body lift, so that attention should be focused on the afterbody for most configurations. The pitching moment of the configuration is also very strongly dependent on the afterbody lift distribution, and thus on the afterbody length. No theory or method for estimating wing-body interference effects which fails to account for the afterbody length can thus be of general utility. Cramer has shown fairly good agreement between the body-lift distribution computed from the Ferrari theory and those obtained from experiment. A normalized body loading curve based on the Ferrari theory which has been calculated by Rae[26] is included herein. This curve can be used directly for all cases in which the wing tip Mach cones do not intersect the body; approximate methods of handling the effects of the wing tips when they do influence the body are discussed in the present paper. The application of slender-body theory as indicated by Ferrari[18] and expanded by Schrenk[27] offers a useful means of obtaining approximate evaluations of such effects.

The interference pressures on the wing should theoretically be obtainable by either the method of Ferari[18, 19] or that of Nielsen.[23] The Ferrari iteration process has, however, not been carried far enough to obtain the wing pressures to a high degree of accuracy. The Nielsen method is set up in such a manner as to favor the determination of wing pressures at the expense of the lift distribution on the afterbody. Thus, the accuracy of Nielsen's wing pressures should be greater than the Ferrari wing pressures for a given amount of numerical effort. As indicated previously, however, Nielsen's method is limited in accuracy for distances downstream of a wing leading edge–body intersection of the order of the body radius. For wings of large chord, the Nielson method should give satisfactory accuracy. Even in this case, the wing span

loadings obtained from the first iteration in the Ferrari method do not differ greatly from those of Nielsen or from experimental results. In studying experimental results for practical configurations, the departures from the theory due to second-order effects on the pressures are found to be significant. Also, the effects of the gap opened at the wing-body juncture in the case of movable wings are marked.[40]

For the case of wing and body at the same angle of attack, Ferrari's iteration solution[18, 19] and the approximate solution of Morikawa[20] provide the only available theoretical data on wing pressures, since Nielsen's method has not yet been extended to this case. Both the first step in the Ferrari method and the Morikawa method estimate a fall in wing lift near the body, although Ferrari's result is in considerably better agreement with experiment. An analysis of experimental results for rectangular wings discloses that the wing pressures in the region between the side of the body and the Mach line from the wing-body intersection average about 90 per cent of the value at the Mach line, at least for distances up to $0.7\sqrt{M^2-1}$ body radii from the wing leading edge. The theoretical value at the Mach line from the leading edge can easily be predicted from linearized wing theory (the result was first given by Kirkby and Robinson[17]). At present, this approach appears to offer the simplest, and at the same time, most practical method for predicting wing pressures for the case of the wing and body at the same angle of attack for the range of wing chord to body diameter considered. Various approximate methods for roughly estimating supersonic wing-body interference effects have been given by several authors, including Laitone,[28] Lagerstrom and Van Dyke,[21] Morikawa,[29] and Beane.[30] These methods are based on the use of strip theory and analogies to planar models at one limit and on slender-configuration theory at the other limit. The results for intermediate cases have been inferred by means of plausible assumptions and approximations. Such methods must be used with care, but when they are skillfully handled, and augmented even by meager experimental results, they can be quite useful in design and in the planning and interpretation of experiments.

General Theory and Concepts

From the discussion in the introduction, it can be noted that a variety of methods applicable to special regimes of flight speed and configuration, and employing different types of approximations, are available. In an attempt to unify the results obtained by different investigators and to clarify the relationships between the various theories, a general formulation of the theory will be developed, and the paths leading to the special theories will be indicated. The general formulation will be applicable to both supersonic and subsonic flows. By proceeding in this manner, the basic similarities and differences between the subsonic and supersonic theories will be brought to the fore. In spite of the complexity of the wing-body problem, there are some general concepts which are applicable to wide classes of configurations and within the limitations of linearized theory to both subsonic and supersonic flows. These concepts will prove to be useful in the discussion of many particular cases and will therefore also be considered in this section.

General Formulation of the Wing-Body Problem

Consider a wing-body configuration immersed in an inviscid uniform free stream flowing with the velocity U_0 parallel to the positive x-axis. The angle between the free stream and every surface element of the wing-body configuration is assumed to be small, so that linearized theory is applicable. The wing is assumed to be so thin that it may be replaced by its mean camber surface, which is assumed to lie in the neighborhood of the plane $z = 0$. The local angle of attack of the wing will be denoted by $\alpha(x,y)$. The curvature of the body will be assumed to be finite everywhere except perhaps at the nose. Aside from this restriction, and the requirements imposed by the applicability of linearized theory, the shape of the body is arbitrary. Effects due to displacements of the wing trailing vortex sheet will be neglected in this formulation, since such effects are difficult to formulate generally. Some special cases will be considered later.

The (x,y,z) components of velocity may be expressed in terms of the perturbation velocity potential φ in the form $(u,v,w) = (U_0 + (\partial\varphi/\partial x), \partial\varphi/\partial y, \partial\varphi/\partial z)$. Necessary and sufficient conditions for specifying a unique potential function may be written in the form:

$$\partial^2\varphi/\partial y^2 + (\partial^2\varphi/\partial z^2) + (1 - M^2)(\partial^2\varphi/\partial x^2) = 0 \quad \text{in the flow field } F \qquad (1)$$

$$\partial\varphi/\partial z = -U_0\,\alpha\cos(x,y) \quad \text{on the wing surface } R_W \qquad (2)$$

$$\partial\varphi/\partial n = -U_0\cos(n,x) \quad \text{on the body surface } R_B \qquad (3)$$

$$\varphi \to 0 \quad \text{as } x \to -\infty \qquad (4)$$

$$\partial\varphi/\partial x = 0 \quad \text{at wing trailing edges } R_{W_T} \qquad (5)$$

Eq. (1) is the well-known linearized differential equation for the velocity potential in a flow at a free-stream Mach Number of M. Eqs. (2) and (3) express the conditions that the flow through any element of the wing or body surface vanishes. The symbol $\partial\varphi/\partial n$ denotes the partial derivative of φ in the direction of the outward normal to the body surface. The symbol $\cos(n,x)$ denotes the cosine of the angle between the outward normal to the body surface and the positive x-axis. Eq. (4) insures that the perturbation velocities vanish far upstream and the Kutta condition at the wing trailing edge is formulized in Eq. (5).

The aerodynamic forces acting on the surface elements of the wing and body are related to the pertur-

bation velocities by the Bernoulli equation

$$\frac{p}{p_0} = \left[1 - \frac{\rho_0}{\gamma p_0}\frac{(\gamma-1)}{2}\left\{2U_0\frac{\partial\varphi}{\partial x} + \left(\frac{\partial\varphi}{\partial x}\right)^2 + \left(\frac{\partial\varphi}{\partial y}\right)^2 + \left(\frac{\partial\varphi}{\partial z}\right)^2\right\}\right]^{\gamma/(\gamma-1)} \quad (6)$$

where p is the pressure, γ is the ratio of specific heats, and ρ_0,p_0 are the density and pressure in the unperturbed free stream.

In view of the fact that the linearized differential Eq. (1) is used to compute the perturbation velocities, the use of the complete Bernoulli equation for the pressures may be questioned on the grounds of internal consistency. The objection may be stated as follows.

The use of the complete Bernoulli equation for computing pressures from the perturbation velocities obtained by solving a linearized differential equation is certainly correct. However, an approximation to the Bernoulli equation which is consistent with the accuracy of the linearized differential equation for the perturbation velocities would yield equally accurate results and would lead to a less complicated expression for the pressure. For the case of slender wing-body configurations in supersonic flow, Broderick[32] and Lighthill[33] have shown that the following approximation to the Bernoulli equation is consistent in accuracy with the linearized differential equation.

$$p_0 - p = \rho_0\left\{\frac{U_0\partial\varphi}{\partial x} + \frac{1}{2}\left(\frac{\partial\varphi}{\partial y}\right)^2 + \frac{1}{2}\left(\frac{\partial\varphi}{\partial z}\right)^2\right\} \quad (7)$$

Adams and Sears[16] have obtained the same result for slender configurations in subsonic flow.

An approximate form of the Bernoulli equation consistent with the linearized differential equation for the potential and applicable to configurations which are not necessarily slender has not been developed. Thus, it appears that a safe procedure would be to use the exact Bernoulli Eq. (6) for nonslender configurations. It should be noted that in any particular case, there is no assurance that use of an approximate Bernoulli equation will not empirically result in better agreement with experiment or nonlinear theory. In practice, the approximate Bernoulli Eq. (7) or the linearized Bernoulli equation

$$p_0 - p = \rho_0 U\frac{\partial\varphi}{\partial x} \quad (8)$$

have been found to yield satisfactory estimates of the pressure in many cases.

In order to avoid the complications introduced by using the nonlinear Bernoulli Eqs. (6) and (7), the results of this paper will be restricted mainly to cases where the linearized Bernoulli Eq. (8) yields accurate results. The general wing-body problem in which the body is cylindrical in the neighborhood of the wing-body intersection may be treated in this fashion if only the difference in pressure between the upper and lower surfaces of the body or wing is computed. It is clear that the results obtained herein may be extended by making use of the exact Bernoulli equation where necessary.

Eqs. (1) through (5) and Eq. (8) represent a mathematical formulation of the linearized wing-body problem in subsonic or supersonic flow. The methods employed by various investigators will be summarized with particular emphasis on the range of applicability of the results and the approximations used in simplifying the problem.

Iterative Procedure

The most general procedure for solving the wing-body problem, at least in principle, is the iterative method first proposed by Ferrari.[18] It will be shown that this method is applicable to all configurations for which the wing-alone and body-alone problem can be solved at both subsonic and supersonic speeds. The convergence of this process may be established in the subsonic case by appeal to the Schwarz "alternierendes Verfahren"[34] and in the supersonic case by the existence proof for Volterra-type integral equations.[35]

The potential φ is written as a sum of the form

$$\varphi = \sum_{k=0}^{N}(\varphi_B^{(k)} + \varphi_W^{(k)}) \quad (9)$$

where each term satisfies the differential Eq. (1) and the condition, Eq. (4), that the perturbations vanish far upstream. It will be shown that the boundary conditions, Eqs. (2) and (3), on the wing and body surface, respectively, are satisfied if $\varphi_B^{(k)}$ and $\varphi_W^{(k)}$ are specified by the following conditions:

$$\partial\varphi_B^{(0)}/\partial n = -U_0\cos(n,x), \quad \partial\varphi_B^{(k)}/\partial n = -(\partial\varphi_W^{(k-1)}/\partial n,\ k = 1,2,\ldots N \text{ on } R_B \quad (10)$$

$$\partial\varphi_W^{(0)}/\partial z = -U_0\alpha(x,y), \quad \partial\varphi_W^{(k)}/\partial z = -(\partial\varphi_B^{(k-1)}/\partial z), \quad k = 1,2,\ldots N \text{ on } R_W \quad (11)$$

$$\frac{\partial\varphi_W^{(k)}}{\partial x} = 0 \quad k = 0,1,2\ldots N \text{ on } R_{W_T} \quad (12)$$

It will be noted that $\varphi_B^{(k)}$ and $\varphi_W^{(k)}$ satisfy boundary conditions only on the body and wing, respectively, and hence require solution of the body-alone and wing-alone problems. It is assumed that a method for solving the body-alone and wing-alone problems is available. It is evident from Eqs. (10), (11), and (12) that the potential functions $\varphi_W^{(k)}$, $\varphi_B^{(k)}$ may be calculated in order of increasing k starting with $k = 0$.

Upon substituting the series, Eq. (9), for φ in the boundary conditions, Eqs. (2) and (3), and making use of the defining Eqs. (10) and (11) for $\varphi_W^{(k)}$ and $\varphi_B^{(k)}$, there result the formulas

$$\partial\varphi/\partial z = -U_0\alpha(x,y) + (\partial\varphi_B^{(N)}/\partial z) \quad R_W \quad (13)$$

$$\partial\varphi/\partial n = -U_0\cos(n,x) + (\partial\varphi_W^{(N)}/\partial n) \quad R_B \quad (14)$$

Upon comparing Eqs. (13) and (14) with the boundary conditions, Eqs. (2) and (3), respectively, it is seen that the series expression, Eq. (9), for φ satisfies all conditions of the problem if $\partial\varphi_B^{(N)}/\partial z$ and $\partial\varphi_W^{(N)}/\partial n$ vanish on the wing and body surfaces, respectively. It can be shown that $\partial\varphi_W^{(N)}/\partial z$ and $\partial\varphi_W^{(N)}/\partial n$ approach zero as $N \to \infty$.

The above iteration process will be useful for numerical calculations only if each iteration is reasonably simple and if the process converges rapidly. In principle, it is immaterial whether the wing be considered as extending through the body or ending at the body, provided the same definition of the wing region is used throughout the analysis. The rapidity of convergence and numerical labor, however, are strongly dependent on the definition of the wing region and the method of starting the calculation. In certain cases, it is possible to use only a finite number of steps in the iteration process, so that the method reduces to simply a superposition of a small number of component potentials. This can be done in the subsonic case if the wing is treated by lifting-line theory, as shown by Multhopp,[3] and in the slender-configuration case. It is also possible in certain supersonic problems, as shown by Lagerstrom and Van Dyke.[21] All of these special cases will be discussed later.

Trefftz-Plane Relationships

The simplest relations of a general type may be obtained by considering the flow far downstream of the wing in the Trefftz plane (x approaching ∞). In this case, $\partial\varphi/\partial x$ and $\partial^2\varphi/\partial x^2$ approach zero and Eq. (1) becomes

$$\frac{\partial^2\varphi}{\partial y^2} + \frac{\partial^2\varphi}{\partial z^2} = 0 \tag{15}$$

This equation is valid for both subsonic and supersonic flows, since the last term of Eq. (1) vanishes in either case. For supersonic flows, however, the region of validity of Eq. (15) is restricted to points near the traces in the Trefftz plane of the configuration under consideration. The treatment of wing-body interference problems in the Trefftz plane has been discussed in detail by Lennertz.[1] The problem of basic importance in wing-body interference is that of a wing-body combination consisting of wings of finite size mounted on an infinite cylindrical body with its generators parallel to the x-axis.

The perturbation pressure on any surface element of wing or body, according to the linearized theory, is given by

$$p = -\rho U_0 \frac{\partial\varphi}{\partial x} \tag{16}$$

Therefore,

$$\int_{-\infty}^{\infty} p\,dx = -\rho U_0 \int_{-\infty}^{\infty} \frac{\partial\varphi}{\partial x} = -\rho U_0 \varphi(\infty) \tag{17}$$

WING-BODY COMBINATION IN THE TREFFTZ PLANE

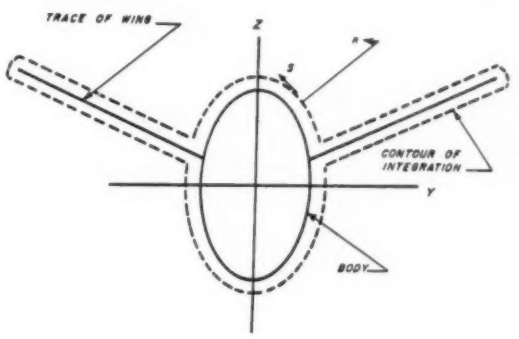

Fig. 1

since $\varphi(-\infty) = 0$. Thus, the integrated pressure which has been experienced by any element of wing or body is completely determined by the value of φ in the Trefftz plane. The total lift on a wing-body combination is then given by

$$L = \rho U_0 \oint \varphi \cos(n,z)\,ds \tag{18}$$

where $\cos(n,z)$ is the cosine of the angle between the outward normal to the surface of the body or the wing traces and the positive z-axis and the integral is taken over the contour enclosing the wings and body as illustrated in Fig. 1. If the lift distribution over the wings is given, so is φ over the trace of the wings in the Trefftz plane. Further, the velocity $\partial\varphi/\partial n$ normal to the body surface must be zero. Thus, the problem of determining the distribution of φ over the body, and hence the integrated body pressure, is reduced to a straightforward problem in two-dimensional potential theory. The circumferential distribution of integrated body pressure on the body is, however, of less interest than the total body lift. This has been found in reference 31 by the use of Green's[31] theorem, to be

$$L_B = \oint_{\text{body}} \rho U_0 \varphi \cos(n,z)\,ds = \oint_{\text{wings}} \rho U_0(\varphi_u - \varphi_l) f(s)\,ds \tag{19}$$

where φ_u is the value of φ on the wing upper surface and φ_l is the value on the wing lower surface; on the wings the outward normal to the upper surface is used to determine $\cos(n,z)$. The function $f(s)$ is the velocity normal to the wing surface which would be produced at the point s on the wing by a unit vertical transverse velocity of the body alone in the negative z direction. Since $(\varphi_u - \varphi_l)$ is equal to the circulation on the wing, the body lift may be written as

$$L_B = \rho U_0 \int_{\text{wings}} \Gamma(s) f(s)\,ds \tag{20}$$

or

$$L_B = \int_{\text{wings}} l(s) f(s)\,ds \tag{21}$$

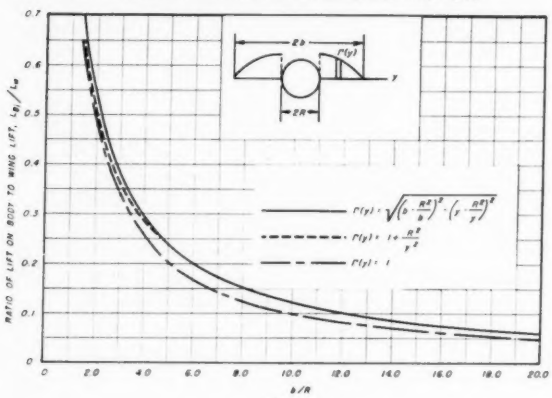

Fig. 2

Here s is taken as the spanwise coordinate over the traces of the wings, and $l(s)$ is the force normal to the wing surface per unit span.

To make Eq. (21) even more concrete, it will be illustrated by application to the common case of a plane wing centrally mounted on a circular cylinder. In this case, the well-known potential for the two-dimensional flow around the cylinder alone is

$$\varphi = (R^2/r) \cos \theta$$

and $s = r$ at $\theta = 90°$

$$f(r) = (1/r)\ (\partial\varphi/\partial\theta)\ \big|_{\theta = 90°}$$

Thus,

$$f(r) = R^2/r^2$$

and

$$L_B = \rho U_0 \int_{\text{wings}} \Gamma(r)\ (R^2/r^2)\ dr \qquad (22)$$

A similar result has been obtained for the antisymmetrical case, but it will not be considered here.

It should be observed that if the lift is computed as the rate of transport of vertical momentum across the Trefftz plane per unit time, it is given by

$$L = -\int\int \rho U_0\ (\partial\varphi/\partial z)\ dy\ dz \qquad (23)$$

By integrating this expression, it can be reduced to

$$L = \oint \rho U_0 \varphi \cos (n,z)\ ds$$

which is identical to Eq. (18). The derivation of Eq. (18) from Eq. (23) rather than from Eq. (17) has, however, deeper significance than is at first apparent. As Ward has shown in the case of slender-body theory, Eq. (18) takes into account more than the linearized Bernoulli equation for pressures used in deriving Eq. (17); in fact, it accounts for, among other things, the quadratic approximation to the Bernoulli equation as given in Eq. (7). In certain problems, the momentum theorem basis for Eq. (18) is essential.

Eq. (21) provides a rapid means for estimating the lift induced on an infinite cylindrical body of any cross section due to any wing lift distribution. As applied to the case of wings centrally mounted on a circular body, Eq. (22), it was first obtained by Lennertz.[1] A result equivalent to Eq. (22) has recently been stated by Zlotnick and Robinson[6] in terms of a representation of the wing lifting elements by horseshoe vortices. Eqs. (21) and (22) show a remarkable property in that the ratio of total lift induced on the body to the total wing lift is relatively insensitive to the details of the wing loading for many practical cases. To illustrate this, the ratio of induced body lift to wing lift, L_{B_i}/L_W, based on Eq. (22) has been plotted versus the ratio of body diameter to wing span R/b in Fig. 2 for the following three cases:

(1) $l(y) = \text{const.}$

(2) $l(y) = \text{const.} \sqrt{[b + (R^2/b)]^2 - [y + (R^2/y)]^2}$

(3) $l(y) = \text{const.}\ (1 + (R^2/y^2))$

The second of these cases is the distribution of lift for minimum induced drag according to Lennertz.[1] It is also the distribution obtained from slender-body theory by Spreiter.[7] The third case is the wing loading obtained from strip theory for a wing operating in the upwash of a circular body at the same angle of attack. It can be seen from Fig. 2 that the ratio, L_{B_i}/L_W, does not vary much with these changes in wing-lift distribution. This result proves to be of considerable value in constructing approximate theories.

The Reverse-Flow Theorem and Its Consequences

A reverse-flow theorem for wings of arbitrary plan form mounted on infinite cylindrical bodies has been derived in reference 31. A statement of the theorem has also been given by Bleakney and Morikawa.[36] For wings mounted on a body at zero angle of attack, the theorem states that

$$\int\int_W \Delta p_2 \bar{w}_1\ dA = \int\int_W \Delta\bar{p}_1 w_2\ dA \qquad (24)$$

where Δp_2 is the normal force per unit area on the wings, w_2 is the specified velocity normal to the wing surface in direct flow, $\Delta\bar{p}_1$ and $\bar{w}_1$ are corresponding quantities for a case in which the flow direction is reversed, and integration is over the wing surfaces. w_2 and $\bar{w}_1$ are defined so as to be of the same sign if the corresponding angles of attack in the respective direct and reversed flows are of the same sign. $\bar{w}_1$ and w_2 may in general be arbitrarily prescribed boundary conditions on the wing surface. As one example of the application of Eq. (24), the case of a rectangular wing in the x,y plane mounted on a body will be considered. Then if $\Delta\bar{p}_1$ is the pressure difference across the wings for the case of the wing at constant unit angle of attack to the x,y plane and $\alpha_2(x,y)$ is an arbitrary camber and twist distribution, the total lift due to $\alpha_2(x,y)$ is given by

$$L_{2W} = \int\int_W \Delta p_2 \, dA = \int\int_W \Delta\bar{p}_1 \, \alpha_2(x, y) \, dA \tag{25}$$

In other words, $\Delta\bar{p}_1$ is the influence function for wing lift. In this case, no reversal of flow is really required, since the rectangular wing presents the same plan form to the flow for either direction of flow. The reversal must, however, be taken into account in specifying the chordwise distribution of $\Delta\bar{p}_1$.

If it is desired to take into account slightly deformed body surfaces in the vicinity of the wings (such as occur in certain stages of iteration or superposition processes) but with the body still at zero angle of attack at $\pm\infty$, the appropriate form of the reverse-flow theorem is more general in form, namely

$$\int\int_{W+B} p_2 \, \bar{w}_{n_1} \, dA = \int\int_{W+B} \bar{p}_1 \, w_{n_2} \, dA \tag{26}$$

where p is the pressure acting on an element of surface and w_n is the value of $\partial\varphi/\partial n$, the fluid velocity normal to the surface; the integration is now to be taken over all surfaces of the wing and bodies, the integration contours in transverse planes being similar to those shown in Fig. 1. An application of Eq. (26) will be given in the discussion of the supersonic wing-body interference problem.

If the body is at uniform angle of attack α_{B_2} in the direct-flow case and $\bar{\alpha}_{B_1}$ in the reversed-flow case, the theorem takes the form

$$\bar{L}_{B_1} \alpha_{B_2} + \int\int_W \Delta\bar{p}_1 \frac{w_2}{U_0} \, dA = L_{B_2} \bar{\alpha}_{B_1} + \int\int_W \Delta p_2 \frac{\bar{w}_1}{U_0} \, dA \tag{27}$$

where $\bar{w}_1$ and w_2 are again arbitrary and L_{B_2} and $\bar{L}_{B_1}$ are the lifts on the body in the direct and reversed-flow cases, respectively. If the configuration is rotated as a unit about the y axis so that the body axis makes a unit positive angle of attack with the x,y plane, then $\bar{\alpha}_{B_1} = 1$, and $\bar{w}_1 = \cos(n,z)$. As in the Trefftz-plane theorem, $\cos(n,z)$ on the wings in this case is the cosine of the angle between the outward normal to the upper wing surface and the z-axis. Then

$$L_{B_2} + \int\int_W \Delta p_2 \cos(n,z) \, dA = \bar{L}_{B_1} \alpha_{B_2} + \int\int_W \Delta\bar{p}_1 \frac{w_2}{U_0} dA \tag{28}$$

The terms on the left are simply the total lift on the wing-body combination in case 2 for arbitrary w_2 and α_{B_2}, so that

$$L_{WB_2} = \bar{L}_{B_1}\alpha_{B_2} + \int\int_W \Delta\bar{p}_1 \frac{w_2}{U_0} \, dA \tag{29}$$

In this instance, $\Delta\bar{p}_1$ and $\bar{L}_{B_1}$ together form the influence function for the total lift of a wing-body combination with arbitrary wing camber and twist, and arbitrary body angle of attack.

By setting $w_2 = 0$ on the wings, $a_{B_2} = 1$ and $\bar{\alpha}_{B_1} = 0$, $(w_1/U_0) = \cos(n,z)$ in Eq. (28), the result is

$$\bar{L}_{B_1} = \int\int_W \Delta p_2 \cos(n,z) \, dA \tag{30}$$

This result has a simple interpretation, if it is recognized that the term on the right is the lift contributed by the wings, so that

$$\bar{L}_{B_1} = L_{W_2} \tag{31}$$

$\bar{L}_{B_1}$ is the lift induced on the body by the wings each at angle of attack $\cos(n,z)$ in case 1, while L_{W_2} is the lift induced on the wings, which are at zero angle of attack, by the body in case 2. If the wings are in the x,y plane, $\cos(n,z) = 1$, and Eq. (31) reduces to the simple statement that the lift induced on the body by the wings at unit angle of attack is equal to the lift induced on the wings by the body at unit angle of attack in reverse flow.

The use of the reverse-flow relations becomes particularly simple if the wing has a spanwise axis of symmetry, or if one is dealing with slender-configuration theory or lifting-line theory, because in these cases the reverse-flow solutions are not really necessary to use the relations. These cases will be considered later.

Another useful result which can be obtained from the reverse-flow theorem is a variational principle which is of value in setting up approximate theories. The procedure used has been explained in some detail in reference 37. The essential result is the variational equation

$$\delta \int\int_{W+B} \left(\bar{p}_1 \frac{\partial\varphi_2}{\partial n} - \bar{p}_1 w_{n_2} - p_2 \bar{w}_{n_1} \right) dA = 0 \tag{32}$$

where the barred quantities correspond to reverse-flow conditions as before. Thus, for first-order variations in $\bar{p}_1$ and p_2 from the exact values corresponding to the specified boundary conditions, this expression deviates from zero only by higher-order terms. The exact solutions correspond to $(\partial\bar{\varphi}_1/\partial n) = \bar{w}_{n_1}$ and $(\partial\varphi_2/\partial n) = w_{n_2}$. $\partial\varphi_2/\partial n$ in this equation is to be regarded as the correct value corresponding to p_2. $\bar{w}_{n_1}$ and w_{n_2} are to be regarded as the values required by the boundary conditions of the problem; they do not vary. If p_2 is exact, $(\partial\varphi_2/\partial n) = w_{n_2}$; if p_2 varies from the exact value of pressure, so does $\partial\varphi_2/\partial n$ vary from w_{n_2}. If $\bar{p}_1$ is taken to be an approximate solution for $\bar{w}_{n_1}$ appropriate to a constant unit angle of attack in reverse flow, and if the solution in direct flow is taken to be $p_2 = cf_2(x,y,z)$ on the surface of the wing-body combination where c is an arbitrary constant which must be determined and $f_2(x,y,z)$ is some plausible distribution of pressure on the boundary in the direct flow case, it can be shown from Eq. (32) and the reverse-flow theorem that the value of total lift obtained from

$$\int\int_{B+W}\left(\frac{\partial\varphi_2}{\partial n} - w_{n_2}\right)\bar{p}_1\,dA = 0 \qquad (33)$$

also has the property of being stationary with variations in $\bar{p}_1$ and p_2 from the correct values. In this sense, $\bar{p}_1$ is a proper weighting factor to use in satisfying the boundary conditions on the average as is often done in approximate solutions. If $\bar{p}_1$ is exact, then Eq. (33) gives the exact answer for the total lift, regardless of what is assumed for the function f_2 representing p_2. This is readily seen, since if the value of $\partial\varphi_2/\partial n$ calculated from the assumed distribution f_2 is given by

$$\partial\varphi_2/\partial n = cg_2(x,y,z)$$

Eq. (33) gives

$$c = \left(\int\int_{W+B} w_{n_2}\bar{p}_1\,dA\right)\Big/\left(\int\int_{W+B} g_2\bar{p}_1 dA\right) \qquad (34)$$

The total lift is given by

$$L_{WB} = c\int\int_{W+B} f_2\cos(n,z)\,dA \qquad (35)$$

so that

$$L_{WB} = \left(\int\int_{W+B} w_{n_2}\bar{p}_1\,dA\right)\Big/\left(\int\int_{W+B} g_2\bar{p}_1\,dA\right)\times \int\int_{W+B} f_2\cos(n,z)\,dA \qquad (36)$$

At this point it should be noted that $U_0\cos(n,z) = \bar{w}_{n1}$, since case 1 in reverse flow corresponds to unit angle of attack of the wing-body combination. Also, because of the reverse-flow theorem as given in Eq. (26)

$$\int\int_{W+B} f_2\frac{\bar{w}_{n_1}}{U_0}\,dA = \int\int_{W+B} g_2\,\bar{p}_1\,dA \qquad (37)$$

since f_2 and g_2 are, respectively, the correct p_2 and $\partial\varphi_2/\partial n$ for some case in direct flow, even though not the one of interest. Therefore,

$$L_{WB} = \int\int_{W+B} w_{n_2}\bar{p}_1\,dA \qquad (38)$$

But by the reverse-flow theorem Eq. (26)

$$\int\int_{W+B} w_{n_2}\bar{p}_1\,dA = \int\int_{W+B} U_0\cos(n,z)p_2\,dA \qquad (39)$$

where p_2 is the exact solution for the specified w_{n_2}. Therefore, $\bar{p}_1$ is the proper influence function for lift of the wing-body combination and Eq. (38) thus gives precisely the correct lift.

This procedure can be generalized to permit the use of several weighting factors in combination with a series of terms for p_2. As shown in reference 37, proper weighting factors to make lift, pitching moment, and rolling moment stationary can be chosen. For the special cases lifting-line theory and slender-body theory, the use of reversed flows becomes unnecessary and simpler variational methods can be derived. These are discussed in the section dealing with these theories.

Subsonic Wing-Body Interference

Multhopp's Formulation

The subsonic problem of a lifting surface mounted on an infinite cylindrical body of any cross-sectional shape will now be formulated, along the lines indicated by Multhopp,[3] and the solutions of this problem for certain limiting cases indicated. The results of such an analysis can, with modifications such as those given by Multhopp, be applied to give approximate results for finite bodies as well.

Consider a thin wing mounted on an infinite cylindrical body, whose generators, which lie approximately in the direction of the x-axis, make a small angle α_B with the x,y plane. The free-stream velocity U_0 is taken to coincide with the x direction, and the wing surface is assumed to lie approximately in the x,y plane. The angle between the wing surface and the x,y plane at any point is denoted by $\alpha(x,y)$. The entire configuration is assumed symmetrical about the y,z plane. It is convenient to consider the flow to be composed of two parts: first, the flow around the isolated body at angle α_B and second, the flow produced by the wings in the presence of the first flow. It may be noted here that the first flow is simply a two-dimensional flow past the body cross section. The second flow must be determined in such a way as not to violate the boundary conditions on the body. The velocity potential, φ_0, describing the isolated body flow field is determined by the condition

$$\nabla^2\varphi_0 = 0 \qquad \text{in the flow field} \qquad (40)$$

$$\partial\varphi_0/\partial n = -U_0\alpha\cos(n,z) \qquad \text{on the body surface} \qquad (41)$$

where $\cos(n,z)$ is the cosine of the angle between the outward normal to the body surface and the z-axis. The velocity potential, φ_1, describing the second flow is determined by the conditions

$$\Delta^2\varphi_1 = 0 \qquad \text{in the flow field}$$

$$\frac{\partial\varphi_1}{\partial z} = -U_0\alpha(x,y) - \partial\varphi_0/\partial z \qquad \text{on the wing surface} \qquad (42)$$

$$\frac{\partial\varphi_1}{\partial n} = 0 \qquad \text{on the body surface} \qquad (43)$$

$$\varphi_1 = 0 \qquad \text{at } x = -\infty \qquad (44)$$

In addition, the pressure difference between the upper and lower surfaces at the wing trailing edge must vanish according to the Kutta condition. The linearized perturbation pressure is given by

$$-p = \rho U_0(\partial\varphi/\partial x) \qquad (45)$$

so that at the trailing edge

$$(\partial\varphi_{1u}/\partial x) - (\partial\varphi_{1l}/\partial x) = 0 \tag{46}$$

where the subscripts u and l are used to identify upper and lower surfaces, respectively.

The conditions on φ_0 and φ_1 give the proper conditions on the solution to the combined problem, since $\varphi = \varphi_0 + \varphi_1$ satisfies the equations previously given in the general formulation, Eqs. (1–5).

The solution for φ_0 can readily be obtained if the body cross section can be mapped conformally onto a circle or a straight line, which can easily be done in a wide variety of cases. The problem of finding φ_1 is considerably more complicated and, in general, can be done only for some simple limiting cases. With further approximations, however, it is possible to find φ_1 in many cases of practical interest. The φ_1 problem is essentially that of a wing mounted on an infinite body at zero of attack with an angle of attack equal to $\alpha(x,y) + (1/U_0)\,(\partial\varphi_0/\partial z)$. For convenience, define

$$f(y) = \frac{1}{U_0\alpha_B}\left.\frac{\partial\varphi_0(y)}{\partial z}\right|_{z=0} \tag{47}$$

The function $f(y)$ is then the vertical velocity produced along the wings by the isolated body in two-dimensional flow for unit vertical velocity of the body. The downwash, w_{1W}, on the plane $z = 0$ produced by the lift on the wings is, according to lifting-surface theory,[13]

$$w_{1W}(x,\,y) = \frac{1}{4\pi}\frac{\partial}{\partial y}\int\int_{Rw}\frac{d\xi\,d\eta}{y-n}\,u_1(\xi,\eta)\times \left\{1 + \frac{\sqrt{(x-\xi)^2 + (y-\eta)^2}}{x-\xi}\right\} \tag{48}$$

where $u_1 = (\partial\varphi_1 u/\partial x) - (\partial\varphi_{1l}/\partial x)$ and $w_1 = (\partial\varphi_1/\partial z)$. It should be noted that the lift per unit area on the wing is given by $l(x,y) = \rho U_0 u_1$, which is directly proportional to u_1. The downwash produced by the lift on the body generally involves more complex considerations which will not be gone into here, because the result is usually so involved that no calculations can be made with it. Since, however, a Green's function for the problem exists, it is possible to set down an operator $K(x,y;\,\xi,\eta)$ such that the additional downwash, w_{1B}, produced by an element of wing lift in the presence of the body is

$$w_{1B} = \int\int_{Rw} d\xi\,d\eta\,u_1(\xi,\eta)K(x,y;\,\xi,\eta) \tag{49}$$

Thus, $w_1 = w_{1W} + w_{1B}$. In accordance with the boundary condition on the wing, Eq. (42),

$$U_0\alpha(x,y) + U_0\alpha_B f(y) = \frac{1}{4\pi}\frac{\partial}{\partial y}\int\int_{Rw} d\xi\,d\eta\times \frac{u_1(\xi,\eta)}{y-\eta}\left\{1 + \frac{\sqrt{(x-\xi)^2 + (y-\eta)^2}}{x-\xi}\right\} + \int\int_{Rw} d\xi\,d\eta u_1(\xi,\eta)K(x,y;\,\xi,\eta) \tag{50}$$

From this integral equation in u_1, the wing lift distribution can, in principle, be solved for any given case, subject to the Kutta condition, $u_1 = 0$ at the wing trailing edge.

One particular case in which the determination of the correction kernel K becomes simple occurs when x approaches ∞; in other words, when the downwash in the Trefftz plane is required. In this case, Eq. (50) becomes

$$w_1 = \frac{1}{2\pi}\frac{\partial}{\partial y}\int_{-b}^{b}\frac{d\eta}{y-\eta}\int_{x_0(\eta)}^{x_1(\eta)} u_1(\xi,\eta)\,d\xi + \int\int_{Rw} d\xi\,d\eta u_1(\xi,\eta)K(\infty,y;\,\xi,\eta) \tag{51}$$

where x_0 and x_1 are the x coordinates of the leading and trailing edges, respectively, while b is the semispan of the wing. In integrating from $-b$ to b, it must be understood that the region of the body itself is excluded. The lift per unit span may be defined as

$$l(\eta) = \rho U_0\int_{x_0(\eta)}^{x_1(\eta)} u_1(\xi,\eta)\,d\xi$$

and the circulation as

$$\Gamma(\eta) = \frac{l(\eta)}{\rho U_0} = \int_{x_0(\eta)}^{x_1(\eta)} u_1(\xi,\eta)\,d\xi$$

Then,

$$w_1 = \frac{1}{2\pi}\frac{\partial}{\partial y}\int_{-b}^{b}\frac{\Gamma(\eta)}{y-\eta}\,d\eta + \int\int_{Rw} d\xi\,d\eta u_1(\xi,\eta)\,K(\infty,\,y;\,\xi,\eta) \tag{52}$$

Integrating the first term by parts and then differentiating under the sign gives

$$w_1 = \frac{1}{2\pi}\int_{-b}^{b}\frac{d\Gamma/d\eta\,d\eta}{y-\eta} + \int\int_{Rw} d\xi\,d\eta u_1(\xi,\eta)K(\infty,\,y;\,\xi,\eta) \tag{53}$$

The exact expression for w_1 in the Trefftz plane is, however, known in another form from the work of Multhopp.[3] If $\bar{l} = g(t)$ is the conformal transformation which takes the body in y,z plane ($t = y + iz$) into the z axis in the $\bar{y},\bar{z}$ plane ($\bar{l} = \bar{y} + i\bar{z}$), then the wing-body combination in the t plane is mapped into a wing-alone in the $\bar{l}$ plane; the vertical slit along the $\bar{z}$ axis representing the body is necessarily a streamline, since the flow component perpendicular to the $\bar{z}$ axis vanishes by symmetry. Thus, the boundary condition on the body is satisfied. In the transformed plane then

$$\bar{w}_1 = \frac{1}{2\pi}\int_{-\bar{b}}^{\bar{b}}\frac{(d\bar{\Gamma}/d\bar{\eta})\,d\bar{\eta}}{\bar{y}-\bar{\eta}} \tag{54}$$

The downwash velocity in the physical plane is given by

$$w_1 = \bar{w}_1 \text{ R.P. } (d\bar{l}/dt) \tag{55}$$

where R.P. denotes "real part of," or

$$w_1 = \text{R.P.} \left(\frac{d\bar{l}}{dt}\right) \frac{1}{2\pi} \int_{-\bar{b}}^{\bar{b}} \frac{(d\bar{\Gamma}/d\bar{\eta})\, d\bar{\eta}}{\bar{y} - \bar{\eta}} \tag{56}$$

It should be noted that this expression for w in terms of $\bar{w}$ is an approximation based on neglecting the sidewash velocity on the transformed wing. Multhopp points out that this effect should usually be small—for a plane wing with a body symmetrical about the plane of the wing the error is zero. A check of some results obtained with this approximation for a body unsymmetrical about the wing plane is given later.

Since the discontinuity in potential $(\varphi_u - \varphi_l)$, and thus the value of Γ, are not altered in a conformal transformation,

$$\bar{\Gamma}(\bar{\eta}) = \Gamma[\bar{\eta}(\eta)] \tag{57}$$

and

$$(d\bar{\Gamma}/d\bar{\eta})\, d\bar{\eta} = (d\Gamma/d\eta)\, d\eta \tag{58}$$

Substituting this relation into Eq. (56)

$$w_1 = \text{R.P.} \left(\frac{d\bar{l}}{dt}\right) \frac{1}{2\pi} \int_{-b}^{b} \frac{(d\Gamma/d\eta)\, d\eta}{\bar{y} - \bar{\eta}} \tag{59}$$

where $\bar{y}$ and $\bar{\eta}$ are explicit functions of y and η, respectively. The velocities of the flow around the cylinder alone may also be given in terms of the transformation. In fact, the upwash function, $f(y)$, is given by

$$f(y) = \text{R.P. } (d\bar{l}/dl) - 1 \tag{60}$$

Thus,

$$\text{R.P. } (d\bar{l}/dt) = 1 + f(y) \tag{61}$$

and

$$w_1(\infty, y) = \frac{[1 + f(y)]}{2\pi} \int_{-b}^{b} \frac{(d\Gamma/d\eta)\, d\eta}{\bar{y} - \bar{\eta}} \tag{62}$$

Comparing this result with Eq. (53), it is clear that the body effect on the downwash is given by

$$\begin{aligned} w_{1B}(\infty, y) &= \int\int_{Rw} d\xi\, d\eta u_1(\xi,\eta)\, K(\infty, y; \xi, \eta) \\ &= \frac{1}{2\pi} \int_{-b}^{b} \frac{d\Gamma}{d\eta} \left\{ \frac{[1 + f(y)]}{\bar{y} - \bar{\eta}} - \frac{1}{y - \eta} \right\} d\eta \end{aligned} \tag{63}$$

For lifting elements located at substantially a single chordwise location, say $x = 0$, the downwash at that location is one-half the value in the Trefftz plane, so that

$$w_1(0,y) = \frac{1}{4\pi} [1 + f(y)] \int_{-b}^{b} \frac{(d\Gamma/d\eta)\, d\eta}{\bar{y} - \bar{\eta}} \tag{64}$$

where, as before, it is understood that the region of the body is excluded from the range of integration. Also,

$$\begin{aligned} w_{1B}(0,y) &= \frac{1}{4\pi} \int_{-b}^{b} \frac{d\Gamma}{d\eta} \left\{ \frac{[1 + f(y)]}{\bar{y} - \bar{\eta}} - \frac{1}{y - \eta} \right\} d\eta \\ &= \int\int_{Rw} d\xi,\ d\eta u_1(\xi,\eta) K(0, y; 0, \eta) \end{aligned} \tag{65}$$

It is convenient at this point to proceed to the discussion of special cases for which the complete formulation and solution of the wing-body problem is possible.

Slender Body Theory

The slender-configuration theories of Munk[38] and Jones[9] as extended to slender wing-body combinations by Spreiter[7] and Ward[8] offer a particularly simple case with which to begin. In these theories, the assumption is implicitly made† that as far as the calculation of induced downwash is concerned, each point on the wing is in the Trefftz plane of all upstream points, and infinitely far ahead of all downstream points. Mathematically, this results from the approximation in Eq. (48)

$$\frac{\sqrt{(x - \xi)^2 + (y - \eta)^2}}{x - \xi} \cong \frac{|x - \xi|}{x - \xi} \tag{66}$$

which would be expected to be valid if $|y - \eta|$ is always small compared to $|x - \xi|$, i.e., for slender configurations. In this case, it is convenient to define

$$\psi(x,y) = \int_{x_0(y)}^{x} u_1(\xi,y)\, d\xi \tag{67}$$

This is $1/\rho U_0$ times the lift on a strip from the leading edge up to the point x. The downwash is given by

$$w_1(x,y) = \frac{[1 + f(y)]}{2\pi} \int_{-b}^{b} \frac{(\partial\psi/\partial\eta)}{\bar{y} - \bar{\eta}}\, d\eta \tag{68}$$

which may also be written as

$$w_1(x,y) = \frac{1}{2\pi} \frac{\partial}{\partial y} \int_{-\bar{b}}^{\bar{b}} \frac{\bar{\psi}}{\bar{y} - \bar{\eta}}\, d\bar{\eta} \tag{69}$$

This must satisfy the boundary condition, Eq. (42), so that

$$U_0\alpha(x,y) + U_0\alpha_B f(y) = \frac{[1 + f(y)]}{2\pi} \int_{-b}^{b} \frac{(\partial\psi/\partial\eta)}{\bar{y} - \bar{\eta}}\, d\eta \tag{70}$$

or

$$U_0 \left[\frac{\alpha(x,y) + \alpha_B f(y)}{1 + f(y)} \right] = \frac{1}{2\pi} \int_{-b}^{b} \frac{(\partial\psi/\partial\eta)}{\bar{y} - \bar{\eta}}\, d\bar{\eta} \tag{71}$$

The most convenient way to solve this integral equation is to convert it entirely to the transformed coordinates, $\bar{y}$ and $\bar{\eta}$. This gives

$$U_0 \left\{ \frac{\alpha[x_1, y(\bar{y})] + \alpha_B f[y(\bar{y})]}{1 + f[y(\bar{y})]} \right\} = \frac{1}{2\pi} \int_{-\bar{b}}^{\bar{b}} \frac{(\partial\bar{\psi}/\partial\bar{\eta})\, d\bar{\eta}}{\bar{y} - \bar{\eta}} \tag{72}$$

† The explicit formulation usually given is quite different from this one, but is equivalent.

This equation may then be inverted directly by well-known methods to give as the solution

$$\frac{\partial \bar{\psi}}{\partial \bar{y}} = \frac{-2U_0}{\pi\sqrt{\bar{b}^2 - \bar{y}^2}} \int_{-\bar{b}}^{\bar{b}} \frac{\{\alpha[x,\eta(\bar{\eta})]\}}{1 + f[\eta(\bar{\eta})]} \frac{\sqrt{\bar{b}^2 - \bar{\eta}^2}}{\bar{y} - \bar{\eta}}\, d\bar{\eta} \quad (73)$$

A simple and important case occurs when $\alpha(x,y)$ is constant as for an uncambered untwisted wing, and when the wing and body are at the same angle of attack, α_0, so that

$$\alpha(x,y) = \alpha_B = \alpha_0 \quad (74)$$

Eq. (72) then becomes

$$U_0\alpha_0 = \frac{1}{2\pi}\int_{-\bar{b}}^{\bar{b}} \frac{(\partial\bar{\psi}/\partial\bar{\eta})\, d\bar{\eta}}{\bar{y} - \bar{\eta}} \quad (75)$$

This corresponds to the case of a slender wing alone of span $2\bar{b}$ at angle of attack α_0. The solution for this case is well known and is

$$\bar{\psi}(x,y) = 2U_0\alpha_0\sqrt{\bar{b}^2 - \bar{y}^2} \quad (76)$$

It should be noted that $\bar{b}$ and $\bar{y}$ are functions of x. The total lift in this case is given by

$$\bar{L} = \pi\rho U_0^2\alpha_0\bar{b}_{\max.}^2 \quad (77)$$

or

$$\frac{\bar{L}}{q} = 2\pi\alpha_0\bar{b}_{\max.}^2 \quad (78)$$

where $\bar{b}_{\max.}$ is the value of $\bar{b}$ at the widest cross section of the wing. It will next be shown that $\bar{L}$ is in fact the total lift on the wing-body combination in the physical plane.

According to the Trefftz plane relation, Eq. (21), the lift on the wing-body combinations in terms of the lift on the wings is given by

$$L = \rho U_0 \int_{-b}^{b} \Gamma(y)\, [1 + f(y)]\, dy \quad (79)$$

where the body is excluded from the range of integration. The lift on the wings in the transformed plane is given by

$$\bar{L} = \rho U_0 \int_{-\bar{b}}^{\bar{b}} \bar{\Gamma}(\bar{y})\, d\bar{y} \quad (80)$$

Now, from the transformation equation and Eq. (61)

$$d\bar{y}/dy = \text{R.P.}\ (d\bar{t}/dt) = 1 + f(y) \quad (81)$$

and in accordance with Eq. (57),

$$\Gamma(\bar{y}) = \Gamma[\bar{y}(y)] \quad (82)$$

so that $\bar{L} = L$. Thus, the following rule may be stated: If in conformal transformation which collapses the body of a slender wing-body combination onto a vertical slit in the plane of symmetry, the transformed wing span is $2\bar{b}$, the lift of the wing-body combination is equal to the lift of an isolated slender wing of span $2\bar{b}$.

Applying this to the simplest case of a wing of span $2b$ mounted on the centerline of a circular cylinder, the conformal mapping function is

$$\bar{t} = t - (R^2/t) \quad (83)$$

and

$$\text{R.P.}(d\bar{t}/dt) = 1 + (R^2/y^2) \qquad \text{when } z = 0 \quad (84)$$

Also,

$$\bar{y} = y - (R^2/y)$$

and

$$\bar{b} = b - (R^2/b)$$

Substituting this into Eq. (78) gives, for the lift of the wing-body combination,

$$L = \pi\rho U_0^2\alpha_0[b - (R^2/y)]^2 \quad (85)$$

which is in agreement with the results of Spreiter. Substituting for $\bar{b}$ and $\bar{y}$ in Eq. (76) leads to

$$\psi(x,y) = 2U_0\alpha\sqrt{[b - (R^2/b)]^2 - [y - (R^2/y)]^2} \quad (86)$$

which is equivalent to the results of Spreiter and Lennertz for the spanwise lift distribution. It should be noted that this expression is identical to

$$\psi(x,y) = 2U_0\alpha\sqrt{[b + (R^2/b)]^2 - [y + (R^2/b)]^2} \quad (87)$$

which is more commonly given.

If the wing is not centrally mounted, but is located a distance h below or above the midplane of the body, the coordinate of the tip is

$$t = b + ih$$

and

$$\bar{b} = b - (R^2b)/(b^2 + h^2)$$

From Eq. (78), the lift of the configuration is then

$$L/q = 2\pi\alpha_0 b^2\{1 - [R^2/(b^2 + h^2)]\}^2 \quad (88)$$

Still another interesting case in slender-body theory may easily be solved, namely that of a wing centrally mounted on a body which is an elliptic cylinder. It is convenient here to use the complex variable $u = z + iy$ rather than $t = y + iz$. For this case, the transformation, which maps the body on to a vertical slit, is

$$\bar{u} = [1/(A - B)]\,[Au - B\sqrt{u^2 - A^2 + B^2}] \quad (89)$$

where B is the axis of the ellipse in the y direction and A is the axis of the ellipse in the z direction. The transformed semispan of the wing is obtained by substituting $u = ib$ into this expression as

$$\bar{b} = [1/(A - B)]\,[Ab - B\sqrt{A^2 - B^2 + b^2}] \quad (90)$$

According to Eq. (78), the lift of the wing-body combination is

$$L/q = 2\pi\alpha_0[(Ab - B\sqrt{A^2 - B^2 + b^2})/(A - B)]^2 \quad (91)$$

This result is in agreement with those of Nonweiler[10] who used Spreiter's[7] approach and Kahane[11] who used methods similar to Ward's.[8]

The virtue of the rule given here is that the total lift on any wing-body combination for which the necessary conformal transformation can be found may be calculated without detailed calculation of the pressure distribution.

The relationship between the solutions obtained from slender wing-body theory and those obtained from the classical theory of wings of minimum induced drag also merits some attention. It has often been observed that the results are intimately related. For example, the Jones theory for a slender wing at constant angle of attack gives an elliptic distribution of lift which is the distribution for minimum induced drag; the Spreiter theory for a slender wing centrally mounted on a circular body gives a distribution of lift identical to the Lennertz solution for minimum induced drag for that case. The relationship between the two theories is easily seen by setting up the slender-body theory in variational form as in Eq. (32). The variational equation is, for the wing at constant angle of attack,

$$\delta\left\{\int_{-b}^{b}\Gamma(y)w(y)\,dy - 2\int_{-b}^{b}\Gamma(y)\,U_0\alpha_0 \times [1 + f(y)]\,dy\right\} = 0 \quad (92)$$

where $w(y)$ is given by Eq. (56) and integration is over the wings only. Carrying out the variational process leads back to the integral Eq. (75). The minimum induced drag problem as set up by Lennertz and, in more general form, by Pepper,[2] requires that the induced drag be made a minimum subject to the constraining condition of constant lift. Since an infinite body at zero angle of attack can contribute no drag, the induced drag arises from the wings only and is given by

$$D = \frac{\rho U_0}{2U_0}\int_{-b}^{b}\Gamma(y)\,w(y)\,dy \quad (93)$$

The lift of the wing-body combination is from Eq. (21)

$$L = \rho U_0\int_{-b}^{b}\Gamma(y)\,[1 + f(y)]\,dy \quad (94)$$

where, as before, the integration is over the wings only The variational problem of finding the minimum induced drag reduces to

$$\delta\left\{\frac{1}{2U_0}\int_{-b}^{b}\Gamma(y)\,w(y)\,dy + \lambda\int\Gamma(y) \times [1 + f(y)]\,dy\right\} = 0 \quad (95)$$

where λ is an undetermined Lagrange multiplier which must be introduced to stipulate the condition of constancy of lift. The variational equations of the two problems are thus identical, except for the constant multipliers of the second integrals in Eqs. (92) and (95). It follows then from the form of these equations that the lift and downwash distributions can differ at most by an arbitrary multiplicative constant. This arbitrariness stems from the fact that the solution of the minimum-induced-drag problem cannot be expected to give a value for the lift in terms of boundary conditions on the wing, but only a relation between lift and drag for the particular distribution which gives minimum drag. It is now possible to state the following rule: For any slender wing-body combination having a cylindrical body with constant angle of attack of the wings and with an equal angle of attack of the body, the distribution of lift over the wings is identically the one giving minimum induced drag for a wing mounted on an infinite cylindrical body of the same shape.

Examining the results in additional detail, it may be seen from Eq. (95) that the Trefftz-plane downwash distribution for minimum induced drag is always

$$w(y) = w_0[1 + f(y)] \quad (96)$$

where w_0 is an arbitrary constant. In order to satisfy the boundary condition in the slender wing-body theory, w_0 must equal $U_0\alpha_0$ (see Eq. (56)). The lift in the minimum-induced-drag problem can be determined in terms of w_0 from momentum considerations (see reference 39), as

$$L = \rho U_0 w_0 \Sigma \quad (97)$$

where Σ is determined from a momentum integral in the Trefftz plane. Thus, the results of the theory of wings of minimum induced drag may be applied with ease, since Σ is the quantity which must be determined to obtain the induced drag in terms of the lift. For instance, in the case of a wing centrally mounted on a circular body, which was considered previously, the theory of minimum induced drag gives[39]

$$\Sigma = \pi[b - (R^2/b)]^2 \quad (98)$$

From this

$$L = \pi\rho U_0^2\alpha_0[b - (R^2/b)]^2 \quad (99)$$

which is in agreement with Eq. (85).

As a further application of the relation between the solution for minimum induced drag and the slender-body solution, consider again the case of a wing mounted on a circular body a distance d below the central plane of the body. As pointed out previously, the solutions obtained in this paper for such cases are approximate because the transformed wing has some dihedral and the mean sidewash at any point is not zero. Pepper has given the exact solution for the minimum induced drag problem in this case. Some of his results for Σ are shown in Fig. 3, and compared with Σ from Eq. (88). It may be seen that the error is small.

A somewhat more complicated problem of some interest may be solved in this same way, namely, the case of a wing-body combination with a gap of span s on

each side between the wing and the body. Consider first the case of a wing alone with gap (the total gap in this case is $2s$), a case which has been treated by Bleviss and Struble.[40] The value of Σ for this case is[39]

$$\Sigma = \pi\left[b^2\left(\frac{K' - 2E'}{K'}\right) + s^2\right] \qquad (100)$$

where K' and E' are elliptic functions of the first and second kind, respectively, of argument $k' = \sqrt{1-(s/b)^2}$. The lift of the slender wing with gap is then

$$L = \pi\rho U_0^2\alpha_0\left[b^2\left(\frac{K' - 2E'}{K'}\right) + s^2\right] \qquad (101)$$

The case of a gap on a slender wing centrally mounted on an infinite circular cylinder may readily be obtained by making use of the earlier result that the lift of the wing-body combination is the same as the lift on the wing alone which is obtained by conformally transforming the body to a slit on the vertical axis. The transformation is again

$$\bar{l} = l - (R^2/l)$$

Thus,

$$\bar{b} = b - (R^2/b)$$

$$\bar{s} = s - (R^2/s)$$

Substituting $\bar{b}$ and $\bar{s}$ for b and s in Eq. (10) gives for the lift on the wing-body combination with gap

$$L = \pi\rho U_0^2\alpha_0\left\{\left(b - \frac{R^2}{b}\right)^2\frac{\bar{K}' - \bar{E}'}{\bar{K}'} + \left(s - \frac{R^2}{s}\right)^2\right\} \qquad (102)$$

where the argument of $\bar{K}'$ and $\bar{E}'$ is $\bar{k} = \sqrt{1-(\bar{s}/\bar{b})^2}$. This result was first obtained by Harold Mirels of Cornell University in a paper as yet unpublished, using methods analogous to Ward's.[8]

The reverse-flow theorem leads to particularly simple results for slender configurations; in fact, no flow reversal at all is required. Results identical to those of the reverse-flow theorem for this case can be obtained directly by considering two distributions $\psi_1(x,y)$ and $\psi_2(x,y)$ corresponding to the angle distributions $\alpha_1(x,y)$ and $\alpha_2(x,y)$, respectively. Then by Eqs. (70) and (69), the integral equations for ψ† in the two cases are

$$U_0\alpha_1(x,y) + U_0\alpha_{B_1}(x,y)\,f(y) = \frac{1}{2\pi}\frac{\partial}{\partial y}\int_{-b}^{b}\frac{\bar{\psi}_1}{\bar{y}-\bar{\eta}}\,d\bar{\eta} \qquad (103)$$

and

† Barred quantities in these equations correspond to conformally transformed values.

COMPARISON OF APPROXIMATE AND EXACT THEORETICAL LIFTS FOR SLENDER WING-BODY COMBINATION UNSYMMETRICAL ABOUT HORIZONTAL PLANE

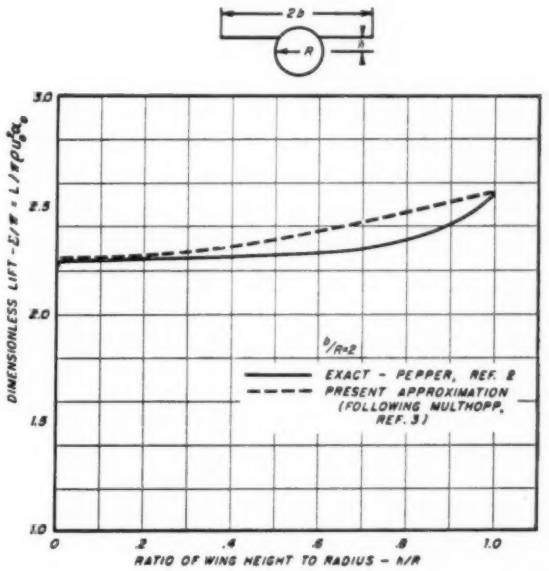

Fig. 3

$$U_0\alpha_2(x,y) + U_0\alpha_{B_2}(x,y)f(y) = \frac{1}{2\pi}\frac{\partial}{\partial y}\int_{-b}^{b}\frac{\bar{\psi}_2}{\bar{y}-\bar{\eta}}\,d\bar{\eta} \qquad (104)$$

Multiplying the first equation by ψ_2 and the second by ψ_1 and integrating over the span gives

$$U_0\int_{-b}^{b}\psi_2\,[\alpha_1 + \alpha_{B_1}f(y)]\,dy = \frac{1}{2\pi}\int_{-b}^{b}\psi_2(y)\frac{\partial}{\partial y}\int_{-b}^{b}\frac{\bar{\psi}_1(\eta)}{\bar{y}-\bar{\eta}}\,d\bar{\eta}\,dy \qquad (105)$$

and

$$U_0\int_{-b}^{b}\psi_1\,[\alpha_2 + \alpha_{B_2}f(y)]\,dy = \frac{1}{2\pi}\int_{-b}^{b}\psi_1(y)\frac{\partial}{\partial y}\int_{-b}^{b}\frac{\bar{\psi}_2(\eta)}{\bar{y}-\bar{\eta}}\,d\bar{\eta}\,dy \qquad (106)$$

where, as usual, the body is omitted from the range of integration. The terms on the left-hand side may easily be shown to be equal by integrating parts, exchanging the order of integration, and taking account of Eqs. (68) and (69). Thus,

$$\int_{-b}^{b}\psi_2\,[\alpha_1 + \alpha_{B1}f(y)]\,dy = \int_{-b}^{b}\psi_1 \times [\alpha_2 + \alpha_{B2}f(y)]\,dy \qquad (107)$$

This is valid for any two angle-of-attack distributions

$\alpha_1(x,y)$ and $\alpha_2(x,y)$. A particular case which will be required in later developments in the case $\alpha_2 = \alpha_{B_2} = 1$, so that ψ_2 is the circulation distribution for unit angle of attack of wing and body given by Eq. (87). Then

$$\int_{-b}^{b} 2U_0 \sqrt{b^2 - \bar{y}^2}\ [\alpha_1 + \alpha_{B_1} f(y)]\, dy = \int_{-b}^{b} \psi_1 [1 + f(y)]\, dy \quad (108)$$

The integral on the right-hand side is the total $1/\rho U_0$ times the lift forward of the location under consideration, $L(x)$, by Eq. (79). Thus

$$L(x) = 2\rho U_0^2 \int_{-b}^{b} \sqrt{b^2 - \bar{y}^2}\ [\alpha_1 + \alpha_{B_1} f(y)]\, dy \quad (109)$$

This expression for the special case of slender wings centrally mounted on a circular body with zero body angle of attack has been given by Morikawa and Puckett.[41]

Low-Aspect-Ratio Wing-Body Combinations

Slender-wing theory, although attractive in its simplicity, proves to be accurate only for wings of very small aspect ratio; for instance, the error in slope of the lift curve of a triangular wing is already of the order of 10 per cent at an aspect ratio of unity. The error in the predicted pitching moment of rectangular wings is even more serious. In reference 13, an approximate theory was developed which gave satisfactory accuracy for many purposes up to an aspect ratio of four. The theory has been extended to wing-body combinations in reference 12. The essential approximation in this analysis is the approximation in Eq. (48).

$$\frac{\sqrt{(x-\xi)^2 + (y-\eta)^2}}{x - \xi} \cong \frac{1}{2}\left\{\frac{|x-\xi| + \sqrt{(x-\xi)^2 + \beta^2}}{x - \xi}\right\} \quad (110)$$

where β is an average local spanwise distance which is a function of x only. This represents a somewhat more accurate approximation than Eq. (66), which is the approximation used in the Jones theory. The approximation of Eq. (110) approaches the Jones theory approximation when $|x - \xi|$ is large compared to the span, β. A good value for $\beta(x)$ has been found to be the local exposed semispan of the wing. Thus, from Eq. (48), the downwash due to the direct effect of the wing lift is

$$w_{1_W}(x,y) = \frac{1}{4\pi}\frac{\partial}{\partial y}\int\int_{R_W} \frac{d\xi\, d\eta}{y - \eta}\, u_1(\xi,\eta) \times \left\{1 + \frac{1}{2}\frac{|x-\xi| + \sqrt{(x-\xi)^2 + \beta^2}}{x - \xi}\right\} \quad (111)$$

The term in braces is a function of x only so that w_1 may be written as

$$w_{1_W}(x,y) = \frac{1}{4\pi}\int_{x_0}^{x_1} d\xi \left\{1 + \frac{|x-\xi| + \sqrt{(x-\xi)^2 + \beta^2}}{2(x-\xi)}\right\} \times \frac{\partial}{\partial y}\int_{-b(\xi)}^{b(\xi)} \frac{u_1(\xi,\eta)}{y - \eta}\, d\eta \quad (112)$$

The term in braces describes the variation of downwash with distance downstream of the location of a lifting element. If it is assumed that the body contributions to the downwash behave in the same way as the direct contributions of the wing lifting elements as far as this variation is concerned, then from Eqs. (112) and (69)

$$\alpha(x,y) + \alpha_B f(y) = w_1(x,y) = \frac{1}{4\pi}\int_{x_0}^{x_1} d\xi \left\{1 + \frac{|x-\xi| + \sqrt{(x-\xi)^2 + \beta^2}}{2(x-\xi)}\right\} \times \frac{\partial}{\partial y}\int_{-\bar{b}(\xi)}^{\bar{b}(\xi)} \frac{u_1(\xi,\bar{\eta})}{\bar{y} - \bar{\eta}}\, d\bar{\eta} \quad (113)$$

To reduce this integral equation in two variables to an integral equation in the spanwise variable only, the method of spanwise integration with weighting factors[13, 37, 42] is employed. The pressure distribution for a constant angle-of-attack distribution on the wing in reverse flow, used as a weighting factor, has the property of providing a stationary (in the sense of the calculus of variations) integral for total lift, as indicated previously. In the present case, the approximate spanwise pressure distribution in reverse flow is taken to be the result obtained from slender-body theory, Eq. (76) for the wing and body at constant angle of attack.

$$p_0(x,y) = \text{const.}\sqrt{\bar{b}^2 - \bar{y}^2} \quad (114)$$

Multiplying Eq. (113) by this factor and integrating over wing span gives

$$\int_{-b}^{b} U_0\, [\alpha(x,y) + \alpha_B f(y)]\, \sqrt{\bar{b}^2 - \bar{y}^2}\, dy = \frac{1}{4\pi}\int_{-b}^{b} dy \int_{x_0}^{x_1} d\xi \left\{1 + \frac{|x-\xi| + \sqrt{(x-\xi)^2 + \beta^2}}{2(x-\xi)}\right\} \times \sqrt{\bar{b}^2 - \bar{y}^2}\, \frac{\partial}{\partial y}\int_{-\bar{b}}^{\bar{b}} \frac{d\bar{\eta}}{\bar{y} - \bar{\eta}}\, u_1(\xi,\bar{\eta}) \quad (115)$$

If the order of integration is changed, this becomes

$$\int_{-b}^{b} U_0\, [\alpha(x,y) + \alpha_B f(y)]\, \sqrt{\bar{b}^2 - \bar{y}^2}\, dy = \frac{1}{4\pi}\int_{x_0}^{x_1} d\xi \left\{1 + \frac{|x-\xi| + \sqrt{(x-\xi)^2 + \beta^2}}{2(x-\xi)}\right\} \times \int_{-b}^{b} dy\, \sqrt{\bar{b}^2 - \bar{y}^2}\, \frac{\partial}{\partial y}\int_{-\bar{b}}^{\bar{b}} \frac{d\bar{\eta}}{\bar{y} - \bar{\eta}}\, u_1(\xi,\bar{\eta}) \quad (116)$$

By virtue of the reciprocal relation Eq. (107), since $\sqrt{\bar{b}^2 - \bar{y}^2}$ is the distribution of p for unit angle of attack

of wing and body, the last double integral is reducible to a very simple form, namely,

$$\frac{1}{2\pi}\int_{-b}^{b} dy\,\sqrt{b^2-\bar{y}^2}\,\frac{\partial}{\partial y}\int_{-b}^{b}\frac{d\bar{\eta}}{\bar{y}-\bar{\eta}}\,u_1(\xi,\bar{\eta}) = \int_{-b}^{b} u_1(\xi,\eta)\,[1+f(\eta)]\,d\eta \quad (117)$$

It is apparent from Eq. (79) that the integral obtained on the right-hand side of the last equation is simply the circulation per unit chord on the wing-body combination. It is convenient to define this quantity as

$$g'(x) = \frac{\partial}{\partial x}\int_{-b}^{b}\psi(x,y)\,[1+f(y)]\,dy \quad (118)$$

where, as before,

$$\psi(x,y) = \int_{x_0}^{x} u_1(\xi,y)\,d\xi$$

Also, the term on the left-hand side of Eq. (116) may be defined as

$$k(x) = \int_{-b}^{b}[\alpha(x,y)+\alpha_B f(y)]\sqrt{b^2-\bar{y}^2}\,dy \quad (119)$$

This latter quantity, as has been shown in Eq. (108) is simply the circulation on the wing-body combination up to a distance x from the origin according to slender configuration theory. Eq. (116) then becomes

$$k(x) = \frac{1}{2}\int_{x_0}^{x}\left\{1+\frac{|x-\xi|}{2(x-\xi)}+\frac{\sqrt{(x-\xi)^2+\beta^2}}{2(x-\xi)}\right\}\times g'(\xi)\,d\xi \quad (120)$$

or

$$k(x) = \frac{1}{2}\,g(x)+\frac{1}{4}\int_{x_0}^{x_1}\left\{1+\frac{\sqrt{(x-\xi)^2+\beta^2}}{x-\xi}\right\}g'(\xi)\,d\xi \quad (121)$$

This one-dimensional integral equation is identical in form to the one derived for low-aspect-ratio wings alone in reference 13. The only differences are that $k(x)$ in this case is the Spreiter-Ward value for the wing-body combination, rather than the Jones value for a wing alone, and β is approximated as the exposed span of the wing rather than as the span of an isolated wing. Methods for solution of Eq. (121) for circulation per unit chord $g(x)$ by collocation have been given in reference 13.

Lifting-Line Theory for Wing-Body Combinations

The theory of wing-body interference for high-aspect-ratio wings mounted on infinite cylindrical bodies according to Prandtl lifting-line theory has been definitively presented by Multhopp.[3] It will be desirable here to briefly indicate how the lifting-line approximation may be arrived at from lifting-surface theory when a body is present. Reissner[42] has shown that for wings alone, the approximation

$$\sqrt{(x-\xi)^2+(y-\eta)^2} \approx |y-\eta| \quad (122)$$

in Eq. (48) for w_{iw} leads to the Prandtl result. With this approximation,

$$w_{iw} = \frac{1}{4\pi}\frac{\partial}{\partial y}\int\int_{Rw}\frac{d\xi\,d\eta}{y-\eta}\left\{1+\frac{|y-\eta|}{x-\xi}\right\}u_1(\xi,\eta) \quad (123)$$

If the wing is considered to be rectangular for simplicity, this may be written

$$w_{iw} = \frac{1}{4\pi}\int\int_{Rw}\frac{d\xi\,d\eta}{y-\eta}\frac{\partial u_1}{\partial\eta}\left\{1+\frac{|y-\eta|}{x-\xi}\right\} \quad (124)$$

or

$$w_{iw} = \frac{1}{4\pi}\int_{-b}^{b}\frac{\partial\Gamma/\partial\eta}{y-\eta}\,d\eta+\frac{1}{2\pi}\int_{c/2}^{c/2}\frac{u_1(\xi,y)}{x-\xi}d\xi \quad (125)$$

where c is the chord and

$$\Gamma(\eta) = \int_{c/2}^{c/2} u_1(\xi,\eta)\,d\xi \quad (126)$$

The first integral in Eq. (125) will be recognized as the downwash of a trailing vortex sheet, of strength $d\Gamma/d\eta$, at the front edge of the sheet, while the second is the downwash of a two-dimensional vortex sheet of strength $u_1(x,y)$ along the chord. The second term does not depend on lifting elements anywhere except at y. Thus, to the lifting-line approximation, the presence or absence of a body should make no difference in this second term on the wing. It may be observed that the first integral which gives the effect of the trailing vortex sheet is one-half the Trefftz-plane downwash due to lifting elements on the wing itself. The corresponding value for a wing plus infinite cylindrical body is given by Eq. (64). Substituting the latter expression for the downwash in place of the first integral in Eq. (125) and setting the downwash equal to the value required by the boundary condition, Eq. (42), gives the following integral equation

$$U_0[\alpha(x,y)+\alpha_B f(y)] = \frac{1}{4\pi}[1+f(y)]\times\int_{-b}^{b}\frac{(d\Gamma/d\eta)\,d\eta}{\bar{y}-\bar{\eta}}+\frac{1}{2\pi}\int_{-c/2}^{c/2}\frac{u_1(\xi,y)}{x-\xi}d\xi \quad (127)$$

Multiplying by the lift distribution in two-dimensional reversed flow as the weighting factor and integrating over the chord gives

$$\int_{-c/2}^{c/2}U_0\,[\alpha(x,y)+\alpha_B f(y)]\sqrt{\frac{(c/2)+x}{(c/2)-x}}\,dx = \frac{1}{4\pi}[1+f(y)]\,\frac{\pi c}{2}\int_{-b}^{b}\frac{(d\Gamma/d\eta)\,d\eta}{\bar{y}-\bar{\eta}}+\frac{\Gamma(y)}{2} \quad (128)$$

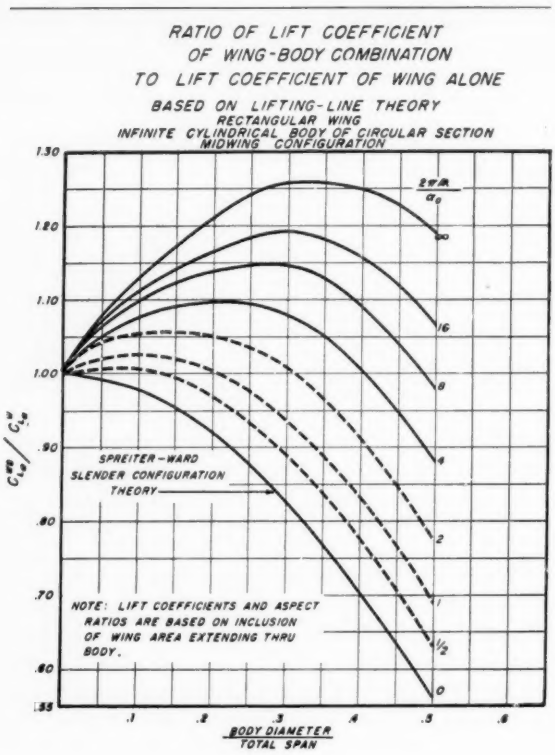

Fig. 4

If α is a function of y only, this becomes

$$U_0[\alpha(y) + \alpha_B f(y)] = \frac{1}{4\pi}[1 + f(y)] \times \int_{-b}^{b} \frac{(d\Gamma/d\eta)\, d\eta}{\bar{y} - \bar{\eta}} + \frac{\Gamma(y)}{\pi c} \quad (129)$$

This is the integral equation for a wing-body combination according to lifting-line theory. It may be solved by any method which can be employed for the lifting-line equation in the case of a wing alone. Multhopp[3] has given solutions for several particular cases.

In order for the lifting-line formulation of the wing-body problem to be valid, not only must the wing aspect ratio be large, but, also the ratio of body diameter to wing chord must be large. This is because there is a rapidly varying angle-of-attack distribution due to flow around the body in the vicinity of the body, and in such regions, lifting-line theory is not accurate. Multhopp points out that, actually, the induced downwash at the 3/4 chord position of the wing (the centroid of the chordwise distribution of lift in reversed flow, and therefore the centroid of the weighting function) will be greater than one-half the Trefftz-plane downwash. Thus, the predicted lifts near the body will be too high. Further, the flow field of a lifting line in the presence of the body is actually readily determinable only in the Trefftz plane, Eq. (62), and at the line, Eq. (64). At other longitudinal locations, it is very difficult to obtain.

A variational method which allows relatively rapid determination of the total lift of a wing-body combination according to lifting-line theory has been given in reference 4. The variational equation is

$$\delta\left[\int_{-b}^{b} \frac{2\Gamma^2}{a_0 c}\, dy - 2U_0 \int_{-b}^{b} [\Gamma\, \alpha(y) + \alpha_B f(y)]\, dy + \int_{-b}^{b} \Gamma w\, dy\right] = 0 \quad (130)$$

where, as usual, the region of the body is excluded from the range of integration and w is given by Eq. (64). Upon performing the variational operations, this gives

$$\frac{2\Gamma}{a_0 c} + w = \{\alpha(y) + \alpha_B f(y)\} U_0 \quad (131)$$

which is identical to Eq. (129) when a_0 is taken as 2π. The total lift obtained in this way, for constant α, must be a maximum as shown in reference 4. In other words, any approximate answer will be less than the exact theoretical lift. The variational equation has been solved by the Rayleigh-Ritz method using a two-term approximation for the lift, namely,

$$cc_l = 8\sqrt{\left(b - \frac{R^2}{b}\right)^2 - \left(y - \frac{R^2}{y}\right)^2} \times \left[(A_1 - A_3) + 4A_3 \frac{(y - (R^2/y))}{(b - (R^2/b))}\right] \quad (132)$$

where A_1 and A_3 are arbitrary constants to be determined from the variational equation. If A_3 is taken as zero in Eq. (132), it may be observed that the cc_l distribution reduces to that of Lennertz and Spreiter, Eq. (86). Calculations by this method have been made for a range of wings of various aspect ratio, taper ratio, and wing span to body diameter ratio in reference 4. Typical results are shown in Figs. 4 and 8.

By manipulations on the integral equation, Eq. (129), similar to those employed to obtain Eq. (107), the following result is obtained

$$\int_{-b}^{b} \Gamma_1[\alpha_2(y) + \alpha_{B_2} f(y)]\, dy = \int_{-b}^{b} \Gamma_2[\alpha_1(y) + \alpha_{B_1} f(y)]\, dy \quad (133)$$

where α_2 and α_{B_2} produce circulation Γ_2, and α_1 and α_{B_1} produce circulation Γ_1. This is again in accord with the reversed-flow theorem except that, for lifting-line theory, flow reversal is not necessary.

The variational principle is sometimes useful in another form, particularly if a rapid estimate of lift is required. In this case, use is made of the fact that the expression

$$\frac{1}{\int_{-b}^{b} \Gamma[\alpha(y) + \alpha_B f(y)]\, dy} =$$

$$\frac{1}{U_0} \frac{\int_{-b}^{b} \Gamma w\, dy + \int_{-b}^{b} \frac{2\Gamma^2}{a_0 c}\, dy}{\left\{\int_{-b}^{b} \Gamma[\alpha(y) + \alpha_B f(y)]\, dy\right\}^2} \quad (134)$$

is stationary and is a minimum. Thus, if an assumed Γ distribution such as Lennertz's and the corresponding w distribution are substituted on the right-hand side the term on the left-hand side will differ from the exact value by terms of higher order than the error in the assumed lift distribution. For $\alpha(y) = \alpha_B =$ unity, the term on the left-hand side is equal to the reciprocal of $1/(\rho U_0)$ times the total lift on the wing plus body.

Theories of the Weissinger Type

One of the shortcomings of lifting-line theory mentioned previously, namely, that the downwash at the 3/4 chord point is actually greater than one-half the Trefftz plane value assumed in lifting-line theory, may be overcome by the use of theories of the Weissinger type. The other shortcoming arising from the lack of a sufficiently tractable form for the correction to the downwash due to the presence of the body w_{1_B} except at the lifting element and in the Trefftz plane still remains, however, and will necessarily limit the accuracy of any theory.

The Weissinger theory can be constructed from the lifting-surface equation by making the approximation in Eq. (48)

$$\sqrt{(x - \xi)^2 + (y - \eta)^2} \approx \sqrt{(c^2/4) + (y - \eta)^2} \quad (135)$$

and then integrating the equation weighted by the function $\sqrt{(c/2 + x)/(c/2 - x)}$ over the chord. The procedure is similar to that used to obtain lifting-line theory, and will not be repeated here. For a rectangular wing alone, the result obtained is

$$U_0\alpha(y) = \frac{\Gamma(y)}{\pi c} + \frac{1}{4\pi}\int_{-b}^{b} \frac{(d\Gamma/d\eta)\, d\eta}{y - \eta} + \frac{1}{4\pi}\int_{-b}^{b} \frac{(d\Gamma/d\eta)\, d\eta}{y - \eta} \times \left\{\sqrt{1 + \frac{4(y - \eta)^2}{c^2}} - \frac{2\,|y - \eta|}{c}\right\} \quad (136)$$

This corresponds to the well-known equation of the Weissinger "L Method." It is equivalent to the satisfaction of the boundary condition at the 3/4 chord position with the lifting line at the 1/4 chord position. The first two terms on the right-hand side are identical to those appearing in the Prandtl lifting-line theory, while the third term represents an additional correction for finite aspect ratio.

The form of Eq. (136) as originally given by Weissinger is obtained by combining the terms on the right-hand side in a different way to give

$$U_0\alpha(y) = \frac{1}{2\pi}\int_{-b}^{b} \frac{(d\Gamma/d\eta)\, d\eta}{y - \eta} + \frac{1}{4\pi}\int_{-b}^{b} \times \frac{(d\Gamma/d\eta)\, d\eta}{y - \eta}\left\{\sqrt{1 + \frac{4(y - \eta)^2}{c^2 - 1}}\right\} \quad (137)$$

Here, the first term on the right-hand side is the downwash in the Trefftz plane and the second contains all corrections due to the finite length of the vortex sheet.

Returning now to consideration of wing-body combinations, it is clear that the main difficulties in the application of this type of theory arise in connection with the last term of Eq. (136). All the other terms have already been treated in the discussion of lifting-line theory. The case of a circular body may be handled approximately by making use of the well-known method of images. For centrally mounted wings, this is particularly simple. In the use of this method, the lifting line is considered to pass through the body, but boundary conditions are satisfied only on the exposed wing, since the images themselves effect the satisfaction of the boundary conditions on the body to some degree. In fact, the body boundary conditions are exactly satisfied at the chordwise location of the lifting line and in the Trefftz plane. The values of $d\Gamma/d\eta$ on the elements of lifting line inside the body are determined by the values on the appropriate point of the wing as

$$\Gamma'(R^2/y) = \Gamma'(y) \qquad y < R \quad (138)$$

With the image approximation, Eq. (136) may be written for a wing-body combination as

$$U_0[\alpha(y) + \alpha_B f(y)] = \frac{\Gamma(y)}{\pi c} + \frac{1}{4\pi}\int_{W,B}^{b} \frac{(d\Gamma/d\eta)\, d\eta}{y - \eta} + \frac{1}{4\pi}\int_{W,B}^{b} \frac{(d\Gamma/d\eta)}{y - \eta}\, d\eta \left\{\sqrt{1 + \frac{4(y - \eta)^2}{c^2}} - \frac{2}{c}|y - \eta|\right\} \quad (139)$$

where the subscript W,B on the integrals over the span indicates that the range of integration includes the surface of the wing passing through the body in contradistinction to what has been done in most other cases in this paper. Eq. (139) is valid over the wing only, since Γ' in the body region is specified by Eq. (138). For wings which are on circular bodies but which are not centrally mounted, the method of images may still be applied, but the equations become more complicated, due to the fact that the image vortices do not lie on the extension of the plane of the wing through the body (the image of a vortex must lie on the line connecting the vortex location with the center of the body). Incidentally, it should be noted that for circular bodies the method of images would give results in slender-body theory and in lifting-line theory com-

pletely equivalent to those given above based on conformal transformation.

In the case of a straight wing mounted on a body of noncircular section, the approximate procedures which may be adopted are not so intuitively obvious as in the case of a circular body, but there are at least two possibilities which can be explored. The first approach would be to adapt Eq. (136) so that it conforms to lifting-line theory at the limit of high aspect ratio and to slender-configuration theory at the limit of low aspect ratio. This can be done by writing Eq. (136) to include the effects of the body (by analogy with Eqs. (129) and (71)) as

$$U_0[\alpha(y) + \alpha_B f(y)] = \frac{\Gamma(y)}{\pi c} + \frac{[1 + f(y)]}{4\pi} \int_{-b}^{b} \times \frac{(d\Gamma/d\eta)\, d\eta}{\bar{y} - \bar{\eta}} + \frac{[1 + f(y)]}{4\pi} \int_{-b}^{b} \frac{(d\Gamma/d\eta)\, d\eta}{\bar{y} - \bar{\eta}} \times \left\{ \sqrt{1 + \frac{4(\bar{y} - \bar{\eta})}{c^2}} - \frac{2}{c} |\bar{y} - \bar{\eta}| \right\} \quad (140)$$

where the range of integration does not include the region of the body and the bars indicate the same transformed coordinates as in Eq. (129). The introduction of the transformed coordinates $\bar{y}$ and $\bar{\eta}$ into the last term of this equation, which represents three-dimensional flow effects, is arbitrary; it does, however, lead to the correct slender-configuration result in the limit as $c \to \infty$. It is also easily seen that as $c \to 0$, Eq. (140) approaches Eq. (129) for lifting-line theory. If the form of the integral equation given by Weissinger, Eq. (137), is used, a possible approximation is

$$U_0[\alpha(y) + \alpha_B f(y)] = \frac{[1 + f(y)]}{2\pi} \int_{-b}^{b} \frac{(d\Gamma/d\eta)\, d\eta}{\bar{y} - \bar{\eta}} + \frac{[1 + f(y)]}{4\pi} \int_{-b}^{b} \frac{(d\Gamma/d\eta)\, d\eta}{\bar{y} - \bar{\eta}} \left\{ \sqrt{1 + \frac{4(\bar{y} - \bar{\eta})}{c^2}} - 1 \right\} \quad (141)$$

where the range of integration excludes the region of the body and the bars again indicate transformed coordinates. This equation approaches the equation of slender-configuration theory as $c \to \infty$, but does not approach the lifting-line equation as $c \to 0$. It has the same interesting property as slender-body theory: for $\alpha = \alpha_B = \text{const.}$, the lift of the wing-body combination is the same as the lift (as given by the Weissinger theory) of a wing alone having the same chord, and the transformed span. Whether Eq. (140) or Eq. (141) gives more satisfactory results in the practical design range of wing parameters is not known and must await detailed comparison with experiment.

For swept wings, the direct application of the Weissinger procedure seems impossible, even where the image approximation is used, since the images of points near the tip may lie aft of the wing root trailing edge. For this case, Zlotnick and Robinson[6] have employed a system of horseshoe vortices and their images to represent the lifting elements of the wing-body combination; the boundary condition, Eq. (42), is then satisfied at the 3/4 chord position on the wing. They also arbitrarily multiplied the downwash due to the bound vortices by $(1 + R^2/y^2)$ in an attempt to account for the presence of the body. This, as they have pointed out, amounts to assuming that the effect of the body on the flow field produced by the bound vortices is the same as the effect of the body in modifying a uniform two-dimensional downflow from infinity. Zlotnick and Robinson[6] also make some reference to work in this field in a paper by Zlotnick and Diederich which is as yet not available to the general public.

For swept wings on bodies of noncircular cross section, it appears necessary at present to resort to quite crude approximation in calculating the spanwise load distribution. It is obviously possible to construct an analogue to the horseshoe-vortex and image method of Zlotnick and Robinson by distributing the lift on the noncircular body arising from a given wing horseshoe vortex, as given by Eq. (21) laterally over the body (this can be done so the total lift is distributed exactly if desired, on the basis of a Trefftz-plane solution as discussed previously). The body lift distribution could then be approximately represented by horseshoe vortices inside the body contour; the longitudinal location of the front edge of the horseshoe must, of course, always coincide with that of the wing horseshoe vortex which induces it. Since the labor involved in this procedure is considerable, it may in many cases be desirable to resort to even cruder approximations such as replacing the body by a plane wall at the side of the body, or replacing the body by the extension of the wing through the body set at zero angle of attack. In each of these two latter approaches, the Weissinger procedure in its original form could be used subject to the modified boundary condition on the wing

$$\alpha = \alpha(y) + \alpha_B f(y)$$

The relative merits of these various methods can only be evaluated by extensive correlation of theory and experiments which are not yet available. For many practical purposes, it may well prove that the simplest approximations are adequate.

The Moment Produced by the Body Lift in Subsonic Flow

The Trefftz-plane theorem for lift may easily be augmented by a similar result for pitching moment. For infinite bodies of circular cross section, this result has already been given by Lennertz[1] and in extended form by Zlotnick and Robinson.[6] Consider a lifting strip of width dx carrying a given spanwise distribution of lift $p(x,y)\, dx$. The potential due to this lifting strip will be $\varphi(x,y,z)$ and in the Trefftz plane it will be $\varphi_\infty(y,z)$. If the same lifting strip with the given spanwise distribution is placed in reversed flow, the potential, denoted by $\bar{\varphi}$, is

$$\tilde{\varphi} = -[\varphi(x,y,z) - \varphi_\infty(y,z)] \tag{142}$$

since the two flows are uniquely determined by the specified distribution of lift and differ only in the requirement that the potential vanish at $x = -\infty$ for the direct flow and at $x = +\infty$ for the reversed flow. The linearized pressure at a point on the body is given by

$$p = \rho U_0(\partial\varphi/\partial x)$$

in direct flow and by

$$\tilde{p} = -\rho U_0(\partial\tilde{\varphi}/\partial x)$$

in reversed flow. Thus, for any point on the body $p = \tilde{p}$, and it may be concluded that the pressure distribution on the body produced by the spanwise lifting strip is longitudinally symmetrical about the location of the strip. The element of body lift produced by the strip is, from the Trefftz-plane theorem, Eq. (21)

$$dL = \int \Delta p(x,y)\, f(y)\, dy$$

The moment of the body lift about $x = 0$ is then given by

$$M_B = \int\int_W xf(y)\Delta p(x,y)\, ds \tag{143}$$

where Δp is the pressure difference per unit area, and the integration is over the wing surface.

Distribution of Lift Along an Infinite Body

In order to apply the various theories discussed thus far to bodies which are finite in length and are noncylindrical, it is expedient to examine first the longitudinal distribution of the lift induced by a wing lifting element on an infinite body. This will be done on the assumption that the body alone is slender, as was done by Multhopp[3] in his treatment of this problem. For a cylindrical body, this assumption of slenderness really has nothing to do with the shape of the body, but is actually an assumption that the wing-induced upwash at the body varies slowly enough in stream direction so that slender-body theory may be employed. This assumption will actually be violated near the wing for lifting elements in close lateral proximity to the body, but great accuracy cannot be obtained in this region without considerable complication. Further, it will be seen that fair agreement with more accurate methods of analysis and with experiment can be obtained even in this region.

Consider a cylindrical body in the presence of two symmetrically disposed lifting elements carrying lifts of amount $\rho U_0\Gamma\Delta y$ at a lateral distance $|y|$ from the axis of the body. For convenience, they will also be assumed to lie in the x,y plane through the body axis parallel to the direction of flow. The upwash induced along the axis of the body may be obtained from the expressions given by von Kármán and Burgers[39] for the induced-flow field of an airfoil of infinitesimal span as

$$w = \frac{\Gamma\Delta y}{4\pi}\left[+\frac{(x^2+y^2)(r-x)+z^2r}{r^3(r-x)^2}\right] \tag{144}$$

Similarly, the longitudinal velocity is

$$u = (\Gamma\Delta y/4\pi)\,(z/r^3) \tag{145}$$

where the origin of coordinates is at the lifting element and

$$r = \sqrt{x^2+y^2+z^2} \tag{146}$$

Taking account of the fact that there are two such lifting elements, the induced upwash at the axis of the body ($z = 0$) is given by

$$w = \frac{\Gamma\Delta y}{2\pi y^2}\left[1 + \frac{x}{\sqrt{x^2+y^2}}\right] \tag{147}$$

The total lift on a circular body due to the upwash according to slender-body theory is given by

$$L_{B_1} = \int_{-\infty}^{\infty}\frac{d}{dx}(\pi\rho R^2U_0w)\, dx \tag{148}$$

Thus,

$$L_{B_1} = \pi\rho R^2U_0\, w_\infty \tag{149}$$

since

$$w_{-\infty} = 0$$

Finally,

$$L_{B_1} = (\rho U_0\Gamma\Delta y)\frac{R^2}{y^2} \tag{150}$$

Since there are two lifting elements carrying lift ($\rho U_0\Gamma\Delta y$), this is just one-half the amount of lift which is induced on the body according to Eq. (22). The other half must arise from the pressure field of the wing lifting elements acting on the body surface. This lift is given by

$$L_{B_2} = \int_{-\infty}^{\infty}\oint \rho U_0 u\cos(n,z)\, ds\, dx \tag{151}$$

where $\cos(n,z)$ is the z direction cosine of the outward normal to the body surface and ds is the element of body circumference. The value of u is positive above the plane $z = 0$ and negative below. If the first term of a Taylor's series expansion in z is used to represent u, u is given by

$$u = \frac{\Gamma\Delta y}{2\pi}\frac{z}{(\sqrt{x^2+y^2})^3} \tag{152}$$

where account has been taken of both lifting elements. The expression for L_{B_2} then becomes with $z = R\cos\theta$

$$L_{B_2} = \int_{-\infty}^{\infty}\frac{\Gamma R^2\Delta y}{2\pi}\frac{\rho U_0}{(\sqrt{x^2+y^2})^3}\int_0^{2\pi}\cos^2\theta\, d\theta\, dx$$

or

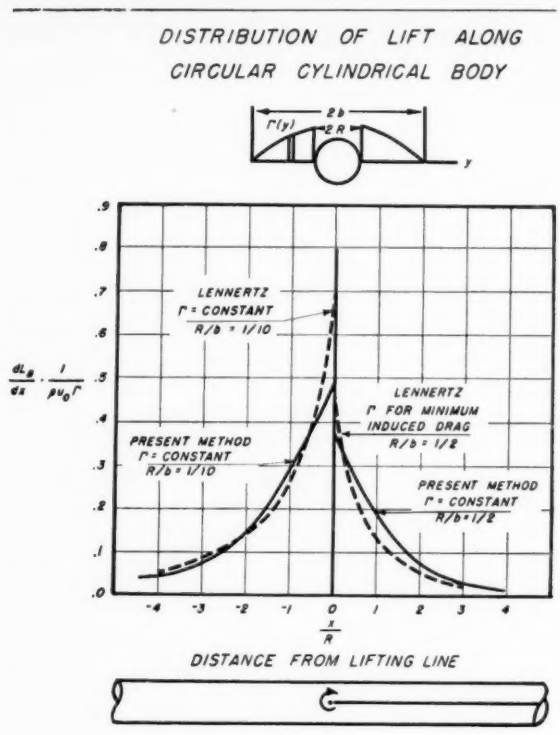

Fig. 5

$$L_{B_2} = \int_{-\infty}^{\infty} \left(\frac{\Gamma R^2}{2}\,\Delta y\right) \rho U_0 \frac{dx}{\left(\sqrt{x^2+y^2}\right)^3}$$

$$= \rho U_0 \frac{\Gamma R^2 \Delta y}{2y^2} \frac{x}{\sqrt{x^2+y^2}}\Bigg|_{-\infty}^{\infty}$$

$$= (\rho U_0 \Gamma \Delta y)\,(R^2/y^2) \tag{153}$$

This then accounts exactly for the other half of the lift on the body. Its distribution along the body is given, to the slender-body approximation, by

$$\frac{dL_{B_2}}{dx} = \rho U_0 \frac{\Gamma R^2 \Delta y}{2} \frac{1}{\left(\sqrt{x^2+y^2}\right)^3} \tag{154}$$

It is now necessary to go back and find the longitudinal distribution of L_{B_1}, the lift induced by the upwash. This is given by

$$dL_{B_1}/dx = \pi \rho R^2 U_0\,(dw/dx) \tag{155}$$

dw/dx is obtained by differentiating Eq. (147), which gives

$$\frac{dw}{dx} = \frac{\Gamma \Delta y}{2\pi} \frac{1}{\left(\sqrt{x^2+y^2}\right)^3}$$

Thus,

$$\frac{dL_{B_1}}{dx} = \frac{\rho U_0 \Gamma \Delta y R^2}{2} \frac{1}{\left(\sqrt{x^2+y^2}\right)^3} \tag{156}$$

This is identical to the expression obtained for dL_{B_2}/dx, so that it may be concluded that not only are the total amounts of both components of lift equal, but that they are identically distributed longitudinally.

The significant thing about the longitudinal distribution of body lift is that it diminishes very rapidly with increasing distance from the lifting element which produces it. As may be seen from Eqs. (154) and (156) for large x it decreases as $1/x^3$.

Lennertz[1] has made calculations for the distribution of lift on a cylindrical body in the presence of a wing without restriction to slender-body theory. Lennertz's results are shown in Fig. 5 for the body lift induced by a uniformly loaded lifting line with $R/b = 0.1$ and by a lifting line carrying the lift distribution for minimum induced drag with $R/b = 1/2$. For comparison, the induced body lift for constant wing circulation according to Eqs. (154) and (156) is shown for $R/b = 1/2$ and 0.1. It is emphasized here that any errors in the present method are only in the longitudinal distribution; the total body lift is exact. The body lift is, according to Eqs. (154) and (156), for constant Γ,

$$\frac{dL_B}{dx} = \rho U_0 \Gamma R^2 \int_R^b \frac{dy}{\left(\sqrt{x^2+y^2}\right)^3}$$

$$\frac{dL_B}{dx} = \frac{\rho U_0 \Gamma}{x^2/R^3}\left[\frac{b}{\sqrt{x^2+b^2}} - \frac{R}{\sqrt{x^2+R^2}}\right] \tag{157}$$

This form is indeterminate at $x = 0$, but it is not difficult to show that the value of dL_B/dx there is

$$(dL_B/dx)_{x=0} = (\rho U_0 \Gamma/2)\,[1 - (R^2/b^2)]$$

Considering the elementary nature of the methods employed here, the agreement between Lennertz's values and those from Eq. (157) is surprisingly good.

Distribution of Lift Along a Finite Body

Applying the slender-body theory to determine the lift distribution on a body of revolution of finite length and varying radius gives

$$dL_B/dx = \oint \rho U_0 u R \cos\theta\, d\theta + [(d/dx)\,(\pi \rho R^2 U_0 w)] \tag{158}$$

If u is represented by $(\partial u/\partial z)_0 z$, as before, this becomes

$$dL_B/dx = \oint \rho U_0 (\partial U/\partial z)_0 R^2 \cos^2\theta\, d\theta + (d/dx)\,(\pi \rho R^2 U_0 w) \tag{159}$$

It may be noted here that because of the irrotationality conditions $\partial u/\partial z = \partial w/\partial x$. Thus,

$$dL_B/dx = \pi \rho R^2 U_0 (\partial w/\partial x) + (d/dx)\,(\pi \rho R^2 U_0 w)$$

The expressions for w and $\partial w/\partial x$ on the axis of the body due to any distribution of lift over the wing span may be obtained from Eq. (147).

Comprehensive experimental data on the distribution of lift over prolate spheroidal bodies in combination with rectangular wings obtained by Möller have been presented by Schlichting[43] in his comprehensive mono-

graph on wing-body interference. These data have been compared by Schlichting with the results of an analysis by Multhopp's method.[3] Multhopp's method, which is mainly intended to serve as a means of predicting the moment about the wing 1/4 chord point due to wing-body interference, is based on a number of approximations to the flow field around the body. First, it is assumed, as has been done here, that the load distribution on the body may be calculated from the slender-body theory of Munk.[38] Second, it is assumed (although not stated in this way) that the total lift which would be produced on an infinite cylindrical body by the wing lifting line acts on the noninfinite body as well; for an infinite body this lift has no moment about the 1/4 chord point and it is assumed that this is the case for a finite body as well. An attempt is therefore made to exclude this part of the body force distribution from the moment calculations. This is done in two ways: first, the forces on the body produced by the direct action of the pressures induced by the wing (dL_{B_2}/dx) are ignored, and second, the induced flow transverse to the body axis is approximated by a flow field which omits any contribution from (dL_{B_1}/dx) in the immediate vicinity of the wing itself. This flow field is obtained by calculating the actual upwash on the axis of the body ahead of the wing from the wing span loading, assuming the flow is parallel to the wing along the wing chord (zero upwash if the wing chord is parallel to the body axis), and assuming that behind the wing the upwash changes linearly from a value of zero at the trailing edge to a value of $\alpha[1 - (d\epsilon/d\alpha)]$ at the tail, where ϵ is the downwash angle at the tail calculated from the wing loading. The load distribution along the body resulting from this special induced flow field is then calculated from Munk's slender-body theory.[38]

A comparison of the load distribution along the body computed according to the present method with experiment and with the load distribution according to Multhopp's method as given by Schlichting[43] is shown in Fig. 6 for a mid-wing configuration having a rectangular wing of aspect ratio 5. In calculating the theoretical upwash for this case, the wing-lift distribution was approximated by one of constant average circulation. The same is usually done in the application of Multhopp's method. The slender-body theory calculations by the present method were also corrected at the ends of the body by substituting $\sin \tau \cos \tau$ for dR/dx, where τ is the angle whose tangent is dR/dx. This correction accounts for the inclination of forces due to normal pressures at the ends; it conforms to the exact solution for an ellipsoid at constant angle of attack. Also, the forces on the afterbody were computed with due allowance for the closing of the vortex sheet around the body according to the method of Adams and Sears[16] which is discussed in the following section.

It may be seen from Fig. 6 that the results obtained from the present theory are in fairly good agreement with experiment. In fairness to Multhopp's method, it must be stated that it serves very well the purpose for which it was intended, namely, the prediction of the shift in neutral point of a wing-body combination caused by interference. Schlichting[43] shows that theoretical predictions of the neutral point shift by Multhopp's theory are in excellent agreement with experiment for a wide range of wing and body parameters. It is felt, however, that the present method is worthy of consideration because it possesses logical consistency which is lacking in Multhopp's method and gives a better approximation to the actual load distribution along the body, while at the same time it requires but little more labor than Multhopp's method. Moreover, the present method can be directly applied to swept wings merely by computing the upwash along the axis due to a swept wing, while Multhopp's cannot be applied without further modification.

Loading on Afterbodies

In slender-configuration theory, the basic assumptions lead inevitably to the result that the lift induced on the body occurs at the same longitudinal location as the wing lifting element inducing it. Thus, if the afterbody of a slender wing-body combination is of constant cross section, no lift can be induced on it behind the wing trailing edge unless displacement and rolling up of the vortex sheet are taken into account. For an afterbody of revolution which closes to a point behind a slender wing-body combination having a straight wing trailing edge, Adams and Sears[16] have given an

COMPARISON OF THEORETICAL AND EXPERIMENTAL BODY LOADINGS ON A BODY OF FINITE LENGTH AT LOW SPEED

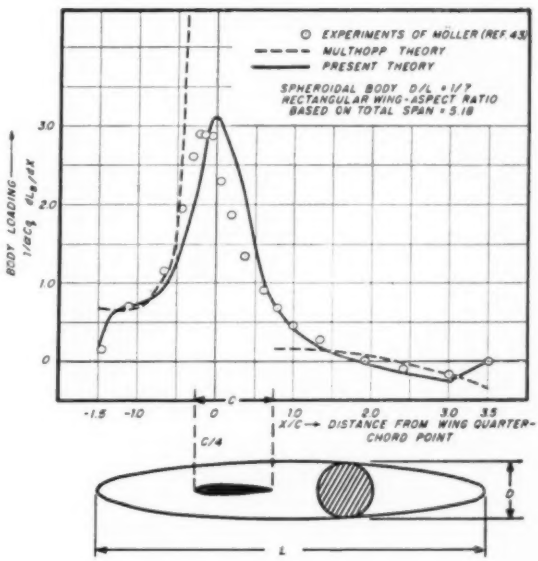

Fig. 6

expression for afterbody lift which takes into account the shifting inward of the wing trailing vortices as they follow the streamlines around an afterbody of decreasing cross-sectional area. Vertical displacements and rolling up of the vortex sheet are neglected, so there is an implied restriction to short bodies and light loadings. Their result for the position, y_2, of a vortex originally at y_1 at the wing trailing edge is

$$y_2^2 - y_1^2 = R_2^2 - R_1^2 \tag{160}$$

where R_1 is the radius of the body at 1 and R_2 is the radius at the location 2 at which the new position of the vortex is desired. Their general expression for the afterbody lift between points 1 and 2 was obtained from the momentum integral in the Trefftz plane, Eq. (18). (Note again that in slender-body theory, every plane is treated as a Trefftz plane insofar as the flow ahead of the plane is concerned.) In the present notation, the afterbody lift as given by Adams and Sears is

$$\frac{\Delta L_{12}}{\rho U_0} = 2\left[\int_{R_2}^{b_2} \Gamma(y)\left(1 + \frac{R_2^2}{y_2^2}\right) dy - \int_{R_1}^{b_1} \Gamma(y)\left(1 + \frac{R_1^2}{y_1^2}\right) dy\right] \tag{161}$$

where y_2 and b_2 are obtained from Eq. (160). This is simply the difference in momentum of the flow between stations 2 and 1. The case of constant circulation (which corresponds to rolled-up vortices) is of interest and can be easily dealt with. For constant circulation, Eq. (161) may be integrated to give

$$\Delta L_{12}/\rho U_0 = 2\Gamma\{[b_2 - (R_2^2/b_2)] - [b_1 - (R_1^2/b_1)]\} \tag{162}$$

so that

$$\Delta L_{12} = 2\rho U_0 \Gamma[(b_2 - b_1) - (R_2^2/b_2) + (R_1^2/b_1)] \tag{163}$$

and from Eq. (160)

$$b_2 = \sqrt{R_2^2 + b_1^2 - R_1^2} \tag{164}$$

If the body closes so that R_2 goes to zero, the afterbody lift becomes

$$\Delta L_{12} = 2\rho U_0 \Gamma[\sqrt{b_1^2 - R_1^2} - b_1 + (R_1^2/b_1)] \tag{165}$$

If b_1/R is large, the radical may be expanded in series and only terms up to order $(R_1/b_1)^2$ retained. Doing this leads to

$$\Delta L_{12} = \rho U_0 \Gamma(R_1^2/b_1) \tag{166}$$

which in the case of large b_1/R amounts to a small positive lift. For comparison, the lift on the body at station 1 is for constant circulation

$$L_{1B} = 2\rho U_0 \Gamma[R_1 - (R_1^2/b_1)] \tag{167}$$

The ratio of afterbody lift to body interference lift for constant circulation based on Eqs. (160) and (165) is shown in Fig. 7. It can be seen that the ratio grows large for R_1/b_1 approaching unity.

Another source of lift on long afterbodies is the displacement of the wing vortex sheet upward from the body as the flow moves downstream. The problem has been studied in detail by Lagerstrom and Graham[14] on the basis of slender-body theory. Moskowitz[15] has estimated the total loss of lift behind a slender wing-body configuration with cylindrical afterbody on the assumption of a very long afterbody. In this case, the wing trailing vortices are eventually displaced to a great enough distance from the body that the wing-induced upwash at the body base becomes effectively zero. Rather sizable losses of lift on the afterbody were predicted in contrast to the results of Lagerstrom and Graham. In fact, it can be shown that Moskowitz's calculations give an afterbody negative lift which is exactly equal to all the positive body interference lift induced ahead of the wing trailing edge. It appears that these results are in error, since only the effect of change in upwash at the body, dL_B/dx, was taken into account in Moskowitz's calculations. Actually, if the trailing vortices are deflected from a position parallel to the body axis, a longitudinal component of lift is induced directly by pressures acting on the body. As was shown by Lagerstrom and Graham, the momentum equations may be applied to this case with simple results if rolled-up concentrated vortices are considered.

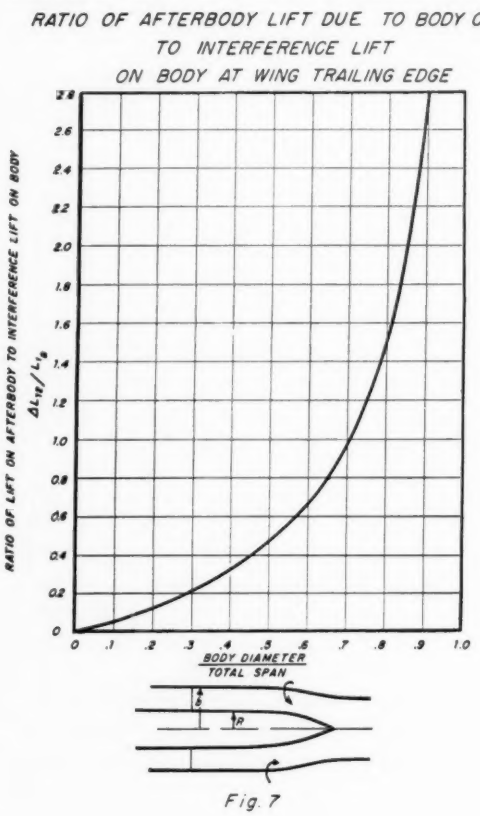

Fig. 7

Far downstream, the rate of flow of momentum (ignoring the uniform flow past the cylinder) is simply the momentum of a vortex pair $\rho U_0 \Gamma 2b_2$ where $2b_2$ is the distance between the two rolled-up vortices. The rate of flow of momentum just behind the trailing edge of the wing is the same as calculated for station 1 in Eq. (162). Thus, the lift on the afterbody, which is the difference of these two values is

$$L_{12} = 2\rho U_0 \Gamma \left\{ b_2 - [b_1 - (R_1^2/b_1)] \right\} \tag{168}$$

or

$$L_{12} = 2\rho U_0 \Gamma \left[(b_2 - b_1) + (R_1^2/b_1) \right] \tag{169}$$

If interactions between the vortices are neglected, it is easy to show from the two-dimensional flow around a circle that

$$b_2 = b_1 - (R_1^2/b_1) \tag{170}$$

Substituting this into Eq. (169), it is seen that to this approximation the afterbody lift is zero. Lagerstrom and Graham have shown that a small positive lift does occur if the interactions of the vortices are considered.

Simplified Method for Estimating Lift of a Wing-Body Combination

Ward[8] has suggested that the result obtained from slender-configuration theory for the lift of a winged body of revolution in terms of the lift, L^*, which the exposed wing would experience if mounted on a plane wall may be applicable to more general wing plan forms than the derivation would imply. His result is

$$L_{W_B} = L_W{}^* [1 + (R/b)]^2 \tag{171}$$

A similar result is suggested by calculations according to lifting-line theory[4] in Fig. 8. It is interesting to note that whereas the lift of the wing-body combination in terms of the lift of the wing including its extension through the body shows a marked dependence on aspect ratio, as shown in Fig. 4, aspect ratio dependence is largely suppressed when the wing-body characteristics are referred to those of the exposed wing in Fig. 8. Also plotted in Fig. 4 are Ward's results and several experimental results[44, 45, 46] for wings of both high and low aspect ratio. The agreement between the two theories and experiment is fair, considering the wide range of configurations covered. For the experimental cases, the lift of the exposed wings alone was in all cases estimated from the Weissinger theory, since whenever wing tests are made to supplement wing-body tests, current experimental practice is to test not the exposed wing, but a hypothetical wing, including the extension of the exposed wing through the body.

From the Trefftz-plane relation, Eq. (21), it is apparent how the method of approximation can be extended to arbitrary body shape. The average angle of attack experienced by the wing is given by

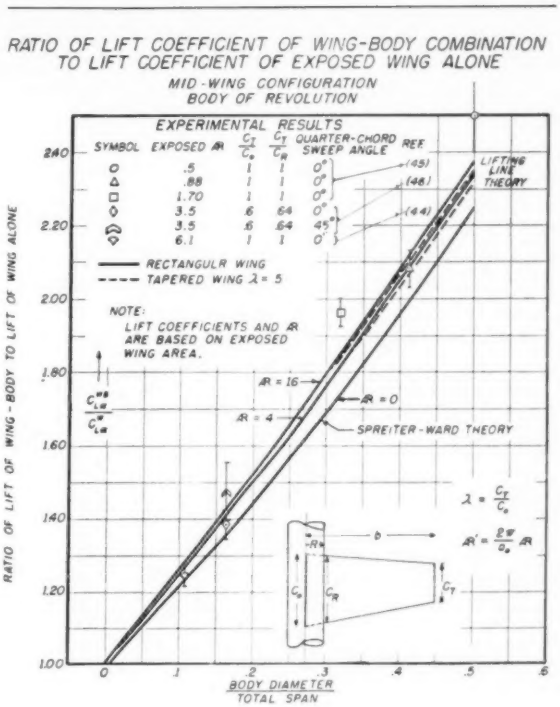
RATIO OF LIFT COEFFICIENT OF WING-BODY COMBINATION TO LIFT COEFFICIENT OF EXPOSED WING ALONE
MID-WING CONFIGURATION
BODY OF REVOLUTION
EXPERIMENTAL RESULTS
SYMBOL EXPOSED AR
QUARTER-CHORD SWEEP ANGLE
RECTANGULR WING
TAPERED WING λ = 5
NOTE: LIFT COEFFICIENTS AND AR ARE BASED ON EXPOSED WING AREA.
AR = 16
AR = 4
AR = 0
SPREITER-WARD THEORY
LIFTING LINE THEORY
RATIO OF LIFT OF WING-BODY TO LIFT OF WING ALONE
BODY DIAMETER / TOTAL SPAN

Fig 8

$$\frac{\bar{\alpha}}{\alpha} = \frac{\int_a^b [1 + f(y)]\, dy}{\int_a^b dy} = \sigma + 1 \tag{172}$$

where $f(y)$ is the same body upwash function introduced previously and a is the distance from the plane of symmetry to the wing-body intersection. If $C_{l_{\alpha W}}{}^*$ is the slope of the lift curve for the exposed wing, then the slope of the lift curve of the wing in the presence of the body will be approximately

$$C_{l_{\alpha W}} = (1 + \sigma) C_{L_{\alpha W}}{}^* \tag{173}$$

The lift induced on the body can be estimated from the Trefftz-plane relation, Eq. (21); assuming the lift on the wing is distributed as $[1 + f(v)]$

$$\frac{C_{l_{\alpha B}}}{C_{l_{\alpha W}}} = \frac{\int_a^b [1 + f(y)] f(y)\, dy}{\int_a^b [1 + f(y)]\, dy} = \mu \tag{174}$$

The slope of the lift curve for the wing-body combination is then

$$C_{l_{\alpha W_B}} = (1 + \mu)\,(1 + \sigma) C_{l_{\alpha W}}{}^* \tag{175}$$

where $C_{l_{\alpha W_B}}$ is based on the exposed wing area. If, in the calculation of the induced lift on the body, the wing-lift distribution is assumed constant, $\mu = \sigma$, and the equation for $C_{l_{\alpha W_B}}$ becomes

$$C_{l_{\alpha W_B}} = (1 + \sigma)^2 C_{l_{\alpha W_B}{}^*} \tag{176}$$

For a body of revolution, this would lead exactly to Ward's equation; for most cases, however, Eq. (175) seems to give slightly better results. Further ways of improving the present method at the expense of additional labor are obvious; better approximations for the wing span-load distribution in the presence of body upwash may be made, the induced body lift could be simply calculated from Eq. (21) once this improved loading were available, and finally, corrections for finite-body length could be estimated where necessary.

Supersonic Wing-Body Interference

The aerodynamics of supersonic aircraft have been subjected to intensive study for a relatively short time, but already there has been a great deal of work on the wing-body interference problem. The various procedures which have been employed in attempts to obtain exact linearized solutions of this problem will first be reviewed in historical order. This will then be followed by a discussion of the practical applications in the light of experimental results. Slender-body theory, which is applicable to sufficiently slender configurations in supersonic flow, will not be discussed further, since the discussion already given in connection with the subsonic problem is directly applicable.

Ferrari Method

Ferrari[18, 19] considered the problem of a flat rectangular wing attached to a body of revolution in supersonic flow where the wing and body are at a common angle of attack. He employed an iterative process in his solution; the basis for this process has already been given under "General Theory and Concepts." The same notation will be employed here. If the wing is assumed to be extended through the body, the projection on the $z = 0$ plane of the region common to both will be denoted by R_{WB}. The four-step iteration procedure employed by Ferrari may be summarized as follows:

$$\left.\begin{aligned}
&\text{Step 1:}\\
&\quad \partial\varphi_W^{(0)}/\partial z = -U_0\alpha \qquad \text{on } R_W + R_{WB}\\
&\text{Step 2:}\\
&\quad \partial\varphi_B^{(0)}/\partial n = -U_0\alpha\cos\theta \qquad \text{on } R_B\\
&\text{Step 3:}\\
&\quad \partial\varphi_W^{(1)}/\partial z = -\partial\varphi_B^{(0)}/\partial z \qquad \text{on } R_W\\
&\quad \partial\varphi_W^{(1)}/\partial z = 0 \qquad \text{on } R_{WB}\\
&\text{Step 4:}\\
&\quad \partial\varphi_B^{(1)}/\partial n = -\partial\varphi_B^{(0)}/\partial n \qquad \text{on } R_B
\end{aligned}\right\} \quad (177)$$

The first two steps of the iteration procedure may be carried out by making use of the Ackeret[49] solution for a two-dimensional wing and the Tsien[56] procedure for a body at angle of attack. In computing the third step, Ferrari makes use of a Fourier expansion of the spanwise lift distribution on the wing which may be regarded as essentially a representation of a doublet distribution.

In the fourth step, the velocity potential of the flow around the body is taken to be of the form

$$\varphi = \sum_{m=1,3}^{\infty} \varphi_m(x,r) r^m \cos m\theta \qquad (178)$$

in polar coordinates with $r = 0$ on the body axis, where the φ_m's are given by

$$\varphi_m = r^m \left(\frac{1}{r}\frac{\partial}{\partial r}\right)^m \int_{\cosh^{-1}(x/\alpha r)}^{0} f_m(x - \alpha r\cosh u)\, du \qquad (179)$$

where the f_m's may be regarded as multipole distributions along the axis and $\alpha = \sqrt{M^2 - 1}$. Cramer[47] has shown that a form of the solution much more convenient for computation is

$$\varphi_m = \frac{(-1)^m \alpha^m}{r^m} \int_{\cosh^{-1}(x/\alpha r)}^{0} f_m \times (x - \alpha r\cosh u)\cosh mu\, du \qquad (180)$$

The f_m's may be found numerically by the methods originally given by von Kármán and Moore for f_0.[48] From the form of Eq. (178), it is clear that only φ_1 contributes to the lift distribution along the body, since the linearized pressures are proportional to $\partial\varphi/\partial x$ and these are multiplied by $\cos\theta$ to obtain the lift.

The Browne-Friedman-Hodes Conical Solution

A conical wing-body configuration is defined as one which can be generated by a line rotating about a fixed point. Browne, Friedman, and Hodes[22] have applied the powerful methods of conical flow and conformal transformation to this problem. Analytic solutions for delta wings with both subsonic and supersonic leading edges were obtained in this fashion. Although the conical configuration is of small practical importance, this work contains the only solution of a wing-body interference problem with subsonic leading edges for nonslender wings. The results of reference 22 have been used to estimate the regime of applicability of the slender-configuration theory of Spreiter[7] and Ward.[8] It is clear that the conical configuration will be of great interest as a check of the more general theories for interference between delta wings and bodies which lie in the future.

The Morikawa Procedure

Morikawa[20] has considered the problem of a rectangular wing attached to a cylindrical body of circular cross section at a common angle of attack α in a supersonic flow field. Upon specializing the results of the general formulation previously given to an infinite circular cylinder at a Mach Number of $\sqrt{2}$, the problem may be formulated in terms of a potential φ_W as follows:

$$\partial^2\varphi_W/\partial x^2 = (\partial^2\varphi_W/\partial y^2) + (\partial^2\varphi_W/\partial z^2) \qquad \text{in flow field } F \qquad (181)$$

$$\partial\varphi_W/\partial r = 0 \qquad \text{on } r = 1 \qquad (182)$$

$$(1/r)\ (\partial\varphi_W/\partial\theta) = -U_0\alpha\,[1 + (1/r^2)] \quad \text{on } x > 0;\ r > 1 \tag{183}$$

Use of the particular Mach Number, $\sqrt{2}$, in the formulation of the problem does not restrict the generality of the result, since the Prandtl-Glauert transformation may be used to obtain results for an arbitrary Mach Number.

The Laplace transform is applied to the differential equation and the boundary conditions. With the definition

$$\psi(r,\theta,s) = \mathfrak{L}\varphi_W\ (r,\theta,x) = \int_0^\infty ds\ e^{-sx}\ \varphi_W(r,\theta,x) \tag{184}$$

the boundary-value problem is reduced to the form

$$s^2\psi = \partial^2\psi/\partial y^2 + \partial^2\psi/\partial z^2 = \partial^2\psi/\partial r^2 + [(1/r)\ (\partial\psi/\partial r)] + [(1/r^2)\ (\partial^2\psi/\partial\theta^2)] \tag{185}$$

$$\partial\psi/\partial r = 0 \qquad \text{on } r = 1 \tag{186}$$

$$(1/r)\ (\partial\psi/\partial\theta) = -[U_0(\alpha/s)]\ [1 + (1/r^2)] \text{ on } \left.\begin{matrix} r = 1 \\ \theta = 0 \end{matrix}\right\} \tag{187}$$

$$(1/r)\ (\partial\psi/\partial\theta) = [U_0(\alpha/s)]\ [1 + (1/r^2)] \text{ on } \left.\begin{matrix} r = 1 \\ \theta = \pi \end{matrix}\right\} \tag{188}$$

The solution obtained by Morikawa for the boundary-value problem in ψ may be written explicitly in the following form

$$\psi(r,\theta,s) = \frac{U_0\alpha}{\pi s}\int_1^\infty d\rho\left(1 + \frac{1}{\rho^2}\right)\{K_0(s\rho_+) + K_0(sp_-)\} - \frac{4U_0\alpha}{\pi s}\int_1^\infty d\rho\left(1 + \frac{1}{\rho^2}\right)\sum_{n=0}^{\infty}\epsilon_n\frac{I_{2n}'(s)}{K_{2n}'(s)} \times K_{2n}(sr)K_{2n}(sp)\cos 2n\theta \tag{189}$$

where I_{2n}, K_{2n}, are the modified Bessel Functions, ϵ_n is equal to one-half when $n = 0$ and equal to 1 otherwise, and ρ_+, ρ_- are defined as follows:

$$\left.\begin{aligned} \rho_+ &= \sqrt{r^2 + 2r\rho\cos\theta + \rho^2} \\ \rho_- &= \sqrt{r^2 - 2r\rho\cos\theta + \rho^2} \end{aligned}\right\} \tag{190}$$

The potential φ_W may be computed from ψ by the inverse Laplace transform

$$\varphi_W(r,\theta,x) = \mathfrak{L}^{-1}\,\psi(r,\theta,s) = \frac{1}{2\pi i}\int_{\gamma-i\infty}^{\gamma+i\infty} ds e^{sx}\,\psi(r,\theta,s) \tag{191}$$

where γ is any real number greater than zero. Thus, the wing-body problem is reduced to two integrations and a summation and may be considered solved in principle. In practice, however, the analytical difficulties are so great that almost no progress has been made in extracting numerical results from the Morikawa formulation in its exact form. Morikawa, however, has approximated the series in Eq. (189) by a simpler function which he constructed semiempirically so as to fit conditions very near the leading edge. The range of validity of this approximation has not been determined mathematically.

Nielsen-Matteson Method

Nielsen and Matteson[55] considered the problem of an untapered wing of double-wedge profile and 60° sweep attached to a cylindrical body of circular cross section in supersonic flow with wing and body at zero angle of attack. The body is replaced by a set of plane areas inscribed in the cylinder. A collocation procedure is used to cancel the normal velocities induced on the body by the disturbances due to the wing. It is clear that the sources distributed over the body in this procedure will cause normal velocities on the wing. Thus, this procedure may be looked upon as the first steps of an interative process. It is evident that the same procedure may be used to treat lifting cases if all edges are supersonic. The difference between the Ferrari and Nielsen-Matteson methods appears to be solely in the method of solving the body-alone problem which arises in the analysis.

Nielsen Procedure

The wing-body problem for a rectangular wing and infinite cylindrical body of circular cross section in supersonic flow has been treated by Nielsen for the case where the body is at zero angle of attack. Nielsen employed the special formulation of the problem suggested by Lagerstrom and Van Dyke[21] in which a basic wing passing through the body gives one component of the solution. The flow set up by this wing violates the boundary condition of zero velocity normal to the body boundary. A second component solution must then be added to the first to cancel the flow across the body. This, thus far, is the same as the Ferrari problem. At this point, however, the Lagerstrom-Van Dyke formulation requires that flow normal to the body surface be cancelled without at the same time producing any new velocities normal to the wing surface. This can be done, for supersonic leading edges, by representing the solution by a Fourier cosine series in the meridional angle ($\theta = 0,\pi$ on the wing) with even terms only. Thus, in effect, the iteration procedure is terminated in two steps.

The potential φ is expressed in the form

$$\varphi = \varphi_W{}^0 + \varphi_B \tag{192}$$

where $\varphi_W{}^0$ satisfies the boundary condition

$$\partial\varphi_W{}^0/\partial z = -U_0\alpha \qquad R_W + R_{WB} \tag{193}$$

and φ_B satisfies the boundary conditions

$$\partial\varphi_B/\partial r = f(x,\theta) - (\partial\varphi_W{}^0/\partial r) \text{ on } r = 1, \quad x > 0 \tag{194}$$

$$\partial\varphi_B/\partial\theta = 0 \qquad \text{on } \theta = 0,\pi, \quad x > 0 \tag{195}$$

and the differential equation

$$\partial^2\varphi_B/\partial x^2 = (\partial^2\varphi_B/\partial y^2) + (\partial^2\varphi_B/\partial z^2)$$

The wing is assumed to extend through the body at angle of attack α so that the Ackeret solution may be used to obtain $\varphi_W{}^0$. The boundary-value problem is solved by taking the Laplace transform of the differential equation and the boundary conditions. With the definitions

$$\psi(r,\theta,s) = \int_0^\infty dx e^{-sx}\varphi_B(r,\theta,x) = \mathfrak{L}\varphi_B \qquad (196)$$

$$F(\theta,s) = \int_0^\infty dx^{-sx} f(\theta,x) = \mathfrak{L}f(\theta,x) \qquad (197)$$

the transformed boundary-value problem may be written as follows

$$s^2\psi = (\partial^2\psi/\partial r^2) + [(1/r)(\partial\psi/\partial r)] + [(1/r^2)(\partial^2\psi/\partial\theta^2)] \qquad (198)$$

$$\partial\psi/\partial r = F(\theta,s) \qquad \text{on } r = 1 \qquad (199)$$

$$\partial\psi/\partial\theta = 0 \qquad \theta = 0,\pi \qquad (200)$$

The solution to the above boundary-value problem may be written in the form

$$\psi(r,\theta,s) = \sum_{n=0,1}^{\infty} \frac{\epsilon_n F_n(s)\cos 2n\theta K_{2n}(s,r)}{s\,K_{2n}{}'(s)} \qquad (201)$$

where the following definitions are used

$$F_n(s) = \frac{2}{\pi}\int_0^\pi d\tau F(\tau,s)\cos 2n\tau \qquad (202)$$

$$\epsilon_n = \frac{1}{2} \qquad n = 0 \qquad (203)$$

$$\epsilon_n = 1 \qquad n > 0$$

It will be noted that the $F_n(s)$ are the Fourier cosine series coefficients of the function $F(\theta,s)$. The potential φ is found by taking the inverse transform of the above expression for ψ or

$$\varphi_B(r,\theta,x) = \sum_{n=0}^{\infty}\epsilon_n\cos 2n\theta\,\mathfrak{L}^{-1}\frac{K_{2n}(sr)\;F_n(s)}{sK_{2n}{}'(s)} \qquad (204)$$

Nielsen has evaluated the inverse Laplace transform appearing in the above formula in terms of known functions and a new function $M_{2n}(x)$ defined below

$$M_{2n}(x) = \mathfrak{L}^{-1}[1/se^sK_{2n}{}'(s)] \qquad (205)$$

The following formulas may be obtained by elementary applications of tables of Laplace transforms (say Van der Pol and Bremmer)

$$\mathfrak{L}^{-1}\frac{K_{2n}(sr)F_n(s)}{s\,K_{2n}{}'(s)} = \left(\frac{2}{r}\right)^{2k}\cdot\frac{\pi(2n)}{\pi(4n)}\int_0^{x-r+1} d\xi g_{2n}(\xi)\times \frac{\partial^{2n-1}}{\partial\xi^{2n-1}}[(x+1-\xi)^2 - r]^{2n-(1/2)} \qquad (206)$$

where $g_{2n}(\xi)$ is defined by the formula

$$g_{2n}(x) = \int_0^x d\xi\, f_{2n}{}'(\xi)M_{2n}(x-\xi) \qquad (207)$$

and $\pi(n) = n!$

Nielsen has tabulated the functions $M_{2n}(x)$ for $n = 0,1,2,3$ and x from 0 to 4 with intervals of approximately 0.2.

It should be noted that since the solution of the second component problem gives no flow across the wing plane, it is not valid behind the trailing edge of the wing. An entirely new solution must be worked out for the body behind the trailing edge based on the downwash field of the wing and body ahead. In the Nielsen solution, by contrast with the Ferrari solution, all terms in the Fourier series for potential contribute to the body lift, not just the first term.

The Status of Supersonic Wing-Body Interference Theory—Comparison with Experiment

Two essentially different procedures have been employed in calculating supersonic wing-body interference for nonslender configurations: the method of iteration and the method of separation of variables. The iteration procedure, which is employed by Ferrari[18, 19] and Nielsen and Matteson,[55] reduces the wing-body interaction problem to a set of general wing-alone and body-alone problems. The wing-alone and body-alone problems are handled exactly in a mathematical sense by Ferrari, and Nielsen and Matteson. In general, the iteration procedure is not entirely satisfactory for two reasons. Although the first stages of the iteration process may be computed rapidly, the numerical calculations of the later stages become very tedious. Furthermore, there is some question as to the rapidity of convergence in regions which are strongly affected by wing-body interferences. In spite of these deficiencies, the iteration procedure is the only method which can be used in its present form to compute the characteristics of general wing-body configurations with subsonic leading edges. It will be noted, however, that such a calculation has not been carried out and appears to require considerable labor.

The method of separation of variables has been employed by Browne, Friedman and Hodes[22] for the conical case and Morikawa[20] and Nielsen[23] for configurations with supersonic wing edges. Separation of the wave equation in conical coordinates is used by Browne, *et al.*, to obtain a relatively simple solution of the conical wing-body problem. Although a conical wing-body configuration is rarely employed in the design of airframes, the solution has been used to establish approximately the regime of applicability of slender-configuration theory and may be used as a test case in evaluating future theories.

The procedures employed by Morikawa[20] and Nielsen[23] are quite similar. By writing the potential as a sum of two terms, Morikawa reduces the wing-body

problem to a problem where the normal velocity is specified on the wing, and is zero on the body. Nielsen makes use of a similar device to reduce the configuration problem to one where the normal velocity is specified on the body and is zero on the wing. The Laplace transform is employed in both theories to reduce the problem to a quasi two-dimensional boundary-value problem. Morikawa determines the Green's function appropriate to the problem as a series expansion. The solution to the problem is then expressed as the inverse Laplace transform of an integral over the wing alone. Morikawa does not evaluate the inverse Laplace transform of the Green's function, which would require the calculation of a hitherto untabulated function $M_{2n}(v)$. Nielsen expresses the solution of the wing-body problem as the inverse Laplace transform of an integral over the body alone. The Green's function derived by Morikawa may be used to obtain the same result. Since the Green's functions for the Morikawa and Nielsen procedures are essentially the same, the same untabulated inverse Laplace transform which arose in the Morikawa theory appears in his result. Nielsen has carried out a numerical evaluation of the function $M_{2n}(x)$ for $n = 0,1,2,3$. It is clear that four terms of the series obtained in the Nielsen and Morikawa theories may be evaluated from the tabulation of M_{2n}. Although both theories are applicable to all configurations with supersonic leading edges, they have been applied only to a rectangular wing. Morikawa's treatment of this problem is based on a semiempirical approximation to the Green's function.

In general, the method of separation of variables leads to a solution in series form, so that the problem of rapidity of convergence arises as in the iteration process. The accuracy of a four-term series turns out to be poor near the leading edge of a wing-body combination. In fact, Nielsen found it necessary to supplement his series solution in the region from the leading edge up to a distance $1.2\sqrt{M^2 - 1}\,R$ downstream of the leading edge (where R is the body radius) by an approximate solution based on a quasi-plane-wall argument. The distance $1.2\sqrt{M^2 - 1}\,R$ is comparable to the wing chord for many configurations, even for $M = 1.4$. The numerical labor required to obtain even one term of the series is comparable with the first stage of the iteration procedure.

It is not possible at present to draw definite conclusions as to the best methods for computing supersonic wing-body interference. However, it does appear that, for wing-body combinations of large wing chord compared to the body radius, which are not followed by afterbodies (tail surfaces), the Nielsen procedure would offer advantages. On the other hand, for configurations having shorter chords and followed by long afterbodies (the more usual wing case) the Ferrari method offers the maximum amount of useful information for a given amount of labor.

A study of the available experimental data has shown that, while available theories fall far short of perfection in their present form, they do provide sufficiently accurate results for most design purposes when applied to cases close to those for which they were derived. Fig. 9, based on experimental data from reference 50, shows the pressures measured on the flat upper surface of a rectangular wing centrally mounted on a body of revolution which was essentially of constant cross section downstream of the wing leading edge. The tests were made with wing and body both at a common angle of attack of 4°. For reference purposes, the pressures are all referred to the theoretical predictions of a formula given by Kirkby and Robinson, Eq. (209). This formula represents the exact solution according to linearized wing theory for the pressures in the region outside the root and tip Mach lines when the wing is operating in the upwash field of an infinite cylinder (Beskin's approximation).[51] For points theoretically inside the root Mach line, Kirkby and Robinson's values on the Mach line were used as reference values. It can be seen that Kirkby and Robinson's result is in very good agreement with experiment outside the root Mach line, being no more than 5 per cent high at the worst. The pressure distributions predicted by the theories of Morikawa and Ferrari (first iteration) are also shown in Fig. 9 for comparison. Morikawa's results for the region outside the root Mach line (which, of course, is not influenced by the body except by upwash) are identical to Kirkby and Robinson's. Ferrari's results for the same region are somewhat high. When the region inside the root Mach line is examined, however, the situation is reversed. Ferrari's result shows fairly good agreement and Morikawa's is too high. It should be emphasized that the test of Morikawa's semiempirical approximation occurs only inside the root Mach line. His solution outside the Mach line was obtained separately in a manner similar to Kirkby and Robinson, and has nothing to do with the solution inside. Ferrari's solutions inside and outside the root Mach line are, however, related since he used a single Fourier series to represent the potential over the span.

The experimental load distributions along the body from reference 52 for a high-aspect-ratio wing mounted on a long cylindrical body are shown in Fig. 10. The body was long enough so that the wing-tip Mach cones did not strike the body until very near the base of the body. The cases of common angle of attack of the wing and body and wing incidence only are included. For the wing incidence study, one test was made with the opening at the wing-body juncture created by the wing angle unsealed, and the other with it sealed. The theory of Ferrari is the only one available for afterbody loading. The results of the first iteration according to this theory are shown in Fig. 10 for comparison with experiment. In the first step of the iteration process, as presently constituted, there is no difference in the computed body loading between the incidence and

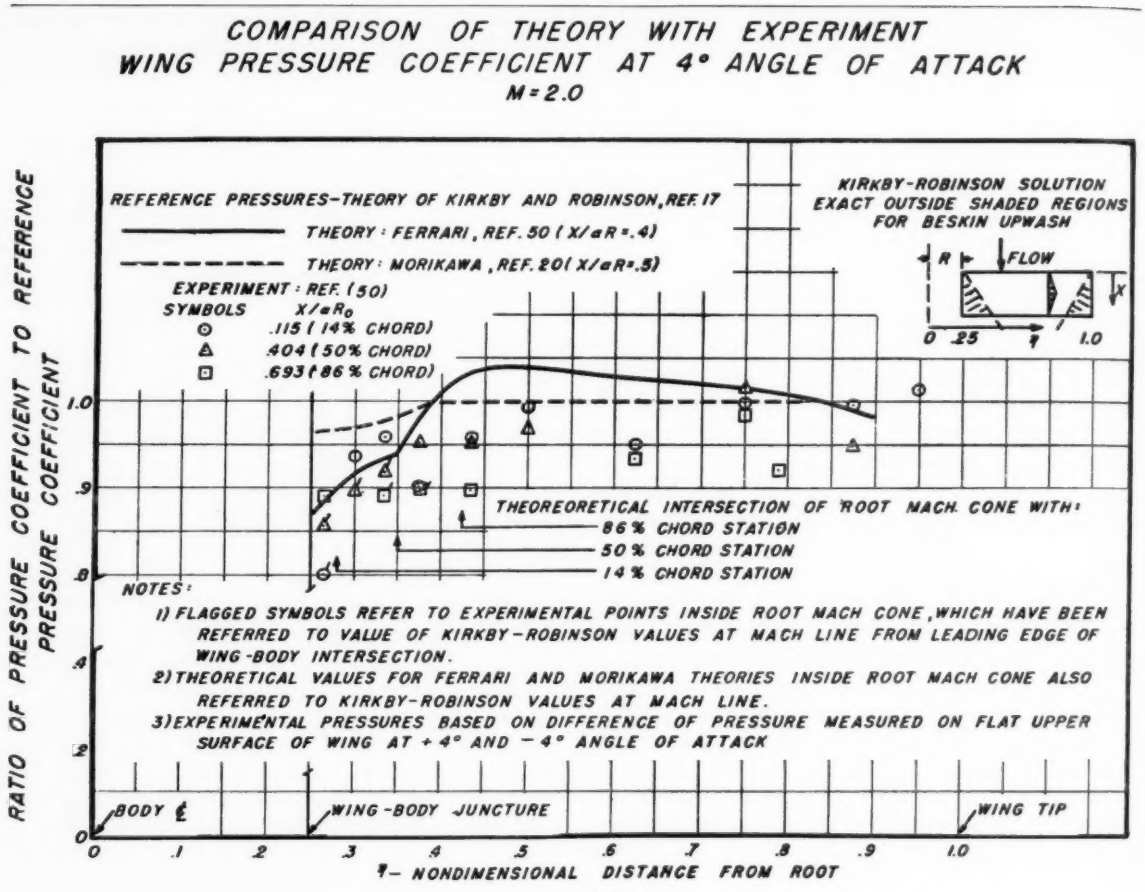
COMPARISON OF THEORY WITH EXPERIMENT
WING PRESSURE COEFFICIENT AT 4° ANGLE OF ATTACK
M = 2.0
RATIO OF PRESSURE COEFFICIENT TO REFERENCE PRESSURE COEFFICIENT
REFERENCE PRESSURES—THEORY OF KIRKBY AND ROBINSON, REF. 17
THEORY: FERRARI, REF. 50 (X/aR = .4)
THEORY: MORIKAWA, REF. 20 (X/aR = .5)
EXPERIMENT: REF. (50)
SYMBOLS X/aR0
.115 (14% CHORD)
.404 (50% CHORD)
.693 (86% CHORD)
KIRKBY-ROBINSON SOLUTION
EXACT OUTSIDE SHADED REGIONS
FOR BESKIN UPWASH
R
FLOW
X
0 .25 1.0
THEOREORETICAL INTERSECTION OF ROOT MACH CONE WITH:
86% CHORD STATION
50% CHORD STATION
14% CHORD STATION
NOTES:
1) FLAGGED SYMBOLS REFER TO EXPERIMENTAL POINTS INSIDE ROOT MACH CONE, WHICH HAVE BEEN REFERRED TO VALUE OF KIRKBY-ROBINSON VALUES AT MACH LINE FROM LEADING EDGE OF WING-BODY INTERSECTION.
2) THEORETICAL VALUES FOR FERRARI AND MORIKAWA THEORIES INSIDE ROOT MACH CONE ALSO REFERRED TO KIRKBY-ROBINSON VALUES AT MACH LINE.
3) EXPERIMENTAL PRESSURES BASED ON DIFFERENCE OF PRESSURE MEASURED ON FLAT UPPER SURFACE OF WING AT + 4° AND − 4° ANGLE OF ATTACK
BODY ℄
WING-BODY JUNCTURE
WING TIP
1.0
.9
.8
.4
½
0
0 .1 .2 .3 .4 .5 .6 .7 .8 .9 1.0
η — NONDIMENSIONAL DISTANCE FROM ROOT

Fig. 9

angle-of-attack cases. This could be improved, but only at the expense of additional labor. It can be seen that the theoretical loading lies between the measured loadings for the wing incidence and angle-of-attack cases, being closest to the case of wing incidence with sealed gap.

No comparison of theory with experiment for the wing pressures in the wing-incidence case was possible because the only wing pressure measurements in such cases were made with large gaps at the wing-body juncture.

Approximate Methods in Supersonic Wing-Body Interference

The theoretical methods which are available for supersonic wing-body interference calculations become extremely laborious and even intractable when applied to many of the practical problems which arise in design. Therefore, less exact and more simple methods for analysis of wing-body combinations have had to be devised. Of course, the results of more exact analyses, particularly if augmented by adequate experiments, serve as major guideposts in any attempt to find approximate methods which can be relied on, at least for some types of configurations. It must be kept in mind that higher-order effects are always present to modify at least some of the results which may be obtained even from the most exact linear theory. For instance, if one has to determine with great accuracy the hinge moments on a movable control surface which is influenced by the body, it will do him little good to seek to determine the pressure distribution from linearized theory with great accuracy. If the effects of gaps and viscosity do not influence the results, second order potential-flow effects most certainly will, unless control-surface thickness and angle of deflection are held down to impractical limits. On the other hand, such things as the overall lift and pitching moment of reasonably conventional configurations can probably be predicted with satisfactory accuracy even by approximate solutions of the linearized equations. At present, only for the case of wings centrally mounted on a circular body of revolution are there sufficient theoretical and experimental data to permit any sort of general conclusions to be drawn.

The earliest attempt at an approximate theory of supersonic wing-body interference was apparently that of Kirkby and Robinson.[17] They considered the case

of a rectangular wing and a conical body at a common angle of attack. Their procedure was to evaluate the body upwash around the conical body and to compute the wing lift on the basis of two-dimensional strip theory (Ackeret)[49] on the additional assumption of constant chordwise upwash equal to the mid-chord value at each spanwise location on the wing. No attempt was made to evaluate the effect of the wing on the body. Their assumption of the applicability of strip theory on the wing would make the method applicable to wings of chord small compared to $R\sqrt{M^2-1}$. In the course of investigating the validity of the strip assumption, Kirkby and Robinson have given in an appendix the simple useful solution, exact within the linearized theory, for a wing of infinite span subjected to the upwash field of an infinite cylinder (in other words, Beskin's approximation[51] when applied to finite-length bodies). This is the same body-induced angle of attack used by Multhopp[3] for finite lergth bodies, namely,

$$\alpha_i = \alpha_B\,(R^2/y^2) \tag{208}$$

where α_B is the body angle of attack. Their solution, for the difference between upper and lower surface pressure coefficients, is

$$\Delta C_p = 4\left\{\frac{\alpha_W}{\sqrt{M^2-1}} + \frac{R^2\alpha_B y(M^2-1)}{[(M^2-1)y^2 - x^2]^{3/2}}\right\} \tag{209}$$

where α_W is the wing angle of attack, α_B is the body angle of attack, and x is measured from the wing leading edge, while y is measured spanwise from the body axis. As may be seen from Fig. 9, this result is in good agreement with experiment in its region of validity.

Returning to Kirkby and Robinson's basic method, their use of strip theory would result in a wing-lift coefficient, based on exposed area,

$$C_{l_W} = \frac{4\alpha}{\sqrt{M^2-1}}\left(1 + \frac{R}{b}\right) \tag{210}$$

where b is the semispan. This neglects wing-tip effects which may be corrected separately, at least for the basic wing lift. On the other hand, Cramer's "Rules

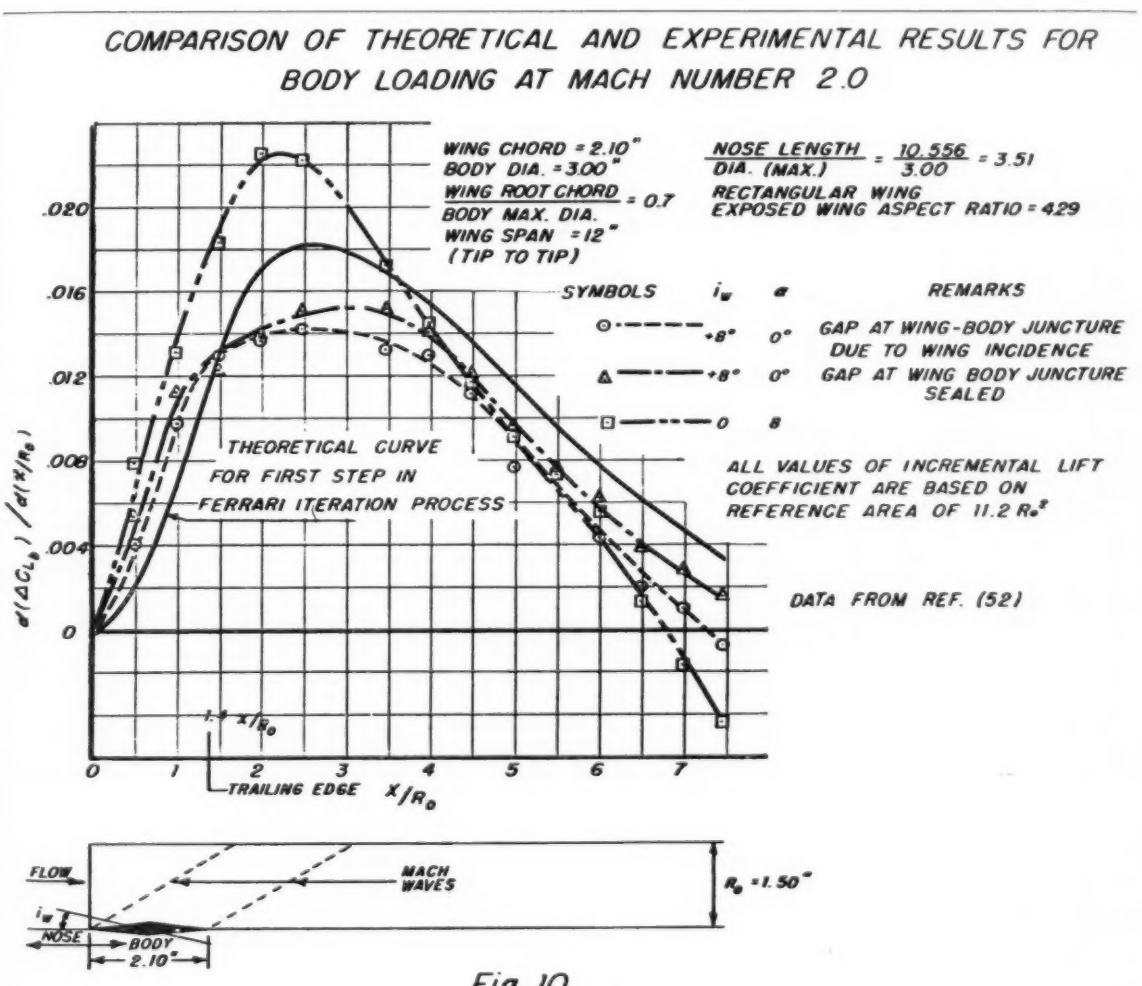
COMPARISON OF THEORETICAL AND EXPERIMENTAL RESULTS FOR BODY LOADING AT MACH NUMBER 2.0
WING CHORD = 2.10"
BODY DIA. = 3.00"
WING ROOT CHORD / BODY MAX. DIA. = 0.7
WING SPAN = 12" (TIP TO TIP)
NOSE LENGTH / DIA. (MAX.) = 10.556 / 3.00 = 3.51
RECTANGULAR WING
EXPOSED WING ASPECT RATIO = 4.29
SYMBOLS
REMARKS
+8° 0° GAP AT WING-BODY JUNCTURE DUE TO WING INCIDENCE
+8° 0° GAP AT WING BODY JUNCTURE SEALED
0 8
THEORETICAL CURVE FOR FIRST STEP IN FERRARI ITERATION PROCESS
ALL VALUES OF INCREMENTAL LIFT COEFFICIENT ARE BASED ON REFERENCE AREA OF 11.2 R₀²
DATA FROM REF. (52)
.020
.016
.012
.008
.004
0
0 1 2 3 4 5 6 7
TRAILING EDGE X/R₀
FLOW
MACH WAVES
R₀ = 1.50"
NOSE
BODY 2.10"

Fig 10

of Thumb"[25] based on experiment lead to the result that, for wings of large span followed by a sufficiently long afterbody, the total lift on the wing-body is

$$C_{l_{WB}} = \frac{4\alpha}{\sqrt{M^2 - 1}}\left(1 + 2\frac{R}{b}\right) \tag{211}$$

The lift due to the body alone must, of course, be added to this result. The interference effect is not equally divided between wing and body, but is somewhat greater on the body. Thus, Kirkby and Robinson's formula is more appropriate for the case of no afterbody. In their theory, they take no account of loading on the body up to the wing trailing edge, but they also do not account for the fall-off of lift in the wing-body juncture. As Cramer has shown, these effects tend to compensate, so that Eq. (210) for total lift is probably not too bad. Qualitative theoretical arguments for the validity of this compensation have been advanced by Lagerstrom and Van Dyke[21] on the basis of analogies to planar lift preservation theorems. As will be shown later, the reverse-flow theorem for wing-body combinations provides a more rigorous basis for this compensation.

If the wing chord is very small compared to the body radius and the wing span is large compared to the body radius, then strip theory should more nearly apply on the wing, since the region affected by the body would be a small part of the wing area. In this case, the lift coefficient along the span would be closely given by

$$C_l(y) = \frac{4\alpha}{\sqrt{M^2 - 1}}\left(1 + \frac{R^2}{y^2}\right) \tag{212}$$

The wing-lift coefficient would then be given by Eq. (210). From the Trefftz-plane theorem, Eq. (22), the lift of a long body in the presence of the wing is given by

$$\frac{L_B}{q} = \frac{4\alpha c}{\sqrt{M^2 - 1}}\, 2\int_R^b \left(1 + \frac{R^2}{y^2}\right)\frac{R^2}{y^2}\, dy \tag{213}$$

Integrating this, and finding the lift coefficient based on exposed wing area, gives

$$C_{l_B} = \frac{4\alpha}{\sqrt{M^2 - 1}}\frac{R}{b}\left[\frac{4}{3} + \frac{1}{3}\frac{R}{b} + \frac{1}{3}\left(\frac{R}{c}\right)^2\right] \tag{214}$$

Adding this to Eq. (210) gives

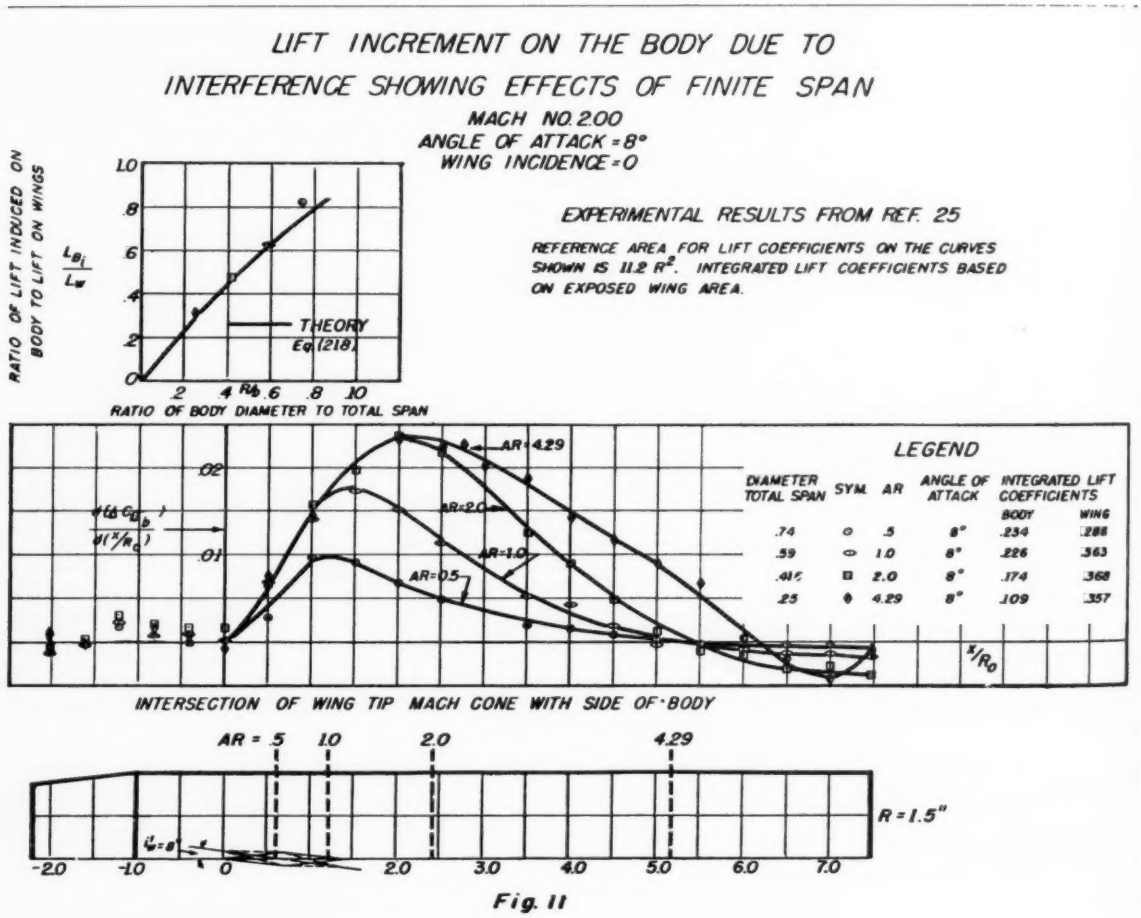
LIFT INCREMENT ON THE BODY DUE TO INTERFERENCE SHOWING EFFECTS OF FINITE SPAN
MACH NO. 2.00
ANGLE OF ATTACK = 8°
WING INCIDENCE = 0
EXPERIMENTAL RESULTS FROM REF. 25
REFERENCE AREA FOR LIFT COEFFICIENTS ON THE CURVES SHOWN IS 11.2 R². INTEGRATED LIFT COEFFICIENTS BASED ON EXPOSED WING AREA.
RATIO OF LIFT INDUCED ON BODY TO LIFT ON WINGS
THEORY Eq (218)
RATIO OF BODY DIAMETER TO TOTAL SPAN
LEGEND
DIAMETER TOTAL SPAN
SYM.
AR
ANGLE OF ATTACK
INTEGRATED LIFT COEFFICIENTS
BODY
WING
.74 5 8° .234 .288
.59 1.0 8° .226 .363
.41 2.0 8° .174 .368
.25 4.29 8° .109 .357
AR=4.29
AR=2.0
AR=1.0
AR=0.5
INTERSECTION OF WING TIP MACH CONE WITH SIDE OF BODY
AR = 5 1.0 2.0 4.29
R = 1.5"

Fig. 11

$$C_{l_{WB}} = \frac{4\alpha}{\sqrt{M^2-1}}\left[1 + \frac{7}{3}\frac{R}{b} + \frac{1}{3}\left(\frac{R}{b}\right)^2 + \frac{1}{3}\left(\frac{R}{b}\right)^3\right] \quad (215)$$

This can be regarded as the limiting value of the lift obtainable from a rectangular wing-body combination. It is undoubtedly too high for most practical cases, and something between Eqs. (210) and (211) will be more appropriate.

The prediction of the pitching moments of wing-body combinations is a somewhat more difficult problem than the determination of the lift, and thus, the approximate methods are not quite so simple. The calculation of the first iteration for the body loading in the Ferrari method in which the wing-tip Mach cones are assumed not to strike the body, consists of two parts: first, the computation of the loading due to the pressure field of the wing acting directly on the body, and second, the loading due to the flow set up around the body to cancel the velocities produced by the wing. On a sufficiently long body, only the first part of the loading produces lift, since the second part of the loading is due to equal positive and negative angle-of-attack changes at the body due to the leading and trailing edge Mach waves. The second loading produces a couple, however. By going to the limiting case of vanishing body radius, Ferrari has computed the moment of the couple as

$$\Delta M_1 = -\pi\rho U_0^2 R^2 c\alpha_0 \quad (216)$$

where the minus sign denotes a nose-down moment, c is the wing chord, and α_0 the angle of attack. The lift acting on the body due to the pressure field of the wing in this approximation is simply equal to the lift which would be carried by the region of the wing going through the body. By a geometrical calculation of the centroid of the surface area intercepted by the Mach planes from the leading and trailing edges, the location of this lift is found to be $(\pi/4)R\sqrt{M^2-1}$ from the wing mid-chord. The moment of this lift about the wing mid-chord is therefore

$$\Delta M_2 = -\frac{4\alpha c R}{\sqrt{M^2-1}}\frac{\pi}{4}R\sqrt{M^2-1}\frac{\rho U_0^2}{2} \quad (217)$$

The total moment about the wing mid-chord is the sum of ΔM_1 and ΔM_2.

Schrenk[27] has reviewed the arguments leading to these expressions starting from slender-body theory, rather than from linearized supersonic theory. In this way, the extension to noncircular bodies and other interference problems is made more obvious.

As the wing aspect ratio becomes smaller, the action of the wing-tip Mach cones on the body alters the simple considerations given above. The lift on the body can no longer be taken to be the lift which would occur on the extension of the wing passing through the body. Fig. 11 shows the loadings produced on the body for a set of wings ranging in exposed aspect ratio from 0.5 to 4.29. The body loading curves all start in substantially the same way, but at the location where the tip effect is felt for each particular wing, the body loading begins to fall away from the $AR = 4.29$ case. It is obviously necessary to modify the Ferrari procedure to account for the wing-tip flow field in these cases. The ratio of lift on the body to lift on the wing for the series of wings tested is shown in the inset in Fig. 11 and compared with calculated values obtained by application of the Trefftz-plane theorem, Eq. (22), on the assumption that the span lift distribution on the wings is given by Eq. (212). The result is

$$\frac{C_{l_B}}{C_{l_W}} = \frac{R}{b}\left\{\frac{(1 - R/b) + 1/3[1 - (R/b)^3]}{[1 - (R/b)^2]}\right\} \quad (218)$$

The agreement between the theoretical and experimental values of this ratio is seen to be quite good, although it is well known that the correct lift distribution is not that of Eq. (212). This is another indication of the insensitivity of this ratio to the loading which was demonstrated earlier for the subsonic case.

The prediction of the moment of the body loading arising with low-aspect-ratio wings requires more care. It appears that the best approach would be to use the Ferrari method for the body loading with a wing of infinite span, and to correct this loading by an increment applied everywhere downstream of the point where the wing-tip Mach cone intersects the body. This increment might well be calculated on the basis of slender-body theory using the local angle of attack on the axis of the body computed from one or another of the simplified theories of wing downwash. To facilitate computation of the infinite wing-body loading, Rae[26] has computed a normalized loading curve for a semi-infinite plane wing centrally mounted on an infinite cylindrical body which is given in Fig. 12. By adding this loading imposed at the wing leading edge to the negative of the same loading imposed at the trailing edge, the solution

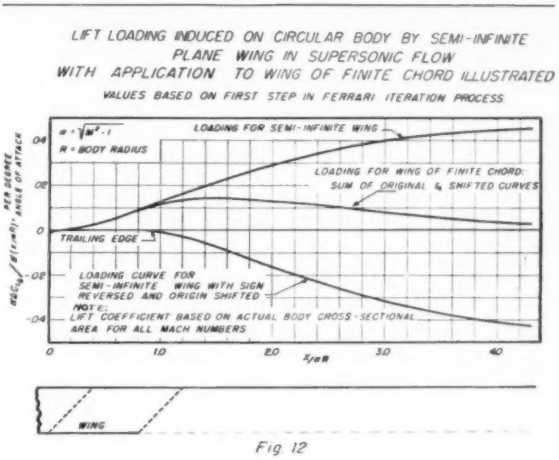
LIFT LOADING INDUCED ON CIRCULAR BODY BY SEMI-INFINITE PLANE WING IN SUPERSONIC FLOW
WITH APPLICATION TO WING OF FINITE CHORD ILLUSTRATED
VALUES BASED ON FIRST STEP IN FERRARI ITERATION PROCESS
LOADING FOR SEMI-INFINITE WING
R = BODY RADIUS
LOADING FOR WING OF FINITE CHORD: SUM OF ORIGINAL & SHIFTED CURVES
TRAILING EDGE
LOADING CURVE FOR SEMI-INFINITE WING WITH SIGN REVERSED AND ORIGIN SHIFTED
NOTE: LIFT COEFFICIENT BASED ON ACTUAL BODY CROSS-SECTIONAL AREA FOR ALL MACH NUMBERS
WING

Fig. 12

for a wing of finite chord may be obtained as illustrated in Fig. 12.

Since the ratio of lift on the body to lift on the wing has been shown to correlate so well with theory, even for low-aspect-ratio configurations, it would be a simple matter to compute the lift of a wing-body combination if an acceptable method for computing the lift on the wings could be devised. Fig. 13, which is based on reference 25, shows the spanwise loading on the various wings corresponding to the body loadings of Fig. 11, with the two-dimensional strip theory values for the wing without upwash, and for the wing subjected to the Beskin upwash also given for comparative purposes. It is clear that the actual wing loadings bear no simple relation to either of these limiting cases of theoretical loading. As a check on the assumption of Beskin upwash for these cases, the upwash produced along the wings by the finite body was computed; the comparison of these values with the Beskin upwash shown in Fig. 14 indicates that while there are differences they are generally small. For practical purposes, the calculation of wing lift can probably be carried out by using the Kirkby-Robinson formula, Eq. (209), in the region outside the root and tip Mach lines, and applying simplified corrections in these regions. For example, examination of Fig. 9 shows that an assumption that the average pressure in this region at any chordwise position is 90 per cent of its value on its value on the Mach line would give good results for total lift at least up to $x = 0.7R\sqrt{M^2 - 1}$. Similarly, simple results have been found for the experimental results on low-aspect-ratio delta and diamond wings with supersonic edges reported by Dye[53]; these wings have the same chord as the rectangular wings of Fig. 13. For these wings too (for the case of body and wings at a common angle of attack), it was found that the ratio of the measured pressures to the theoretical pressures on a delta wing alone did not vary by more than 10 per cent from the value at the Mach line inside the root Mach line.

In the formulation of approximations for wing-body interference problems, it is often useful to have available some general ideas as to the carry-over of lift from the wing to the body in the region of the wing rather than all along the body. Lagerstrom and Van Dyke have used what they have called "lift preservation theorems" based on planar configurations to arrive at such ideas. The reverse-flow theorems for wing-body combinations may be applied to arrive at such results for nonplanar configurations. Consider a rectangular wing of large span mounted on a body of revolution. Assume also that the wing is at angle of attack and the

SPANWISE - LIFT DISTRIBUTIONS ON WINGS
OF WING - BODY COMBINATIONS
M = 2.00

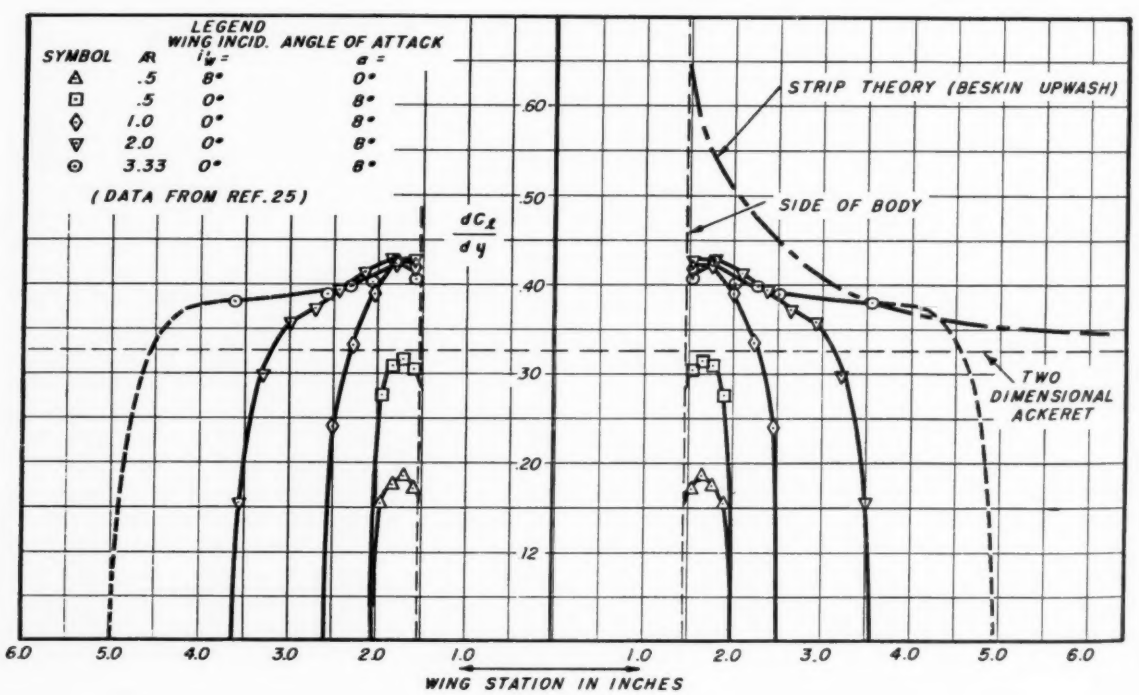

Fig. 13

body at zero. Then any amount of lift which is lost by the exposed wings (relative to the two-dimensional value) is recovered by a region on the surface of the body which is bounded by the intersection of the body with the plane Mach wave from the trailing edge at the rear and by the intersection of the body with the Mach cone from the wing root at the front. This region of "lift preservation" is shown in Fig. 15. The proof of this result may be obtained by the use of Eq. (26). In reverse flow, consider the wing at unit angle of attack, but without the body. This induces normal components of velocity at the location of the surface of the body of amount equal to the z direction cosine of the normal to the body at every point. In direct flow, consider the exposed wings at unit angle of attack and with the body at zero angle of attack. The velocity normal to the body surface must be zero. The reverse-flow theorem is applied to the region outside the exposed wings and body contour. Eq. (26) then leads directly to the result that the total lift on the body plus exposed wings in direct flow must equal the lift carried by the exposed wings alone in reverse flow. Contributions to the integrals in Eq. (26) can only arise from the region of perturbed flow common to both the direct and reverse cases. This explains the particular shape of the bounding curves on the surface of the body. If analogies to the planar case are employed, the entire region of the body influenced by the direct flow up to the trailing edge is the region "preserving" the wing lift. On the other hand, the nonplanar theorem shows that the lift on the body up to the wing-trailing edge is somewhat greater than that necessary to make up for any loss in two-dimensional lift on the exposed wings.

Lagerstrom and Van Dyke,[21] and Morikawa[29] have used the planar analogs of the "lift preservation" theorem as the basis for calculating the lift on a wing-body combination without afterbodies by strip theory. They have then used slender-body theory to obtain an opposite limiting case for comparison, and have attempted to infer conclusions for intermediate cases by interpolation between these limiting cases. This procedure provides a reasonable estimate of the total lift, but provides no information relative to lift on the individual components. Further, the prediction of moments for configurations with long after bodies is not possible by such methods. For wing-body combinations with highly swept wings, slender-body theory probably gives good results both for total lift and for the components lifts. In this theory, however, the entire body lift is supposed to occur between the leading and trailing edges of the wings. For configurations of only moderate sweep, this may result in sizable errors in moment. A promising attack on the problem of "not-so-slender" wing-body combinations is being made at Cornell University by means of an extension of the Adams-Sears second-order theory.[16]

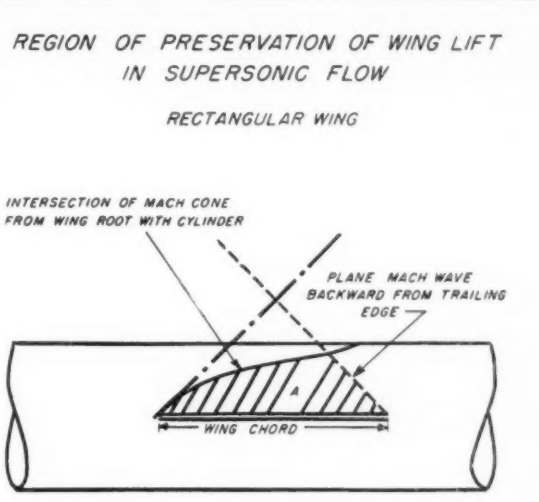

Fig. 15

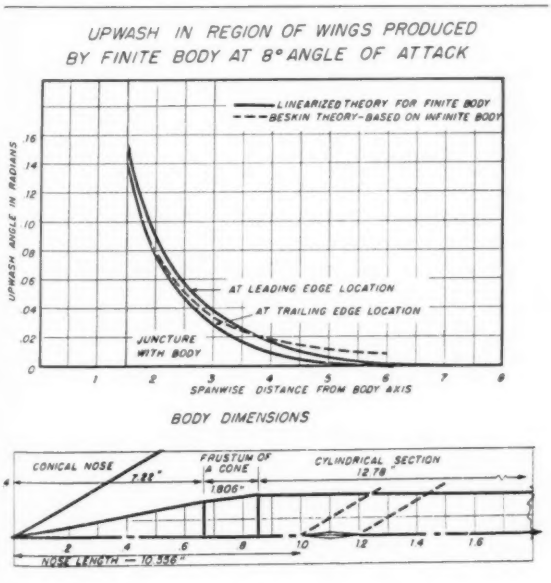

Fig. 14

References

[1] Lennertz, J., *Influence of the Airplane Body on the Wings*, Aerodynamic Theory; W. F. Durand, Editor, Vol. IV, Division K, Chapter III, Durand Reprinting Committee, 1943.

[2] Pepper, P. A., *Minimum Induced Drag in Wing-Fuselage Interference*, NACA TN 812, September, 1941.

[3] Multhopp, H., *Aerodynamics of the Fuselage*, NACA TM 1036, December, 1942.

[4] Flax, A. H., and Treanor, C. E., *A Variational Calculation of Subsonic Wing-Body Interference According to Lifting-Line Theory*, Cornell Aeronautical Laboratory. (To be published.)

[5] Weissinger, J., *The Lift Distribution of Sweptback Wings*, NACA TM 1120, March, 1947.

[6] Zlotnick, M., and Robinson, S. W., Jr., *A Simplified Mathematical Model for Calculating Aerodynamic Loading and Downwash for Midwing Wing-Fuselage Combinations with Wings of Arbitrary Planform*, NACA RN L52J27a, January, 1953.

[7] Spreiter, John R., *Aerodynamic Properties of Slender Wing-Body Combinations at Subsonic, Transonic, and Supersonic Speeds*, NACA TN 1662, July, 1948.

[8] Ward, G. N., *Supersonic Flow Past Slender Pointed Bodies*, Quarterly Journal of Mechanics and Applied Mathematics, Vol. II, Part I, pp. 76–97, 1949.

[9] Jones, R. T., *Properties of Low-Aspect-Ratio Pointed Wings at Speeds below and above the Speed of Sound*, NACA TR 835, 1946.

[10] Nonweiler, T., *The Theoretical Lift and Pitching Moment of a Highly-Swept Delta Wing on a Body of Elliptic Cross Section*, British ARC C.P. No. 58 (13,696), 1951.

[11] Kahane, A., *The Lift and Moment of Slender Elliptical Cross-Section, Body-Wing and -Fin Combinations*, Republic Aviation Corporation, Report No. EDR-57-152, November, 1952.

[12] Lawrence, H. R., *The Aerodynamic Characteristics of Low-Aspect-Ratio Wing-Body Combinations in Steady Subsonic Flow*, Cornell Aeronautical Laboratory Report, No. AF-743-A-6, November, 1952.

[13] Lawrence, H. R., *The Lift Distribution on Low-Aspect-Ratio Wings at Subsonic Speeds*, Journal of the Aeronautical Sciences, Vol. 18, No. 10, pp. 683–695, October, 1951.

[14] Lagerstrom, P. A., and Graham, M. E., *Aerodynamic Interference in Supersonic Missiles*, Douglas Aircraft Company, Report No. SM-13743, 1950.

[15] Moskowitz, B., *Approximate Theory for Calculation of Lift of Bodies, Afterbodies, and Combinations of Bodies*, NACA TN 2669, April, 1952.

[16] Adams, Mac C., and Sears, W. R., *Slender Body Theory—Review and Extension*, Journal of the Aeronautical Sciences, Vol. 20, No. 2, pp. 85–98, February, 1953.

[17] Kirkby, S., and Robinson, A., *Wing-Body Interference at Supersonic Speeds*, College of Aeronautics, Cranfield Report No. 7, April, 1947.

[18] Ferrari, C., *Interference between Wing and Body at Supersonic Speeds—Theory and Numerical Application*, Journal of the Aeronautical Sciences, Vol. 15, No. 6, pp. 317–336, June, 1948.

[19] Ferrari, C., *Interference between Wing and Body at Supersonic Speeds—Note on Wind Tunnel Results and Addendum to Calculations*, Journal of the Aeronautical Sciences, Vol. 16, No. 19, pp. 542–546, September, 1949.

[20] Morikawa, G. K., *The Wing-Body Problem for Linearized Supersonic Flow*, Progress Report No. 4-116, ORDICT Project, Jet Propulsion Laboratory, California Institute of Technology, December 19, 1949.

[21] Lagerstrom, P. A., and Van Dyke, M. D., *General Considerations about Planar and Non-Planar Lifting Systems*, Douglas Aircraft Company, Report SM-13432, June, 1949.

[22] Browne, S. H., Friedman, L., and Hodes, I., *A Wing-Body Problem in a Supersonic Conical Flow*, Journal of the Aeronautical Sciences, Vol. 15, No. 8, pp. 443–452, August, 1948.

[23] Nielsen, J. N., *Supersonic Wing-Body Interference*, Thesis, California Institute of Technology, 1951.

[24] Nielsen, J. N., and Pitts, W. C., *Wing-Body Interference at Supersonic Speeds with an Application to Combinations with Rectangular Wings*, NACA TN 2677, April, 1952.

[25] Cramer, R. H., *Wing-Body Interference at Supersonic Speeds—Recent Experimental Results and their Bearing on Advances in Theory*. Presented at Navy Bureau of Ordnance Symposium on Aeroballistics, May 13, 1952.

[26] Rae, W. J., *Generalized Distribution along the Body Axis of the Increment in Lift Produced by Interference from the Wing*, Cornell Aeronautical Laboratory Bumblebee Report CAL/CM-794. (To be published.)

[27] Schrenk, O., *Angenäherte Berechnung der gegenseitigen Beinflussung swischen Flügel und Rumpf im Überschallbereich* (Approximate Calculation of the Mutual Interference between Wing and Fuselage in the Supersonic Region), Z. angew. Math. Phys. 1, No. 3, pp. 202–209, May 15, 1950.

[28] Laitone, E. V., *First-Order Wing-Body Interference Effects*, Journal of Aeronautical Sciences, Readers' Forum, Vol. 16, No. 8, p. 510, August, 1949.

[29] Morikawa, G. K., *Supersonic Wing-Body Lift*, Journal of the Aeronautical Sciences, Vol. 18, No. 4, pp. 217–228, April, 1951.

[30] Beane, B., *The Effect of Planform on the Lift to Drag Ratio of Wing-Body Combinations at Supersonic Speeds*, Douglas Aircraft Company, Report No. SM-14454, July 30, 1952.

[31] Flax, A. H., *Integral Relations in the Linearized Theory of Wing-Body Interference*, Cornell Aeronautical Laboratory, Report No. CAL-45, November, 1952.

[32] Broderick, J. B., *Supersonic Flow round Pointed Bodies of Revolution*, Quarterly Journal of Mechanics and Applied Mathematics, Vol. 2, Part 1, pp. 98–120, 1949.

[33] Lighthill, M. J., *Methods for Predicting Phenomena in the High-Speed Flow of Gases*, Journal of the Aeronautical Sciences, Vol. 16, No. 2, pp. 69–83, 1949.

[34] Kellogg, O., *Foundations of Potential Theory*, p. 323, 1929; Ungar Publishing Company, New York.

[35] Lovitt, W. V., *Linear Integral Equations*, pp. 13–17, 1924; McGraw-Hill Book Company, Inc.

[36] Bleakney, W. M., and Morikawa, G. K., *Reciprocity Relations in Wing-Body Systems*, Journal of the Aeronautical Sciences, Vol. 19, No. 11, pp. 784–785, November, 1952.

[37] Flax, A. H., *General Reverse Flow and Variational Theorems in Lifting-Surface Theory*, Journal of the Aeronautical Sciences, Vol. 19, No. 6, pp. 361–374, June, 1952.

[38] Munk, Max M., *The Aerodynamic Forces on Airship Hulls*, NACA TR 184, 1924.

[39] von Kármán, Th., and Burgers, J. M., *General Aerodynamic Theory—Perfect Fluids*, Aerodynamic Theory; W. F. Durand, Editor, Vol. II, Div. E, Durand Reprinting Committee, 1943.

[40] Bleviss, Z. O., and Struble, R. A., *Some Aerodynamic Effects of Streamwise Gaps in Low-Aspect-Ratio Lifting Surfaces at Supersonic Speeds*, IAS Preprint No. 396, January, 1953.

[41] Morikawa, G. K., and Puckett, A. E., *Equivalence of the Spanwise Lift Distribution to the Spanwise Lift-Influence Function for Slender Wings and Wing-Bodies*, Journal of the Aeronautical Sciences, Readers' Forum, Vol. 18, No. 7, pp. 503–504, July 1951.

[42] Reissner, E., *Note on the Theory of Lifting Surfaces*, Proceedings of the National Academy of Sciences, Vol. 35, No. 4, pp. 208–215, April, 1949.

[43] Schlichting, H., *Monograph on the Aerodynamics of Mutual Interference between the Components of the Airplane*, National Research Council of Canada, Technical Translation No. TT-92, July, 1949.

[44] Jacobs, E. N., and Ward, K. E., *Interference of Wing and Fuselage from Tests of 209 Combinations in the NACA Variable-Density Tunnel*, NACA TR 540, 1935.

[45] Low, L., and Stone, H. N., *The Subsonic Aerodynamic Characteristics of Wings in Combination with Slender Bodies of Revolution*, Cornell Aeronautical Laboratory, Bumblebee Report No. CAL/CM-679, July, 1951.

[46] Goodman, A., *Effects of Wing Position and Horizontal-Tail Position on Static Stability Characteristics of Models with Unswept and 45° Sweptback Surfaces with some Reference to Mutual Interference*, NACA TN 2502, October, 1951.

[47] Cramer, R. H., *Interference between Wing and Body at Supersonic Speeds—Theoretical and Experimental Determination of Pressures on the Body*, Journal of the Aeronautical Sciences, Vol. 18, No. 9, pp. 629–632, September, 1951.

[48] von Kármán, Th., and Moore, N. B., *The Resistance of Slender Bodies Moving with Supersonic Velocities with Special Reference to Projectiles*, Transactions of the A.S.M.E., Vol. 54, pp. 303–310, December, 1932.

[49] Ackeret, J., *Air Forces on Airfoils Moving Faster than Sound*, NACA TM 317, June, 1925.

(*Continued on page 328*)

On the Stability of a Vortex Sheet in an Inviscid Compressible Fluid*

SHIH-I PAI†
University of Maryland

SUMMARY

The stability of a vortex sheet in an inviscid compressible fluid with respect to two-dimensional small disturbances is investigated. A new simple criterion for complete stability of this case is found. The significance of "supersonic," "sonic," and "subsonic" disturbances is discussed. It is found that only the "supersonic neutral stable disturbance" with respect to the free stream gives continuous eigen values. The determinantal equation for "supersonic" damped or self-excited disturbance with respect to the free stream here may be reduced to the same simple form as those for other subsonic or sonic disturbance and the eigen values so obtained are discrete.

INTRODUCTION

IN THE STUDY of the stability of flow of a compressible fluid, one of the most interesting problems is that the laminar flow of very high Mach Number tends to be completely stable with respect to small disturbances. To show such a complete stability, it is customary to discuss either the smallest eigen value[1, 2] of the determinantal equation which in general has an infinite number of eigen values, or the nonexistence of the "subsonic neutral stable disturbance" with respect to free stream velocity.[1, 2, 3] The following questions have never been fully clarified: (1) if the smallest eigen value shows a complete stability, what would be the effect of other higher eigen values? In other words, is it possible to show that all the eigen values of the determinantal equations give the possibility of complete stability? (2) We know that for the supersonic neutral disturbances with respect to the free stream the eigen values are continuous and not discrete. But is there any possibility of the existence of damped or self-excited supersonic disturbances with respect to the free stream? If so, what will be the eigen values of these disturbances? In this paper, we study one of the most simple examples of the stability of compressible flow, i.e., the stability of a vortex sheet or ideal jet in an inviscid compressible fluid with respect to two-dimensional small disturbances in order to throw some light on the above questions.

The problem of the stability of a vortex sheet in an inviscid compressible fluid has been studied by Landau[4] and Hiroshi Hatanaka[5] who both showed the possibility of complete stability at high Mach Numbers. Here we find a new simple criterion for the stability of the vortex sheet in a compressible fluid [Eq. (26)] and (Fig. 2). We also discuss the significance of the supersonic disturbances with respect to the free stream for this problem which has not been discussed before.

FUNDAMENTAL EQUATION AND SOLUTIONS

We consider a straight vortex sheet between two parallel streams within the domain $y = y_1$ and $y = y_2$ where y_1 and y_2 may be finite or infinite (Fig. 1). The velocity in the upper half plane ($y > 0$) is U_1 and that in the lower half plane ($y < 0$) is U_2. The vortex sheet is situated along the x-axis at the beginning, $t = 0$. We assume that the flows on both sides of the vortex sheet are potential flows because it is known that no vorticity can be produced in the interior of an inviscid fluid which is initially in irrotational motion and where the stagnation enthalpy and entropy are constant; hence the vorticity remains concentrated in the vortex sheet. The velocity potentials of the flows on both sides of the vortex sheet may be written as

$$\Phi_j = U_j x + \varphi_j \tag{1}$$

where $j = 1$ or 2. Subscript 1 refers to flow in the upper half plane ($y > 0$) and subscript 2, that in the lower half plane ($y < 0$). φ_j are the perturbed velocity potentials which are produced when the vortex sheet is slightly disturbed so that it has the shape $\eta = \eta(x,t)$.

The differential equation which governs the small disturbances φ_j is

$$1/a_j^2\,[(\partial^2\varphi_j/\partial t^2) + 2U_j(\partial^2\varphi_j/\partial x\partial t)] = [(1 - M_j^2)\,(\partial^2\varphi_j/\partial x^2)] + (\partial^2\varphi_j/\partial y^2) \tag{2}$$

where a_j is the sound speed corresponding to the basic flow velocity U_j and $M_j = U_j/a_j$, the Mach Number of the basic flow.

Since the disturbance $\eta = \eta(x,t)$ is two-dimensional in nature, we may assume that

$$\varphi_j = \Psi_j(y)e^{i\alpha(x - Ct)} \tag{3}$$

where $\Psi_j(y)$ is the disturbance amplitude function, α is

Received September 1, 1953.

* This paper was written when the author visited the Aeronautical Engineering Department of The Pennsylvania State College during August of 1953, supported by ONR Contract Nonr 656(01). The author wishes to express his appreciation to Professor Martin Lessen for his interest in this problem and to Mr. John A. Fox for his help in numerical calculations and the drawings.

† Associate Research Professor, Institute for Fluid Dynamics and Applied Mathematics.

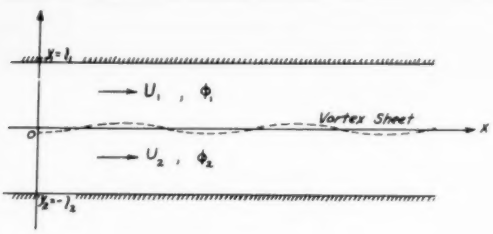

Fig. 1 Vortex Sheet in Inviscid Compressible Fluid

the disturbance wave number, C is the disturbance phase velocity which may be complex, i.e.,

$$C = C_r + iC_i \tag{4}$$

Substituting Eq. (3) into Eq. (2), we have

$$\Psi_j'' - \alpha^2\sigma_j^2\Psi_j = 0 \tag{5}$$

where

$$\sigma_j^2 = 1 - [(U_j - C)/a_j]^2 \tag{6}$$

and prime means differentiation with respect to y.

The general solution of Eq. (5) is

$$\Psi_j(y) = A_{j1} \sinh \alpha\sigma_j y + A_{j2} \cosh \alpha\sigma_j y \tag{7}$$

where A_{j1} and A_{j2} are arbitrary constants. Since Eq. (2) is a linear equation, the method of superposition may be used here to find complicated solutions.

Subsonic, Sonic, and Supersonic Disturbances

It is convenient in the study of the stability of flow of a compressible fluid to classify the disturbances as "subsonic," "sonic," and "supersonic" relative to a certain local velocity when the x-component of the phase velocity of the disturbance relative to the local velocity is less than, equal to, or greater than the mean speed of sound at that point, respectively. In the present problem, such disturbances may be classified with respect to U_j. For such classified disturbances we have

(1) $C_i = 0$ neutral stable disturbance

$$\sigma_j = \begin{cases} \text{pure imaginary—supersonic} \\ \text{zero—sonic} \\ \text{real—subsonic} \end{cases} \text{ with respect to } U_j.$$

(2) $U_j = C_r$

σ_j = real, for all cases.

(3) $C_i \neq 0$ damped or self-excited disturbances

σ_j = complex number, for all cases.

The significant result is that only for supersonic neutral stable disturbances with respect to U_j, is σ_j pure imaginary which will give continuous eigen values. For all other disturbances, it will be shown later that the eigen values for the stability of a vortex sheet are discrete.

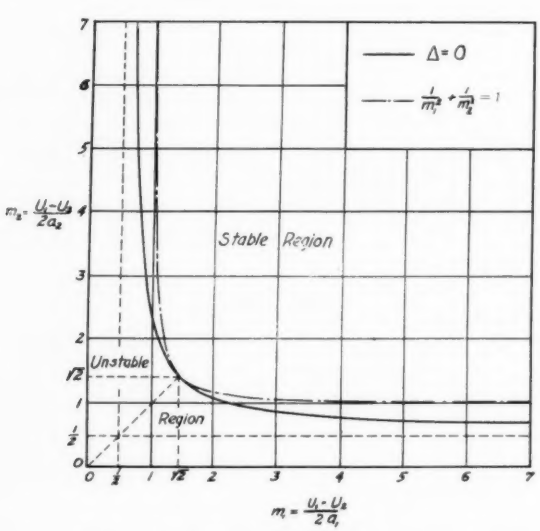

Fig. 2 Stability Criterion of Vortex Sheet in Compressible Flow

Boundary Conditions

The boundary conditions on the vortex sheets are:

(1) the velocity components of the fluid perpendicular to the vortex sheet are equal on both sides and equal to the movement of the vortex sheet itself in that direction. If the higher order terms are neglected, this condition may be written as:

$$\partial\eta/\partial t = (\partial\varphi_j/\partial y) - [U_j(\partial\eta/\partial x)] \tag{8}$$

where the expression of η may be written as

$$\eta(x,t) = Be^{i\alpha(x - Ct)} \tag{9}$$

where B is a small constant. The expression of Eq. (9) is assumed because of the expression of Eq. (3).

(2) The other boundary condition is that the pressures on both sides of the vortex sheet are equal, i.e.,

$$\frac{\gamma_1}{a_1^2}\left[U_1\frac{\partial\varphi_1}{\partial x} + \frac{\partial\varphi_1}{\partial t}\right] = \frac{\gamma_2}{a_2^2}\left[U_2\frac{\partial\varphi_2}{\partial x} + \frac{\partial\varphi_2}{\partial t}\right] \tag{10}$$

where γ_j = the ratio of specific heats (C_p/C_v) on each side of the vortex sheet.

As to the boundary conditions at y_1 and y_2, the following three different problems may be studied:

(1) Vortex sheet between solid walls at $y = y_1$ and $y = y_2$. In this case, the disturbance velocity components perpendicular to the walls are zero, i.e.,

$$\begin{aligned} \partial\varphi_1/\partial y &= 0 \quad \text{at } y = y_1 = l_1 \\ \partial\varphi_2/\partial y &= 0 \quad \text{at } y = y_2 = -l_2 \end{aligned} \tag{11}$$

where l_1 and l_2 are positive real numbers.

(2) Two-dimensional jet with $y = y_2$ as the axis of symmetry of the jet. It is well known that in this case the disturbances may be separated into antisymmetrical and symmetrical disturbances. These disturbances may be treated independently. For anti-

symmetrical disturbances, the boundary conditions at $y = y_i$ are the same as those of Eq. (11) while for a symmetrical disturbance, the value of $\partial v/\partial y$ must be zero at $y = y_2$, and then the boundary conditions at $y = y_i$ are

$$\begin{aligned} \partial\varphi_1/\partial y &= 0 \qquad \text{at } y = y_1 = l_1 \\ \partial^2\varphi_2/\partial y^2 &= 0 \qquad \text{at } y = y_2 = -l_2 \end{aligned} \tag{12}$$

Eigen Value Equations

If we substitute the general solution Eq. (7) into the boundary conditions Eqs. (8), (10), (11), or (12) with the help of Eq. (9) the eigen value equation may be obtained. For a vortex sheet and an antisymmetrical disturbance of a two-dimensional jet, we have

$$\{\sigma_1/[\gamma_1(1 - \sigma_1^2)]\} \tanh \alpha\sigma_1 l_1 = -\{\sigma_2/[\gamma_2(1 - \sigma_2^2)]\} \tanh \alpha\sigma_2 l_2 \tag{13}$$

For a symmetrical disturbance of a two-dimensional jet we have

$$\{\sigma_1/[\gamma_1(1 - \sigma_1^2)]\} \tanh \alpha\sigma_1 l_1 = -\{\sigma_2/[\gamma_2(1 - \sigma_2^2)]\} \coth \alpha\sigma_2 l_2 \tag{14}$$

Cases for Semi-infinite or Infinite Domain

It is usually desirable to study the stability of the vortex sheet itself without the influence of the solid wall $y = y_j$. Then we may assume that l_j tends to be infinite. We have to find the limiting value of $\tanh \alpha\sigma_j l_j$ as l_j tends to be infinite in Eqs. (13) and (14). Now

$$\tanh \alpha\sigma_j l_j = (\tanh \alpha\sigma_{jr} l_j + \tanh i\alpha\sigma_{ji} l_j) \div (1 + \tanh \alpha\sigma_{jr} l_j \tanh i\alpha\sigma_{ji} l_j) \tag{15}$$

where

$$\sigma_j = \sigma_{jr} + i\sigma_{ji} \tag{16}$$

If $\sigma_{jr} \neq 0$, we have

$$\lim_{l_j \to \infty} \tanh \alpha\sigma_j l_j = \pm 1 \tag{17}$$

If $\sigma_{jr} = 0$, we have

$$\lim_{l_j \to \infty} \tanh \alpha\sigma_j l_j = \lim_{l_j \to \infty} i \tan \alpha\sigma_{ji} l_j \tag{18}$$

Since $\tan \infty$ may be any value, the limiting value of Eq. (18) may be any value.

From the analysis of the classification of disturbances, we know that only for the supersonic neutral disturbance with respect to U_j, is the value of σ_j pure imaginary. Only for such supersonic neutral disturbances, the eigen value α may be any value, i.e., both Eqs. (13) and (14) give a continuous spectrum of α. For all the other disturbances, including supersonic damped or self-excited disturbances with respect to U_j the eigen values are discrete and may be obtained from Eqs. (13) or (14) with the help of Eq. (17).

Vortex Sheet in an Infinite Domain of Fluid

For a vortex sheet in an infinite domain of fluid, both l_1 and l_2 tend to be infinite. With the exception of supersonic neutral disturbances with respect to U_j, Eq (13) becomes

$$\sigma_1^2/[\gamma_1^2(1 - \sigma_1^2)^2] = \sigma_2^2/[\gamma_2^2(1 - \sigma_2^2)^2] \tag{19}$$

Now we assume that $\gamma_1 = \gamma_2$ and put

$$M_1 = (U_1 - C)/a_1, \quad M_2 = (U_2 - C)/a_2 \tag{20}$$

Eq. (19) becomes

$$M_1^2 M_2^2 = M_1^2 + M_2^2 \tag{21}$$

where $M_1 \neq M_2$.

We write

$$\left.\begin{aligned} A &= \frac{C_1}{U} \\ C &= C_1 + [(U_1 + U_2)/2] \\ U &= (U_1 - U_2)/2 = m_1 a_1 = m_2 a_2 \end{aligned}\right\} \tag{22}$$

then Eq. (21) becomes

$$A^4 - [2 + (1/m_1^2) + (1/m_2^2)]A_2^2 - 2[(1/m_1^2) - (1/m_2^2)]A + [1 - (1/m_1^2) - (1/m_2^2)] = 0 \tag{23}$$

The complete stability condition is that all of the four roots of Eq. (23) must be real. Since $1/m_1^2 + 1/m_2^2 > 0$, the sufficient conditions that all the roots of Eq. (23) are real are: (a)

$$(1/m_1^2) + (1/m_2^2) \geq 1 \tag{24}$$

and (b) the discriminant Δ of Eq. (23) is greater than zero,[6] i.e.,

$$\Delta > 0 \tag{25}$$

By Eq. (24) and the Descartes rule of sign, we see that Eq. (23) has at least two real roots, because without loss of generality, if we take $1/m_1^2 - 1/m_2^2 > 0$, there will be one positive real root since there is only one change in sign of Eq. (23) and one or three negative roots since there are three changes in sign. But $\Delta > 0$ means that Eq. (23) has four distinct real roots or two pairs of complex roots.[6] Combining these two conditions, we have that Eq. (23) has four real roots.

The discriminant of Eq. (23) after simplification may be written as follows:

$$\Delta = [64 - (48/m_1^2) - (48/m_2^2) + (12/m_1^4) - (84/m_1^2 m_2^2) + (12/m_2^4) - (1/m_1^6) - (3/m_1^4 m_2^2) - (3/m_1^2 m_2^4) - (1/m_2^6)]\, 64/m_1^2 m_2^2 \tag{26}$$

The boundary line of stability in m_1, m_2 plane* is

* Dr. F. W. Geiger of Cornell Aeronautical Laboratory has informed the author that he found by geometrical considerations a criterion in place of Eqs. (26) and (27). Even though it is difficult to reduce Eq. (26) into the formula of Dr. Geiger analytically, by numerical calculation (Fig. 2) the result of Eq. (26), $\Delta = 0$, is identical to that given by the formula of Dr. Geiger whose result will be published by Cornell Aeronautical Laboratory.

$$\Delta = 0 \tag{27}$$

which is shown in Fig. 2. Since the condition of Eq. (24) always holds for the point just on the right side of $\Delta = 0$ curve in Fig. 2, the region on the right side of $\Delta = 0$ curve is the stable region, i.e., in this region, the vortex sheet is completely neutrally stable with respect to small two-dimensional disturbances. Only neutrally stable disturbances can occur in this region with definite velocity of propagation for subsonic neutral disturbances with respect to U_j and with all kinds of velocity of propagation for supersonic neutral disturbances with respect to U_j. The stability condition Eq. (27) also holds for $(1/m_1^2) + (1/m_2^2) < 1$ which shows also that the four roots may be all real.

When $m_1 = m_2 = m$, i.e., $a_1 = a_2 = a$, we have the complete stability criterion as

$$m > \sqrt{2} \tag{28}$$

When either one of m_1 and m_2 is infinity, the other for stability condition will be larger than one half, i e.,

$$m_2 > 1/2 \qquad \text{if} \qquad m_1 = \infty \tag{29}$$

The interesting result in this section is that it is possible to show that all the eigen values of the determinantal equation show complete stability for flow of high Mach Numbers, i.e., large value of m_j.

The above analysis gives the same order of magnitude of Mach Number for complete stability, i.e., $(U_1 - U_2)/a > 2\sqrt{2}$ as the analyses of references 2 and 3 where the stability condition is $(U_1 - U_2)/a > 2.5$. Here we do not use the unconvincing argument of the nonexistence of subsonic neutral stable disturbances with respect to free stream but solve the complete determinantal equation which includes the "supersonic" damped or self-excited disturbances with respect to the free stream if they exist.

References

[1] Lees, L., *The Stability of the Laminar Boundary Layer in a Compressible Fluid*, NACA TN 1360, 1947.

[2] Pai, S. I., *On the Stability of Two-Dimensional Laminar Jet Flow of Gas*, Journal of the Aeronautical Sciences, Vol. 18, No. 11, pp. 731–742, 1951.

[3] Lin, C. C., *On the Stability of the Laminar Mixing Region between Two Parallel Streams in a Gas*, NACA TN 2887, 1953.

[4] Landau, L., *Stability of Tangential Discontinuities in Compressible Fluid*, Akademiia Nauk S.S.S.R. Comptes rendus Doklady), Vol. 44, No. 4, pp. 139–141, 1944.

[5] Hiroshi Hatanaka, *On the Stability of a Surface of Discontinuity in a Compressible Fluid*, Jour. Soc. Sci. Culture, Japan, Vol. 2, pp. 3–7, 1947.

[6] Conkwright, N. B., *Introduction to the Theory of Equations* Ginn and Company, 1941.

Wing-Body Interference at Subsonic and Supersonic Speeds—Survey and New Developments

(*Continued from page 324*)

[50] Cramer, R. H., *Interference between Wing and Body at Supersonic Speeds—Part V: Phase One Wind-Tunnel Tests Correlated with Linear Theory*, Cornell Aeronautical Laboratory, Bumblebee Report No. CAL/CM-597, December, 1950.

[51] Beskin, L., *Determination of Upwash around a Body of Revolution at Supersonic Velocities*, Consolidated-Vultee Aircraft Corporation, Bumblebee Report No. CM-251, May, 1946.

[52] Nichols, S., *Interference between Wing and Body at Supersonic Speeds—Part VIII: Data Report—Pressure Distribution Tests of Wing-Body Interference Models at a Mach No. of 2.00–Phase IV Tests*, Cornell Aeronautical Laboratory, Bumblebee Report No. CAL/CF-1571, July, 1951.

[53] Dye, F. E., Jr , *Interference between Wing and Body at Supersonic Speeds—Part X: Data Report—Pressure Distribution Tests of Wing-Body Interference Models at a Mach No. of 2.00–Phase VI Tests*, Cornell Aeronautical Laboratory, Bumblebee Report No. CAL/CF-1856, September, 1952.

[54] Rae, W. J., *Interference between Wing and Body at Supersonic Speeds—Part XI: Data Report—Pressure Distribution Tests of Wing-Body Interference Models at a Mach No. of 2.00—Phase VII Tests*, Cornell Aeronautical Laboratory, Bumblebee Report No. CAL/CF-1886. (To be published.)

[55] Nielsen, J. N., and Matteson, F. H., *Calculative Method for Estimating the Interference Pressure Field at Zero Lift on a Symmetrical Sweptback Wing Mounted on a Circular Cylindrical Body*, NACA RM 495, August, 1949.

[56] Tsien, Hsue-Shen, *Supersonic Flow over an Inclined Body of Revolution*, Journal of the Aeronautical Sciences, Vol. 5, No. 12. pp. 480–483, October, 1938.

Postbuckling Behavior of Axially Compressed Circular Cylindrical Shells*

JOSEPH KEMPNER†
Polytechnic Institute of Brooklyn

SUMMARY

The postbuckling characteristics of an axially compressed thin-walled circular cylindrical shell loaded either by dead weights or by a rigid testing machine are determined. It is shown that for either loading condition the minimum applied stress in the postbuckling region is $0.182(Et/R)$ and that the region of stable equilibrium corresponding to loading by the rigid testing machine includes and extends beyond that obtained with dead weight loading. The work here described is a continuation of work done earlier by von Kármán and Tsien, by Michielsen, and by Leggett and Jones.

INTRODUCTION

THE EXPLANATION OF THE discrepancies between experimentally determined failing stresses and those computed by the small deflection theory for axially compressed thin-walled circular cylindrical shells appears to have been attempted first with the aid of a large deflection theory by L. H. Donnell[1] in 1934. Including second order terms in the expressions for the median surface strains, Donnell derived a second-approximation compatibility equation which with energy considerations was applied to the determination of the postbuckling behavior of thin-walled circular cylindrical shells under axial compression. However, as pointed out by Donnell and Wan,[2] the analysis was oversimplified and hence led to an unsatisfactory solution.

In 1941 Th. von Kármán and H. S. Tsien[3] presented second approximation compatibility and equilibrium equations for the same problem. It is shown in reference 4, and in the present text, that their equilibrium equation was incomplete. However, these investigators did not use the equilibrium equation but, like Donnell, applied the principle of stationary potential energy. The results presented in reference 3 indicated that a buckled cylinder could be maintained in equilibrium under an axial stress considerably below the critical stress computed from small deflection theory.

In the past ten years the work of von Kármán and Tsien has been refined and extended by several investigators.[2, 5, 6] In references 5 and 6 the compatibility equation, energy expressions, and assumed deflected shape were accepted from reference 3 and the principle of stationary potential energy was again applied. However, in contrast to the analysis of reference 3, in references 5 and 6 the energy was made stationary with respect to all arbitrary deflection parameters, whereas in reference 3 parameters characterizing the number of circumferential waves and the ratio of the circumferential and axial wave lengths were fixed. From the more rigorous analysis it was found that the smallest applied axial compressive stress σ required to maintain the cylinder in a state of equilibrium with finite wave amplitude corresponded to $\sigma R/Et = 0.195$. This value is considerably less than the critical value of the classical linear theory which is $\sigma R/Et = 0.605$.

In reference 2, the analyses of references 5 and 6 were extended to include the effect of an additional arbitrary parameter in the assumed deflected shape, as well as the effect of various types of initial imperfections in the cylinder. However, the solutions of the resulting set of equations for the deflection parameters were calculated rigorously only for loads between 100 and 75 per cent of the classical critical load; at lower loads certain restrictions on the parameters were introduced. With these approximations the minimum postbuckling value of $(\sigma R/Et)$ for an initially perfect cylinder was found to be approximately 0.26 (Fig. 8, reference 2). Since the investigators were primarily interested in the greatest axial load a cylinder with given imperfections could resist, the postbuckling region investigated was considerably smaller than that of references 5 and 6.

The present investigation is an extension of Michielsen's and Leggett and Jones' continuation of von Kármán and Tsien's work.[6, 5, 3] The energy expressions of reference 3 are used to derive the corresponding equilibrium equations. The equations for equilibrium of membrane stresses are then used in the determination of a suitable compatibility equation. With the expression for the radial displacements at buckling obtained from classical linear theory as a first approximation, the equation of equilibrium of radial forces and the compatibility equation are iterated to obtain a suitable second approximation. This approximation includes the deflected shape assumed in reference 2 which in turn includes the shape assumed in refer-

Received March 23, 1953.

* Based upon a dissertation submitted to the Polytechnic Institute of Brooklyn, August, 1949, in partial fulfillment of the requirements for the degree of Doctor of Philosophy. The work reported on was jointly sponsored by the Office of Naval Research and the Bureau of Ships under Contract No. N6onr-26303, Project No. NR 064-167 and Contract No. N6onr-26308, Project No. NR 064-298. The author is indebted to Professor N. J. Hoff for his encouragement and to Mr. Sharad A. Patel for his assistance during the course of the analysis.

† Assistant Professor of Aeronautical Engineering.

ences 3, 5, and 6. In order to make tractable the computations involved in the energy solution of the problem, only that part of the second approximation for the deflected shape which corresponds to that assumed in reference 2 (in that region where the parameters were unrestricted) was considered. Thus in the present investigation one more arbitrary deflection parameter is introduced than in references 3, 5, and 6.

The analysis shows that, for a cylinder axially compressed by either a dead weight or a rigid testing machine, the minimum value of $(\sigma R/Et)$ consistent with finite-deflection equilibrium configurations is 0.182. Furthermore, it is seen that the equilibrium configurations are identical for the two types of loading. However, the results of a stability analysis indicate that the rigid testing machine affords a range of stable equilibrium including and extending beyond that obtained with a dead-weight loading.

Symbols

A_{11}, A_{19}, A_{91}	= functions of wave-length ratio
D	= $(1/12)Et^3/(1-\nu^2)$
E	= modulus of elasticity
$F(x,y)$	= airy stress function
L	= shell length
R	= mean shell radius
U_1, U_2, U_3	= nondimensional energy quantities
W_1, W_2, W_3, W_4	= extensional strain energy, bending strain energy, potential of applied axial load, potential of applied lateral load, respectively
a, b, c, d, e	= deflection parameters
d_{11}, d_{20}, d_{02}	= stress function parameters for first approximation
$f_{11}, f_{22}, f_{13}, f_{31}, f_{20}, f_{02}$	= stress function parameters
m, n	= numbers of axial and circumferential waves, respectively
p	= inward radial pressure
t	= wall thickness
u, v, w	= axial, circumferential, and radial displacements, respectively
x, y	= axial and circumferential coordinates on median surface of shell, respectively
$\gamma_{xy}, \epsilon_x, \epsilon_y$	= median surface shear, axial, and circumferential strains, respectively
ϵ	= unit end shortening
η	= $(t/R)n^2$
λ_x, λ_y	= axial and circumferential half wave lengths, respectively
μ	= (λ_y/λ_x)
ν	= Poisson's ratio (0.3)
ξ	= deflection parameter
$\sigma_x, \sigma_y, \tau_{xy}$	= axial, circumferential, and shear median surface stresses, respectively
σ	= applied average axial compressive stress
ω	= $\xi\eta$
∇^4	= $(\partial^4/\partial x^4) + 2(\partial^4/\partial x^2\,\partial y^2) + (\partial^4/\partial y^4)$

Underlying Assumptions

In the ensuing analysis the thin-walled circular cylindrical shell of uniform thickness is assumed to be stressed elastically and to be of sufficient length such that the effects of end restraints are negligible. N. Nojima and S. Kanemitsu have shown that the latter assumption is valid if the length is greater than 1.5 times the radius. The results of their investigations are described in reference 7. With only axial stresses applied to the shell, omission of the effects of end restraint leads to the condition of zero average circumferential and shear stresses.

In addition to the foregoing assumptions, the changes of curvatures in the axial and circumferential directions and the twist of the median surface are assumed to be $(\partial^2 w/\partial x^2)$, $(\partial^2 w/\partial y^2)$, and $(\partial^2 w/\partial x \partial y)$, respectively, where w is the inward radial displacement and x and y the coordinates of a point on the median surface of the shell (Fig. 1). Justification of the use of these simple expressions was given by Donnell in reference 8.

Basic Relations

The following relations upon which the present analysis is based are given in reference 3.

Median Surface Strains

With terms up to the second order included, the axial and circumferential median surface strains ϵ_x and ϵ_y, and the median surface shear strain γ_{xy} of a thin circular cylindrical shell of radius R are

$$\left.\begin{aligned} \epsilon_x &= (\partial u/\partial x) + (1/2)\,(\partial w/\partial x)^2 \\ \epsilon_y &= (\partial v/\partial y) + (1/2)\,(\partial w/\partial y)^2 - (w/R) \\ \gamma_{xy} &= (\partial u/\partial y) + (\partial v/\partial x) + (\partial w/\partial x)\,(\partial w/\partial y) \end{aligned}\right\} \quad (1)$$

in which u, v, and w are displacements of a point of the median surface in the axial, circumferential, and inward radial directions, respectively (Fig. 1).

Median Surface Stresses

The axial, circumferential, and shear stresses in the median surface are from Eqs. (1) and from the usual form of Hooke's law for thin shells

$$\left.\begin{aligned} \sigma_x &= [E/(1-\nu^2)]\,\{(\partial u/\partial x) + (1/2)\,(\partial w/\partial x)^2 + \nu[(\partial v/\partial y) + (1/2)\,(\partial w/\partial y)^2 - (w/R)]\} \\ \sigma_y &= [E/(1-\nu^2)]\,\{(\partial v/\partial y) + (1/2)\,(\partial w/\partial y)^2 - (w/R) + \nu[(\partial u/\partial x) + (1/2)\,(\partial w/\partial x)^2]\} \\ \tau_{xy} &= [E/2(1+\nu)]\,\{(\partial u/\partial y) + (\partial v/\partial x) + (\partial w/\partial x)\,(\partial w/\partial y)\} \end{aligned}\right\} \quad (2)$$

in which σ_x and σ_y are positive in tension; E is the modulus of elasticity; and ν is Poisson's ratio (0.3 in subsequent calculations).

Extensional Stain Energy

The elastic energy corresponding to the median surface stresses can be expressed as

$$W_1 = (t/2E)\int_0^L \int_0^{2\pi R} [(\sigma_x + \sigma_y)^2 - 2(1+\nu)\,(\sigma_x\sigma_y - \tau_{xy}^2)]\,dx\,dy \quad (3)$$

in which L is the length and t the wall thickness of the shell.

Bending Strain Energy

With the curvatures and twist mentioned under "Underlying Assumptions," the energy of bending becomes

$$W_2 = (D/2)\int_0^L\int_0^{2\pi R}\{[(\partial^2 w/\partial x^2) + (\partial^2 w/\partial y^2)]^2 - 2(1-\nu)[(\partial^2 w/\partial x^2)(\partial^2 w/\partial y^2) - (\partial^2 w/\partial x\ \partial y)^2]\}dx\,dy \quad (4)$$

in which $D = (1/12)Et^3/(1-\nu^2)$.

Potential of External Loads

The potential energy of the axial stresses applied to the ends of the shell can be expressed as

$$W_3 = -t\int_0^{2\pi R}(\sigma_x)_{x=L}\,dy\int_0^L(\partial u/\partial x)\,dx \quad (5)$$

The potential energy of an applied external radial pressure p is

$$W_4 = -\int_0^L\int_0^{2\pi R} pw\,dx\,dy \quad (6)$$

If a variation of the total potential is contemplated for axial loads applied by a rigid testing machine, then $\delta W_3 = 0$ since no axial displacements are permitted.

Equilibrium and Compatibility Equations

Addition of Eqs. (3) to (6) and subsequent variation of the total potential yields the following three equilibrium equations, as well as boundary conditions which are not given here:

$$(D/t)\nabla^4 w = (p/t) + (\partial/\partial x)(\sigma_x\partial w/\partial x) + (\partial/\partial y)(\tau_{xy}\partial w/\partial x) + (\partial/\partial x)(\tau_{xy}\partial w/\partial y) + (\partial/\partial y)(\sigma_y\partial w/\partial y) + (\sigma_y/R) \quad (7)$$

$$(\partial\sigma_x/\partial x) + (\partial\tau_{xy}/\partial y) = 0 \quad (8)$$

$$(\partial\tau_{xy}/\partial x) + (\partial\sigma_y/\partial y) = 0 \quad (9)$$

in which $\nabla^4 = (\partial^4/\partial x^4) + 2(\partial^4/\partial x^2\,\partial y^2) + (\partial^4/\partial y^4)$.

In the derivation of Eqs. (7) to (9), Eqs. (2) were used to relate the stresses and displacements. It may be noted that the energy term W_3 of Eq. (5) does not contribute to Eqs. (7) to (9), but rather enters into the expressions for the boundary conditions.

Elimination of the stress derivatives obtained upon performance of the operations indicated in Eq. (7) with the aid of Eqs. (8) and (9) yields the following equilibrium equation:[4, 5]

$$(D/t)\nabla^4 w = (p/t) + \sigma_x(\partial^2 w/\partial x^2) + 2\tau_{xy}(\partial^2 w/\partial x\partial y) + \sigma_y(\partial^2 w/\partial y^2) + (\sigma_y/R) \quad (10)$$

Eqs. (8) and (9), which express the conditions of equilibrium of forces in the median surface, are identically satisfied by the introduction of the Airy stress function $F(x,y)$ defined by the relations

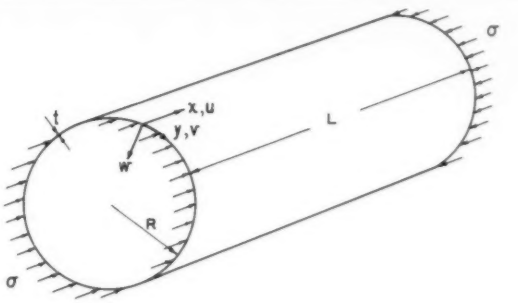

FIG. 1 COORDINATES AND COMPONENTS OF DISPLACEMENTS OF A POINT ON MEDIAN SURFACE OF AXIALLY COMPRESSED THIN-WALLED CYLINDER

$$\sigma_x = (\partial^2 F/\partial y^2), \qquad \tau_{xy} = -(\partial^2 F/\partial x\,\partial y), \qquad \sigma_y = (\partial^2 F/\partial x^2) \quad (11)$$

Combination of Eqs. (2), (8), (9), and (11) yields

$$\nabla^4 F = E[(\partial^2 w/\partial x\,\partial y)^2 - (\partial^2 w/\partial x^2)(\partial^2 w/\partial y^2) - (1/R)(\partial^2 w/\partial x^2)] \quad (12)$$

This compatibility equation was first developed in reference 1.

With the aid of Eqs. (11) and (12), an alternative form of the equilibrium Eq. (10) is found to be

$$(D/t)\nabla^8 w + (E/R^2)(\partial^4 w/\partial x^4) = \nabla^4[(p/t) + (\partial^2 F/\partial y^2)(\partial^2 w/\partial x^2) - 2(\partial^2 F/\partial x\,\partial y)(\partial^2 w/\partial x\,\partial y) + (\partial^2 F/\partial x^2)\times(\partial^2 w/\partial y^2)] + (E/R)(\partial^2/\partial x^2)[(\partial^2 w/\partial x\,\partial y)^2 - (\partial^2 w/\partial x^2)(\partial^2 w/\partial y^2)] \quad (13)$$

Except for the last term on the right-hand side, Eq (13), with $p = 0$, is identical to von Kármán and Tsien's Eq. (12) of reference 3. It was indicated in reference 4 that omission of this term, which is of the same order

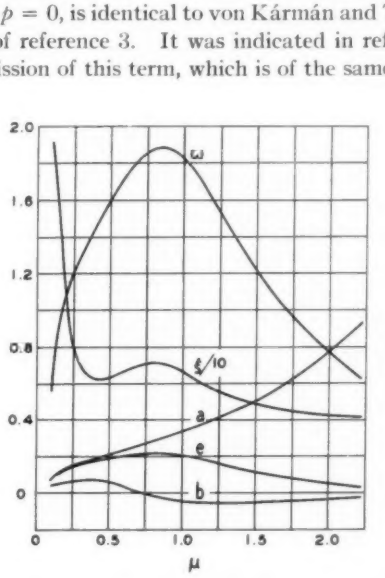

FIG. 2 VARIATION OF PARAMETERS a, b, e, ξ AND ω WITH WAVE-LENGTH RATIO μ

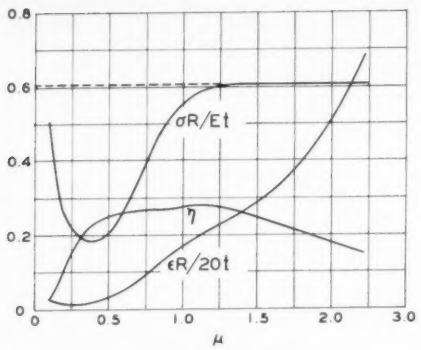

FIG. 3 VARIATION OF APPLIED STRESS, UNIT END SHORTENING AND WAVE NUMBER PARAMETER WITH WAVE-LENGTH RATIO

of magnitude as those remaining, may lead to considerable error in the analysis of the postbuckling behavior of axially compressed cylinders.

The form of the equilibrium equation used in the present analysis is from Eqs. (10) and (11) with $p = 0$

$$(D/t)\nabla^4 w = (\partial^2 F/\partial y^2)(\partial^2 w/\partial x^2) - 2(\partial^2 F/\partial x\,\partial y)(\partial^2 w/\partial x\,\partial y) + (\partial^2 F/\partial x^2)(\partial^2 w/\partial y^2) + (1/R)(\partial^2 F/\partial x^2) \quad (14)$$

Approximate Deflected Shape

The well-known deflection function which satisfies the linearized form of Eq. (13) can be expressed as

$$w_1 = \xi_1 t[\cos(\pi x/\lambda_{1x})\cos(\pi y/\lambda_{1y}) + e_1] \quad (15)$$

in which ξ_1, e_1, λ_{1x}, and λ_{1y} are independent of x and y, and the subscript 1 indicates a first approximation. Substitution of this approximation to w into the right-hand side of Eq. (12) and subsequent solution of the resulting equation yields

$$F_1 = d_{11}\cos(\pi x/\lambda_{1x})\cos(\pi y/\lambda_{1y}) + d_{20}\cos(2\pi x/\lambda_{1x}) + d_{02}\cos(2\pi y/\lambda_{1y}) - (\sigma_1/2)y^2 \quad (16)$$

in which d is a parameter and σ_1 is the average applied axial compressive stress. This expression for F satisfies the condition of zero average circumferential and shear stress and hence, as discussed earlier, reflects the neglect of edge restraints. Introduction of the expressions for w and F from Eqs. (15) and (16) into the right-hand side of Eq. (14) and determination of a particular solution of the resulting equation lead to the following form for a second approximation to w:

$$w = \xi t[\cos(\pi x/\lambda_x)\cos(\pi y/\lambda_y) + a\cos(2\pi x/\lambda_x) + b\cos(2\pi y/\lambda_y) + c\cos(\pi x/\lambda_x)\cos(3\pi y/\lambda_y) + d\cos(3\pi x/\lambda_x)\cos(\pi y/\lambda_y) + e] \quad (17)$$

in which ξ, a, b, c, d, and e are undetermined coefficients, and λ_x and λ_y are the half wave lengths in the axial and circumferential directions, respectively. That Eq. (17) represents a suitable choice for the form of the deflection function of an axially compressed thin-walled circular cylindrical shell is seen from reference 3. The deflection function assumed in this reference which was arrived at from physical observations is equivalent to Eq. (17) if $c = d = 0$ and $a = b$.

For the present analysis Eq. (17) will be applied with $c = d = 0$, and thus the undetermined quantities are ξ, a, b, e, λ_x, and λ_y. The resulting simplified expression for w corresponds to that used in the analysis of reference 2. In the present paper all the deflection parameters are determined from the principle of stationary potential energy whereas in much of the work presented in reference 2 it was found necessary to assume fixed values of a, b, and (λ_y/λ_x).

Stress Function

The expression for F obtained from the solution of Eq. (12) with w introduced from Eq. (17) is for $c = d = 0$:

$$F = -(Et^2/\mu^2\eta^2)[f_{11}\cos(\pi x/\lambda_x)\cos(\pi y/\lambda_y) + f_{22}\cos(2\pi x/\lambda_x)\cos(2\pi y/\lambda_y) + f_{13}\cos(\pi x/\lambda_x)\cos(3\pi y/\lambda_y) + f_{31}\cos(3\pi x/\lambda_x)\cos(\pi y/\lambda_y) + f_{20}\cos(2\pi x/\lambda_x) + \mu^4 f_{02}\cos(2\pi y/\lambda_y)] - (\sigma/2)y^2 \quad (18)$$

in which σ is the applied average axial compressive stress,

$$f_{11} = A_{11}\omega[2\omega(a+b) - 1]$$
$$f_{22} = A_{11}\omega^2 ab$$
$$f_{13} = 2A_{91}\omega^2 b$$
$$f_{31} = 2A_{19}\omega^2 a$$
$$f_{20} = (1/32)\omega(\omega - 8a)$$
$$f_{02} = (1/32)\omega^2$$

and

$$\omega = \xi\eta, \qquad \mu = (\lambda_y/\lambda_x), \qquad \eta = (t/R)n^2 = (\pi^2 Rt/\lambda_y^2)$$

$$A_{11} = \mu^4/(1+\mu^2)^2, \qquad A_{19} = \mu^4/(1+9\mu^2)^2, \qquad A_{91} = \mu^4/(9+\mu^2)^2$$

It may be noted that μ is the ratio of the circumferential and axial wave lengths and n is the number of circumferential waves. The number of axial waves m is related to λ_x by the expression $m = L/2\lambda_x$.

Unit End Shortening

Since the operator of a standard type testing machine has control only of the distance between movable and fixed platens, the unit end shortening of an axially compressed shell is one of the principal parameters of the present problem. It is defined as[3]

$$\epsilon = -(1/L)\int_0^L (\partial u/\partial x)\,dx \quad (19)$$

and is the ratio of the total shortening in the axial direction to the cylinder length. From the first two of Eqs. (2) and the first and third of Eqs. (11),

$$(\partial u/\partial x) = (1/E)\ [(\partial^2 F/\partial y^2) - \nu(\partial^2 F/\partial x^2)] - (1/2)\ (\partial w/\partial x)^2 \quad (20)$$

Hence from Eqs. (17) to (20) for $c = d = 0$,

$$(\epsilon R/t) = (\sigma R/Et) + (1/8)\ (\omega^2\mu^2/\eta)\ (1 + 8a^2) \quad (21)$$

Uniform Inward Displacement

That component of the total displacement which corresponds to a uniform inward displacement is given in Eq. (17) as ξte. Consideration of the condition that the displacement v must be a periodic function of y readily leads to the determination of e (reference 3). From Eqs. (2) and (11)

$$(\partial v/\partial y) = (1/E)\ [(\partial^2 F/\partial x^2) - \nu(\partial^2 F/\partial y^2)] - (1/2)\ (\partial w/\partial y)^2 + (w/R) \quad (22)$$

Eq. (22) together with Eqs. (17) and (18) and the periodicity condition yield (for $c = d = 0$)

$$\xi e = (1/8)\ (\omega^2/\eta)\ (1 + 8b^2) - \nu(\sigma R/Et) \quad (23)$$

in which $\xi = \omega/\eta$. Thus in Eq. (17), e is not an independent parameter.

Determination of the Deflection Parameters

The deflection parameters of Eq. (17) can be expressed in terms of a, b, η, μ, and ω. These parameters are determined from the condition that at equilibrium their values are such that the total potential energy of the system has a stationary value for any small variation of the parameters. This condition can be enforced for σ = constant (dead-weight loading) or ϵ = constant (rigid testing machine loading, $\delta W_3 = 0$). However, it can be readily verified that these two conditions lead to the same expressions for the deflection parameters.

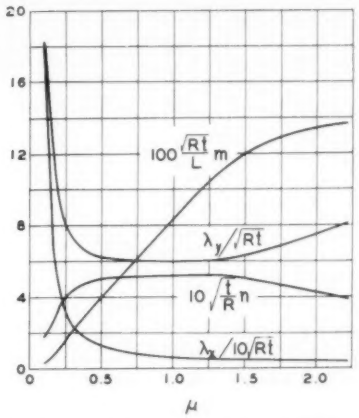

FIG. 4 VARIATION OF AXIAL AND CIRCUMFERENTIAL HALF WAVE LENGTHS AND NUMBERS OF WAVES WITH WAVE-LENGTH RATIO

From Eqs. (3), (4), (5), (11), (17), (18), and (20), the three energy quantities entering into the calculations become

$$U_1 = (\omega^2/\eta^2)\ \big(\omega^2\{A_{11}[(a + b)^2 + 4a^2b^2] + A_{19}a^2 + A_{91}b^2 + (\mu^4/128)\} + A_{11}[(1/4) - \omega(a + b)] + (1/128)\ (\omega - 8a)^2\big) + (\sigma R/Et)^2 \quad (24)$$

$$U_2 = [1/48(1 - \nu^2)]\omega^2[(1 + \mu^2)^2 + 32(\mu^4a^2 + b^2)] \quad (25)$$

$$U_3 = -2(\sigma R/Et)\ [(\sigma R/Et) + (1/8)\ (\omega^2\mu^2/\eta)\ (1 + 8a^2)] \quad (26)$$

in which

$$U_1 = (R/\pi Et^3L)W_1, \text{ etc.}$$

Expressed in terms of σ, the following five equations are obtained from enforcing the condition that the sum of U_1, U_2, and U_3 has a stationary value with respect to a, b, η, μ, and ω, respectively, for constant σ. With the aid of Eq. (21) these relations can be expressed in terms of the unit end shortening ϵ rather than the average axial compressive stress σ.

$$a = [(\omega/16)\ (8A_{11} + 1) - A_{11}\,\omega^2 b]/\{\omega^2[A_{11}\,(1 + 4b^2) + A_{19}] + [2/3(1 - \nu^2)]\mu^4\eta^2 - 2\mu^2\eta(\sigma R/Et) + (1/2)\} \quad (27)$$

$$b = [(A_{11}/2)\omega - A_{11}\omega^2 a]/\{\omega^2[A_{11}(1 + 4a^2) + A_{91}] + [2/3(1 - \nu^2)]\eta^2\} \quad (28)$$

$$\eta = \big(\omega^2\{A_{11}[(a + b)^2 + 4a^2b^2] + A_{19}a^2 + A_{91}b^2 + (\mu^4/128)\} + A_{11}[(1/4) - \omega(a + b)] + (1/128)\ (\omega - 8a)^2\big)/[(\mu^2/8)\ (\sigma R/Et)\ (1 + 8a^2)] \quad (29)$$

$$(\sigma R/Et) = \{8/[\mu^2\eta(1 + 8a^2)]\}\ \big(\omega^2\{[A_{11}/(1 + \mu^2)]\ [(a + b)^2 + 4a^2b^2] + [A_{19}a^2/(1 + 9\mu^2)] + [9A_{91}b^2/(9 + \mu^2)] + (\mu^4/128)\} + [A_{11}/(1 + \mu^2)]\ [(1/4) - \omega(a + b)] + [1/48(1 - \nu^2)]\ (1 + \mu^2 + 32\mu^2a^2)\mu^2\eta^2\big) \quad (30)$$

$$\omega^2\{A_{11}[(a + b)^2 + 4a^2b^2] + A_{19}a^2 + A_{91}b^2 + (1/128)\ (1 + \mu^4)\} - \omega(3/32)\ [8A_{11}(a + b) + a] + (1/8)\ \{A_{11} + 2a^2 + [1/12(1 - \nu^2)]\ [(1 + \mu^2)^2 + 32(\mu^4a^2 + b^2)]\eta^2 - \mu^2\eta(\sigma R/Et)\ (1 + 8a^2)\} = 0 \quad (31)$$

Eqs. (29) and (31) can be combined to yield an equation independent of σ.

$$\eta^2 = 3(1 - \nu^2)\left\{4A_{11} + 8a^2 - \omega[8A_{11}(a + b) + a]\right\}/[(1 + \mu^2)^2 + 32(\mu^4 a^2 + b^2)] \tag{32}$$

Similarly Eqs. (30), (31), and (32) yield a relation which is independent of σ and η.

$$\omega^2\left\{A_{11}^{3/2}[(a + b)^2 + 4a^2b^2] + 9A_{19}^{3/2}a^2 + A_{91}^{3/2}b^2 + (1/128)\right\} - \omega\Big(A_{11}^{3/2}(a + b) + (a/8) - (\mu^2/16)\left\{(1 + \mu^2 + 32\mu^2a^2)\,[8A_{11}(a + b) + a]/[(1 + \mu^2)^2 + 32(\mu^4a^2 + b^2)]\right\}\Big) + (A_{11}^{3/2}/4) + (a^2/2) - \left\{(\mu^2/4)\,(1 + \mu^2 + 32\mu^2a^2)\,(A_{11} + 2a^2)/[(1 + \mu^2)^2 + 32(\mu^4a^2 + b^2)]\right\} = 0 \tag{33}$$

Hence, simultaneous solution of Eqs. (27), (28), (30), (32), and (33) for constant σ or constant ϵ [Eq. (21)] determines the parameters a, b, η, μ, and ω such that the total potential is stationary. It may be noted that if a, b, η, μ, and ω constitute a solution, then so does the set $-a$, $-b$, η, μ, and $-\omega$. However, the deflected shape of the shell [Eq. (17) with $c = d = 0$] is the same for the two solutions.

Stability Considerations

Although any solution of Eqs. (27), (28), (30), (32), and (33) corresponds to a state of equilibrium, it does not generally correspond to a state of stable equilibrium. For such a solution to represent a stable equilibrium state, it must correspond not only to the vanishing of the first variation of the total potential but also to a positive value of the second variation of this potential. Thus, since a solution of the aforementioned equations enforces the vanishing of the first variation of the potential, the condition that the solution correspond to a stable equilibrium configuration is that the second variation must be a positive definite quantity. The second variation is such a quantity provided that the determinant

$$|U_{ij}| > 0,\ i, j = a, b, \eta, \mu, \text{ and } \omega \tag{34}$$

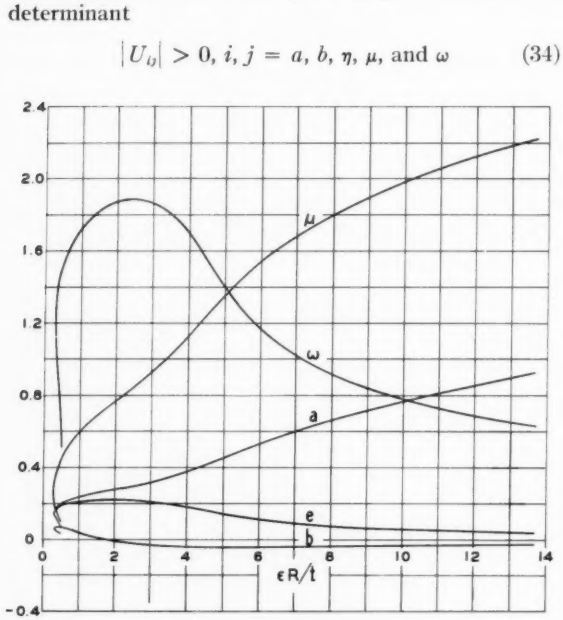

FIG. 5 VARIATION OF PARAMETERS a, b, e, ω AND μ WITH UNIT END SHORTENING

and each of its four leading subdeterminants is likewise positive. The quantity U_{ij} represents the total potential differentiated twice partially with respect to the parameters indicated by the subscripts. Although the first variation of the total potential led to identical relations among the deflection parameters for σ = constant (i.e., $\delta U = \delta U_1 + \delta U_2 + \delta U_3$) and ϵ = constant (i.e., $\delta U = \delta U_1 + \delta U_2$) such is not the case for the second variation; thus, the set of five stability determinants is not the same for σ = constant and ϵ = constant. Hence, in general, the two methods of loading can be distinguished on the basis of stability considerations.

Numerical Solution

In order to determine the postbuckling characteristics of the axially compressed shell, it is necessary to solve for the deflection parameters a, b, η, μ, and ω from the set of nonlinear algebraic Eqs. (27), (28), (30), (32), and (33) for a range of the applied compressive stress σ (or unit end shortening ϵ). Such solutions can be obtained with a suitable numerical successive approximation procedure. Since the wave-length ratio parameter appears in these equations in a rather complicated manner, it is more expedient to fix μ and solve for $(\sigma R/Et)$ along with the remaining deflection parameters than it is to fix $(\sigma R/Et)$ and solve for all the deflection parameters. Thus for a given value of μ, first approximations are assumed for a and b, thereby reducing Eq. (33) to a quadratic in ω. A value of ω obtained from the solution of this equation together with the given μ and the assumed a and b permit the direct computation of the corresponding η and $(\sigma R/Et)$ parameters from Eqs. (32) and (30), respectively. Substitution of the calculated values of ω, η, and $(\sigma R/Et)$ into Eqs. (27) and (28) determines new values for a and b which in general differ from those first assumed. In the procedure used, for each assumed value of a, several values of b are chosen until the calculated value of b [Eq. (28)] is equal to the assumed value. Thus a set of values for a and b is determined such that the difference Δb between the assumed and calculated values of b is zero. Similarly, for each assumed value of a, a value of b is also determined such that Δa is zero. In these calculations plots of Δa and Δb vs. b for each assumed a are helpful. To assist in the determination of a set of values a, b for which Δa and Δb are simultaneously zero, $\Delta a = 0$ and $\Delta b = 0$-curves are plotted

in the ab-plane. The intersection of these curves determines a and b, which in turn determine ω, η, and $(\sigma R/Et)$, such that Eqs. (27), (28), (30), (32), and (33) are satisfied for the assumed value of μ. The entire procedure must be repeated for a suitable number of μ-values. By means of Eq. (21) the stress parameter $(\sigma R/Et)$ can be related to the end shortening parameter $(\epsilon R/t)$ once a solution of the simultaneous equations is found.

Results and Discussion

The results of the solution of Eqs. (27), (28), (30), (32), and (33) are presented in Figs. 2 to 4 as functions of the wave length ratio μ, and in Figs. 5 to 7 as functions of the unit end shortening parameter $(\epsilon R/t)$. In Fig. 6 the deflection parameter ξ and the applied stress σ are compared with the corresponding quantities determined by Michielsen in reference 6. In this reference, as well as in reference 5, the minimum value of the applied stress in the postbuckling region was found to be $0.195(Et/R)$ at $\mu \approx 0.40$. In the present analysis this minimum stress was found to be $0.182(Et/R)$ at $\mu = 0.362$. These results compare favorably, and both are considerably below the critical value of classical theory $0.605(Et/R)$. In reference 6 Michielsen points out that the value of $(\sigma R/Et)$ reaches a maximum of 0.77, whereas the present solution leads to no such maximum but rather indicates that for large values of $(\epsilon R/t)$ or μ the value of $(\sigma R/Et)$ approaches asymptotically the critical value of classical theory 0.605 (Fig. 3 or 6). In Fig. 6 the straight line segment of the $(\sigma R/Et)$ vs. $(\epsilon R/t)$-curve drawn from the origin corresponds to the prebuckled state of the shell. It terminates at the classical buckling stress $0.605(Et/R)$.

Application of the stability conditions discussed earlier showed that in the postbuckling region for a deadweight loading the solution described corresponds to stable equilibrium configurations for the region of the curves defined by $\mu > 0.362$. The lower bound of μ corresponds to the minimum value of applied stress $0.182(Et/R)$. However, if the load is applied by a rigid testing machine, the region of stability increases to $\mu > 0.25$, the lower bound of which corresponds to the minimum value of the unit end shortening found to be $0.307(t/R)$. Thus from the $(\sigma R/Et)$ vs. $(\epsilon R/t)$-curve of Fig. 6, the region of postbuckling stable equilibrium configurations is represented by the portion of the curve to the right of the point of minimum stress for deadweight loading and to the right of the point of minimum unit end shortening for rigid testing machine loading. The remaining region of the postbuckling curve for each case of loading represents unstable configurations. The results of the stability analysis for loading by means of a rigid testing machine are in complete agreement with the analysis of Tsien in reference 9. In this reference it was found that a column supported laterally by nonlinear supports and loaded

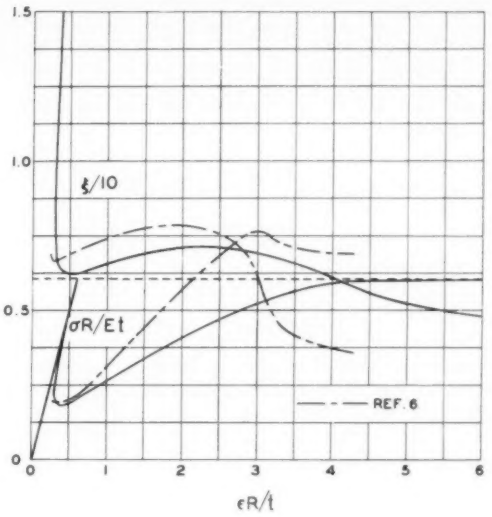

FIG. 6 VARIATION OF DEFLECTION PARAMETER ξ AND STRESS σ WITH UNIT END SHORTENING AND COMPARISON WITH REF. 6

axially by a rigid testing machine became unstable when $d\epsilon/d\sigma = 0$. Tsien has also proposed a method with which the results of analyses of the type presented here can be used to determine conditions which correspond to the transition from an unbuckled to a buckled state.[10]

References

[1] Donnell, L. H., *A New Theory for the Buckling of Thin Cylinders under Axial Compression and Bending*, Trans. ASME, Vol. 56, p. 795, 1934.

[2] Donnell, L. H., and Wan, C. C., *Effect of Imperfections on Buckling of Thin Cylinders and Columns under Axial Compression*, Jour. App. Mech., Vol. 17, No. 1, p. 73, March, 1950.

(*Continued on page 342*)

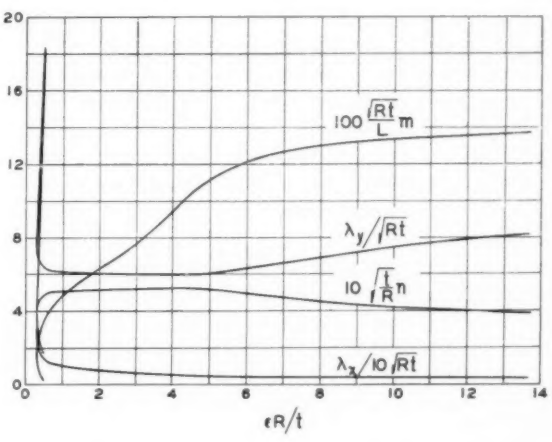

FIG. 7 VARIATION OF AXIAL AND CIRCUMFERENTIAL HALF WAVE LENGTHS AND NUMBERS OF WAVES WITH UNIT END SHORTENING

A Guide to the Use of the M.I.T. Cone Tables*

RICHARD C. ROBERTS† AND JAMES D. RILEY†
U.S. Naval Ordnance Laboratory

SUMMARY

The second and third volumes of the M.I.T. cone tables have been found to be unsatisfactory in two respects. They have been criticized because of their inconvenient tabulation and because the theory on which they are based is inadequate near the cone surface. The former is eliminated by means of a coordinate transformation. Empirical evidence is presented to show that the latter may be ignored in practice. The exact nature of certain numerical errors in the table is also pointed out.

INTRODUCTION

THE THREE VOLUMES of the M.I.T. tables[1, 2, 3] for supersonic flow over right circular cones with attached shocks were originally prepared to provide a handy catalog of this important type of conical flow. The first volume, containing the results for unyawed cones, is tabulated so as to give easy access to the variables in any part of the flow field. However, several authors[4, 7–10] have noted that the results for yawing cones, contained in the latter two volumes, are not so satisfactory.

The two reasons for the unsatisfactory character of these two volumes of tables may be stated briefly as follows:

(1) The tables are not tabulated in the most convenient coordinate system for practical use.

(2) The method of solution used to compute the tables is not valid near the surface of the cone.

The first of these difficulties may be easily remedied by a change of coordinates as noted by Van Dyke, Young, and Siska.[4] This brief note was expanded by Young and Siska[9] into a report giving formulas for the flow variables in a coordinate system which is still not the most desirable one, since one of the angles is measured from the wind axis. This present report completes the transformation along the lines of their method A, which assumes that the intermediate surfaces are yawed with the solid cone and remain circular cones. However, their method B, although more complicated, has merit in that it renders the approximation for the complete flow uniformly valid, somewhat in the spirit of Lighthill's straining of coordinates.[15] The present method, as does their method A, has the disadvantage that it is not appropriate for part of the region just behind the shock. However, at the shock and for most of the flow field, the present method is entirely appropriate and is the most simple and direct.

The second difficulty was first noticed by Ferri.[7] He pointed out that the form of the Stone solution[5, 6] used to compute the tables was not valid near the surface of the cone. Briefly, Ferri showed that the entropy must be constant on the cone, while the perturbation solution of Stone gives a cosine variation in the entropy to the first order in the angle of yaw. He also gave a method for correcting the Stone solution near the cone.

The present authors have found that, although these corrections are logically necessary, they may be neglected in practice, as will be seen later. This is especially desirable since these corrections are difficult to apply in an unambiguous manner in the first order, and the second order corrections have never been derived.

This paper is intended to give a descriptive review of the problems mentioned above together with a collection of formulas that facilitate the use of the tables. Any one who is merely interested in using the formulas may turn immediately to the last section.

DESCRIPTION OF THE PROBLEM

The Stone theory[5, 6] has been developed in terms of spherical polar coordinates (r, θ, ϕ), with the axis $\theta = 0$ parallel to the flow at infinity. (These coordinates will hereafter be referred to as the wind coordinates.) The axis of the cone has the equation $\theta = \epsilon$, $\phi = 0$ (see Fig. 1). In the nonyaw case ($\epsilon = 0$), the axis of the cone and the axis $\theta = 0$ coincide. This means that the equations for the cone and the shock are $\theta = \theta_s$ and $\theta = \theta_w$, respectively. However when $\epsilon \neq 0$ (in our coordinate system ϵ is negative for positive angle of attack), then the cone axis does not lie parallel to the wind axis, and the flow quantities at $\theta = \theta_s$ are not generally those on the surface of the cone. Likewise the flow quantities at $\theta = \theta_w$ are not in general those at the shock. In spite of this the range of the M.I.T. tables is $\theta_s \leq \theta \leq \theta_w$.

The range of θ given in the tables arises from the fact that Stone satisfied his boundary conditions at θ_s and θ_w instead of at the true positions of the cone and shock. This procedure is perfectly consistent with the perturbation method used by Stone, but can cause some confusion when the tables are to be used. The situation

Received November 11, 1953. Revised and received February 17, 1954.

* The authors wish to express their appreciation to the reviewing committee for the detailed constructive criticism.

† Mathematicians, Applied Mathematics Division.

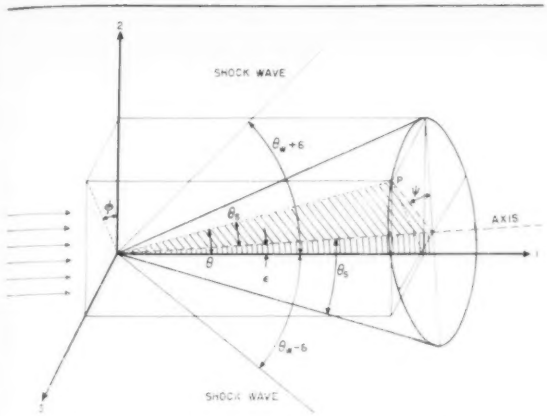

FIG. 1. Wind and body coordinate systems.

at the surface of the cone may be remedied by transforming the flow variables from wind coordinates to body coordinates (r, θ_r, ψ), where the polar axis is now the axis of the cone. When this is done, the equation $\theta_r = \theta_s$ is the equation for the cone. The equation for the shock is somewhat more complicated since the cone and the shock are not inclined at the same angle. This will be treated in a later section.

The perturbation method already referred to uses the angle of attack as the perturbing element. That is, the solution is expanded in powers of the angle of attack and the coefficients are calculated by substituting the expansions into the exact equations of motion and equating like powers of ϵ. Because of the assumption of conical flow these coefficients are functions of θ and ϕ alone. Reference 1 gives the zero order coefficients while references 2 and 3 give the first and second order coefficients, respectively.

The Coordinate Transformation

If the coordinates of a point in body coordinates (r, θ_r, ψ) are given and the flow quantities are desired at this point, one could compute to first or second order the coordinates (r, θ, ϕ) with respect to the wind axis and then compute the flow quantities by the Stone-Kopal equations. This procedure has the disadvantage that certain regions of the flow will be outside the range of the tables;* in particular, that section of the surface of the cone where $0 \leq \psi < \pi/2$ will be out of the range.

The following procedure is much more satisfactory and will be developed here. Transform the Stone-Kopal equations to body coordinates and then compute the flow quantities using the coordinates of the point (r, θ_r, ψ) as arguments directly.

This method has the advantages that the entire surface of the cone may be reached and that the formulas may be specialized to the surface of the cone, where the coefficients may be looked up with no interpolation; except between the tables for Mach Number, if desired.

It should then be noted that the velocity components computed will be the components in the wind coordinate system. Only the arguments of the components have so far been changed. The velocity components must then be changed to components in the body coordinate system.

The first and second order expansions will be discussed separately.

First Order Theory

In the first order theory the Stone-Kopal formulas associated with the tables are the following:

$$u = \bar{u} + \epsilon x \cos \phi \tag{1a}$$

$$v = \bar{v} + \epsilon y \cos \phi \tag{1b}$$

$$w = \epsilon z \sin \phi \tag{1c}$$

$$p = \bar{p} + \epsilon \eta \cos \phi \tag{1d}$$

$$\rho = \bar{\rho} + \epsilon \xi \cos \phi \tag{1e}$$

where u, v, w are the velocity components, p the pressure, and ρ the density. The coefficients $\bar{u}$, x, $\bar{v}$, y, z, $\bar{p}$, η, $\bar{\rho}$, and ξ are functions of θ alone, and the bars indicate the nonyaw quantities.

The above formulas refer to the wind coordinate system, and the velocity components are the components in this system. The quantities of general interest are those in which the axis of the cone itself is the central reference line, as is pointed out by Van Dyke, Young, and Siska.[4]

To the first order in ϵ, the transformation between the coordinate systems is $r = r$, $\theta = \theta_r + \epsilon \cos \psi$, $\phi = \psi - \epsilon \cot \theta_r \sin \psi$. Now if u, v, w are the velocity components with respect to the wind axis and u, V, W the components with respect to the body axis (the u component is the same in both systems), then Eqs. (1) become

$$u(\theta_r, \psi) = \bar{u} + [x + \bar{v}]\epsilon \cos \psi \tag{2a}$$

$$V(\theta_r, \psi) = \bar{v} + \left[y - \frac{\bar{a}^2(\bar{u} + \bar{v} \cot \theta_r)}{\bar{a}^2 - \bar{v}^2} - \bar{u} \right] \epsilon \cos \psi \tag{2b}$$

$$W(\theta_r, \psi) = (z - \bar{v} \csc \theta_r)\, \epsilon \sin \psi \tag{2c}$$

$$p(\theta_r, \psi) = \bar{p} + \left[\eta + \frac{\bar{a}^2 \bar{\rho} \bar{v} (\bar{u} + \bar{v} \cot \theta_r)}{\bar{a}^2 - \bar{v}^2} \right] \epsilon \cos \psi \tag{2d}$$

$$\rho(\theta_r, \psi) = \bar{\rho} + \left[\xi + \frac{\bar{\rho} \bar{v} (\bar{u} + \bar{v} \cot \theta_r)}{\bar{a}^2 - \bar{v}^2} \right] \epsilon \cos \psi \tag{2e}$$

where $\bar{a}$ is the nonyaw velocity of sound. Here the coefficients are to be evaluated from the tables, using for θ the angle θ_r measured from the body axis.

On the surface of the solid cone $\theta_r = \theta_s$, $\bar{v} = 0$, and $y = 2\bar{u}$. In this case Eqs. (2) reduce to Eqs. (1) with ψ replaced by ϕ and (1b) replaced by

* The tables could have been extended to cover these regions.

$$v = 0 \tag{1b'}$$

If the flow quantities are desired at the shock on the downstream side, a slight modification of the Eqs. (2), as pointed out in reference 4, is necessary. In each bracket, each term except the first should be multiplied by $\alpha = \delta/\epsilon$, where δ is the yaw of the shock cone, except in the formula for W. For example, at the shock wave,

$$u = \bar{u} + [x + \alpha\bar{v}]\epsilon \cos \psi \tag{3}$$

where the coefficients are to be taken from the tables with $\theta = \theta_w$. Since δ and ϵ are of like sign, α is a positive quantity. W is independent of α in the first order.

This coordinate transformation provides, in a sense, an extrapolation to certain regions neglected in the computations. This neglect was due to the simplification, mentioned previously, of shifting the boundary conditions.

Second Order Theory

When the yaw of the cone is larger, and second order approximations are desired, the formulas become considerably more complicated. In wind coordinates the formulas are as follows:

$$\left.\begin{aligned} u &= \bar{u} + \epsilon x \cos \phi + \epsilon^2(u_0 + u_2 \cos 2\phi) \\ v &= \bar{v} + \epsilon y \cos \phi + \epsilon^2(v_0 + v_2 \cos 2\phi) \\ w &= \epsilon z \sin \phi + \epsilon^2 w_2 \sin 2\phi \\ p &= \bar{p} + \epsilon\eta \cos \phi + \epsilon^2(p_0 + p_2 \cos 2\phi) \\ \rho &= \bar{\rho} + \epsilon\xi \cos \phi + \epsilon^2(\rho_0 + \rho_2 \cos 2\phi) \end{aligned}\right\} \tag{4}$$

where u, x, u_0, u_2, etc., are functions of θ.

To second order the relation between the coordinate systems is as follows (see also reference 6):

$$\left.\begin{aligned} r &= r \\ \theta &= \theta_r + \epsilon \cos \psi + {}^1/_2\epsilon^2 \cot \theta_r \sin^2 \psi \\ \phi &= \psi - \epsilon \cot \theta_r \sin \psi + \\ &\qquad {}^1/_4\epsilon^2(1 + 2 \cot^2\theta_r) \sin 2\psi \end{aligned}\right\} \tag{5}$$

Thus if f is any analytic function of θ, the value of f in body coordinates may be computed, to second order, by the formula:

$$f(\theta) = f(\theta_r) + \epsilon f'(\theta_r) \cos \psi + {}^1/_2\epsilon^2[f'(\theta_r) \cot \theta_r \sin^2 \psi + f''(\theta_r) \cos^2\psi] \tag{6a}$$

The following second order approximations also hold:

$$\left.\begin{aligned} \epsilon \cos \phi &= \epsilon \cos \psi + \epsilon^2 \cot \theta_r \sin^2 \psi \\ \epsilon \sin \phi &= \epsilon \sin \psi - {}^1/_2\epsilon^2 \cot \theta_r \sin 2\psi \\ \epsilon^2 \cos 2\phi &= \epsilon^2 \cos 2\psi \\ \epsilon^2 \sin 2\phi &= \epsilon^2 \sin 2\psi \end{aligned}\right\} \tag{6b}$$

The following formulas relate the velocity components to second order. (The radial component is the same in both systems.) (See also reference 6.)

$$\left.\begin{aligned} V &= v(1 - {}^1/_2\epsilon^2 \csc^2 \theta_r \sin^2 \psi) + \\ &\qquad w\epsilon \csc \theta_r \sin \psi \\ W &= w - v(\epsilon \csc \theta_r \sin \psi - \\ &\qquad {}^1/_2\epsilon^2 \csc \theta_r \cot \theta_r \sin 2\psi) \end{aligned}\right\} \tag{7}$$

Note that since w is itself a first order quantity the change in v is entirely second order and the first order change is nil.

Eqs. (4) transformed by Eqs. (6) and (7) are listed below.

$$u = \bar{u} + \epsilon(x + \bar{v}) \cos \psi + \epsilon^2(u_0 + {}^1/_4\bar{v}' + {}^1/_4\bar{v} \cot \theta_r + {}^1/_2y + {}^1/_2x \cot \theta_r) + \epsilon^2(u_2 + {}^1/_4\bar{v}' - {}^1/_4\bar{v} \cot \theta_r + {}^1/_2y - {}^1/_2x \cot \theta_r) \cos 2\psi \tag{8}$$

$$v = \bar{v} + \epsilon(y + \bar{v}') \cos \psi + \epsilon^2(v_0 + {}^1/_4\bar{v}'' + {}^1/_4\bar{v}' \cot \theta_r + {}^1/_2y' + {}^1/_2y \cot \theta_r) + \epsilon^2(v_2 + {}^1/_4\bar{v}'' - {}^1/_4\bar{v}' \cot \theta_r + {}^1/_2y' - {}^1/_2y \cot \theta_r) \cos 2\psi \tag{9}$$

$$V = \bar{v} + \epsilon(y + \bar{v}') \cos \psi + \epsilon^2(v_0 + {}^1/_4\bar{v}'' + {}^1/_4\bar{v}' \cot \theta_r - {}^1/_4\bar{v} \csc^2 \theta_r + {}^1/_2y' + {}^1/_2y \cot \theta_r + {}^1/_2z \csc \theta_r) + \epsilon^2(v_2 + {}^1/_4\bar{v}'' - {}^1/_4\bar{v}' \cot \theta_r + {}^1/_4\bar{v} \csc^2 \theta_r + {}^1/_2y' - {}^1/_2y \cot \theta_r - {}^1/_2z \csc \theta_r) \cos 2\psi \tag{10}$$

$$w = \epsilon z \sin \psi + \epsilon^2(w_2 + {}^1/_2z' - {}^1/_2z \cot \theta_r) \sin 2\psi \tag{11}$$

$$W = \epsilon(z - \bar{v} \csc \theta_r) \sin \psi + \epsilon^2\{w_2 + {}^1/_2z' - {}^1/_2z \cot \theta_r + {}^1/_2[\bar{v} \cot \theta_r - (y + \bar{v}')] \csc \theta_r\} \sin 2\psi \tag{12}$$

$$p/\bar{p} = 1 + [(\eta/\bar{p}) + (\bar{p}'/\bar{p})]\epsilon \cos \psi + \epsilon^2[(p_0/\bar{p}) + (\eta/2\bar{p}) \cot \theta_r + (\eta'/2\bar{p}) + (\bar{p}'/4\bar{p}) \cot \theta_r + (\bar{p}''/4\bar{p})] + \epsilon^2[(p_2/\bar{p}) - (\eta/2\bar{p}) \cot \theta_r + (\eta'/2\bar{p}) - (\bar{p}'/4\bar{p}) \cot \theta_r + (\bar{p}''/4\bar{p})] \cos 2\psi \tag{13}$$

$$\rho/\bar{\rho} = 1 + [(\xi/\bar{\rho}) + (\bar{\rho}'/\bar{\rho})]\epsilon \cos \psi + \epsilon^2[(\rho_0/\bar{\rho}) + (\xi/2\bar{\rho}) \cot \theta_r + (\xi'/2\bar{\rho}) + (\bar{\rho}'/4\bar{\rho}) \cot \theta_r + (\bar{\rho}''/4\bar{\rho})] + \epsilon^2[(\rho_2/\bar{\rho}) - (\xi/2\bar{\rho}) \cot \theta_r + (\xi'/2\bar{\rho}) - (\bar{\rho}'/4\bar{\rho}) \cot \theta_r + (\bar{\rho}''/4\bar{\rho})] \cos 2\psi \tag{14}$$

where the quantities are to be evaluated from the tables using for θ the value θ_r measured from the body axis, and (see also reference 9)

$$\bar{v}' = -\{[\bar{a}^2(\bar{u} + \bar{v} \cot \theta_r)]/(\bar{a}^2 - \bar{v}^2)\} - \bar{u} \tag{15}$$

$$\bar{v}'' = -\bar{v}'[\cot \theta_r + (\bar{p}'/\gamma\bar{p})] + \bar{v}[\cot^2 \theta_r - 1 + (1/\gamma)(\bar{p}'/\bar{p})^2 + (\bar{p}''/\gamma\bar{p})] \tag{16}$$

$$\bar{p}'/\bar{p} = [\gamma\bar{v}(\bar{u} + \bar{v} \cot \theta_r)]/(\bar{a}^2 - \bar{v}^2) \tag{17}$$

$$\bar{p}''/\bar{p} = \{(\bar{a}^2 - \gamma\bar{v}^2)/[\gamma(\bar{a}^2 - \bar{v}^2)]\}\,(\bar{p}'/\bar{p})^2 + (\bar{v}'/\bar{v})\cdot[(\bar{a}^2 + \bar{v}^2)/(\bar{a}^2 - \bar{v}^2)]\cdot(\bar{p}'/\bar{p}) + [\gamma\bar{v}\cot\theta_r(\bar{v}' - \bar{v}\cot\theta_r)]/(\bar{a}^2 - \bar{v}^2) \quad (18)$$

$$y' = -\{[\cot\theta_r + (\bar{p}'/\gamma\bar{p})]y + 2x + z\csc\theta_r + (\bar{v}/\gamma)\,[(\eta'/\bar{p}) - (\eta/\bar{p})\cdot(\bar{p}'/\bar{p})]\} \quad (19)$$

$$\frac{\eta'}{\bar{p}} = \frac{1}{\bar{a}^2 - \bar{v}^2}\left\{\left[\bar{a}^2\frac{\xi}{\bar{p}} - \bar{v}^2\frac{\eta}{\bar{p}}\right]\frac{\bar{p}'}{\bar{p}} - \gamma y(\bar{u} + \bar{v}') + \gamma\bar{v}x + y\bar{v}\left(\gamma\cot\theta_r + \frac{\bar{p}'}{\bar{p}}\right) + z\gamma\bar{v}\csc\theta_r\right\} \quad (20)$$

$$\xi'/\bar{\rho} = (1/\gamma)\,\{[(\xi/\bar{\rho}) - (\eta/\bar{p})]\,(\bar{p}'/\bar{p}) + (\eta'/\bar{p})\}; \qquad \bar{\rho}'/\bar{\rho} = \bar{p}'/\gamma\bar{p} \quad (21)$$

$$\bar{\rho}''/\bar{\rho} = [(1 - \gamma)/\gamma^2]\,(\bar{p}'/\bar{p})^2 + (1/\gamma)\,(\bar{p}''/\bar{p}) \quad (22)$$

$$z' = (\bar{a}^2/\gamma\bar{v})\cdot(\eta/\bar{p})\csc\theta_r - [(\bar{u}/\bar{v}) + \cot\theta_r]z \qquad (\theta_r \neq \theta_s) \quad (23)$$

These formulas are not strictly accurate, due to the change in coordinate system. However when used in the formulas for the flow variables all discrepancies fortunately become third order or higher.

The following alternative formulas for y' and $\bar{v}''$ also hold

$$\bar{v}'' = -(\bar{v}'A + \bar{v}B) \quad (16a)$$

where

$$A = \cot\theta_r + \lambda[2\bar{u} + 3\bar{v}\cot\theta_r + (\gamma + 1)\lambda\bar{v}(\bar{u} + \bar{v}\cot\theta_r)]$$
$$B = 1 - \cot^2\theta_r + \lambda[\lambda(\gamma - 1)\bar{u}(\bar{u} + \bar{v}\cot\theta_r) - \bar{v}\cot^2\theta_r]$$
$$\lambda = \bar{v}/(\bar{a}^2 - \bar{v}^2)$$

$$y' = -(Ay + Bx + Cd) \quad (19a)$$

where

$$Cd = [(1 + \lambda\bar{v})/(\sin^2\theta_r)]\,(x + z\sin\theta_r)$$

On the surface of the solid cone

$$\theta_r = \theta_s,\ \bar{v} = 0,\ y = 2\bar{u},\ \bar{v}' = -2\bar{u},\ \bar{p}' = 0$$
$$\bar{\rho}' = 0,\ \bar{\rho}''/\bar{\rho} = -2(\bar{u}/\bar{a})^2,\ \eta' = 2\bar{\rho}\bar{u}^2$$
$$\bar{p}'' = -2\bar{\rho}\bar{u}^2,\ \bar{v}'' = 2\bar{u}\cot\theta_s,\ \xi'/\bar{\rho} = 2(\bar{u}/\bar{a})^2$$
$$y' = -2\bar{u}\cot\theta_s - 2x - z\csc\theta_s,\ v_0 = x$$
$$v_2 = \bar{u}\cot\theta_s + z\csc\theta_s + x$$
$$z'^{*} = -2\bar{u}\csc\theta_s - z\cot\theta_s$$

Therefore

$$u(\theta_s, \psi) = \bar{u} + \epsilon x\cos\psi + \epsilon^2(u_0 + {}^1/_2\bar{u} + {}^1/_2x\cot\theta_s) + \epsilon^2(u_2 + {}^1/_2\bar{u} - {}^1/_2x\cot\theta_s)\cos 2\psi \quad (24)$$

$$v(\theta_s, \psi) = -\epsilon^2 z\csc\theta_s\sin^2\psi \quad (25)$$

$$V(\theta_s, \psi) = 0 \quad (26)$$

$$w(\theta_s, \psi) = \epsilon z\sin\psi + \epsilon^2(w_2 - \bar{u}\csc\theta_s - z\cot\theta_s)\sin 2\psi \quad (27)$$

$$W(\theta_s, \psi) = \epsilon z\sin\psi + \epsilon^2(w_2 - \bar{u}\csc\theta_s - z\cot\theta_s)\sin 2\psi \quad (28)$$

$$[p(\theta_s, \psi)]/[\bar{p}(\theta_s)] = 1 + \epsilon(\eta/\bar{p})\cos\psi + \epsilon^2[(p_0/\bar{p}) + (\gamma\bar{u}^2/2\bar{a}^2) + (\eta/2\bar{p})\cot\theta_s] + \epsilon^2[(p_2/\bar{p}) + (\gamma\bar{u}^2/2\bar{a}^2) - (\eta/2\bar{p})\cot\theta_s]\cos 2\psi \quad (29)$$

$$[\rho(\theta_s, \psi)]/[\bar{\rho}(\theta_s)] = 1 + \epsilon(\xi/\bar{\rho})\cos\psi + \epsilon^2[(\rho_0/\bar{\rho}) + (\bar{u}^2/2\bar{a}^2) + (\xi/2\bar{\rho})\cot\theta_s] + \epsilon^2[(\rho_2/\bar{\rho}) + (\bar{u}^2/2\bar{a}^2) - (\xi/2\bar{\rho})\cot\theta_s]\cos 2\psi \quad (30)$$

Note that on the cone $w = W$ to second order.

Use and Validity of the Theory

The transformed formulas of the previous section may now be easily used to compute the flow variables at points between the shock and the cone. We illustrate this by indicating the methods of computing the pressure coefficient C_p on the surface of the cone, where

$$C_p = (2/\gamma M^2)\,[(p/\bar{p})\cdot(\bar{p}/p_1) - 1]$$

In the above equation M is the free stream Mach Number and the subscript 1 refers to the free stream.

* Using L'Hospital's rule, as in reference 9.

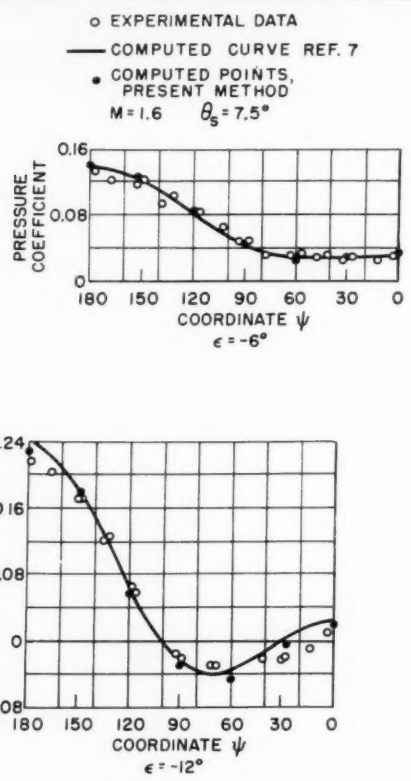

FIG. 2. Pressure distribution around the cone at $M = 1.6$.

C_p may be computed in either of two ways for both first and second order theory. We present both ways here and give only the recommended method in the next section. These methods consist of (a) computing $p/\bar{p}$ to the first or second order using the tables and previous formulas and computing $\bar{p}/p_1$ exactly to give p/p_1, or (b) computing the square of the speed q^2 using the tables and formulas, and obtaining p/p_1 from

$$p/p_1 = \Pi[(1 - q^2)/(1 - q_1^2)]^{\gamma/(\gamma-1)} \tag{31}$$

where

$$\Pi = \left(\frac{\gamma + 1}{2}\right)^{(\gamma+1)/(\gamma-1)} \left(\frac{\bar{M}^2}{1 + \frac{\gamma - 1}{2}\bar{M}^2}\right)^{\gamma/(\gamma-1)} \times \frac{1}{\left(\gamma\bar{M}^2 - \frac{\gamma - 1}{2}\right)^{1/(\gamma-1)}} \tag{32}$$

and

$$\bar{M}^2 = M^2 \sin^2 \theta_w \tag{33}$$

It has been pointed out[7] that when using (b) to first order better agreement with experimental data is obtained if the second order terms in $q^2 = u^2 + V^2 + W^2$ are retained, i.e., if u, V, and W are computed to first order before squaring.

So far we have tacitly assumed that the Stone theory, and as a consequence the last two volumes of the M.I.T. tables, are mathematically correct. However Ferri[7] has shown that the entropy distribution given by Stone is not correct at the surface of the cone. In fact the entropy must be constant there. Ferri then gives some corrections to the Stone theory which are designed to make it consistent with his general conclusions.

The actual method of applying these corrections is not clearly stated, so that we have been unable to reproduce his results. It turns out that the present theory may be applied without these corrections to give good results, as we shall show.

We now present some empirical evidence to support our thesis that the M.I.T. tables may still be used for practical results in spite of any theoretical objections to the Stone theory. In the following calculations we have used method (a) above, where $p/\bar{p}$ has been found to second order.

Figs. 2 and 3 show plots of the pressure coefficient on the cone surface against ψ. Also appearing in the graphs are Ferri's corrected results, which are first order, and some experimental data taken from references 7 and 8. The computations carried out by our method agree with the experimental data extremely well in all cases with the possible exception of the last graph. In making the computations for $M = 6.86$ it was necessary to use the fact that the pressure coefficient for hypersonic flow is essentially independent of the Mach Number. The data in the third volume of the M.I.T. tables go up only to $M = 4+$, which was the Mach Number used in our calculations. This may account for some of the discrepancy in the last graph.

It is really surprising that the theory gives such excellent results for angles of yaw as large as 14°. This is certainly better than would be expected from any preliminary analysis.

Our recommendation is that for a yaw less than about 6° method (b) be used to first order and that for a yaw greater than this the second order form of method (a) be used. Method (a) is more direct and is to be preferred for second order computation. However, using method (b) for first order permits the retention of the important second order terms (mentioned previously) without the use of any second order theory. No really sharp limits on the yaw angle can be set for the first order theory to hold since it will vary slightly with Mach Number, cone angle, etc. In all cases it would seem that the Ferri corrections may be neglected.

TABULAR ERRORS

Although many precautions were taken to avoid errors in computing the M.I.T. cone tables the second volume does contain a systematic error.[13] The tabulated values of z are incorrect. The error comes from

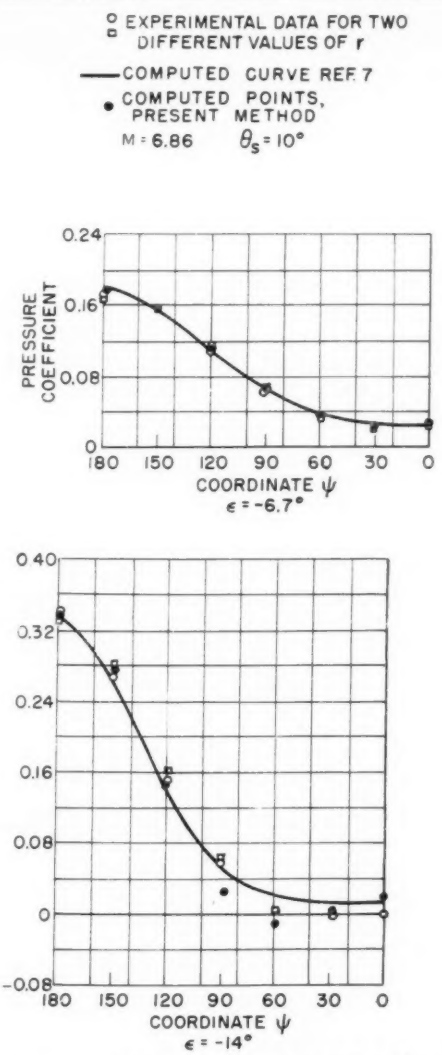

FIG. 3. Pressure distribution around the cone at $M = 6.86$.

using the wrong sign for C in computing from Eq. (34) of that report. The correct value of z is found as follows:

$$(\text{correct } z) = -(z \text{ from tables}) - (2x/\sin\theta)$$

Ferri, Ness, and Kaplite[12] suggested that the error just mentioned might have carried over into the third volume of the tables. By performing an indirect check it is easy to see that this is not the case.* Thus it appears that the only correction that need be made is one for z.

PROCEDURE FOR COMPUTATIONS

(A) On the Surface of the Cone

First Order.—Use Eqs. (1a)–(1e) for the flow quantities. Look up $\bar{u}$, x, z, $\eta/\bar{p}$ and $\xi/\bar{p}$ at a value of θ equal to the semi-apex angle θ_s of the solid cone. Use for ϵ the value of the angle of yaw in radians. If the pressure coefficient is desired, use formula (31) for p/p_1, keeping the second order terms which appear in q^2. Note also that $v = 0$.

Second Order.—Use formulas (24), (26), (28), (29), and (30) looking up all quantities at $\theta = \theta_s$ in the tables. If the pressure coefficient is desired, use formula (29) to compute $p/\bar{p}$, then compute $\bar{p}/p_1$ exactly, etc.

(B) Between the Shock Wave and the Solid Cone

In general, the flow quantities will be desired at points around the cone at a uniform distance from the surface of the cone. Therefore body coordinates will be used.

First Order.—Use formulas (2a)–(2e) looking up all quantities in the table using for θ the angle measured from the axis of the solid cone. If the pressure coefficient is desired, see the suggestion made for the surface of the cone.

Second Order.—Use formulas (8), (10), (12), (13), (14), and formulas (15)–(23) looking up all quantities in the tables using for θ the angle measured from the axis of the solid cone.

(C) At the Shock Wave on the Downstream Side

First Order.—Modify formulas (2a), (2b), (2d), and (2e) by multiplying each term in the coefficient of ϵ, except the first, by $\alpha = \delta/\epsilon$. The value of α may be obtained from the tables. Then use the modified formulas to compute the flow quantities, with $\theta_r = \theta_w$, and looking up all quantities in the tables using for θ the angle θ_w as given in the tables. Use formula (2c) without the above modification. These formulas are, of course, the terms remaining in the second order formulas (stated below) after neglecting terms with ϵ^2.

* In a private communication Prof. Kopal has confirmed the fact that the correct values of z were used in computing the third volume of the tables.

Second Order.—Use the formulas stated below together with formulas (15)–(23) with all quantities looked up in the tables at $\theta = \theta_w$.

$$u = \bar{u} + \epsilon(x + \alpha\bar{v})\cos\psi + \epsilon^2[u_0 + \tfrac{1}{2}x\cot\theta_w + \tfrac{1}{2}\alpha y + (\beta_0 + \tfrac{1}{2}\alpha\cot\theta_w)\bar{v} + \tfrac{1}{4}\alpha^2\bar{v}'] + \epsilon^2[u_2 - \tfrac{1}{2}x\cot\theta_w + \tfrac{1}{2}\alpha y + (\beta_2 - \tfrac{1}{2}\alpha\cot\theta_w)\bar{v} + \tfrac{1}{4}\alpha^2\bar{v}']\cos 2\psi \quad (34)$$

$$V = \bar{v} + \epsilon(y + \alpha\bar{v}')\cos\psi + \epsilon^2[v_0 + (1/2)y\cot\theta_w + \tfrac{1}{2}\alpha y' + (\beta_0 + \tfrac{1}{2}\alpha\cot\theta_w)\bar{v}' + \tfrac{1}{4}\alpha^2\bar{v}'' - \tfrac{1}{4}\bar{v}\csc^2\theta_w + \tfrac{1}{2}z\csc\theta_w] + \epsilon^2[v_2 - (1/2)y\cot\theta_w + \tfrac{1}{2}\alpha y' + (\beta_2 - \tfrac{1}{2}\alpha\cot\theta_w)\bar{v}' + \tfrac{1}{4}\alpha^2\bar{v}'' + \tfrac{1}{4}\bar{v}\csc^2\theta_w - \tfrac{1}{2}z\csc\theta_w]\cos 2\psi \quad (35)$$

$$W = \epsilon(z - \bar{v}\csc\theta_w)\sin\psi + \epsilon^2[w_2 + {}^1/_2\alpha z' - {}^1/_2 z\cot\theta_w + {}^1/_2\alpha\bar{v}\csc\theta_w\cot\theta_w - {}^1/_2(y + \alpha\bar{v}')\csc\theta_w]\sin 2\psi \quad (36)$$

$$p/\bar{p} = 1 + \epsilon[(\eta/\bar{p}) + \alpha(\bar{p}'/\bar{p})]\cos\psi + \epsilon^2\{(p_0/\bar{p}) + [(1/2)(\eta/\bar{p})\cot\theta_w + (\alpha/2)\cdot(\eta'/\bar{p}) + [\beta_0 + (\alpha/2)\cot\theta_w](\bar{p}'/\bar{p}) + (\alpha^2/4)\cdot(\bar{p}''/\bar{p})\} + \epsilon^2\{(p_2/\bar{p}) - [(1/2)(\eta/\bar{p})\cot\theta_w] + (\alpha/2)\cdot(\eta'/\bar{p}) + [\beta_2 - (\alpha/2)\cot\theta_w](\bar{p}'/\bar{p}) + (\alpha^2/4)\cdot(\bar{p}''/\bar{p})\}\cos 2\psi \quad (37)$$

$$\rho/\bar{\rho} = 1 + \epsilon\{(\xi/\bar{\rho}) + [\alpha(\bar{\rho}'/\bar{\rho})]\}\cos\psi + \epsilon^2\{(\rho_0/\bar{\rho}) + [{}^1/_2(\xi/\bar{\rho})]\cot\theta_w + (\alpha/2)\cdot(\xi'/\bar{\rho}) + [\beta_0 + (\alpha/2)\cot\theta_w](\bar{\rho}'/\bar{\rho}) + (\alpha^2/4)\cdot(\bar{\rho}''/\bar{\rho})\} + \epsilon^2\{(\rho_2/\bar{\rho}) - [{}^1/_2(\xi/\bar{\rho})]\cot\theta_w + (\alpha/2)\cdot(\xi'/\bar{\rho}) + [\beta_2 - (\alpha/2)\cot\theta_w](\bar{\rho}'/\bar{\rho}) + (\alpha^2/4)\cdot(\bar{\rho}''/\bar{\rho})\}\cos 2\psi \quad (38)$$

REFERENCES

[1] Staff of the Computing Section, Center of Analysis (under direction of Zdeněk Kopal), *Tables of Supersonic Flow Around Cones*, Tech. Report No. 1, M.I.T., 1947.

[2] Staff of the Computing Section, Center of Analysis (under direction of Zdeněk Kopal), *Tables of Supersonic Flow Around Yawing Cones*, Tech. Report No. 3, M.I.T., 1947.

[3] Staff of the Computing Section, Center of Analysis (under direction of Zdeněk Kopal), *Tables of Supersonic Flow Around Cones of Large Yaw*, Tech. Report No. 5, M.I.T., 1949.

[4] Van Dyke, Milton D., Young, George B. W., Siska, Charles, *Proper Use of the M.I.T. Tables for Supersonic Flow Past Inclined Cones*, Readers' Forum, Journal of the Aeronautical Sciences, Vol. 18, pp. 355–356, 1951.

[5] Stone, A. H., *On Supersonic Flow Past a Slightly Yawing Cone*, Jour. Math. and Phys., Vol. XXVII, No. 1, pp. 67–81, April, 1948.

[6] Stone, A. H., *On Supersonic Flow Past a Slightly Yawing Cone. II*, Jour. Math. and Phys., Vol. XXX, No. 4, pp. 200–213, January, 1952.

[7] Ferri, Antonio, *Supersonic Flow Around Circular Cones at Angles of Attack*, NACA TN No. 2236, November, 1950 (now NACA Report No. 1045, 1951).

[8] Cooper, Morton, and Webster, Robert A., *The Use of an Uncalibrated Cone for Determination of Flow Angles and Mach Numbers at Supersonic Speeds*, NACA TN No. 2190, March, 1951.

[9] Young, G. B. W., and Siska, C. P., *Supersonic Flow Around Cones at Large Yaw*, Journal of the Aeronautical Sciences, Vol. 19, pp. 111–119, 1952.

[10] Young, G. B. W., *An Elucidation of Stone's Solution for a Slightly Yawing Supersonic Cone*, RM-48; The RAND Corporation, Santa Monica, Calif., July, 1948.

[11] Van Dyke, Milton D., *First and Second-Order Theory of Supersonic Flow Past Bodies of Revolution*, Journal of the Aeronautical Sciences, Vol. 18, pp. 161–179, 1951.

[12] Ferri, Antonio, Ness, Nathan, and Kaplite, Thaddeus T., *Supersonic Flow over Conical Bodies Without Axial Symmetry*, Journal of the Aeronautical Sciences, Vol. 20, pp. 563–571, 1953.

[13] Moore, Franklin K., *Laminar Boundary Layer on the Circular Cone in Supersonic Flow at a Small Angle of Attack*, NACA TN No. 2521, 1951.

[14] Stone, A. H., *Corrections to the Paper "On Supersonic Flow Past a Slightly Yawing Cone. II,"* Jour. Math. and Phys., Vol. XXXI, No. 4, p. 300, January, 1953.

[15] Lighthill, M. J., *A Technique for Rendering Approximate Solutions to Physical Problems Uniformly Valid*, Philosophical Mag., Ser. 7, Vol. XL, pp. 1179–1201, 1949.

Postbuckling Behavior of Axially Compressed Circular Cylindrical Shells

(*Continued from page 335*)

[3] von Kármán, Th., and Tsien, Hsue-Shen, *The Buckling of Thin Cylindrical Shells under Axial Compression*, Journal of the Aeronautical Sciences, Vol. 8, No. 8, p. 303, June, 1941.

[4] Chien, W. Z., *Intrinsic Theory of Thin Shells and Plates*, Quart. App. Math., Vol. II, No. 2, p. 120, July, 1944.

[5] Leggett, D. M. A., and Jones, R. P. N., *The Behavior of a Cylindrical Shell under Axial Compression when the Buckling Load has been Exceeded*, A.R.C.R. and M. No. 2190, August, 1942.

[6] Michielsen, Herman F., *The Behavior of Thin Cylindrical Shells after Buckling under Axial Compression*, Journal of the Aeronautical Sciences, Vol. 15, No. 12, p. 738, December, 1948.

[7] von Kármán, Th., Dunn, Louis G., and Tsien, Hsue-Shen, *The Influence of Curvature on the Buckling Characteristics of Structures*, Journal of the Aeronautical Sciences, Vol. 7, No. 7, p. 276, May, 1940.

[8] Donnell, L. H., *Stability of Thin-Walled Tubes under Torsion*, NACA Report No. 479, 1934.

[9] Tsien, H. S., *Buckling of a Column with Non-Linear Lateral Supports*, Journal of the Aeronautical Sciences, Vol. 9, No. 4, p. 119, February, 1942.

[10] Tsien, Hsue-Shen, *A Theory for the Buckling of Thin Shells*, Journal of the Aeronautical Sciences, Vol. 9, No. 10, p. 373, August, 1942.

Thermal and Creep Effects in Work-Hardening Elastic-Plastic Solids*

ALEXANDER J. WANG† AND WILLIAM PRAGER‡
Brown University

EXTREMUM PRINCIPLES GOVERNING the isothermal deformation of a work-hardening elastic-plastic solid have been given by Hodge and Prager[1] and Hill.[2] In the present note it is shown how these principles can be extended to include thermal and creep effects.

Using rectangular Cartesian coordinates x_i ($i = 1, 2, 3$), denote the infinitesimal displacement from the standard state by u_i, the infinitesimal strain by ϵ_{ij}, the stress by σ_{ij}, the mean normal stress by σ, and the stress deviation by s_{ij}. The mean normal stress is defined as

$$\sigma = (1/3)\sigma_{ii} \tag{1}$$

where the usual summation convention regarding repeated subscripts is used; the stress deviation is defined as

$$s_{ij} = \sigma_{ij} - \sigma\delta_{ij} \tag{2}$$

δ_{ij} being the Kronecker delta. The mean normal stress is an invariant of the stress tensor. Further invariants useful in the theory of isotropic plastic solids are

$$J_2 = (1/2)s_{ij}s_{ji}, \qquad J_3 = (1/3)s_{ij}s_{jk}s_{ki} \tag{3}$$

To specify the mechanical behavior of the isotropic solid, consider an element that, at the generic instant t, has the temperature θ and the strain ϵ_{ij} and is under the stress σ_{ij}. In the interval between the instants t and $t + dt$, let the temperature be changed by $d\theta$ and the stress by $d\sigma_{ij} = ds_{ij} + d\sigma\delta_{ij}$.

The corresponding change of strain, $d\epsilon_{ij}$, will then be assumed to consist of the following components:

(1) The *elastic* component

$$d\epsilon_{ij}{}^{e} = \alpha(\theta)\, ds_{ij} + \beta(\theta) d\sigma\delta_{ij} \tag{4}$$

where $\alpha(\theta)$ is one-half of the reciprocal of the temperature-dependent shear modulus, and $\beta(\theta)$ is one-third of the reciprocal of the temperature-dependent bulk modulus.

(2) The *thermal* component

$$d\epsilon_{ij}{}^{\theta} = [\alpha'(\theta)s_{ij} + \beta'(\theta)\sigma\delta_{ij}]\, d\theta + \gamma(\theta)\delta_{ij}\, d\theta \tag{5}$$

where the prime denotes differentiation with respect to the temperature and $\gamma(\theta)$ is the coefficient of linear thermal expansion at zero stress.

(3) The *creep* component

$$d\epsilon_{ij}{}^{c} = \Phi(\theta, J_2, J_3)\, (\partial\varphi/\partial\sigma_{ij})\, dt \tag{6}$$

where $\varphi = \varphi(\theta, J_2, J_3)$.

(4) The *plastic* component

$$d\epsilon_{ij}{}^{p} = \begin{cases} 0 \text{ if } \psi(\theta,J_2,J_3) < h \\ \Psi(\theta,J_2,J_3)\, (\partial\psi/\partial\sigma_{ij})\ \ (d\psi + |d\psi|) \text{ if} \\ \qquad\qquad\qquad\qquad \psi(\theta,J_2,J_3) = h \end{cases} \tag{7}$$

where the scalar h describes the state of hardening of the considered element at the time t.

Eqs. (4) and (5) result from a generalized form of Hooke's law in which the elastic constants are functions of the temperature.

In Eq. (6) the derivative $\partial\varphi/\partial\sigma_{ij}$ must be evaluated for the state of stress existing at the time t. The expression $\Phi\partial\varphi/\partial\sigma_{ij}$ then represents the rate of secondary creep corresponding to this state of stress. This expression is sufficiently general to comprise all isotropic laws of secondary creep that have so far been proposed in the literature on creep.

In Eq. (7), the equation $\psi(\theta,J_2,J_3) = h$ represents the temperature-dependent yield limit for the state of hardening achieved at the instant t. The first line of Eq. (7) therefore states that there will be no change in plastic strain where the state of stress is below the yield limit. The differential $d\psi$ in the second line of Eq. (7) must be evaluated from the given temperature and stress at the instant t and the changes in temperature and stress during the considered time interval. On account of the absolute value in the second line of Eq. (7), there will be no change in plastic strain even if the state of stress is at the yield limit provided that $d\psi < 0$. A special case of the combination of creep and plastic flow described by Eqs. (6) and (7) has been investigated by Odqvist.[3]

The extremum principles that are to be established concern the following boundary value problem. Consider a mass of work-hardening plastic material that has been deformed and, at the time t, occupies a region V bounded by the surface S. Suppose that the temperature θ, the stress σ_{ij}, and the state of hardening h are known throughout V. If the unit vector along the exterior normal of S is denoted by n_j, the surface traction in the considered state is $T_i = \sigma_{ij}n_j$. Prescribe now infinitesimal changes $d\theta$ of the temperature

Received January 6, 1954.
* The results presented in this paper were obtained in the course of research conducted under Contract N7onr-35801 between the Office of Naval Research and Brown University.
† Research Associate in Applied Mathematics.
‡ Professor of Applied Mechanics.

throughout V, infinitesimal changes dT_i of the surface traction on the portion S_T of the surface and infinitesimal displacements dU_i on the remainder S_U of the surface. What are the corresponding changes of stress $d\sigma_{ij}$ and the corresponding displacement du_i throughout V?

The infinitesimal displacement du_i causes the strain to change by

$$d\epsilon_{ij} = (1/2)\ [(\partial/\partial x_i)\ (du_j) + (\partial/\partial x_j)\ (du_i)] \quad (8)$$

The change of stress must satisfy the equation of equilibrium which, to within higher order terms, can be written as

$$(\partial/\partial x_j)\ (d\sigma_{ij}) = 0 \quad (9)$$

Finally, the following boundary conditions must be satisfied

$$d\sigma_{ij}n_j = dT_i \text{ on } S_T \quad (10)$$

$$du_i = dU_i \text{ on } S_U \quad (11)$$

The problem thus consists in determining the change of stress $d\sigma_{ij}$ and the displacement du_i in such a manner that the boundary conditions, Eqs. (10) and (11), and the equation of equilibrium, Eq. (9), are satisfied, and that the strain change computed from Eq. (8) is related to the given values of θ, $d\theta$, σ_{ij} and h and to the sought stress change $d\sigma_{ij}$ by means of Eqs. (4) through (7).

The first extremum principle compares the actual changes of stress and strain, $d\sigma_{ij}$ and $d\epsilon_{ij}$, to a fictitious change of stress $d\sigma_{ij}^*$ and the corresponding change of strain $d\epsilon_{ij}^*$. The stress change $d\sigma_{ij}^*$ is supposed to satisfy the equation of equilibrium and the boundary condition on S_T, and the strain change $d\epsilon_{ij}^*$ is associated with θ, $d\theta$, σ_{ij}, h, and $d\sigma_{ij}^*$ by means of Eqs. (4) through (7), but need not be derivable from a displacement field. The principle of virtual work then furnishes the equation

$$\int [(d\sigma_{ij}^* - d\sigma_{ij})\ d\epsilon_{ij}]\ dV = \int [(dT_i^* - dT_i)\ dU_i]\ dS_U \quad (12)$$

where $dT_i^* = d\sigma_{ij}^*\ n_j$.

The integrand of the left-hand side of Eq. (12) can be transformed as follows:

$$2(d\sigma_{ij}^* - d\sigma_{ij})\ d\epsilon_{ij} = (d\sigma_{ij}^* d\epsilon_{ij}^* - d\sigma_{ij} d\epsilon_{ij}) - [d\sigma_{ij}^*(d\epsilon_{ij}^* - d\epsilon_{ji}) + d\epsilon_{ij}(d\sigma_{ij} - d\sigma_{ij}^*)] \quad (13)$$

On the right-hand side of this equation, introduce the components, Eqs. (4) through (7), of the change of strain. Since $d\epsilon_{ij}^{*\theta} = d\epsilon_{ij}^{\theta}$ and $d\epsilon_{ij}^{*c} = d\epsilon_{ij}^{c}$,

$$2(d\sigma_{ij}^* - d\sigma_{ij})\ d\epsilon_{ij} = d\sigma_{ij}^*(d\epsilon_{ij}^* + d\epsilon_{ij}^{*\theta} + d\epsilon_{ij}^{*c}) - d\sigma_{ij}(d\epsilon_{ij} + d\epsilon_{ij}^{\theta} + d\epsilon_{ij}^{c}) - [d\sigma_{ij}^*(d\epsilon_{ij}^{*e} + d\epsilon_{ij}^{*p} - d\epsilon_{ij}^{e} - d\epsilon_{ij}^{p}) + (d\epsilon_{ij}^{e} + d\epsilon_{ij}^{p})\ (d\sigma_{ij} - d\sigma_{ij}^*)] \quad (14)$$

The bracket in Eq. (14) involves only elastic and plastic changes of strain. When the case $d\sigma_{ij}^* \equiv d\sigma_{ij}$ is excluded, it can be shown that this bracket is positive. This is done in exactly the same manner as in the proof of the extremum principle for isothermal deformation of a work-hardening plastic material (see Hill,[2] pp. 63–64). Thus, the left-hand side of Eq. (14) is smaller than the first two terms on the right-hand side unless $d\sigma_{ij}^* \equiv d\sigma_{ij}$. When this result is introduced into Eq. (12), the following relation is obtained:

$$(1/2) \int [d\sigma_{ij}^*(d\epsilon_{ij}^* + d\epsilon_{ij}^{*\theta} + d\epsilon_{ij}^{*c})]\ dV - \int (dT_i^* dU_i)\ dS_U \geq (1/2) \int [d\sigma_{ij}(d\epsilon_{ij} + d\epsilon_{ij}^{\theta} + d\epsilon_{ij}^{c})]\ dV - \int (dT_i\ dU_i)\ dS_U \quad (15)$$

where the equality sign holds only if $d\sigma_{ij}^* \equiv d\sigma_{ij}$. The relation (15) establishes a minimum property of the actual change of state.

Before the second extremum principle can be discussed, it must be shown that Eqs. (4) through (7) can be transformed so as to represent $d\sigma_{ij}$ as function of $d\epsilon_{ij}$. We note first that $d\epsilon_{ij}^{\theta}$ and $d\epsilon_{ij}^{c}$ follow immediately from the data of the considered boundary value problem. Since these two components of the change of strain are known, giving $d\epsilon_{ij}$ is equivalent to giving $d\epsilon_{ij}^{e} + d\epsilon_{ij}^{p} = d\epsilon_{ij} - d\epsilon_{ij}^{\theta} - d\epsilon_{ij}^{c}$. The proof that the sum $d\epsilon_{ij}^{e} + d\epsilon_{ij}^{p}$ specifies a unique $d\sigma_{ij}$ then proceeds exactly as in the case where $d\epsilon_{ij}^{e} + d\epsilon_{ij}^{p}$ represents the entire change of strain (see Hill,[2] pp. 68–69).

The second extremum principle compares the actual changes of strain and stress, $d\epsilon_{ij}$ and $d\sigma_{ij}$, to a fictitious change of strain $d\epsilon_{ij}^*$ and the corresponding change of stress $d\sigma_{ij}^*$. The strain change $d\epsilon_{ij}^*$ is supposed to be derivable from a displacement field du_i^* that satisfies the boundary conditions on S_U; the stress change $d\sigma_{ij}^*$ is associated with θ, $d\theta$, σ_{ij}, h, and $d\epsilon_{ij}^*$ by means of Eqs. (4) through (7), but need not satisfy the equation of equilibrium or the boundary condition on S_T. The principle of virtual work then furnishes the equation

$$\int [d\sigma_{ij}(d\epsilon_{ij}^* - d\epsilon_{ij})]\ dV = \int [dT_i(du_i^* - du_i)]\ dS_T \quad (16)$$

The integrand on the left-hand side of Eq. (16) equals

$$d\sigma_{ij}(d\epsilon_{ij}^{*e} + d\epsilon_{ij}^{*p} - d\epsilon_{ij}^{e} - d\epsilon_{ij}^{p}) \quad (17)$$

and does not involve the thermal or creep effects; it can therefore be transformed in exactly the same manner as in the case where the sum of elastic and plastic strain changes represents the total strain change (see Hill,[2] pp. 65–66). As a result of this transformation, the following relation is obtained:

$$\int (dT_i du_i^*)\ dS_T - (1/2) \int [d\sigma_{ij}^*(d\epsilon_{ij}^{*e} + d\epsilon_{ij}^{*p})]\ dV \leq \int (dT_i du_i)\ dS_T - (1/2) \int [d\sigma_{ij}(d\epsilon_{ij}^{e} + d\epsilon_{ij}^{p})]\ dV \quad (18)$$

where the equality sign holds only if $d\epsilon_{ij}^* = d\epsilon_{ij}$. The relation (18) establishes a maximum property of the actual change of state.

(*Continued on page 360*)

Readers' Forum

BRIEF REPORTS of investigations in the aeronautical sciences and discussions of papers published in the JOURNAL are presented in this special department. The publication will be completed as soon as possible after receipt of the material. The Editorial Committee does not hold itself responsible for the opinions expressed by the correspondents.

The Compressible Laminar Boundary Layer on a Rotating Body of Revolution

Sheng To Chu and A. N. Tifford
Department of Aeronautical Engineering, The Ohio State University, Columbus, Ohio
January 27, 1954

A RELATIVELY GENERAL analysis of the "constant property" laminar boundary layer on a rotating body of revolution in axial motion has been given in reference 1. As a sequel, constituting a portion of his doctoral research, the senior author is undertaking the investigation of the detailed effect therein of the variability of fluid properties. The initial result obtained is a Crocco-like energy relation applicable when the Prandtl Number is unity. By means of this relation, the compressible laminar boundary layer on a rotating body of revolution may be correlated with a fictitious incompressible laminar boundary layer under more general circumstances than those reported by Illingworth (reference 2). Furthermore, the analogy between the frictional torque and the surface rate of heat transfer of reference 1 is readily seen to be unaffected by the variability of fluid properties.

The steady compressible boundary layer equations for a rotating body of revolution are

$$(\partial/\partial x)(r\rho u) + (\partial/\partial y)(r\rho v) = 0 \tag{1}$$

$$\rho[u(\partial u/\partial x) + v(\partial u/\partial y) - (w^2/r)(dr/dx)] = \rho_1 u_1(du_1/dx) + (\partial/\partial y)[\mu(\partial u/\partial y)] \tag{2}$$

$$\rho\{u[\partial(rw)/\partial x] + v[\partial(rw)/\partial y]\} = (\partial/\partial y)\{\mu[\partial(rw)/\partial y]\} \tag{3}$$

$$\rho[u(\partial i/\partial x) + v(\partial i/\partial y)] + up_1u_1(du_1/dx) = (1/\sigma)(\partial/\partial y)[\mu(\partial i/\partial y)] + \mu[(\partial u/\partial y)^2 + (\partial w/\partial y)^2] \tag{4}$$

$$[(\gamma - 1)/\gamma]\rho i = p = p_1 = [(\gamma - 1)/\gamma]\rho_1 i_1 \tag{5}$$

Here x is the distance along the surface of the body in a meridian plane, y is the distance measured normal to the surface, r is the distance of the surface from the axis of symmetry measured normal to the latter, u and v are the velocity components along the x and y directions, respectively, w is the rotational velocity component, and the other quantities are denoted by conventional symbols. The energy equation in the free stream is

$$i_1 + (1/2)u_1^2 = h_1 = \text{constant} \tag{6}$$

It is assumed that the Prandtl number, σ, of the fluid is unity, and the enthalpy, i, is a function of H alone, where

$$H = (u^2/2) + (w^2/2) + k\omega rw \tag{7}$$

ω is the angular velocity of the rotating body, and k is an abritrary constant. Combining this assumption and Eqs. (2), (3), and (4), it may be shown that

$$di/dH = -1 \tag{8}$$

is a particular solution of the energy equation, Eq. (4). Eq. (9) follows:

$$i + (u^2/2) + (w^2/2) + k\omega rw = \text{constant} \tag{9}$$

For Eq. (9) to be valid at both edges of the boundary layer, $(u_1^2/2) + i_1$ must equal $[(1/2) + k]\omega^2r^2 + i_w$ and be identically the integration constant. In other words, Eq. (9) applies, in general, only when the surface enthalpy varies parabolicly with r. The arbitrary constant, k, may be adjusted, however, so as to allow a variety of parabolic representations of the surface enthalpy distribution to be covered. Additional interesting points worth noting are:

(a) Eq. (9) reduces to the well-known Crocco integral (reference 3) when the body does not rotate.

(b) The analogy of reference 1 between the frictional torque and the surface rate of heat transfer is readily shown to apply despite the variability of the fluid properties.

(c) An insulated rotating surface acquires the surface enthalpy distribution, $i_w = h_1 + (\omega r)^2/2$, i.e., $k = -1$. Conversely, a rotating body having a surface enthalpy (temperature) corresponding to the free stream total enthalpy (temperature)—$k = -1/2$—does experience heat transfer.

Aside from its general character, Eq. (9) may be used advantageously in obtaining a correlation between the compressible boundary layer on a rotating body of revolution having a surface pressure gradient and an associated fictitious incompressible boundary layer by a method somewhat analogous to that employed by Illingworth (reference 2). However, neither his restrictive condition of constant enthalpy inside the boundary layer nor his limitation of the local free stream Mach number variation along the surface to $M_1 = (\alpha r + \beta)^{1/2}$ is required any longer.

Assuming that the coefficient of absolute viscosity is proportional to the absolute temperature, Eqs. (2) and (3) may be transformed into Eqs. (10) and (11),

$$(1/u_1)(du_1/ds)(\bar{u}^2 - \bar{\imath}) + \bar{u}(\partial\bar{u}/\partial s) - (\omega^2/u_1^2)r(dr/ds)\bar{w}^2 = \bar{u}(\partial/\partial\psi)[\bar{u}(\partial\bar{u}/\partial\psi)] \tag{10}$$

and

$$[\partial(r^2\bar{w})]/\partial s = \partial/\partial\psi\{\bar{u}[\partial(r^2\bar{w})]/\partial\psi\} \tag{11}$$

where the stream function, ψ, satisfied the relations,

$$r\rho u = \partial\psi/\partial y \text{ and } r\rho v = -(\partial\psi/\partial x) \tag{12}$$

$$\bar{u} = u/u_1,\ \bar{w} = w/\omega r,\ \bar{\imath} = i/i_1 = \rho/\rho_1 \tag{13}$$

and

$$s = \int_0^x r^2\mu_1\rho_1u_1dx \tag{14}$$

Essentially this transformation is a combination of that of von Mises (reference 4) and that of Mangler (reference 5). From Eq. (8) we can write,

$$(\bar{u}^2 - \bar{\imath}) = (\bar{u}^2 - 1)\{1 + [1/2(u_1^2/i_1)]\} + [1/2(\omega^2 r^2/i_1)]\bar{w}^2 + (k\omega^2 r^2/i_1)\bar{w} \quad (15)$$

Substituting Eq. (15) into Eq. (10), we have

$$[(1 + b)(1/u_1)][(du_1/ds)(\bar{u}^2 - 1)] + \bar{u}(\partial\bar{u}/\partial s) - (\omega^2/u_1^2)[r(dr/ds)]\bar{w}^2 + [(1 + b)(1/u_1)](du_1/ds) \times [1/2(\omega^2 r^2/h_1)\bar{w} + (k\omega^2 r^2/h_1)\bar{w}] = \bar{u}(\partial/\partial\psi)[\bar{u}(\partial\bar{u}/\partial\psi)]$$

where $b = u_1^2/2i_1$. The term dr/ds may be expressed as

$$dr/ds = (dr/db)(db/ds) = (1 + b)^2[(u_1/h_1)(du_1/ds)]$$

Thus the above equation becomes

$$[(1 + b)(1/u_1)][(du_1/ds)(\bar{u}^2 - 1)] + \bar{u}(\partial\bar{u}/\partial s) - (\omega^2/h_1)[r(dr/db)]\bar{w}^2(1 + b)^2[(1/u_1)(du_1/ds)] + [(1 + b)(1/u_1)(du_1/ds)][1/2(\omega^2 r^2/h_1)\bar{w}^2 + (k\omega^2 r^2/h_1)\bar{w}] = \bar{u}(\partial/\partial\psi)[\bar{u}(\partial\bar{u}/\partial\psi)] \quad (16)$$

and Eq. (11) retains its original form

$$\partial(r^2\bar{w})/\partial s = (\partial/\partial\psi)\{\bar{u}[\partial(r^2\bar{w})/\partial\psi]\} \quad (17)$$

The boundary conditions are

$$\left.\begin{array}{lll} \text{at } \psi = 0, & \bar{u} = 0, & \bar{w} = 1 \\ \text{at } \psi \to \infty, & \bar{u} = 1, & \bar{w} = 0 \end{array}\right\} \quad (18)$$

It will be found possible to establish a correspondence between the compressible boundary layer problem represented by the differential system, Eqs. (16), (17), and (18), for the rotating body of revolution having a surface pressure gradient and an associated fictitious incompressible boundary layer problem.

Consider the following system of equations

$$\partial U/\partial X + \partial V/\partial Y = 0 \quad (19)$$

$$U(\partial U/\partial X) + V(\partial U/\partial Y) - (W^2/R)(dR/dX) \times [1 + (1/2)(U_1/U_r)^2] + U_1(dU_1/dX)[(1/2)(W/U_r)^2 + (k\Omega RW/U_r^2) - 1] = N_*(\partial^2 U/\partial Y^2) \quad (20)$$

and

$$U[\partial(RW)/\partial X] + V[\partial(RW)/\partial Y] = N_*[\partial^2(RW)/\partial Y^2] \quad (21)$$

Here the capitalized letters denote corresponding quantities in the fictitious incompressible boundary layer problem, U_r is a constant reference velocity, and N_* is the uniform kinematic viscosity. Note that when $W = 0$, these equations reduce to that of a two-dimensional boundary layer flow of an impressible fluid about a cylinder. By changing to s and ψ coordinates, Eqs. (19), (20), and (21) may be transformed into Eqs. (22) and (23)

$$(1/U_1)[(dU_1/ds)(\bar{u}^2 - 1)] + \bar{u}(\partial\bar{u}/\partial s) - (\Omega^2/U_r^2)R(dR/dB)\bar{w}^2[1 + 1/2(U_1/U_r)^2](1/U_1)(dU_1/ds) + (1/U_1)(dU_1/ds)\{(\Omega R/U_r)^2[(1/2)\bar{w}^2 + k\bar{w}]\} = \bar{u}(\partial/\partial\psi) \times [\bar{u}(\partial\bar{u}/\partial\psi)] \quad (22)$$

$$\partial(R^2\bar{w})/\partial s = (\partial/\partial\psi)\{\bar{u}[\partial(R^2\bar{w})/\partial\psi]\} \quad (23)$$

The following definitions and nondimensional quantities have been used in obtaining the above differential equations:

$$LP_*U = \partial\psi/\partial Y, \qquad LP_*V = -(\partial\psi/\partial X) \quad (24)$$

and

$$\bar{u} = U/U_1, \quad \bar{w} = W/\Omega R, \quad B = (1/2)(U_1/U_r)^2, \quad s = L^2M_*P_*\int_0^X U_1 dX \quad (25)$$

where P_* is the uniform density; M_*, the uniform viscosity; and L, the characteristic length of the incompressible problem. After comparing Eqs. (22) and (23) with Eqs. (16) and (17), we choose

$$(1/r)(dr/ds) = (1/R)(dR/ds) \quad (26)$$

and

$$(1 + b)(1/u_1)(du_1/ds) = (1/U_1)(dU_1/ds) \quad (27)$$

The integrals of Eqs. (26) and (27) are, respectively,

$$r(s) = c_1R(s) \quad (28)$$

and

$$(u_1^2/i_1)(s) = c_2U_1^2(s) \quad (29)$$

where c_1 and c_2 are integration constants. Furthermore, we choose

$$\Omega = \omega, \quad c_1 = 1, \quad c_2 = 1/U_r^2 = 1/h_1 \quad (30)$$

The last relation gives $b(s) = B(s)$. It is therefore obvious that with these choices the two sets of equations, Eqs. (16), (17) and Eqs. (22), (23) are now identical to each other. Besides, the boundary conditions for both sets are the same, as given in Eq. (18).

The correlation mentioned previously is thus established. That is, under the conditions given in Eqs. (28), (29), and (30), the nondimensional functions $\bar{u}$ and $\bar{w}$ may be found from the incompressible flow Eqs. (19), (20), and (21) instead of the more complicated Eqs. (1), (2), and (3).

References

[1] Tifford, A. N., and Chu, S. T., *The Laminar Boundary Layer on Spinning Axisymmetric Bodies*, Proceedings of the Third Midwestern Conference on Fluid Mechanics, p. 579, 1953.

[2] Illingworth, C. R., *The Laminar Boundary Layer of a Rotating Body of Revolution*, Phil. Mag., Vol. 44, No. 351, p. 389, April, 1953.

[3] Crocco, L., *Transmission of Heat From a Flat Plate to a Fluid Flowing at High Velocity*, NACA TM No. 690, October, 1932.

[4] Mises, R. von, *Bemerkungen zur Hydrodynamik*, Z. angew. Math. Mech., Vol. 7, p. 425, 1927.

[5] Mangler, W., *Zusammenhang zwischen ebenen und rotationssymmetrischen Grenzschichten in kompressiblen Flussigkeiten*, Z. angew. Math. Mech., Vol. 28, p. 97, 1948.

Controlled Motion with Time Lag in Autopilot

G. M. Andrew
North American Aviation, Inc., Downey, Calif.

December 31, 1954

THE EQUATIONS developed below apply to a second order system with arbitrary initial conditions, controlled by the autopilot, having an average time lag T. The method illustrated on one degree of freedom can be readily adapted for two or three degrees of freedom. Denote the natural frequency and the damping ratio of the uncontrolled system by ω_n and ζ and the forcing function by $\delta(t)$ then the equation of motion can be written.

$$\ddot{\theta}(t) + 2\zeta\omega_n\dot{\theta}(t) + \omega_n^2\theta(t) = M_\delta\delta(t) \quad (1)$$

Assume that the control surface deflection having the time lag T is proportional to displacement $\theta(t)$ and rate $\dot{\theta}(t)$. Then the control surface deflection is represented by

$$\delta(t) = \delta_0 + K_\theta\theta(t - T) + K_{\dot{\theta}}\dot{\theta}(t - T) \quad (2)$$

where generally constants K_θ and $K_{\dot{\theta}}$ are negative.

Substituting Eq. (2) into Eq. (1) gives an operational equation (in the time domain) of controlled system

$$(D^2 + 2\zeta\omega_nD + \omega_n^2)\theta(t) = M_\delta\delta_0 + M_\delta(K_\theta + K_{\dot{\theta}}D)\theta(t - T) \quad (3)$$

For the initial conditions (at $t = 0$) δ_0; θ_0 and $\dot{\theta}_0$, the Laplace Transformation of Eq. (3) yields

$$(s^2 + 2\zeta\omega_n s + \omega_n^2)\theta(s) = s\theta_0 + \dot{\theta}_0 + 2\zeta\omega_n\theta_0 + [(M_\delta\delta_0)/s] + [M_\delta(K_\theta + K_{\dot\theta}s)\theta(s) - M_\delta K_{\dot\theta}\theta_0]e^{-sT} \quad (4)$$

For technical purpose a very good approximation can be obtained expanding e^{-sT} into a series and taking the first two terms

$$e^{-sT} \cong (1 - Ts) \quad (5)$$

Eq. 5 substituted into Eq. (4) gives

$$s^2\theta(s) + 2\zeta\omega_n s\theta(s) + \omega_n^2\theta(s) = s\theta_0 + 2\zeta\omega_n\theta_0 + \dot{\theta}_0 + [(M_\delta\delta_0)/s] + M_\delta K_\theta\theta(s) + M_\delta K_{\dot\theta}s\theta(s) - M_\delta K_{\dot\theta}\theta_0 - TM_\delta K_\theta s\theta(s) - TM_\delta K_{\dot\theta}s^2\theta(s) + TM_\delta K_{\dot\theta}s\theta_0 \quad (4a)$$

rearranging

$$[(1 + TM_\delta K_{\dot\theta})s^2 + (2\zeta\omega_n + TM_\delta K_\theta - M_\delta K_{\dot\theta})s + (\omega_n^2 - M_\delta K_\theta)]\theta(s) = (1 + TM_\delta K_{\dot\theta})s\theta_0 + (2\zeta\omega_n - M_\delta K_{\dot\theta})\theta_0 + [(M_\delta\delta_0)/s] + \dot{\theta}_0 \quad (4b)$$

Or

$$\left[s^2 + \left(\frac{2\zeta\omega_n + TM_\delta K_\theta - M_\delta K_{\dot\theta}}{1 + TM_\delta K_{\dot\theta}}\right)s + \left(\frac{\omega_n^2 - M_\delta K_\theta}{1 + TM_\delta K_{\dot\theta}}\right)\right]\theta(s) = s\theta_0 + \frac{(2\zeta\omega_n - M_\delta K_{\dot\theta})\theta_0 + \dot{\theta}_0}{1 + TM_\delta K_{\dot\theta}} + \frac{M_\delta\delta_0}{s(1 + TM_\delta K_{\dot\theta})} \quad (4c)$$

To simplify the notations let

$$[(2\zeta\omega_n + TM_\delta)K_\theta - M_\delta K_{\dot\theta}]/(1 + TM_\delta K_{\dot\theta}) = 2\zeta_c\omega_{nc} \quad (6)$$

and

$$(\omega_n^2 - M_\delta K_\theta)/(1 + TM_\delta K_{\dot\theta}) = \omega_{nc}^2 \quad (7)$$

where ω_{nc} and ζ_c are equivalent natural frequency and damping ratio of the controlled system with the time lag T.

Then:

$$s(s^2 + 2\zeta_c\omega_{nc} + \omega_{nc}^2)\theta(s) = s^2\theta_0 + [(2\zeta\omega_n - M_\delta K_{\dot\theta})\theta_0 + \dot{\theta}_0]s/(1 + TM_\delta K_{\dot\theta}) + (M_\delta\delta_0)/(1 + TM_\delta K_{\dot\theta}) \quad (4d)$$

Let us shorten the notation as follows:

$$[(2\zeta\omega_n - M_\delta K_{\dot\theta})\theta_0 + \dot{\theta}_0]/[\theta_0(1 + TM_\delta K_{\dot\theta})] = a_1 \quad (8)$$

$$(M_\delta\delta_0)/[\theta_0(1 + TM_\delta K_{\dot\theta})] = a_0 \quad (9)$$

$$2\zeta_c\omega_{nc} = b \quad (10)$$

$$\omega_{nc}^2 = k \quad (11)$$

Then Eq. (4d) solved for $\theta(s)$ gives

$$\theta(s) = \theta_0\{(s^2 + a_1 s + a_0)/[s(s^2 + bs + k)]\} = \theta_0\{(s^2 + a_1 s + a_0)/s[(s + \alpha)^2 + \beta^2]\} \quad (4e)$$

where the roots of the characteristic equation are:

$$s_{1,2} = \alpha \pm j\beta \quad (12)$$

The inverse Laplace transform of Eq. (4e) yields the time history of the motion (for $t > T$) as:

$$\theta(t) = \theta_0\{(a_0/\beta_0^2) + (1/\beta\beta_0)[(\alpha^2 - \beta^2 - a_1\alpha + a_0)^2 + \beta^2(a_1 - 2\alpha)^2]^{1/2}e^{-\alpha t}\sin(\beta t + \psi)\} \quad (13)$$

where

$$\psi = \tan^{-1}\{[\beta(a_1 - 2\alpha)]/(\alpha^2 - \beta^2 - a_1\alpha + a_0)\} - \tan^{-1}(\beta/-\alpha) \quad (14)$$

$$\beta_0^2 = \alpha^2 + \beta^2 \quad (15)$$

REFERENCES

[1] *Automatic and Manual Control*, papers contributed to the conference at Cranfield, 1951, London; Butterworths Scientific Publications, 1952.

[2] Gardner, M. F., and Barnes, J. L., *Transients in Linear Systems*, Vol. I; John Wiley & Sons, Inc., New York.

The Shock Strength in the Regular Reflection of Weak Shock Waves

William Chester
Mathematics Department, Bristol University, England

December 7, 1953

LET A PLANE FRONTED SHOCK be incident upon an infinite wedge whose leading edge is yawed through an angle β relative to the direction of propagation of the shock (see Fig. 1). If the faces of the wedge are only slightly inclined to the direction of propagation of the shock, Mach reflection takes place. The strength of the resulting Mach shock has been obtained correct to the second order of small quantities by Tan[1] and Chester.[2] The same problem is considered in this note, but for a thick wedge and weak incident shock (an acoustic pulse). In the latter case regular reflection takes place, and the boundary of the perturbed region consists of the Mach cone with vertex at the junction of the shock and the wedge leading edge, and possibly by the tangent plane to this cone from the intersection of the shock and the face of the wedge [this latter part of the boundary is the ordinary reflected shock which occurs in the elementary theory of reflection and does not appear when the face of the wedge is so inclined that there is a region of shadow and, hence, a diffraction effect—see Figs. 2(a) and 2(b)].

The pressure and sonic velocity in the undisturbed flow ahead of the shock will be denoted by p_0 and a_0, respectively. Corresponding quantities in the region of uniform flow behind the shock, and in the region of perturbed flow, will be distinguished by the suffixes 1 and 2, respectively. The dependence on time is eliminated by taking the origin of a Cartesian system of coordinates $0(x', y', z')$ at the vertex of the Mach cone with the z' axis along the leading edge of the wedge and the y' axis perpendicular to the direction of propagation of the incident shock

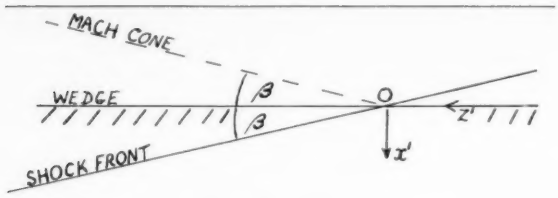

FIG. 1. Configuration in the (x', z') plane.

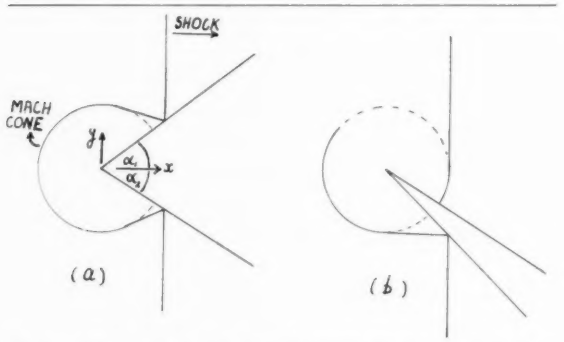

FIG. 2. Configuration in the (x, y) plane for (a) $0 < \alpha_1 < \pi/2$, $0 < \alpha_2 < \pi/2$ and (b) $-\pi/2 < \alpha_1 < 0$, $0 < \alpha_2 < \pi/2$.

On the assumption that $(p_1 - p_0)$ is small, the main flow velocity behind the shock is approximately $a_0/\sin\beta$ parallel to the leading edge, and the pressure in the region of perturbed flow satisfies

$$\partial^2 p/\partial x'^2 + \partial^2 p/\partial y'^2 = \cot^2\beta(\partial^2 p/\partial z'^2) \tag{1}$$

where

$$p = (p_2 - p_1)/(p_1 - p_0) \tag{2}$$

Since there is no fundamental length in the data defining the problem, the pressure must be a function only of x and y, where

$$x = x'/(z' \tan\beta), \qquad y = y'/(z' \tan\beta) \tag{3}$$

If, further, the Busemann transformation be made, namely

$$x = (2\rho\cos\theta)/(1 + \rho^2), \qquad y = (2\rho\sin\theta)/(1 + \rho^2) \tag{4}$$

Eq. (1) reduces to Laplace's equation with (ρ, θ) as polar coordinates.

Angular distances remain unchanged by the transformation. Furthermore the Mach cone becomes the unit circle in both the (x, y) and the (ρ, θ) planes. We thus require a harmonic function which satisfies certain boundary conditions on the unit circle and the lines $\theta = \alpha_1$, $\theta = 2\pi - \alpha_2$, where α_1 and α_2 are the angles which the faces of the wedge make with the x' axis. Such a solution can be obtained by a method similar to that used by Lighthill.[3] When the conformal transformations

$$\{\rho \exp[i(\theta - \alpha_1)]\}^{\pi/(2\pi - \alpha_1 - \alpha_2)} = Z \tag{5}$$

$$x_1 + iy_1 = z_1 = -(1/2)[Z + (1/Z)] \tag{6}$$

are effected, that part of the boundary consisting of $\theta = \alpha_1$ (between the origin and the unit circle) in the (ρ, θ) plane then becomes $y_1 = 0$, $-\infty < x_1 < -1$ in the z_1-plane. The unit circle between $\theta = \alpha_1$ and $\theta = 2\pi - \alpha_2$ becomes $y_1 = 0$, $-1 < x_1 < 1$ and finally $\theta = 2\pi - \alpha_2$ becomes $y_1 = 0$, $1 < x_1 < \infty$.

In the z_1-plane, the boundary conditions on the real axis may be written

$$\partial p/\partial y_1 = 0, \qquad |x_1| > 1; \qquad \partial p/\partial x_1 = 0 \qquad |x_1| < 1 \tag{7}$$

together with

$$\left.\begin{aligned} \int_{-\epsilon - \cos\alpha_1\tau}^{\epsilon - \cos\alpha_1\tau} \frac{\partial p}{\partial x_1}\,dx_1 &= -\left(\frac{\sin\alpha_1\tau}{\sin\alpha_1\tau}\right) \\ \int_{-\epsilon + \cos\alpha_2\tau}^{\epsilon + \cos\alpha_2\tau} \frac{\partial p}{\partial x_1}\,dx_1 &= \frac{\sin\alpha_2\tau}{\sin\alpha_2\tau} \end{aligned}\right\} \tag{8}$$

where

$$\tau = \pi/(2\pi - \alpha_1 - \alpha_2)$$

We now define the complex function

$$W(z_1) = \partial p/\partial y_1 + i(\partial p/\partial x_1) \tag{9}$$

The boundary conditions, expressed in terms of W, are that on the real axis W is real for $|x_1| < 1$ and wholly imaginary for $|x| > 1$. Near $z_1 = -\cos\alpha_1\tau$, Eq. (8) suggests that

$$W \sim \frac{1}{\pi}\frac{\sin\alpha_1\tau}{\sin\alpha_1\tau}\frac{1}{z + \cos\alpha_1\tau}$$

with an analoguos relation near $z_1 = \cos\alpha_2\tau$.

A function which satisfies all these conditions, and is integrable at all points in the upper half-plane except the specified singularities, is

$$W = (1/\pi)\{(\sin\alpha_1\tau)/[(1 - z_1^2)^{1/2}(z_1 + \cos\alpha_1\tau)]\} - (1/\pi)\{(\sin\alpha_2\tau)/[(1 - z_1^2)^{1/2}(z_1 - \cos\alpha_2\tau)]\} \tag{10}$$

It is, of course, possible to deduce the actual pressure field using Eq. (10) and the pressure distribution on the Mach cone. This has, however, already been investigated by Keller and Blank[4] using a different technique, and Eq. (10) is sufficient for the purpose of this note.

The above theory predicts a singularity in the normal derivative of the pressure at the Mach cone. For if $\partial p/\partial n$ denotes the pressure derivative along the inward normal to the circle $\rho = 1$ in the (ρ, θ) plane, and if (r, θ) are polar coordinates in the (x, y) plane, we have near $r = 1$,

$$p - (p)_{r=1} \sim (1 - \rho)(\partial p/\partial n) \sim [2(1 - r)^{1/2}](\partial p/\partial n) \tag{11}$$

and hence

$$\partial p/\partial r \sim -(1 - r)^{-1/2}(\partial p/\partial n) \tag{12}$$

Now Lighthill[5] has shown quite generally that the true behavior near the Mach cone depends on the sign of $\partial p/\partial n$. If

$$p_2 - (p_2)_{r=1} \sim \rho_1 V_1^2(1 - r)^{1/2}F(\theta) \tag{13}$$

then the Mach cone is a linear approximation to a shock wherever $F(\theta) > 0$. The discontinuity in pressure across this shock is

$$\Delta p_2 = (3/4)\gamma(\gamma + 1)\{p_1 V_1^6/[a_1^4(V_1^2 - a_1^2)]\}F^2(\theta) \tag{14}$$

where γ denotes the adiabatic index.

When $F(\theta) < 0$ there is probably a weaker (third order) shock followed immediately by a relatively stronger (second order) expansion.

In the present case, it follows from Eq. (11) and (13) that

$$F(\theta) = \{[2^{1/2}(p_1 - p_0)]/\rho_1 V_1^2\}(\partial p/\partial n) \tag{15}$$

Since a_1 and V_1 are, to the present order of approximation, a_0 and $a_0/\sin\beta$, respectively, Eqs. (14) and (15) show that, when $\partial p/\partial n > 0$,

$$\Delta p_2 = [3(\gamma + 1)/2\gamma\cos^2\beta][(p_1 - p_0)^2/p_0](\partial p/\partial n)^2 \tag{16}$$

Now

$$\frac{\partial p}{\partial n} = \left|\frac{dz_1}{d\rho}\right|\frac{\partial p}{\partial y_1} \tag{17}$$

and, on the circle $\rho = 1$,

$$\left|\frac{dz_1}{d\rho}\right| = \tau\sin\tau(\theta - \alpha_1) \tag{18}$$

$$x_1 = -\cos\tau(\theta - \alpha_1) \tag{19}$$

by virtue of Eqs. (5) and (6). It follows, with the help of Eq.

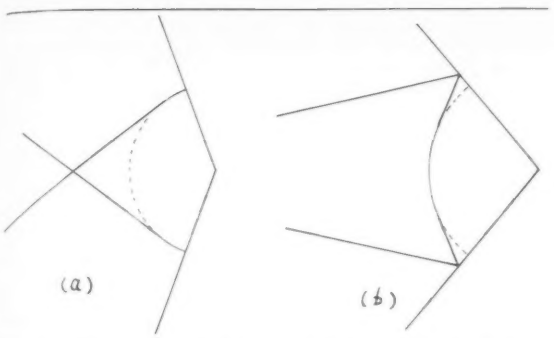

FIG. 3. Diffraction pattern produced in a corner for $\alpha_1 = \alpha_2 = \alpha$ and (a) $\pi/2 < \alpha < 2\pi/3$, (b) $2\pi/3 < \alpha < 3\pi/4$.

(10), that on $\rho = 1$

$$\frac{\partial p}{\partial n} = \frac{-1}{2\pi - \alpha_1 - \alpha_2}\left\{\frac{\sin[\alpha_1\pi/(2\pi - \alpha_1 - \alpha_2)]}{\cos\phi - \cos[\alpha_1\pi/(2\pi - \alpha_1 - \alpha_2)]} - \frac{\sin[\alpha_2\pi/(2\pi - \alpha_1 - \alpha_2)]}{\cos\phi + \cos[\alpha_2\pi/(2\pi - \alpha_1 - \alpha_2)]}\right\} \quad (20)$$

where $\phi = (\theta - \alpha_1)\pi/(2\pi - \alpha_1 - \alpha_2)$, so that $0 \leq \phi \leq \pi$ on the Mach cone.

In the symmetrical case, for example, with $\alpha_1 = \alpha_2 = \alpha$, Eq. (20) simplifies to

$$\partial p/\partial n = \frac{-\sin[\pi\alpha/(\pi - \alpha)]}{(\pi - \alpha)\{\cos 2\phi - \cos[\pi\alpha/(\pi - \alpha)]\}} \quad (21)$$

When $0 < \alpha < \pi/2$, $\partial p/\partial n$ is positive for $\pi\alpha/2(\pi - \alpha) < \phi < \pi - \pi\alpha/2(\pi - \alpha)$, that is for $2\alpha < \theta < 2(\pi - \alpha)$ if terms of the third order are neglected. Thus if terms of the third order are neglected a shock is predicted only along that part of the Mach cone which contributes to the boundary of the disturbed region (the continuation of the plane reflected shocks—see Fig. 2). The remaining part of the Mach cone probably represents a weaker shock followed immediately by an expansion.

When $\pi/2 < \alpha < 2\pi/3$, $\partial p/\partial n$ is positive in the intervals $\alpha < \theta < 2(\pi - \alpha)$ and $2\alpha < \theta < (2\pi - \alpha)$. These sections of the Mach cone still represent the continuations of the plane reflected shocks [see Fig. 3(a)]. As α is further increased multiple reflections of the incident shock wave occur at the two walls before the actual corner is reached,[4] and the flow pattern in the neighborhood of the corner is determined by the last pair of reflected waves. Fig. 3(b) for example, shows the configuration near the corner for $2\pi/3 < \alpha < 3\pi/4$. The factor $(\pi - \alpha)$ in the denominator of Eq. (21) suggests that strong shocks will be produced by reflection in corners of small angle.

Diffraction by a half-plane is also a simple special case. With $-\alpha_1 = \alpha_2 = \alpha$, Eq. (20) becomes

$$\partial p/\partial n = [2 \sin \alpha/2 \cos(\theta/2 + \alpha/2)] \div \{\pi[\cos(\theta + \alpha) - \cos\alpha]\} \quad (22)$$

In this case the reflected shock appears on one side only of the plane (see Fig. 2(b)), and is continued along the Mach cone as a weaker shock whose strength is deducible from Eqs. (16) and (22) as far as the point $\theta = (\pi - \alpha)$. Finally, in the region of shadow the Mach cone represents a continuation of the incident shock as far as the boundary.

REFERENCES

[1] Tan, H. S., *Strength of Reflected Shock in Mach Reflection*, Journal of the Aeronautical Sciences, Vol. 18, No. 11, p. 768, November, 1951.

[2] Chester, W., *The Reflection and Diffraction of Shock Waves*. To be published in the Quart. Jour. Mech. and App. Maths.

[3] Lighthill, M. J., *The Diffraction of Blast*, Proc. Roy. Soc. (A), Vol. 198, p. 454, 1949.

[4] Keller, J. B., and Blank, A., *Diffraction and Reflection of Pulses by Wedges and Corners*, Comm. Pure App. Maths., Vol. 4, p. 75, 1951.

[5] Lighthill, M. J., *The Shock Strength in Supersonic Conical Fields*, Phil. Mag., Vol. 40, p. 1202, 1949.

Allowable Stresses for Channels and Zees in Bending

B. E. Gatewood and D. W. Breuer

Mechanics Department, USAF Institute of Technology, Wright-Patterson Air Force Base, Ohio

January 4, 1954

THIS NOTE CORRECTS AN ERROR in the paper by Gatewood and Williams[1] "Allowable Compressive Stresses in Aircraft Structures" and presents some test results on channels in bending.

Several readers have been so kind as to point out an error in the bending buckling coefficient (K) curves in Fig. 6 of the original paper, the error being of the order of 15 per cent conservative in the region of $b_w/b_s = 1$ to 5. Fig. 1 shows the corrected curves, as well as additional curves for $t_w/t_s = 1.25$ and 1.50.

The table for the maximum stress coefficient M in Fig. 1 (Fig. 6 of original paper) was based on analogy to channels in compression and on seven bending tests on 24S-T formed channels.[2, 3] Recently, the authors have conducted a few more tests on standard 24S-T channel extrusions. A constant moment (zero shear) was applied to two channels back to back, separated by spacers outside the test region. To obtain failure in the test region instead of at the ends, the thickness of the compression leg was reduced about 10 per cent in the test region. Fig. 2 shows the test results as compared to the calculated values. K and M

M

$\frac{b_s}{t_s}$	M-formed in "T" cond.	M-extrusions; formed in "O" cond.
0-25	0.85	0.80
40	0.75	0.67
75	0.67	0.60

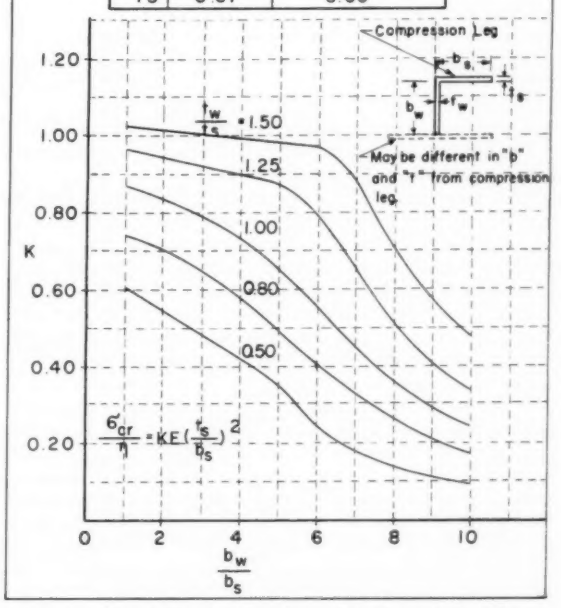

FIG. 1. M and K values for channels and zees in bending.

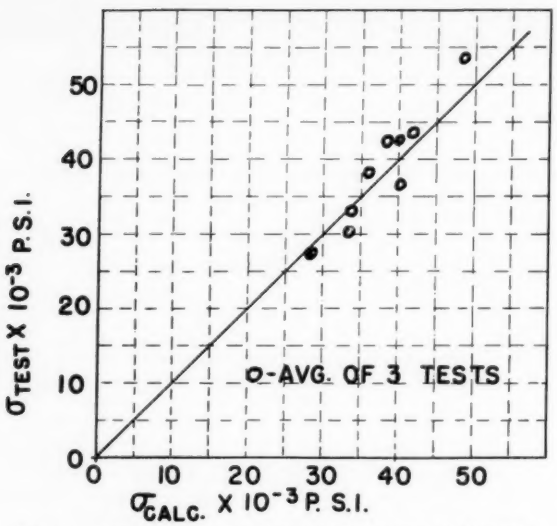

FIG. 2. Test results on bending of 24S-T extruded channels.

of Fig. 1, together with the crippling stress curves of Fig. 4 in reference 1, were used to calculate the allowable crippling stresses.

REFERENCES

[1] Gatewood, B. E., and Williams, E. L., *Allowable Compressive Stresses in Aircraft Structures*, Journal of the Aeronautical Sciences, Vol. 18, No. 10, pp. 657–664, October, 1951.

[2] Newton, R. E., *Bending Strength of Formed Sheet Metal Channels*, Curtiss-Wright (St. Louis) Report No. R-162, February, 1945.

[3] Charleville, J., *Bending Tests of 0.032 24 ST Alclad Formed Channels*, Curtiss-Wright (St. Louis) Report No. T-19, December, 1944.

Propagation of Turbulence from an Instantaneous Point Disturbance

Morton Mitchner
Research Fellow, Combustion Aerodynamics Laboratory
Harvard University, Cambridge, Mass.
January 6, 1954

EMMONS[1] has recently proposed a mechanism for the manner in which transition occurs from a laminar to a turbulent boundary layer. The mechanism assumes that unavoidable sources of disturbance carried within the laminar boundary layer may appear at random as "point" sources of turbulent spots. Once initiated, these individual turbulent regions will continue to grow in extent as they travel downstream until they coalesce with adjacent turbulent regions and eventually produce a fully developed turbulent boundary layer. The following contains a brief account of the flow distortion resulting from an artificial "instantaneous, point" disturbance produced in two different types of shear flow.

If the steady laminar motion of water flowing in an inclined rectangular channel is externally disturbed by allowing a drop of water to fall into the fluid, the development of the resulting region of turbulence may be observed visually by the roughness of the free surface associated with the turbulence. Observations were made at a constant mass flow rate of 0.81 lb./sec. ft. (or at Reynolds Number of 1230 corresponding to a water temperature of 21.0°C.) for channel slopes of 1.18°, 2.98°, and 5.26°. The corresponding mean velocities were 17.5, 25.0, and 31.0 in./sec., respectively. In all cases the developed turbulent spots were observed to be very closely geometrically similar in shape. Each spot is characterized by a well-defined upstream boundary with a more vaguely defined downstream edge, a typical shape being indicated in Fig. 1. The half-angle of the spots with respect to their point of origin, α, was found to remain essentially the same and equal to 6.6°. The half-angle of the spots with respect to their own vertex, β, was found to vary as 50°, 48°, and 45°, respectively. The velocity of the upstream edge of the spots, s', varied as 14.4, 20.2, and 25.4 in./sec., respectively, while the velocity of the downstream edge, s'', varied as 15.9, 23.0, and 28.8 in./sec., respectively. The experimental values for s' were found to agree moderately well with a theory treating the upstream edge as a particular form of hydraulic jump.[2]

A low turbulence level wind tunnel was employed to produce a critical laminar boundary layer over the length of a 30-in. flat plate at a free stream velocity of 550 in./sec. Point disturbances having a time duration of less than $^1/_{200}$ sec. were produced periodically 10 in. from the leading edge, and the development of the consequent turbulent flow patterns downstream was observed with a hot-wire. Disturbances were produced both by popping a small projection into the laminar boundary layer from the undersurface, and by producing a spark discharge in the boundary layer. The plan and side view shapes of an average spot are indicated in Fig. 2. At a distance of 14.5 in. from the disturbance source, the upstream and downstream edges of the turbulent spot were found to have velocities of 310 and 450 in./sec., respectively. The half-angle of the spot with respect to the disturbance origin, α, was found to be 8.6°. It is of some interest to note that the vertex of the turbulent spot for the flat plate case points downstream, in exact contradistinction to the free surface case. The inference is that in the latter case the free surface, in addition to the turbulence, plays an essential role in establishing the spot shape.

The observation that turbulent spots may be created artificially does not offer a complete verification of Emmons' mechanism of transition by any means, and considerable work

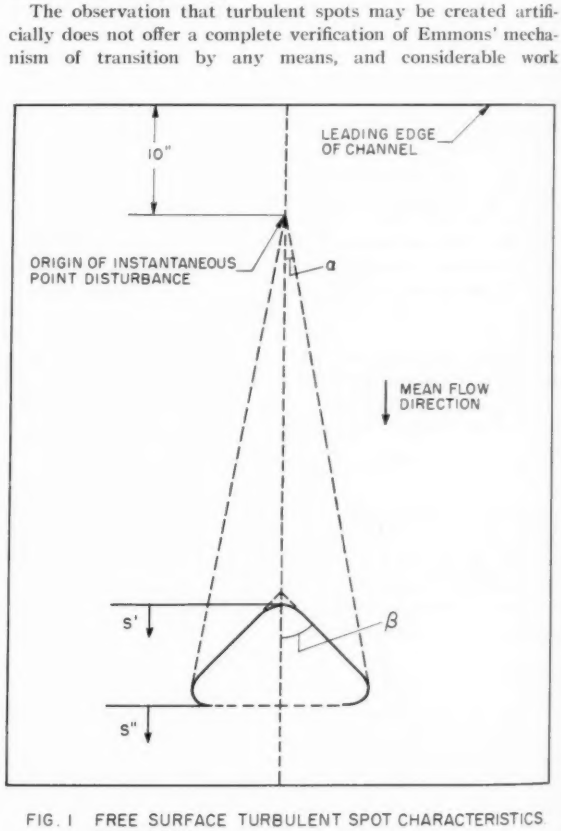

FIG. 1 FREE SURFACE TURBULENT SPOT CHARACTERISTICS PLAN VIEW

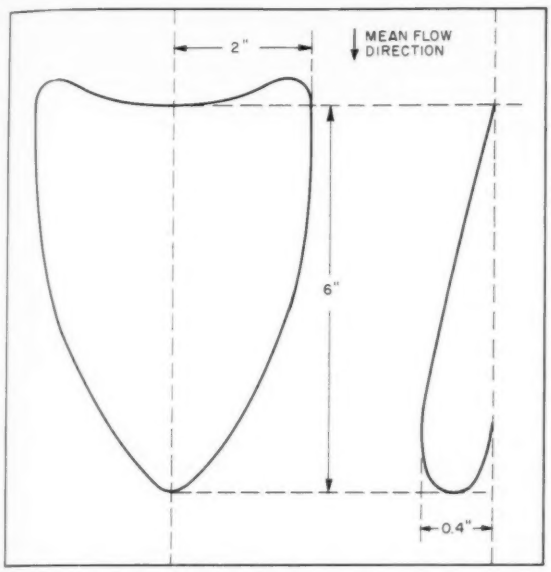

FIG 2 FLAT PLATE TURBULENT SPOT CHARACTERISTICS. PLAN AND SIDE VIEW.

remains to be done. The observation that spots appear to have heads projecting well above the flat plate surface suggests the interesting speculation that these heads are associated with the ragged turbulent high spots in the intermittent region above a fully-developed turbulent boundary layer. If this were the case there should exist a high degree of correlation between the properly time-delayed turbulence readings of two hot-wires placed in the intermittent region and separated along the direction of flow. It is also suggested that an obstacle, such as a cylinder, placed in a uniform flow acts as an intermittent source of turbulent spots, and that the wake consists of a moving pattern of such spots, the observed wake puffs being merely the passage of successive spot wings.

The author would like to express his thanks to Dr. A. A. Townsend for both his invaluable advice and his permission to use the low turbulence level wind tunnel at Cambridge University.

References

[1] Emmons, H. W., *The Laminar-Turbulent Transition in a Boundary Layer, Part I*, Journal of the Aeronautical Sciences, Vol. 18, No. 7, pp. 490–498, 1951.

[2] Mitchner, M., *The Propagation of Turbulence into a Laminar Boundary Layer*, Combustion Tunnel Laboratory Interim Technical Report No. 3, Harvard University, 1952.

An Integral Equation Occurring in the Theory of a Slender Quasi-Axisymmetrical Body

Paul F. Byrd
Aeronautical Research Scientist, Ames Aeronautical Laboratory, NACA, Moffett Field, Calif.

January 22, 1954

W. T. LORD[1] in a recent report derives an integral equation for a quasi-axisymmetrical, slender body having a specified sidewash on the wing. He states, however, that no published solution has yet been given. It is the purpose of this note to present an inversion of the equation.

The integral equation is

$$g(x, \psi) = \int_{-1}^{1} \frac{H(x, \zeta)\, d\zeta}{\psi - \zeta} \tag{1}$$

where ψ lies *outside* the interval of integration and all variables are real. This equation may also be written in the form

$$T(x, a) = \int_{-1}^{1} \frac{H(x, \zeta)\, d\zeta}{1 - 2a\zeta + a^2} \tag{1a}$$

where the prescribed function T is related to the sidewash, and H is an unknown function defining the boundary condition on the body. (See reference 1.) Eq. (1a) can easily be inverted by methods of complex variables or potential theory, and lends itself also to direct treatment by expansion of the kernel. We shall employ here the latter method.

Formal expansion of the kernel in terms of Tchebycheff's polynomials[2] of the second kind yields

$$\frac{1}{1 - 2a\zeta + a^2} = \frac{1}{\sqrt{1 - \zeta^2}} \sum_{j=0}^{\infty} a^j U_{j+1}(\zeta) \tag{2}$$

where the polynomials are given by

$$U_{j+1}(\zeta) = (1 + j)\sqrt{1 - \zeta^2} \int_0^{\pi} (\zeta + i\sqrt{1 - \zeta^2} \times \cos\theta)^j \sin\theta\, d\theta \tag{3}$$

Assuming now that the unknown

$$H(x, \zeta) = \sum_{m=0}^{\infty} b_{m+1}(x)\, U_{m+1}(\zeta) \tag{4}$$

we thus have for Eq. (1a)

$$T(x, a) = \sum_{m=0}^{\infty} b_{m+1}(x) \sum_{j=0}^{\infty} a^j \int_{-1}^{1} \frac{U_{j+1}(\zeta) U_{m+1}(\zeta)}{\sqrt{1 - \zeta^2}} \tag{5}$$

If we further assume that

$$T(x, a) = \sum_{m=0}^{\infty} c_m \xi_1(x)\, a^m \tag{6}$$

it follows from Eqs. (5) and (6) that $\pi b_{m+1} = c_{m+1}$. Hence, from Eqs. (3) and (4) we have the expression

$$H(x, \zeta) = \frac{\sqrt{1 - \zeta^2}}{\pi} \sum_{m=0}^{\infty} (1 + m)\, c_{m+1}(x) \int_0^{\pi} (\zeta + i\sqrt{1 - \zeta^2} \cos\theta)^m \sin\theta\, d\theta \tag{7}$$

The series occurring in this equation for H is summable.

From Eq. (6)

$$\sum_{m=0}^{\infty} (1 + m)\, c_{m+1}(x)\, \sigma^m = T(x, \sigma) + \sigma \frac{d}{d\sigma} T(x, \sigma)$$

and thus upon setting $\sigma = \zeta + i\sqrt{1 - \zeta^2} \cos\theta$, one can write for Eq. (7) the inversion formula in the closed form

$$H(x, \zeta) = \frac{i}{\pi} \int_{\zeta + i\sqrt{1 - \zeta^2}}^{\zeta - i\sqrt{1 - \zeta^2}} [T(x, \sigma) + \sigma \frac{d}{d\sigma} T(x, \sigma)] d\sigma \tag{8}$$

or finally

$$H(x, \zeta) = \frac{2}{\pi} \mathrm{Im}[(\zeta + i\sqrt{1 - \zeta^2})\, T(x, \zeta + i\sqrt{1 - \zeta^2})] \tag{8a}$$

where the symbol Im means that the imaginary part is to be taken.

References

[1] Lord, W. T., *Supersonic Flow Past a Particular Type of Slender Wing-Body Combination at Zero Incidence*, R.A.E. Tech Note No. Aero. 2134, December, 1951.

[2] Magnus, Wilhelm, and Oberhettinger, Fritz, *Formulas and Theorems for the Special Functions of Mathematical Physics*. Reprinted by Chelsea Pub. Co., 1949.

On Heat Transfer in a Compressible Laminar Boundary Layer

Alfred H. Silver
General Electric Company, Cincinnati, Ohio
December 24, 1953

Notation

c_p = specific heat at constant pressure, ft.lbs./slug °F.
h = film coefficient of heat transfer, ft.lbs./sec. ft.^{2} °F.
k = thermal conductivity, ft.lbs./sec. ft. °F.
p = pressure, lbs. per sq.ft.
t = function of x defined in text
u = velocity in x direction, ft. per sec.
v = velocity in y direction, ft. per sec.
w = value at wall, subscript
x = distance along airfoil measured from forward stagnation point, ft.
y = distance perpendicular to and measured from airfoil surface, ft.
I = modified Bessel function of first kind
Q = unit heat flux, ft.lbs./sec. ft.^{2}
T = total temperature, $T_s + (u^2/2c_p)$, °R.
T_s = static temperature, °R.
Γ = gamma function
δ = function of x defined in text
θ = momentum thickness of boundary layer, ft.
μ = absolute viscosity, lbs. sec./ft.^{2}
ν = kinematic viscosity, ft.^{2} per sec. $= \mu/\rho$
ρ = mass density, slugs per cu.ft.
σ = Prandtl Number $\mu c_p/k$, dimensionless
τ_0 = shear stress at wall
ψ = stream function, $\rho u = \partial\psi/\partial y$, $\rho v = -\partial\psi/\partial x$

Analysis

The solution of heat transfer in a two-dimensional laminar gas boundary layer, considering compressibility effects and with arbitrary pressure and surface temperature distributions, involves the simultaneous solution of the momentum, continuity, and energy equations. The exact solution of the equations has not, to the knowledge of the writer, been found as yet. This note, which is a condensation of work done for General Electric in 1951, attempts to extend the approximations of Lighthill[1] and Tifford[2] to include the effects of compressibility.

For the analysis, c_p is considered constant, σ is considered constant and near unity, and the effects of curvature of the surface and pressure gradient normal to the surface are neglected. The equations to be solved are

Momentum:
$$\rho u \frac{\partial u}{\partial x} + \rho v \frac{\partial u}{\partial y} = -\frac{dp}{dx} + \frac{\partial}{\partial y}\left(\mu \frac{\partial u}{\partial y}\right) \tag{1}$$

Continuity:
$$\frac{\partial}{\partial x}(\rho u) + \frac{\partial}{\partial y}(\rho v) = 0 \tag{2}$$

Energy:
$$\rho c_p u \frac{\partial T_s}{\partial x} + \rho v c_p \frac{\partial T_s}{\partial y} = u \frac{dp}{dx} + \frac{c_p}{\sigma}\frac{\partial}{\partial y}\left(\mu \frac{\partial T_s}{\partial y}\right) + \mu\left(\frac{\partial u}{\partial y}\right)^2 \tag{3}$$

Transformation of the equations into the x, ψ coordinate system yields

$$\rho u \frac{\partial u}{\partial x} = -\frac{dp}{dx} + \rho u \frac{\partial}{\partial \psi}\left(\rho \mu u \frac{\partial u}{\partial x}\right) \tag{1a}$$

$$\rho u c_p \frac{\partial T_s}{\partial x} = u \frac{dp}{dx} + \frac{\rho u c_p}{\sigma}\frac{\partial}{\partial \psi}\left(\rho \mu u \frac{\partial T_s}{\partial \psi}\right) + \mu \rho^2 u^2 \left(\frac{\partial u}{\partial \psi}\right)^2 \tag{3a}$$

Multiplication of Eq. (1a) by u and adding yields

$$\frac{\partial T}{\partial x} = \frac{1}{\sigma}\frac{\partial}{\partial \psi}\left\{\rho \mu u \frac{\partial}{\partial \psi}\left[T + (\sigma - 1)\frac{u^2}{2}\right]\right\} \tag{4}$$

The boundary conditions on the total temperature are:

$$T(0, \psi) = T(x, \infty) = 0, \quad T(x, 0) = T_0(x)$$

Since the analysis is concerned with heat transfer, which is a surface phenomenon, and since σ is assumed near unity, the second term in the bracket is neglected in comparison with the first. This yields

$$\frac{\partial T}{\partial x} = \frac{1}{\sigma}\frac{\partial}{\partial \psi}\left(\rho \mu u \frac{\partial T}{\partial \psi}\right) \tag{4a}$$

A final assumption about the nature of the gas properties is that the viscosity can be expressed as $\mu = C_1 T_s$. The applicability of this assumption has been shown by Chapman and Rubesin.[3] This means that $\rho\mu = C_2 p$ and

$$\partial(\rho\mu)/\partial\psi = C_2(\partial p/\partial\psi) = 0$$

Therefore

$$\partial T/\partial x = (\rho\mu/\sigma)(\partial/\partial\psi)[u(\partial T/\partial\psi)] \tag{4b}$$

Similarly, from Eq. (1a)

$$\frac{\partial u}{\partial x} = \frac{-1}{\rho u}\frac{dp}{dx} + \rho\mu \frac{\partial}{\partial \psi}\left(u \frac{\partial u}{\partial \psi}\right) \tag{1b}$$

The simultaneous solution of Eqs. (1b) and (4b) is a formidable task in the general case. Therefore, a power series approximation to the velocity distribution which is valid close to the wall will be used.

Let

$$u/\sqrt{2} = a(x) + b(x)\psi^{1/2} + c(x)\psi + \ldots$$

Since $u(x, 0) = 0$

$$\tau(x, 0) \equiv \tau_0(x) = \mu_w[\rho u(\partial u/\partial\psi)]_{\psi=0}$$

$$a(x) \equiv 0 \text{ and } b^2(x) = \tau_0(x)/\rho_w\mu_w$$

Applying Eq. (1b) at $\psi = 0$ yields

$$dp/dx = \rho_w^2\mu_w u(\partial/\partial\psi)\,[u(\partial u/\partial\psi)]_{\psi=0}$$

or

$$(1/\rho_w^2\mu_w)(dp/dx) = (3/\sqrt{2})b^2 c$$

This gives

$$\frac{u^2}{2} = \frac{\tau_0(x)}{\rho_w \mu_w}\psi + \frac{2\sqrt{2}}{3}\left(\frac{\nu_w}{\tau_0}\right)^{1/2}\frac{1}{\rho_w\mu_w}\frac{dp}{dx}\psi^{3/2} + \cdots$$

If the first term only is used, the velocity distribution of Lighthill is obtained. This, however, neglects the effect of pressure gradient in the direction of flow on the velocity distribution. Tifford suggested that the term involving dp/dx be accounted for in some way while retaining only the first power of ψ. This can be done, in this case, by letting

$$\delta(x) = (2\sqrt{2}/3)\,(\nu_w/\tau_0)^{1/2}\psi^{1/2}$$

Then

$$u^2/2 = (1/\rho_w\mu_w)\,[\tau_0(x) + \delta(dp/dx)]\psi$$

The validity of the use of δ and its exact nature will be determined after the analysis is complete by comparing the results of the equation obtained with those from the special cases that have been solved exactly.

Letting $F(x) \equiv \tau_0 + \delta(dp/dx)$ and remembering that $\rho\mu$ is independent of ψ, Eq. (4b) yields

$$\frac{\sigma}{\sqrt{2\rho\mu F}}\frac{\partial T}{\partial x} = \frac{\partial}{\partial\psi}\left(\psi^{1/2}\frac{\partial T}{\partial\psi}\right) \tag{5}$$

Letting

$$t = \int_0^x \frac{\sqrt{2\rho\mu F(z)}}{\sigma}\,dz$$

$$\partial T/\partial t = (\partial/\partial\psi)\,[\psi^{1/2}(\partial T/\partial\psi)] \tag{6}$$

subject to

$$T(0, \psi) = T(t, \infty) = 0, \quad T(t, 0) = T_0(t)$$

Eq. (6) can be solved by Laplace Transformation obtaining a Bessel function ($I_{\pm 1/3}$) solution. If the Bessel function is written in its power series form, the following is obtained:

$$T(t) = T_0(t)\left\{1 - \frac{(2/3)^{2/3}}{\Gamma(4/3)}\left[\int_0^t \frac{T_0'(t_1)\,dt_1}{(t - t_1)^{2/3}} + \frac{T_0(0+t)}{t^{1/3}}\right]\psi^{1/2} + f(t)\psi + \cdots\right\} \tag{7}$$

Since T has a finite discontinuity at $t = 0$ due to the change in temperature from the free-stream value to the stagnation point surface temperature, the coefficient of $\psi^{1/2}$ in Eq. (7) can be expressed as the Stieltjes integral

$$-\frac{(2/3)^{2/3}}{\Gamma(4/3)}\int_0^t \frac{dT_0(t_1)}{(t - t_1)^{1/3}}$$

Therefore

$$T(x) = T_0(x)\left\{1 - \frac{(2/3)^{2/3}}{\Gamma(4/3)}\int_0^x \frac{dT_0(\xi)}{(t - t_1)^{1/3}}\psi^{1/2} + g(x)\psi + \cdots\right\}$$

where t_1 is the value of t at which $x = \xi$. But

$$t - t_1 = \frac{1}{\sigma}\int_\xi^x \sqrt{2\rho\mu F(z)}\,dz$$

so that

$$T(x) = T_0(x)\left\{1 - \left[\frac{(2/3)^{2/3}\,\sigma^{1/3}}{\Gamma(4/3)}\int_0^x\left(\int_\xi^x \sqrt{2\rho\mu F(z)}\,dz\right)^{-1/3} dT_0(\xi)\right]\psi^{1/2} + g(x)\psi + \cdots\right\} \tag{8}$$

The heat transfer from the surface, $Q(x)$, may be determined from

$$Q(x) = -k_w\left.\frac{\partial T_s}{\partial y}\right|_{y=0} = -k_w\left.\frac{\partial T}{\partial y}\right|_{y=0} = -k_w\rho u\left.\frac{\partial T}{\partial\psi}\right|_{\psi=0}$$

or

$$Q(x) = \frac{k_w}{\Gamma(4/3)}\frac{\sqrt{\rho_w F}}{2\mu_w}\left(\frac{4\sigma}{9}\right)^{1/3}\int_0^x\left[\int_\xi^x \sqrt{2\rho\mu F(z)}\,dz\right]^{-1/3} dT_0(\xi) \tag{9}$$

Since $\sigma \approx 1$, the effective and total temperatures are nearly equal. Therefore

$$h(x) = \frac{Q(x)}{T_0} = \frac{k_w}{\Gamma(4/3)T_0}\left(\frac{4\sigma}{9}\right)^{1/3}\frac{\sqrt{\rho_w F}}{2\mu_w}\int_0^x\left[\int_\xi^x \sqrt{2\rho\mu F(z)}\,dz\right]^{-1/3} dT_0(\xi) \tag{10}$$

For the average heat-transfer coefficient of a fluid of constant properties on an isothermal surface, Eq. (10) simplifies to

$$\frac{\bar{h}l}{k} = 0.807\left(\frac{\sigma\rho}{\mu^2}\right)^{1/3}\int_0^l \sqrt{F(z)}\,dz$$

Tifford compared Eq. (22) with the solution obtained by numerical integration of the differential equations for isothermal wedges with widely varying wedge angles. He determined that an excellent correlation (±1.3 per cent) could be obtained if the value of δ be chosen as

$$\delta = (4/3)\theta(x)/\sigma^{1/4}$$

and the resulting value of F be multiplied by $0.98\sigma^{0.02}$.

It is therefore recommended that Eqs. (9) and (10) be used with

$$F(x) = 0.98\sigma^{0.02}\left[\tau_0(x) + \frac{(4/3)\theta(x)}{\sigma^{1/4}}\frac{dp}{dx}\right] \tag{11}$$

References

[1] Lighthill, M. J., *Contributions to the Theory of Heat Transfer Through a Laminar Boundary Layer*, Proceedings of the Royal Society (London), Series A, Vol. 202, No. 1070, pp. 359–377, August, 1950.

[2] Tifford, A. N., *On the Theory of Heat Transfer Through a Laminar Boundary Layer*, Readers' Forum, Journal of the Aeronautical Sciences, Vol. 18, No. 9, pp. 284–285, April, 1951.

[3] Chapman, D. R., and Rubesin, M. W., *Temperature and Velocity Profile in the Compressible Laminar Boundary Layer with Arbitrary Distribution of Surface Temperature*, Journal of the Aeronautical Sciences, Vol. 16, No. 9, pp. 547–565, September, 1945.

Buckling of Thin Cylindrical Shells Subject to Hydrostatic Pressure

William A. Nash

Associate Professor, Department of Engineering Mechanics, University of Florida, Gainesville, Fla.

January 19, 1954

SEVERAL ANALYSES have appeared in the literature for the elastic buckling of a thin cylindrical shell subject to hydrostatic pressure.[1–6] These have all been based upon the classical small deformation theory of thin shells presented by Love,[7] and have assumed a geometrically perfect cylinder prior to loading. The procedure adopted in most of these papers has been that of minimization of the total potential, which leads to a stability determinant for calculating the buckling pressure. The labor of computing the elements of such a determinant is considerable and it is the purpose of this note to present approximate formulas for the elastic buckling pressure for several boundary conditions.

In 1934 Donnell[8] presented a second-approximation shell theory for finite deflections in which two of the displacement components were eliminated and the following relation between the stress function F of the membrane stresses and the radial displacement w was developed:

$$\left(\frac{\partial^2}{\partial x^2}+\frac{\partial^2}{\partial s^2}\right)^2 F = EK\left[\left(\frac{\partial^2 w}{\partial x \partial s}\right)^2 - \frac{\partial^2 w}{\partial x^2}\cdot\frac{\partial^2 w}{\partial s^2}\right] - \frac{E}{R}\frac{\partial^2 w}{\partial x^2} \tag{1}$$

Here x and s are axial and tangential coordinates in the middle surface of the shell, R denotes the mean radius of the shell, and K involves the ratio between the initial deviation from perfect shape w_0 and the displacement during loading w. The second-order terms on the right-hand side correspond to membrane stresses due to finite displacements, while the last term corresponds to membrane stresses due to the curvature. For the case of small displacements of an initially perfect shell, this equation reduces to

$$[(\partial^2/\partial x^2)+(\partial^2/\partial s^2)]^2 F = -(E/R)\cdot(\partial^2 w/\partial x^2) \tag{2}$$

Thus, if w is assumed, then F can be readily obtained. Knowing w and F the internal strain energy of the shell is given by[8]

$$\bar{E} = \frac{Eh^3}{24(1-\nu^2)}\int_0^L\int_0^{2\pi R}\left\{\left(\frac{\partial^2 w}{\partial x^2}+\frac{\partial^2 w}{\partial s^2}\right)^2 + 2(1-\nu)\left[\left(\frac{\partial^2 w}{\partial x \partial s}\right)^2 - \frac{\partial^2 w}{\partial x^2}\cdot\frac{\partial^2 w}{\partial s^2}\right]\right\} dx\,ds + \frac{h}{2E}\int_0^L\int_0^{2\pi R}\left\{\left(\frac{\partial^2 F}{\partial x^2}+\frac{\partial^2 F}{\partial s^2}\right)^2 + 2(1+\nu)\left[\left(\frac{\partial^2 F}{\partial x \partial s}\right)^2 - \frac{\partial^2 F}{\partial x^2}\cdot\frac{\partial^2 F}{\partial s^2}\right]\right\} dx\,ds \tag{3}$$

where h is the shell thickness and ν represents Poisson's ratio.

The potential energy of the forces acting upon the shell has previously been demonstrated to be[5]

$$W_1 = pR\int_0^L\int_0^{2\pi R}\left[-\frac{w_s^2}{2}+\frac{w^2}{2R^2}-\frac{w_x^2}{4}\right] dx\,ds \tag{4}$$

where L is the length of the shell. Consequently, the total potential is given by the sum of $\bar{E}$, W_1, and a constant term which corresponds to the mean axial and circumferential stresses.

Let us first consider the case of a clamped-end cylinder subject to hydrostatic pressure. The shell is not reinforced. If the deflection of a generator is represented by the function

$$w = ah\cos(ms/R)(1-\cos 2\delta x) \tag{5}$$

where a is an arbitrary parameter, m is the number of waves in the circumferential direction, and $\delta = \pi/L$, then from Eq. (2) we have

$$F = -\frac{4E\delta^2 ah}{[4\delta^2+(m^2/R^2)]^2 R}\cos\frac{ms}{R}\cos 2\delta x \tag{6}$$

Minimizing the total potential with respect to the parameter a and solving the resulting equation for the buckling pressure p we obtain

$$p = \frac{\dfrac{Eh^3}{24(1-\nu^2)}\left\{8\delta^4+\dfrac{3m^4}{2R^4}+\dfrac{4\delta^2 m^2}{R^2}\right\}+\dfrac{4Eh\delta^4}{[4\delta^2+(m^2/R^2)]^2R^2}}{\left\{\dfrac{3m^2}{4R}+\dfrac{R\delta^2}{2}-\dfrac{3}{4R}\right\}} \tag{7}$$

Because of the simplified expressions used for the bending strain energy, the above equation for buckling pressure is accurate only if the square of the number of circumferential waves m is large compared to unity.

Secondly, the case of a cylindrical shell having simply supported ends and subject to hydrostatic pressure may be treated by this technique. This is the problem considered by von Mises[1] and if the deflection of the generator is taken to be

$$w = ah\sin(ms/R)\sin\delta x \tag{8}$$

as he assumed, then after minimization of the total potential, the buckling pressure is found to be

$$p = \frac{\dfrac{Eh^3}{48(1-\nu^2)}\left\{\delta^2+\dfrac{m^2}{R^2}\right\}^2+\dfrac{Eh\delta^4}{4[\delta^2+(m^2/R^2)]^2R^2}}{\left\{\dfrac{m^2}{4R}+\dfrac{R\delta^2}{8}-\dfrac{1}{4R}\right\}} \tag{9}$$

TABLE 1

Model	L, In.	h, In.	R, In.	A, Ref. 1	B, Eq. 9	C, Ref. 6	D, Eq. 7	b	h_0	E, Ref. 4	F, Ref. 6
1	32	0.031	8	7.0(6)	7.2(6)	10.1(7)	10.4(7)	0.12	0.40	7.9(6)	9.8(6)
2	32	0.050	8	23.1(5)	24.1(5)	34.0(6)	35.2(6)	0.12	0.40	29.7(6)	32.5(6)
3	16	0.053	8	51.2(7)	53.2(7)	73.0(8)	74.5(8)	0.12	0.40	65.5(8)	68.4(8)
4	32	0.109	8	152.2(4)	162.1(4)	224.1(5)	235.2(5)	0.12	0.40	197.7(5)	213.5(5)
5	8	0.0635	8	164.7(9)	166.6(9)	229.1(10)	246.5(10)	0.12	0.40	226.0(10)	210.9(10)
6	8	0.0901	8	384.9(8)	390.6(8)	534.2(9)	538.7(9)	0.12	0.40	463.7(9)	492.5(9)
7	5.08	0.065	13.38	137.6(15)	138.1(15)	189.0(17)	189.9(17)	0.1875	0.719	175.1(17)	179.0(16)
8	6.686	0.1324	13.41	613.2(11)	617.5(11)	849.7(12)	852.8(12)	0.231	1.0824	781.0(10)	823.2(10)

This is equivalent to the result von Mises obtained using three differential equations of equilibrium. It was also presented by Salerno and Levine[2] as a special case of their analysis of a cylinder reinforced by elastic circumferential rings.

It is of interest to compare the numerical results indicated by Eqs. (7) and (9) with those found from existing theories derived from minimum energy considerations in which three orthogonal components of displacement were considered and the potential minimized with respect to at least three parameters. In Table 1 are listed the geometries of eight cylindrical shells together with buckling pressures given by various theories. In column A is listed the buckling pressure indicated by von Mises[1] for simply-supported cylinders, and in column B appears the value given by Eq. (9). Column C lists the buckling pressure for a shell having clamped ends[6] and column D lists the buckling pressure for this same shell as given by Eq. (7). In columns E and F appear buckling pressures indicated by the theories of references 4 and 6, respectively, for multiple-bay cylindrical shells, each bay having the geometry indicated in Table 1 but reinforced by rectangular circumferential stiffening rings having the width b and overall ring-shell depth h_0 indicated. The pressures given in C and D could, of course, be regarded as buckling pressures for a multiple-bay shell having infinitely rigid reinforcing rings, each bay being of length L. The number in parentheses after each buckling pressure is the number of circumferential waves which corresponds to the minimum buckling load. It is to be borne in mind that all of these pressures are for a geometrically perfect shell having no initial imperfections and being free from initial stress. The presence of initial imperfections is known to reduce the buckling pressures from those given by classical treatments of idealized shells.

REFERENCES

[1] von Mises, R., *Der kritische Aussendruck für allseits belastete zylindrische Rohre*, Fest. zum 70 Geburstag, von Prof. A. Stodola, Zurich, pp. 418–430, 1929.

[2] Salerno, V. L., and Levine, B., *Buckling of Circular Cylindrical Shells with Evenly Spaced, Equal Strength Circular Ring Frames*, Parts I and II, Polytechnic Institute of Brooklyn, Reports Nos. 167, 169, 1950.

[3] Salerno, V. L., Levine, B., and Pulos, J. G., *Charts for the Determination of the Upper and Lower Limit of Hydrostatic Buckling Pressures for Reinforced Circular Cylindrical Shells*, Polytechnic Institute of Brooklyn Report No. 177, 1950.

[4] Salerno, V. L., and Levine, B., *The Determination of the Hydrostatic Buckling Pressures for Circular Cylindrical Shells Reinforced with Rings*, Polytechnic Institute of Brooklyn Report No. 182, 1951.

[5] Batdorf, S. B., *A Simplified Method of Elastic-Stability Analysis for Thin Cylindrical Shells*, NACA Report 874, 1947.

[6] Nash, W. A., *Buckling of Multiple-Bay Ring-Reinforced Cylindrical Shells Subject to Hydrostatic Pressure*, Journal of Applied Mechanics, Vol. 20, No. 4, pp. 469–474, 1953.

[7] Love, A. E. H., *A Treatise on the Mathematical Theory of Elasticity*, Dover Publications, New York, 1944.

[8] Donnell, L. H., *A New Theory for the Buckling of Thin Cylinders Under Axial Compression and Bending*, Trans. A.S.M.E., Vol. 56, p. 795, 1934.

An Empirical Method for Calculation of the Growth of a Turbulent Boundary Layer*

Donald Ross† and J. M. Robertson‡
Ordnance Research Laboratory, The Pennsylvania State College

November 4, 1953

SUMMARY

A new, simplified method for calculating the momentum thickness of a symmetrical turbulent boundary layer has been developed empirically. In regions of strong adverse pressure gradient, a simple algebraic expression may be used involving an exponent which is a function of the Reynolds Number. Limitations of the method are presented.

INTRODUCTION

THE USUAL EQUATION for the growth of a two-dimensional boundary layer is the von Kármán integral momentum equation for the rate of change of the momentum thickness θ as a function of the wall-shear-stress coefficient c_f and the pressure gradient

$$d\theta/dx = c_f/2 + \{(2 + H)[(\theta/\rho u_1^2)(dp/dx)]\} \quad (1)$$

where H is the shape parameter and u_1 the velocity outside of the boundary layer. This equation was originally derived by von Kármán[1] in 1921 for laminar boundary layers and later applied to turbulent boundary layers by Buri[2] and Gruschwitz.[3] Although the equation has generally been verified for turbulent flows with zero pressure gradient, and by Clauser[4] for equilibrium flows of all types, it has been found faulty for nonequilibrium turbulent boundary layers both with and without adverse pressure gradients. The cause of the discrepancies was discovered in 1949 by Newman[5] and Wallis,[6] who pointed out that the turbulent normal stresses are not negligible and must be included in the differential equation for the growth of the momentum thickness.

The revised equation derived by Goldschmied,[7] Bidwell,[8] Van Le,[9] and Ross[10] may be written

$$\frac{d\theta}{dx} = \frac{c_f}{2} + (2 + H)\frac{\theta}{\rho u_1^2}\frac{dp}{dx} + \frac{1}{u_1^2}\int_0^\delta \frac{\partial}{\partial x}(\overline{u'^2} - \overline{v'^2})dy \quad (2)$$

where p refers to the wall static pressure. The term involving the anisotropy of the turbulence has been related to the shear stress and thence to mean flow quantities by Ross,[10,11] resulting in a new approximate differential equation; while Rubert and Persh[12] have obtained an empirical correction term of similar

* Work partially supported by the Office of Naval Research under Project NR 062-139.

† Associate Professor of Engineering Research.

‡ Professor of Engineering Research.

form. In any case, it is now agreed that some correction of the original von Kármán equation is required for turbulent flows. We may write the revised equation

$$d\theta/dx \cong c_f/2 - \{(2 + H)[(\theta/u_1)(du_1/dx)]\} + [C\theta(dH/dx)] \quad (3)$$

where the term involving the wall pressure is replaced by one with the outer velocity, and the correction term includes the fact that the static pressure at the outer edge of the boundary layer is not equal to that at the wall.

Eq. 3 reveals why Clauser[4] found good agreement with Eq. 1 for equilibrium boundary layers even in fairly strong adverse pressure gradients. For such flows, H is practically constant and the correction term is negligible. The equation also shows why some cases of redistributing flows have not agreed with Eq. 1, even though there was practically zero pressure gradient. For such flows, the correction is negative and the momentum thickness grows less rapidly than as predicted by the simple von Kármán equation.

Integrated forms of Eq. 1 have been developed by several authors, often based on erroneous assumptions concerning the behavior of the wall-shear-stress coefficient. None of the equations is particularly simple to use and all of them are inaccurate near separation. The solution presented in the present paper is quite simple mathematically, and it is usually more accurate than the other methods.

Equilibrium Boundary Layers

For conditions close to equilibrium, H is practically constant and the only major problem is the determination of a suitable equation for the wall-shear-stress coefficient. The recently developed equation of Ludwieg and Tillmann[13]

$$c_f = 0.246/(10^{0.678H}R_\theta^{0.268}) \quad (4)$$

is applicable at any value of the shape parameter. Expressing Eq. 3 as a difference equation:

$$\Delta\theta = (c_f/2)\Delta x - (2 + H)\theta\Delta\ln u_1 \quad (5)$$

and using this with Eq. 4, step-by-step integration is possible. This is the usual method for the solution of the von Kármán equation. However, because of the relative constancy of c_f and H and the usual small pressure gradient, large intervals may be used and the solution requires only a few steps.

Strong Adverse Pressure Gradients

For comparatively large pressure gradients, such as those on the suction surface of a lifting airfoil or in a diffuser, the step-by-step solution requires many more steps, as well as simultaneous solution of an equation for H. Here a new solution is presented. The complete momentum equation (Eq. 3) may be written:

$$d\theta/\theta \cong -du_1/u_1\{2 + H - [c_f/2(\theta/u_1)(du_1/dx)] - Cu_1(dH/du_1)\} \quad (6)$$

All of the functions in the brackets are variable with distance; but it has been observed in a large number of cases that their sum is approximately constant for any single experiment. If we make this assumption and replace the quantity in brackets by $2 + G$, then the solution of Eq. 6 is simply:

$$\theta/\theta_i = [u_{1i}/u_1]^{2+G} \quad (7)$$

where the subscript i refers to some initial station. This solution of the integral momentum equation is very simple and allows the replacement of the usual laborious step-by-step solution by an algebraic equation. It remains to confirm this solution experimentally, determine its limitations, and evaluate the exponent.

Confirmation for Two-Dimensional Flows

To verify a solution of the momentum equation of the form of Eq. 7, the data from more than twenty two-dimensional experiments were plotted in the form of θ as a function of u_1^2 on log-log paper. These experiments were chosen to cover a wide variety of two-dimensional configurations. The result of the log-log plot was encouraging, as a general linear trend was found for most of the data. Closer examination revealed consistent discrepancies for weak pressure gradients, and also close to separation. By trial and error it was found that one criterion for the applicability of Eq. 7 is that the pressure gradient term dominate. This is expressed approximately by the inequality

$$-[(\theta/u_1)(du_1/dx)] \geq c_f/4 \quad (8)$$

Restricting the data to those satisfying this inequality, a second plot was made to confirm Eq. 7. The result is presented in Fig. 1, the key to the experimental points being given by Table 1. The general linear trend is found for most of the experiments, with an average value of G of about 2.8 fitting most of the data. Particularly impressive is the verification for the diffuser tested by Hall[14] for which particular care was exercised in obtaining two-dimensional flow. The only divergent set of data is that of Wieghardt and Tillmann[15] in a channel. These data have been criticized elsewhere, and Tillmann has attributed the divergence to observed secondary flows. Ignoring this one test, the rest of the data give a reasonable confirmation of Eq. 7.

The explanation of the success of Eq. 7 lies in the approximate constancy of the relation

$$G = H - [c_f/2(\theta/u_1)(du_1/dx)] - Cu_1(dH/du_1) \quad (9)$$

all terms of which are usually positive in an adverse pressure gradient. Apparently, as the boundary layer progresses, the decrease in the skin friction term closely equals the increase in both H and the correction term, thus keeping G approximately constant. Near separation, the sum of H and the correction term is large, and the momentum thickness may be expected to exceed the value given by the simple equation. However, for redistributing flows, such as a reattached boundary layer following separation, the correction term is negative and so Eq. 7 is valid even at high values of H close to separation.

Axisymmetric Boundary Layers

For flows with rotational symmetry the momentum equation is quite similar to the two-dimensional one, and so a similar solution is to be expected. Unfortunately, bodies of revolution exhibit only relatively weak pressure gradients and such data are not applicable. However, strong adverse pressure gradients are found in conical diffusers. For flow in conical diffusers, the momentum integral equation becomes

$$\frac{d(\theta r)}{\theta r} = -\frac{du_1}{u_1}\left[2 + \mathrm{H} - \frac{c_f/2}{(\theta/u_1)(du_1/dx)} - Cu_1\frac{dH}{du_1}\right] \quad (10)$$

where r is the local pipe radius and the three-dimensional momentum thickness is defined by

$$\theta \equiv \frac{1}{r}\int_0^\delta \left(1 - \frac{u}{u_1}\right)\frac{u}{u_1}\left(1 - \frac{y}{r}\right)dy \quad (11)$$

The corresponding solution for the momentum thickness in strong adverse pressure gradients is

$$(\theta r/\theta_i r_i) = [(u_{1i}/u_1)]^{2-G} \quad (12)$$

This is the form in which the present solution of the momentum equation was originally derived by the authors[16] for application to a diffuser experiment.

To confirm Eq. 12, data from several conical diffuser experiments have been used. Fig. 2 shows the results of a study of three diffuser angles and several entrance boundary layer thicknesses carried out by the authors[17] preliminary to the design of a large water tunnel. These data are seen to confirm Eq. 12.

Variation with Reynolds Number

Examination of Eq. 9 for G would lead one to expect a Reynolds number effect. At lower Reynolds numbers, both H and c_f

FIG.

TABLE 1 SYMBOLS FOR EXPERIMENTS

SYMBOLS	INVESTIGATORS	TEST OBJECT	EXPERIMENT IDENTIFICATION
⊘	FAGE, FALKNER (1930)	JOUKOWSKI AIRFOIL, 0°	$R_c = 1.25 \times 10^6$
⊘	FAGE, FALKNER (1930)	JOUKOWSKI AIRFOIL, 0°	$R_c = 1.67 \times 10^6$
⊕	PRESTON, SWEETING (1943)	JOUKOWSKI AIRFOIL, 0°	$R_c = 4.2 \times 10^5$
⊖	PRESTON, SWEETING (1943)	JOUKOWSKI AIRFOIL, 6°	$R_c = 4.2 \times 10^5$
⊙	SCHUBAUER, KLEBANOFF (1950)	SIMULATED AIRFOIL,	$R_c = 15.3 \times 10^6$
△	GRUSCHWITZ (1931)	GÖTTINGEN 387 AIRFOIL, 12°	$R_c = 8.4 \times 10^5$
<	VON DOENHOFF, TETERVIN (1942)	66, 2-216 AIRFOIL, 10°	$R_c = 2.6 \times 10^6$
∨	VON DOENHOFF, TETERVIN (1943)	65(216)-222 AIRFOIL, 8.1°	$R_c = 0.9 \times 10^6$
∧	VON DOENHOFF, TETERVIN (1943)	65(216)-222 AIRFOIL, 8.1°	$R_c = 2.7 \times 10^6$
>	VON DOENHOFF, TETERVIN (1943)	65(216)-222 AIRFOIL, 10.1°	$R_c = 2.6 \times 10^6$
◫	KEHL (1943)	CHANNEL AK III	
⊟	KEHL (1943)	CHANNEL K3	
▨	KEHL (1943)	CHANNEL K7a	
▨	KEHL (1943)	CHANNEL K7b	
▯	WIEGHARDT, TILLMANN (1944)	CHANNEL IV	208 FT. PER SEC
⊡	HALL (1946)	CHANNEL B	10.2° DIFFUSER
●	BURSNALL, LOFTIN (1951)	66_3-018 AIRFOIL, 0°	$R_c = 2.4 \times 10^6$
▲	NEWMAN (1949)	AIRFOIL WITH SPOILER, 0°	$R_c = 3.3 \times 10^6$
▼	NEWMAN (1949)	AIRFOIL WITH SPOILER, 10°	$R_c = 3.3 \times 10^6$

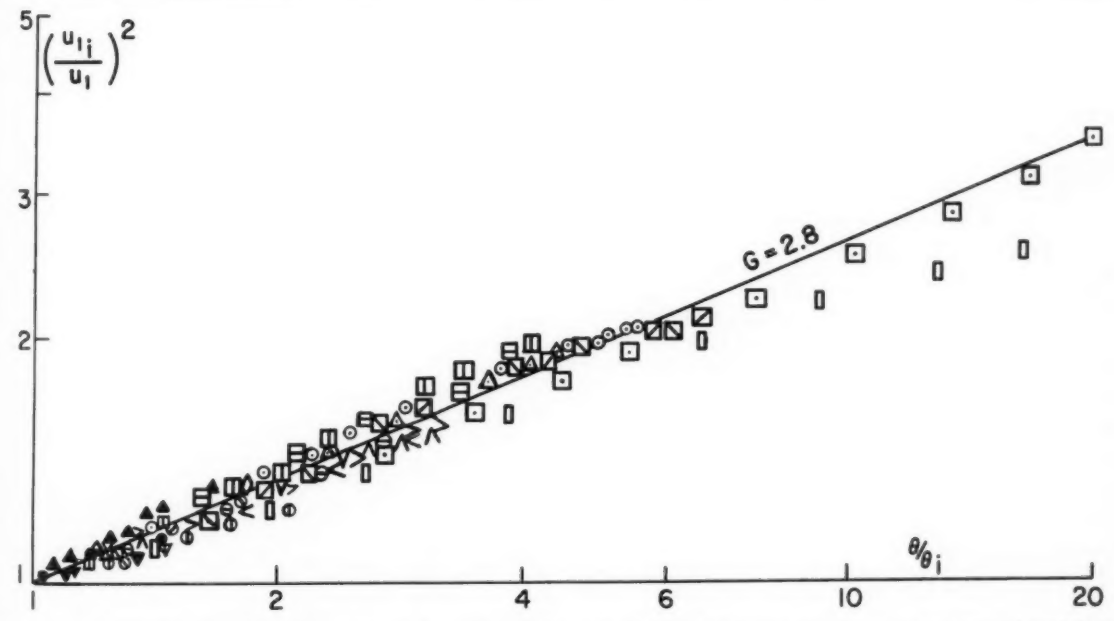

FIG. 1. Verification of relation for momentum thickness for two-dimensional flows in strong adverse pressure gradients (symbols are defined in Table 1).

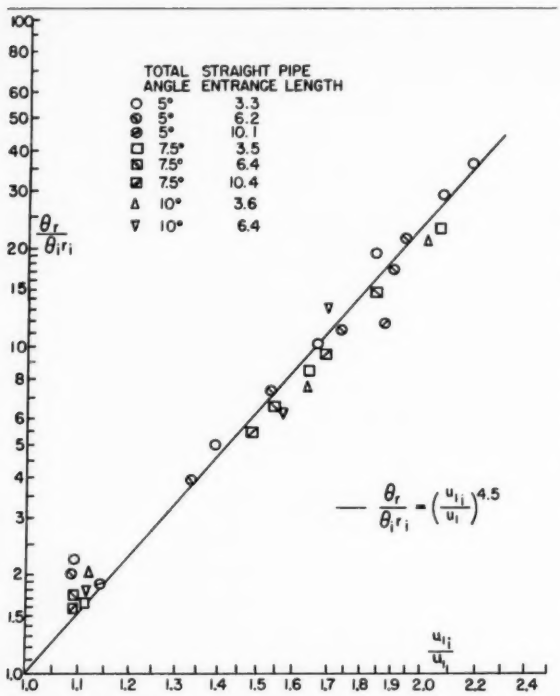

FIG. 2. Verification of relation for momentum thickness in conical diffusers.

tend to be higher, so that G should be somewhat higher. Examination of the data in Fig. 1 shows consistent deviations from the single average curve. To test for Reynolds number effects, the values of G which best fit each individual set of data were determined, and these were plotted, together with the diffuser results, as a function of Reynolds number in Fig. 3. The more reliable data do show the expected trend. It is also noteworthy that the results of the conical diffuser experiments agree well with the two-dimensional data. It should be remarked that the entrance momentum-thickness Reynolds number is used as the independent variable. The point at the highest Reynolds number was obtained from measurements made at only one station in the diffuser of the 48-inch water tunnel[18] at The Pennsylvania State College. Also included are data obtained by Uram[19] in a recent study of conical diffuser boundary layers.

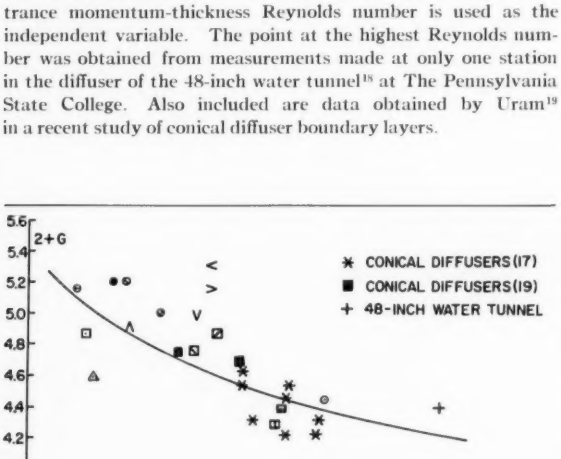

FIG. 3. Variation in exponent with Reynolds number (except as noted, symbols are defined in Table 1).

CONCLUSION

A solution of the integral momentum equation has been presented which is particularly simple for flows in adverse pressure gradients. The solution is a power relation, the exponent being a function of the Reynolds number. The limitations of the method, both at low pressure gradients and near separation, have been discussed and defined.

To solve a typical boundary layer problem, the step-by-step solution given by Eqs. 4 and 5 should be used from transition to the point where the inequality of Eq. 8 is satisfied. Calling this point the origin (subscript i) Eq. 7 may then be used directly for any subsequent station. In using this equation, the value of G may be taken from Fig. 3, or a mean value of $G = 2.8$ may be assumed if only a rough approximation is required.

For the cases for which the present method has been compared with experiment, the results are in each case at least as good as any other published method. The simplicity, when compared to the step-by-step solution of simultaneous differential equations required by most methods, should appeal to most workers in this field.

The authors wish to thank Mr. E. M. Uram for the use of his unpublished data on conical diffuser flow.

REFERENCES

[1] von Kármán, Th., *Über laminare und turbulente Reibung*, Zeitschrift für angewandte Mathematik und Mechanik, Vol. 1, pp. 235–252, 1921.

[2] Buri, A., *Eine Berechnungsgrundlage für die turbulente Grenzschicht bei beschleunigter und verzögerter Strömung*, Thesis 652, Federal Technical College, Zurich, 1931; R.T.P. Trans. 2073, British Ministry of Aircraft Production.

[3] Gruschwitz, E., *Die turbulente Reibungsschicht in ebener Strömung bie Druckabfall und Druckanstieg*, Ingenieur-Archiv, Vol. 2, pp. 321–346, 1931.

[4] Clauser, Francis H., *Turbulent Boundary Layers in Adverse Pressure Gradients*, The Johns Hopkins University, Department of Aeronautics, Contract AF 33(038)9862, June, 1953.

[5] Newman, B. G., *The Re-Attachment of a Turbulent Boundary Layer Behind a Spoiler*, Report A64 of the Aeronautical Research Laboratories, Australia, October, 1949.

[6] Wallis, R. A., *Turbulent Energy Considerations in Turbulent Boundary Layer Flow*, Aerodynamics Note 86 of the Aeronautical Research Laboratories, Australia, November, 1949.

[7] Goldschmied, Fabio R., *Skin Friction of Incompressible Turbulent Boundary Layers Under Adverse Pressure Gradients*, NACA TN No. 2431, August, 1951.

[8] Bidwell, Jerold M., *Application of the von Kármán Momentum Theorem to Turbulent Boundary Layers*, NACA TN No. 2571, December, 1951.

[9] Van Le, Nguyen, *The von Kármán Integral Method as Applied to a Turbulent Boundary Layer*, Readers' Forum, Journal of the Aeronautical Sciences, Vol. 19, No. 9, pp. 647–648, September, 1952.

[10] Ross, Donald, *Integration of the Reynolds Equations for Incompressible Turbulent Boundary Layers*, The Pennsylvania State College, Ordnance Research Laboratory Report NOrd 7958-268, ONR Project NR 062-139, May, 1953.

[11] Ross, Donald, *Evaluation of the Momentum Integral Equation for Turbulent Boundary Layers*, Readers' Forum, Journal of the Aeronautical Sciences, Vol. 20, No. 7, p. 502, July, 1953.

[12] Rubert, Kennedy F., and Persh, Jerome, *Procedure for Calculating the Development of Turbulent Boundary Layers Under the Influence of Adverse Pressure Gradients*, NACA TN No. 2478, September, 1951.

[13] Ludwieg, H., and Tillmann, W., *Untersuchungen über die Wandschubspannung in turbulenten Reibungsschichten*, Ingenieur-Archiv, Vol. 17, pp. 288–299, 1949; Trans. NACA TM No. 1285, May, 1950.

[14] Hall, A. H., *Investigation of Separation in Two-Dimensional Flow*, Ph.D. Thesis, Purdue University, June, 1946; Data published by R. C. Binder, Journal of Applied Mechanics, Vol. 14, pp. 213–216, 1947.

[15] Wieghardt, K., and Tillmann, W., *Zur turbulenten Reibungsschicht bei Druckanstieg*, ZWB U and M 6617, November, 1944; Trans. NACA TM No. 1314, October, 1951.

[16] Ross, Donald, and Robertson, J. M., *Water Tunnel Diffuser Flow Studies, Part 3—Analytical Research*, The Pennsylvania State College, Ordnance Research Laboratory External Report NOrd 7958-230, March, 1952.

[17] Robertson, J. M., and Ross, Donald, *Effect of Entrance Conditions on Diffuser Flow*, American Society of Civil Engineers, Proceedings Separate No. 141, July, 1952.

[18] Ross, Donald, Robertson, J. M., and Power, R. B., *Hydrodynamic Design of the 48-Inch Water Tunnel at The Pennsylvania State College*, Transactions of the Society of Naval Architects and Marine Engineers, Vol. 56, pp. 5–29, 1948.

[9] Uram, E. M., *Investigation of the Growth of an Axisymmetric Turbulent Boundary Layer in an Adverse Pressure Gradient*, MS Thesis, The Pennsylvania State College, Dept. of Engineering Mechanics, June, 1953.

Corrections and Additions to "A Modification of the Holzer Method for Computing Uncoupled Torsion and Bending Modes"[1]

Henry E. Fettis
Mathematics Branch, Aeronautical Research Laboratory, Wright Patterson Air Force Base, Ohio
January 29, 1954

SINCE THE PUBLICATION of the subject paper,[1] experience has indicated that some revisions in the procedure originally recommended would render the method more useful. Also, two typographical errors have been noted which are hereby corrected:

(1) Eq. 10(c) should read

$$\left[\frac{M_{n+1}}{EI_{n+1}}\right]\left(\frac{\Delta x_n}{2}\right)^2 = [p_{n+1} - p_n]\left(\frac{\Delta x_n}{2}\right) - \left[\frac{M_n}{EI_n}\right]\left(\frac{\Delta x_n}{2}\right)^2$$

(2) The heading of column 14 of Table 2 should read:

$$(2/\Delta x_n)$$

In the original paper it was suggested that the computations for bending frequencies be carried out in one table, with each entry consisting of two portions, one depending on the initial amplitude and the other on the initial slope. In actual practice it was found preferable to carry these two calculations out in separate tables. It was also found that in some problems it is more suitable to use the wing root as the starting point rather than the tip as originally suggested. This is particularly advantageous when the tip mass is subject to variation, since then the conditions at the free end can be used to directly determine the tip mass as a function of the frequency. The disadvantage is, of course, that the symmetric and antisymmetric cases must be treated separately. For symmetric modes, the solution is started with zero slope and known shear at the root, while for antisymmetric notes, the solution begins with zero deflection and a known moment. At the tip, the conditions of shear and moment are applied to determine the tip mass corresponding to the assumed frequency. If rotary inertia of the tip mass is neglected, then the moment is set equal to zero and the mass determined from the resulting value of the shear force. If rotary inertia is included, then it is necessary to assume (at least as a first approximation) that the radius of gyration of the tip mass is constant. The conditions of shear and moment then result in two simultaneous equations from which the unknown mass may be found. When computations are carried out by this procedure, an interesting result is obtained concerning the effect of rotary inertia which might not otherwise be recognized. It is first noted that if rotary inertia is neglected, the tip mass is a one-valued function of frequency, the relation being somewhat as shown in Fig. 2 of the original paper. However, when rotary inertia is included, the tip mass becomes two-valued. That is, for each value of the frequency, two values of the tip mass can be found which satisfy the end conditions of shear and moment.* The result is a plot of the type shown in Fig. 1. It can be seen that values on the second branch of the curve, which correspond to the second mode may actually lie below other values in the first branch. In other words, for sufficiently large masses, the frequency of the second mode may be less than that of the first mode for smaller tip masses, a result which could not be obtained from the theory if rotary inertia were not considered. The

* One of these values may sometimes be negative.

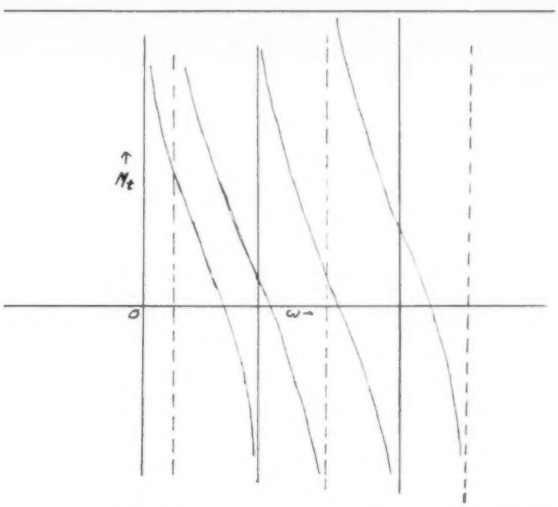

FIG. 1. Manner of variation of tip mass with frequency when rotary inertia is not neglected.

reason for this is that rotary inertia is more critical in higher modes as pointed out previously in a note in this JOURNAL.[2]

Finally the following extensions to cases not considered in the original paper are noted:

I. BEAMS WITH DISCONTINUITIES AT AN INBOARD POINT

To illustrate the treatment of this general type of problem by the present method, we consider the case of transverse vibrations and a cantilever beam, simply supported at some inboard point. If the coordinates of the root, support, and free end are, respectively, $x = 0$, $x = x_1$, $x = L$, the problem may be formulated as follows:

For all x,

$$(d^2/dx^2)EI(d^2h/dx^2) = \omega^2\mu h$$

At $x = 0$, $\begin{cases} h = 0 \\ (dh/dx) = 0 \end{cases}$

At $x = L$, $\begin{cases} EI(d^2h/dx^2) = 0 \\ (d/dx)EI(d^2h/dx^2) = 0 \end{cases}$

At $x = x_1$, $h = 0$

In addition to the above five conditions, we require that (dh/dx) and M be continuous at $x = x_1$. However the shear force at this point will suffer a discontinuity corresponding to the reaction of the support. Numerically, the problem is handled by considering separately the cases $0 < x < x_1$ and $x_1 < x < L$. Starting at the point $x = 0$, and using an assumed value of ω, the tabular method is employed to obtain two linearly independent solutions of the equation which satisfy the initial conditions of zero deflection and slope. The process is carried up to the point $x = x_1$, at which point the condition of zero deflection is applied which determines the ratio of the initial values of moment and shear. Similarly, starting at $x = L$ and proceeding inward to the point $x = x_1$, two solutions satisfying the free end conditions are obtained. These are likewise combined to satisfy the condition of zero deflection at $x = x_1$. The two portions of the solutions are thus uniquely determined with the exception of numerical factors, which now are chosen in the proper ratio necessary to render the slope continuous. Had the proper value of ω been used, the moments would then *a priori* be continuous. Thus by plotting the moment discontinuity against the assumed values of frequency, the correct values of ω may be located.

II. Extension to Coupled Modes

The differential equations for coupled bending-torsion oscillations are

$$(d^2/dx^2)EI(d^2h/dx^2) = \omega^2(\mu h + S\theta)$$

$$(d/dx)GJ(d\theta/dx) = -\omega^2(Sh + I\theta)$$

where S is the mass static moment per unit span about the torsion axis. The resulting algebraic equations for h_{n+1} and θ_{n+1} in terms of previous values of deflection, slope, moment and shear are*

$$\begin{cases} h_{n+1}\left[EI_{n+1} - \omega^2\left(\frac{\Delta x}{2}\right)^4 \mu_{n+1}\right] + \theta_{n+1}\left[-\omega^2\left(\frac{\Delta x}{2}\right)^4 S_{n+1}\right] = h_n\left[EI_{n+1} + \omega^2\left(\frac{\Delta x}{2}\right)^4 \mu_n\right] + \\ \qquad \theta_n\left[\omega^2\left(\frac{\Delta x}{2}\right)^4 S_n\right] + p_n\left(\frac{\Delta x}{2}\right)[2EI_{n+1}] + \frac{M_n}{EI_n}\left(\frac{\Delta x}{2}\right)^2 [EI_{n+1} + EI_n] + 2F_n\left(\frac{\Delta x}{2}\right)^2 \\ h_{n+1}\left[\omega^2\left(\frac{\Delta x}{2}\right)^2 S_{n+1}\right] + \theta_{n+1}\left[GJ_{n+1} + \omega^2\left(\frac{\Delta x}{2}\right)^4 I_{n+1}\right] = h_n\left[-\omega^2\left(\frac{\Delta x}{2}\right)^2 S_n\right] + \\ \qquad \theta_n\left[GJ_{n+1} - \omega^2\left(\frac{\Delta x}{2}\right)^2 I_n\right] + \theta_n'\left(\frac{\Delta x}{2}\right)[GJ_{n+1} + GJ_n] \end{cases}$$

which may be solved simultaneously for h_{n+1}, θ_{n+1} in terms of h_n, θ_n, θ_n', p_n, M_n, and F_n. Advance values of θ, p, M, and F are then found as in the uncoupled case. Since three initial values are not specified, it is necessary in this case to construct three linearly independent solutions for an arbitrarily chosen value of ω. At the opposite end, application of the three remaining conditions will result in three homogeneous equations which will only be consistent if the correct value of ω had been chosen.

References

[1] Fettis, Henry E., *A Modification of the Holzer Method of Computing Uncoupled Torsion and Bending Modes*, Journal of the Aeronautical Sciences, Volume 16, No. 10, October, 1949.

[2] Fettis, Henry E., *Effect of Rotary Inertia on Higher Modes of Vibration*, Journal of the Aeronautical Sciences, Volume 16, No. 7, July, 1949.

* Δx is assumed constant.

Errata on Alternative Forms for the Basic Equations of Transonic Flow Theory*

John R. Spreiter
National Advisory Committee for Aeronautics, Ames Aeronautical Laboratory, Moffett Field, Calif.
February 26, 1954

I have discovered that the ordinates of Figs. 3 and 4 in my recent note in the Readers' Forum are mislabeled. The exponent in the numerator should have been $^1/_3$ instead of $^2/_3$ so that the ordinate of Fig. 3 should read

$$(\gamma + 1)^{1/3}c_{d_0}/(t/c)^{5/3}$$

instead of $(\gamma + 1)^{2/3}c_{d_0}/(t/c)^{5/3}$

and of Fig. 4,

$$[(\gamma + 1)M_0^2]^{1/3}c_{d_0}/(t/c)^{5/3}$$

rather than $[(\gamma + 1)M_0^2]^{2/3}c_{d_0}/(t/c)^{5/3}$

All the calculations and discussions are correct as are the curves themselves when relabeled.

* Readers' Forum, Journal of the Aeronautical Sciences, Vol. 21, No. 1, pp. 70–72, January, 1954.

Thermal and Creep Effects in Work-Hardening Elastic-Plastic Solids

(*Continued from page 344*)

References

[1] Hodge, P., and Prager, W., *A Variational Principle for Plastic Materials with Strain Hardening*, J. Math. Phys., Vol. 27, pp. 1–10, 1948.

[2] Hill, R., *The Mathematical Theory of Plasticity;* Clarendon Press, Oxford, 1950.

[3] Odgvist, Folke K. G., *Influence of Primary Creep on Stresses in Structural Parts*, Transactions, Royal Institute of Technology, Stockholm, Sweden, No. 66 (1953).

INSTITUTE of the AERONAUTICAL SCIENCES

President

J. L. ATWOOD

Vice-Presidents

W. A. M. BURDEN
J. W. LARSON
E. T. PRICE
E. S. THOMPSON

Director

S. PAUL JOHNSTON

Past-Presidents

J. C. HUNSAKER
CHARLES L. LAWRANCE (Deceased)
DONALD W. DOUGLAS
GLENN L. MARTIN
CLARK B. MILLIKAN
T. P. WRIGHT
GEORGE W. LEWIS (Deceased)
JAMES H. DOOLITTLE
FRANK W. CALDWELL
HALL L. HIBBARD
HUGH L. DRYDEN
R. H. FLEET
CHARLES H. COLVIN
ARTHUR E. RAYMOND
P. R. BASSETT
JOHN K. NORTHROP
W. A. M. BURDEN
J. H. KINDELBERGER
LAWRENCE B. RICHARDSON
WELLWOOD E. BEALL
CHARLES J. MCCARTHY

Secretary

ROBERT R. DEXTER

Treasurer

ELMER A. SPERRY, JR.

Controller

JOSEPH J. MAITAN

Counsel

ALLAN D. EMIL

COUNCIL

J. E. BARFOOT
P. R. BASSETT
G. W. BAUGHMAN
M. G. BEARD
WILLIAM B. BERGEN
V. E. CARBONARA
RALPH S. DAMON
R. N. DUBOIS
W. M. DUKE
J. A. HERLIHY
W. T. IMMENSCHUH
E. M. LESTER
CHARLES J. MCCARTHY
CLARK B. MILLIKAN
E. M. POWERS
ARTHUR E. RAYMOND
LAWRENCE B. RICHARDSON
R. C. SEBOLD
EDWARD R. SHARP
PHILIP B. TAYLOR
H. F. WARING
T. P. WRIGHT

ADVISORY COMMITTEE

E. E. ALDRIN
CHARLES H. COLVIN
KENNETH S. M. DAVIDSON
SMITH J. DE FRANCE
JAMES H. DOOLITTLE
SHERMAN M. FAIRCHILD
R. H. FLEET
R. M. HAZEN
HALL L. HIBBARD
J. C. HUNSAKER
THOMAS A. KNOWLES
GROVER LOENING
GLENN L. MARTIN
THOMAS A. MORGAN
F. W. REICHELDERFER
LAURANCE S. ROCKEFELLER
W. C. ROCKEFELLER
T. CLAUDE RYAN
TH. VON KÁRMÁN
EDWARD WARNER

HONORARY FELLOWS

J. ACKERET
P. R. BASSETT
FRANK W. CALDWELL
SIR GEOFFREY DE HAVILLAND
WALTER S. DIEHL
JAMES H. DOOLITTLE
DONALD W. DOUGLAS
HUGH L. DRYDEN
W. F. DURAND
SIR RICHARD FAIREY
SIR WILLIAM (SCOTT) FARREN
SIR ROY FEDDEN
LEROY R. GRUMMAN
SIR FREDERICK HANDLEY PAGE
J. C. HUNSAKER
SIR MELVILL JONES
J. H. KINDELBERGER
GLENN L. MARTIN
CLARK B. MILLIKAN
J. H. PARKIN
J. LAURENCE PRITCHARD
D. R. PYE
ARTHUR E. RAYMOND
IGOR I. SIKORSKY
SIR GEOFFREY TAYLOR
SIR HENRY TIZARD
TH. VON KÁRMÁN
CHARLES C. WALKER
EDWARD WARNER
T. P. WRIGHT

BENEFACTORS

E. E. ALDRIN
HART O. BERG (Deceased)
W. A. M. BURDEN
E. L. CORD
DONALD W. DOUGLAS
ALLAN D. EMIL
SHERMAN M. FAIRCHILD
SIR RICHARD FAIREY
R. H. FLEET
LESTER D. GARDNER
FLORENCE GUGGENHEIM (Deceased)
C. D. HANSCOM
JOHN P. V. HEINMULLER
ALEXANDER KLEMIN (Deceased)
PAUL KOLLSMAN
BELLA C. LANDAUER
WILLIAM LANDAUER
GROVER LOENING
EDMUND C. LYNCH (Deceased)
F. W. MAGIN
GLENN L. MARTIN
GEORGE J. MEAD (Deceased)
S. A. REED (Deceased)
LAURANCE S. ROCKEFELLER
EDWARD WARNER

AMERICAN FELLOWS

IRA H. ABBOTT
JOHN D. AKERMAN
E. E. ALDRIN
H. JULIAN ALLEN
MILTON B. AMES
HARRY G. ARMSTRONG
KARL ARNSTEIN
J. L. ATWOOD
PAUL S. BAKER
RALPH S. BARNABY
P. R. BASSETT
WELLWOOD E. BEALL
M. G. BEARD
REX B. BEISEL
G. M. BELLANCA
DON R. BERLIN
HENRY A. BERLINER
CARLTON BIOLETTI
MAURICE A. BIOT
WILLIAM BOLLAY
CALVIN M. BOLSTER
GEORGE W. BRADY
LYMAN J. BRIGGS
W. G. BROMBACHER
WILLIAM G. BROWN
EDWARD F. BURTON
KENNETH CAMPBELL
GEORGE F. CHAPLINE
CHARLES H. CHATFIELD
BENJAMIN W. CHIDLAW
ALLAN CHILTON
FRANCIS H. CLAUSER
FRANKLIN R. COLLBOHM
PHILIP A. COLMAN
CHARLES H. COLVIN
A. T. COLWELL
KARL T. COMPTON
EMERSON W. CONLON
JOHN W. CROWLEY, JR.
RALPH S. DAMON
KENNETH S. M. DAVIDSON
LUIS DE FLOREZ
SMITH J. DE FRANCE
J. P. DEN HARTOG
LEO J. DEVLIN, JR.
ROBERT R. DEXTER
F. N. DICKERMAN
C. S. DRAPER
IVAN H. DRIGGS
LOUIS G. DUNN
WILLIAM K. EBEL
OLIVER P. ECHOLS
C. L. EGTVEDT
SHERMAN M. FAIRCHILD
FRANK W. FINK
FREDRIC FLADER
CHARLES FROESCH
JACK FRYE
GARLAND FULTON
C. C. FURNAS
LESTER D. GARDNER
RICHARD C. GAZLEY
MICHAEL E. GLUHAREFF
MELVIN N. GOUGH
ROBERT L. HALL
HAROLD R. HARRIS
R. M. HAZEN
EDWARD H. HEINEMANN
S. D. HERON
HALL L. HIBBARD
L. S. HOBBS
HAROLD D. HOEKSTRA
NICHOLAS J. HOFF
PAUL E. HOVGARD
JOHN J. IDE
ROBERT INSLEY
EASTMAN N. JACOBS
C. L. JOHNSON
S. PAUL JOHNSTON
CARL KAPLAN
ALEXANDER KARTVELI
PAUL H. KEMMER
CARLTON KEMPER
OTTO E. KIRCHNER
ARTHUR L. KLEIN
W. B. KLEMPERER
PAUL KOLLSMAN
OTTO C. KOPPEN
B. V. KORVIN-KROUKOVSKY
S. M. KRAUS
ARNOLD M. KUETHE
I. M. LADDON
E. S. LAND
JEROME LEDERER
JOHN G. LEE
JOHN C. LESLIE
HANS W. LIEPMANN
CHARLES A. LINDBERGH
WILLIAM LITTLEWOOD
GROVER LOENING
ALBERT E. LOMBARD
T. C. LONNQUEST
F. A. LOUDEN
W. RANDOLPH LOVELACE, II
EUGENE E. LUNDQUIST
R. D. MACCART
JOHN R. MARKHAM
ERLE MARTIN
WM. H. MCAVOY
CHARLES J. MCCARTHY
JAMES S. MCDONNELL
ROBERT J. MINSHALL
ALFRED S. NILES
JOHN K. NORTHROP
ARTHUR NUTT
SHATSWELL OBER
ROBERT R. OSBORN
W. BAILEY OSWALD
GEORGE A. PAGE, JR.
F. W. PENNOYER, JR.
FRANK N. PIASECKI
E. M. POWERS
P. W. PRATT
A. A. PRIESTER
DONALD L. PUTT
F. W. REICHELDERFER
ELLIOTT G. REID
H. J. E. REID
LAWRENCE B. RICHARDSON
RUSSELL G. ROBINSON
L. EUGENE ROOT
C. E. ROSENDAHL
ADDISON M. ROTHROCK
DANIEL SAYRE
GEORGE S. SCHAIRER
GALEN B. SCHUBAUER
WILLIAM T. SCHWENDLER
W. R. SEARS
E. E. SECHLER
FRANCIS R. SHANLEY
EDWARD R. SHARP
IGOR ALEXIS SIKORSKY
ABE SILVERSTEIN
C. RICHARD SODERBERG
SELDEN B. SPANGLER
ELMER A. SPERRY, JR.
JOHN STACK
ROBERT M. STANLEY
ERNEST G. STOUT
WILLIAM B. STOUT
C. FAYETTE TAYLOR
EDWARD S. TAYLOR
PHILIP B. TAYLOR
TH. THEODORSEN
F. L. THOMPSON
T. E. TILLINGHAST
S. TIMOSHENKO
H. S. TSIEN
RALPH H. UPSON
J. PARKER VAN ZANDT
J. G. VINCENT
WALTER G. VINCENTI
FRANK L. WATTENDORF
P. V. H. WEEMS
FRED E. WEICK
E. C. WELLS
JOHN B. WHEATLEY
CARLOS WOOD
DONALD H. WOOD
ROBERT J. WOODS
JOHN E. YOUNGER
ALBERT F. ZAHM
STEPHEN J. ZAND

EDITORIAL COMMITTEE

HUGH L. DRYDEN, *Chairman*

Aerodynamics

Francis H. Clauser
Howard Emmons
Antonio Ferri
Alexander Flax
R. Paul Harrington
R. T. Jones
Carl Kaplan
H. W. Liepmann
C. C. Lin
H. F. Ludloff
Harold Luskin
John R. Markham
Clark B. Millikan
Shatswell Ober
W. Bailey Oswald
Allen E. Puckett
Elliott G. Reid
H. J. E. Reid
Russell Robinson
G. B. Schubauer
W. R. Sears
John Stack
Theodore von Kármán

Air Transport

Charles Froesch
J. A. Herlihy
R. D. Kelly
Otto E. Kirchner
Jerome Lederer
John C. Leslie
R. Dixon Speas

Flight Testing

W. K. Ebel
R. R. Gilruth
Melvin N. Gough
Ernest G. Stout

Structures and Materials

W. B. Bleakney
E. W. Conlon
L. H. Donnell
E. C. Hartmann
N. J. Hoff
Samuel Levy
E. E. Lundquist
Alfred S. Niles
W. Ramberg
F. R. Shanley
H. W. Sibert
C. R. Strang
S. Timoshenko
H. S. Tsien
Chi-Teh Wang

Rotating Wing Aircraft

F. B. Gustafson
K. H. Hohenemser
Bartram Kelley
R. B. Maloy
Ralph McClarren
R. H. Miller
R. H. Prewitt
Igor I. Sikorsky

Vibration and Flutter

Lee Arnold
M. A. Biot
R. L. Bisplinghoff
William Bollay
Chieh-Chien Chang
I. E. Garrick
Martin Goland
J. P. Den Hartog

Aircraft Design

W. E. Beall
W. K. Ebel
Hall L. Hibbard
Richard Hutton
C. L. Johnson
A. A. Kartveli
C. J. McCarthy
Fred E. Weick
Robert J. Woods

Electronics in Aviation

K. C. Black
E. F. Herzog
David S. Little
D. K. Martin
George Rappaport
Paul Rosenberg
L. M. Sherer

Physiologic Problems

H. G. Armstrong
Louis H. Bauer
Robert J. Benford
Eugene Du Bois
W. Randolph Lovelace, II
Ross A. MacFarland

Fuels and Oils

D. P. Barnard
J. H. Doolittle
Graham Edgar
R. T. Goodwin
S. D. Heron
A. M. Rothrock

Flight Propulsion

George W. Brady
Frank W. Caldwell
L. S. Hobbs
E. E. Johnson
Joseph Keenan
R. P. Kroon
Hans Reissner
Abe Silverstein
C. Fayette Taylor
E. S. Taylor
P. B. Taylor
E. S. Thompson
H. S. Tsien

Instruments

Allan G. Binnie
J. R. Bradburn
Charles H. Colvin
C. S. Draper
S. G. Eskin
O. E. Esval
H. W. Holzapfel
W. L. Howland
George H. Purcell
C. F. Savage
O. Hugo Schuck
C. L. Seward, Jr.
L. D. Statham
R. C. Sylvander
D. K. Warner

Meteorology

C. F. Brooks
D. M. Little
E. J. Minser
F. W. Reichelderfer
H. C. Willett